STEREOSELECTIVE CONSTRUCTION OF 2-OXINDOLE FUSED SPIROCYCLE PRECURSORS

A THESIS SUBMITTED TO
THE GRADUATE SCHOOL OF NATURAL AND APPLIED SCIENCES
OF
MIDDLE EAST TECHNICAL UNIVERSITY

BY

SEDA KARAHAN

IN PARTIAL FULFILLMENT OF THE REQUIREMENTS
FOR
THE DEGREE OF DOCTOR OF PHILOSOPHY
IN
CHEMISTRY

JANUARY 2019

Approval of the thesis:

STEREOSELECTIVE CONSTRUCTION OF 2-OXINDOLE FUSED SPIROCYCLE PRECURSORS

submitted by **SEDA KARAHAN** in partial fulfillment of the requirements for the degree of **Doctor of Philosophy in Chemistry Department, Middle East Technical University** by,

Prof. Dr. Halil Kalıpçılar
Dean, Graduate School of **Natural and Applied Sciences** _____

Prof. Dr. Cihangir Tanyeli
Head of Department, **Chemistry** _____

Prof. Dr. Cihangir Tanyeli
Supervisor, **Chemistry Dept., METU** _____

Examining Committee Members:

Prof. Dr. Canan Ünaleroğlu _____
Chemistry Dept., Hacettepe University

Prof. Dr. Cihangir Tanyeli _____
Chemistry Dept., METU

Prof. Dr. Metin Zora _____
Chemistry Dept., METU

Prof. Dr. Özdemir Doğan _____
Chemistry Dept., METU

Assist. Prof. Dr. Yunus Emre Türkmen _____
Chemistry Dept., Bilkent University

Date: 11.01.2019

I hereby declare that all information in this document has been obtained and presented in accordance with all academic rules and ethical conduct. I also declare that, as required by these rules and conduct, I have fully cited and referenced all material and results that are not original to this work.

Name, Last name: Seda Karahan

Signature :

ABSTRACT

STEREOSELECTIVE CONSTRUCTION OF 2-OXINDOLE FUSED SPIROCYCLE PRECURSORS

Karahan, Seda

PhD, Department of Chemistry

Supervisor: Prof. Dr. Cihangir Tanyeli

January 2019, 257 pages

Recent literature on the bioactivity of isatin (indoline-2,3-dione) derivatives triggered organic chemists to make use of the unique potential of isatin in asymmetric organocatalytic synthesis. Due to extensive presence of 2-oxindole skeleton, especially spiro-fused cycles, in many natural products, they drew the special interest in the disciplines of medicinal chemistry and agrochemistry. Due to highly reactive prochiral carbonyl group, isatins are potent precursors for the synthesis of 3,3-disubstituted spirooxindoles. Direct nucleophilic addition to isatin-derived ketimines is one of the straightforward approaches leading to α-chiral amines which are frequent subunits of pharmaceuticals and agrochemicals besides being heterocycle precursors. In this respect, asymmetric organocatalytic synthesis offers facile and environmentally benign reaction process and selectivity as well. Remarkable advantages of cooperative activation of substrates via bifunctional organocatalysts bearing H-bond donor components such as urea, thiourea and squaramide are indispensable. Modulation of sterically encumbered units such as 1-adamantyl, 2-adamantyl and *t*-butyl in the structure of organocatalyst reveals distinct changes in stereoselectivity of the synthetic transformations. In this thesis study, we aimed to utilize new quinine-based squaramides in the asymmetric aza-Friedel-Crafts and Mannich reactions of isatin

ketimines to obtain corresponding chiral 2-oxindoles with 1,3-aminonaphthol and 2-azidoethanamine functionalities, respectively. A new quinine-derived squaramide organocatalyst revealed excellent stereoselectivity up to >99% ee in aza-Friedel-Crafts reaction also up to 96% ee and 24:1 diastereomeric ratio in Mannich reaction of *N*-carbamate protected isatin ketimines. Additionally, representative examples of 1,4-naphthoxazepines, 1,2,3-triazoles and cyclic ureas were synthesized to demonstrate the synthetic potential of these novel chiral 3,3-disubstituted 2-oxindoles as being heterocycle precursors. Reaction scope, limitations and activation modes of organocatalysts were discussed in detail.

Keywords: Asymmetric synthesis, organocatalysis, squaramide, isatin ketimine, 2-oxindole, aza-Friedel-Crafts, Mannich

ÖZ

2-OKSİNDOL BİTİŞİK SPİROHALKA ÖNCÜ BİLEŞİKLERİNİN STEREOSEÇİCİ SENTEZİ

Karahan, Seda
Doktora, Kimya Bölümü
Tez Yöneticisi: Prof. Dr. Cihangir Tanyeli
Ocak 2019, 257 sayfa

İsatin (indolin-2,3-dion) türevlerinin sahip olduğu biyoaktivite ile ilgili yayımlanmış son çalışmalar organik kimyacıları bu yapıyı asimetrik organik sentezde de kullanmaya teşvik etmiştir. 2-Oksindol iskeleti, özellikle de bitişik halkalılar, birçok doğal üründe bulunması nedeniyle medikal kimya ve tarım kimyası alanlarının özel ilgisini çekmektedir. Oldukça reaktif prokiral karbonil grubu sayesinde isatin yapısı, 3,3-disübstitüe spirooksindol yapılarına geçişte kullanılabilen öncü bileşiklerdir. İsatin türevi iminlere direkt nükleofilik katılma sonucu elde edilecek α-kiral aminler, farmasötiklerin ve tarım kimyasallarının sıklıkla rastlanılan birimleri olmanın yanı sıra heterohalka öncüleridir. Bu bağlamda asimetrik organokatalitik sentez, kolay ve çevre dostu tepkime şartlarının yanı sıra ürünlerin stereoseçici sentezini de sağlamaktadır. Reaktiflerin, H-bağ yapıcı özellikteki üre, tiyoüre ve skuaramit gibi birimler ile eşzamanlı aktivasyonunu sağlaması nedeniyle bifonksiyonel organokatalizörlerin bu alandaki önemi göz ardı edilemez. Bifonksiyonel katalizörlerde sterik açıdan kalabalık 1-adamantil, 2-adamantil ve *t*-bütil gibi grupların kullanılması stereoseçicilikte farklı sonuçlar gösterebilmektedir. Bu tez çalışmasında, yeni kinin temelli skuaramit organokatalizörlerin 1,3-aminonaftol ve 2-azidoetanamin

fonksiyonel gruplarına sahip kiral 2-oksindollerin sentezi için asimetrik aza-Friedel-Crafts ve Mannich tepkimelerinde kullanılması amaçlanmıştır. Bahsedilen yeni kinin türevi organokatalizör ile *N*-karbamat korumalı isatin ketiminlerinin aza-Friedel-Crafts tepkimesinde %>99 ee, Mannich tepkimesinde %96 ee ve 24:1 dr'ye varan yüksek stereoseçicilikler elde edilmiştir. Ayrıca özgün kiral 3,3-disübstitüe 2-oksindollerin heterosiklik yapılara geçişteki sentetik potansiyellerini örneklemek amacıyla bu yapılar, 1,4-naftoksazepin, 1,2,3-triazol ve siklik ürelere dönüştürüldü. Tepkime kapsamları, limitleri ve organokatalizörlerin aktifleme biçimleri ayrıntılarıyla ele alınmıştır.

Anahtar kelimerler: Asimetrik sentez, organokataliz, skuaramit, isatin ketimin, 2-oksindol, aza-Friedel-Crafts, Mannich

To My Devoted Husband and Family…

ACKNOWLEDGEMENTS

Firstly, I would like to express my sincere gratitude to my advisor Prof. Dr. Cihangir Tanyeli for his continuous guidance, support, motivation and confidence in me throughout my PhD study and related research. I really appreciate how he could spare time from his schedule full of administrative works whenever I need.

I am also grateful to my thesis monitoring committee, Prof. Dr. Özdemir Doğan and Assist. Prof. Dr. Yunus Emre Türkmen, for their insightful comments widening my perspective in synthesis and encouragement. I would like to thank all faculty members of Department of Chemistry since I have learnt lots of valuable information that improved my scientific point of view.

For the financial support I would like to thank Scientific and Technological Research Council of Turkey (TÜBİTAK Grant No: 113Z156) and Research Fund of Middle East Technical University. Specially, I am thankful to TÜBİTAK for 2211/A graduate scholarship for national students.

I would like to thank NMR specialist Betül Eymur and Zeynep Erdoğan from Bilkent University for HRMS analysis. Also I am very grateful to Dr. Ferdi Karadaş for his help in XRD measurement.

Apart from the fun already inherent in organic chemistry☺, I would like to express my great thanks to my whole current and former lab mates making the lab environment an enjoyful working place. Besides D-251 members Dilşad Susam, Ezgi Bayer, Abdul Rouf and my lovely former undergraduate students (Sinem Ulusan and Baran Dingiloğlu), I also thank all Tanyeli Research Group members Deniz Tözendemir, Esra Kanberoğlu Dündar, Duygu İşibol, Selin Sağesen, Merve

Bozdemir, Arzu Bilgin and M. Faik Tümer for their help and understanding during my experimental period.

I am also thankful to my M.Sc. supervisor, late Prof. Dr. Ayhan Sıtkı Demir, who made me meet with scientific vision in my early ages and teach how hard I have to work for this. I would like to thank my faithful friends Melek Parlak Khalily and Eylem Canbolat from ASD Research Group for listening me with patience and making me feel the indispensable peace of being understood.

I feel really lucky for having such great friends Aysun Gülseven, Eda Çağlı, Eda Karadeniz, Halil İpek and Gökçen Çetinkaya. They are the people that I can consult about any topic related to my personal life. Therefore, I can sincerely describe them as my family in Ankara.

I am extremely grateful to my family: my father, brother and family of my husband for their endless trust, encouragement and understanding. Without their love and support it would be impossible to complete this PhD study. I know that how much they triggered for keeping me away from the problems during this period in order not to disturb my concentration at work. I would like to apologize to my brother Furkan Burak Okumuş for not being able to be with him when he needs. But I witnessed how much prudent and wise he is. I am really proud of him, my dear lawyer brother ☺.

Last but no means least, thanks go to my dear husband. I don't really know how I could dare living apart together for the last three years for the sake of my PhD degree. By leaving three hundred eighty kilometers behind almost each weekend, he came to me and spend his time at the lab with no complaints. Words fail to describe how he was compassionate, devoted and tolerant to my emotional turbulences. But I will never forget how he sabotaged my reaction flask ☺. I would like to thank him with all my heart for always believing in me.

LIST OF ABBREVIATIONS

Boc	*tert*-Butoxycarbonyl
Cbz	Carboxybenzyl
CuAAC	Copper-catalyzed azide-alkyne cycloaddition
DEPT	Distortionless enhancement by polarization transfer
DIAD	Diisopropyl azodicarboxylate
DMAP	4-Dimethylaminopyridine
DNA	Deoxyribonucleic acid
DPPA	Diphenyl phosphoryl azide
EWG	Electron withdrawing group
FG	Functional group
HSQC	Heteronuclear single quantum correlation
PG	Protecting group
PMP	*p*-Methoxyphenyl
RNA	Ribonucleic acid
TEA	Triethylamine
TFA	Trifluoroacetic acid
TMSCN	Trimethylsilyl cyanide
Tol-BINAP	2,2′-Bis(di-*p*-tolylphosphino)-1,1′-binaphthyl

TABLE OF CONTENTS

LIST OF TABLES

TABLES

LIST OF FIGURES

FIGURES

LIST OF SCHEMES

SCHEMES

CHAPTER 1

INTRODUCTION

1.1 Isatin as Privileged Scaffold

Indoline 2,3-dione, which is commonly known as isatin (Figure 1), is a well-known natural product found in the plants of genus *Isatis*, such as *Isatis tinctoria*, *Calanthe discolor*, *Couroupita guianensis*.[1] It was initially obtained as the oxidation product of indigo dye by nitric acid and chromic acid by Erdmann[2] and Laurent[3] in 1840. Almost thirty years later, its structure was first enlightened by Kekule.[4] From a structural point of view, possessing an indole unit together with a ketone and γ-lactam functionalities isatin is a privileged scaffold capable of reacting as a both nucleophile and electrophile (Figure 1). Its unique potential as a building block unfolds various aspects of organic synthesis such as electrophilic aromatic substitutions at C-5 and C-7 of the phenyl ring, *N*-substitutions and nucleophilic additions to C-3 carbonyl group.[1]

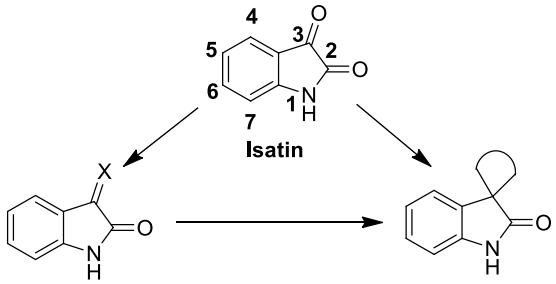

Figure 1 Isatin and its general transformations.

Most frequently, prochiral C-3 center has been exploited because of its undoubted high reactivity. Reactions of this centre, mostly nucleophilic additions and spiroannulations, afford 2-oxindole derivatives (Figure 1). Construction of spiro-

cyclic framework has always been a great challenge due to the necessity of well-designed synthetic strategies and overcoming steric issues. However, exploration of isatin chemistry in the past decade offered successful design and synthesis of various spiro-fused 2-oxindole rings.

Specifically, 3-aminooxindole moiety has been encountered as the core entity of many architecturally complex natural products and pharmaceuticals such as AG-041R gastrin/CCK-B receptor agonist,[5a] CRTH2 antagonist as anti-bacterial agent and an anti-tuberculosis agent,[5b] vasopressin V_{1b} receptor antagonist SSR-149415 which is used in treatment of anxiety and depression,[5c] an anti-malarial agent NITD609,[5d] HIV-1 protease inhibitor[5e] and an anti-mycobacterial against *M.tuberculosis* H37Rv[5f] (Figure 2).

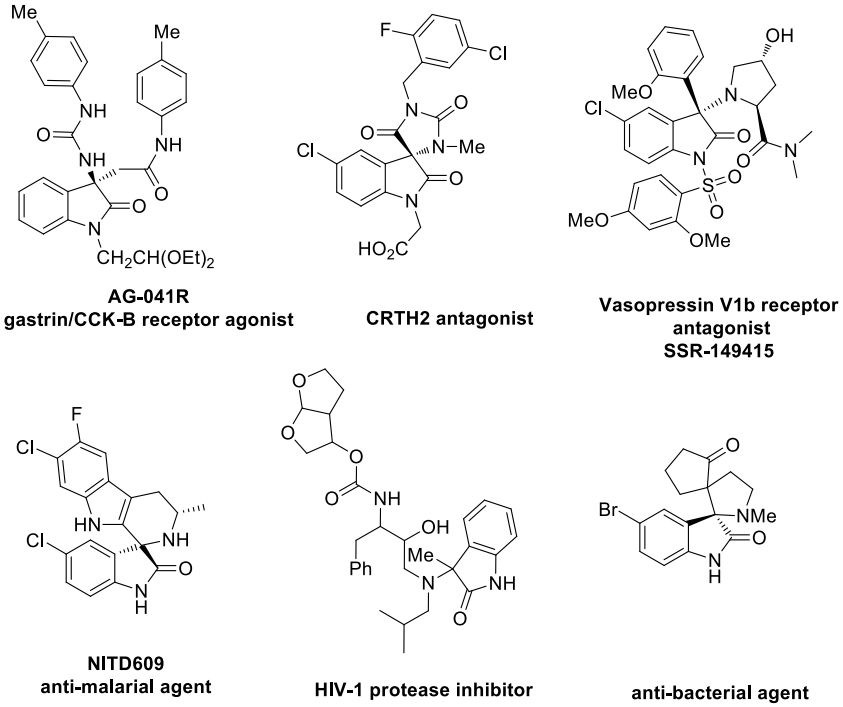

Figure 2 Representative examples of biologically active compounds containing 3-amino-2-oxindole skeleton.

1.1.1 Chiral Spirooxindoles

Chiral spirooxindoles, a class of spiro-cyclic frameworks, is prevalent in natural alkaloids and therapeutic agents. Their scope of biological mode of action is so wide that, apart from the examples given in Figure 2, they have frequent utility in therapeutic areas as being anti-tumor, antimicrobial, anti-HIV, antimalarial, antiviral, antipyretic agents and sodium-channel blockers.[6] Structurally rigid nature of spirooxindoles provides an affinity to three-dimensional proteins.[7]As a result of broad and promising biological activity of chiral spirooxindole skeleton, investigation of robust and facile strategies for their synthesis are of interest for the communities in both industry and academia.

Organocatalysis is a milestone for construction of stereochemically complex spiro-cyclic frameworks. Its ready availability, mild reaction conditions and stability makes enantioselective organocatalysis attractive in organocascade and domino strategies designed for the enantioselective synthesis of high-order products.[8]

Asymmetric catalysis has been efficiently utilized for the construction of spirooxindoles from oxindole and derivatives in the last decade (Figure 3). Isatin and isatinimines **1** are good acceptors due to highly reactive C-3 position which can be readily attacked by a nucleophile. With well-designed reaction partners possessing both nucleophilic and electrophilic sites subsequent to addition, cyclization affords chiral spirooxindoles. 3-Alkylidene indolinones **2** reveal similar reactivity pattern; however, the control of regioselectivity may alter due to influence of substituents on two carbon atoms.[8] Secondly, 3-substituted oxindoles **3** couple with convenient reaction partners via an addition-annulation process. Moreover, isatin-derived 3-indolylmethanols **4** have drawn attention because of zwitterion generated under acidic conditions are good substrates for [3+2] cycloadditions and [3+3] cyclizations to form 5- and 6-membered rings.[9] A

variety of enantioenriched spirooxindoles **5-9** with three to seven membered cycles are known in the literature. Depending on the substituents on the rings, annulation reactions may lead to the formation of multiple stereocenters.

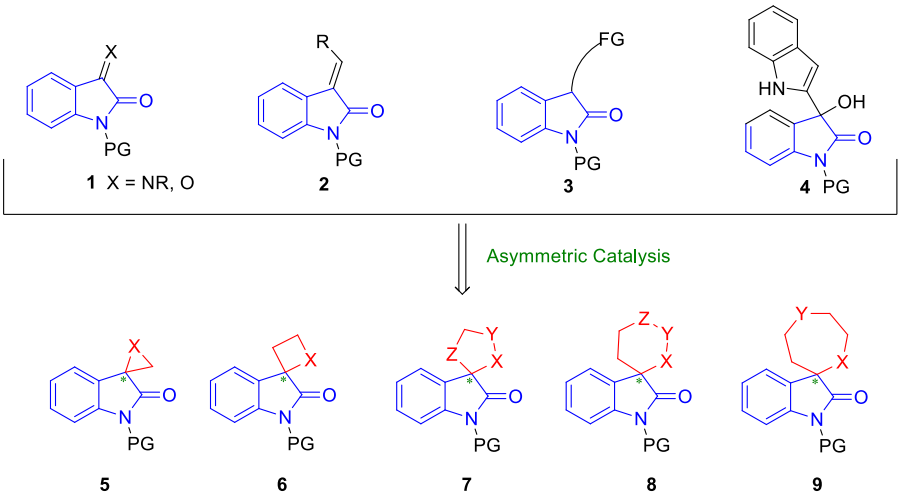

Figure 3 Strategies for catalytic asymmetric synthesis of chiral spirooxindoles.

1.2 Why Do We Need Asymmetric Synthesis?

Asymmetric synthesis is the ability to control the three-dimensional structure of the molecular architecture. This control brings about a chemical synthesis in which one or more new chirality elements are produced so that the stereoisomeric (enantiomeric and diastereomeric) products are unequal in amounts.[10] In other words, in the course of the synthesis of a compound, the molecular interactions between the substrates and catalysts selectively favor one enantiomeric form. This selectivity is advantageous since the majority of medicinal agents and natural products exist already as the single enantiomer.

1.2.1 Applications in Medicinal Chemistry

Selectivity of enzymes and information carrier molecules such as RNA and DNA are dependent to their monomeric subunits, amino acids and nucleotides,

respectively. Therefore, a biological system can differentiate and respond differently to both enantiomers of a biologically active compound. Generally, only one of the enantiomers is therapeutically active while the other is categorized as medicinal pollutant. Most of the natural medicinal agents exist in their optically pure form such as quinine, quinidine, (-)-morphine and (+)-digitoxin (Figure 4).[11]

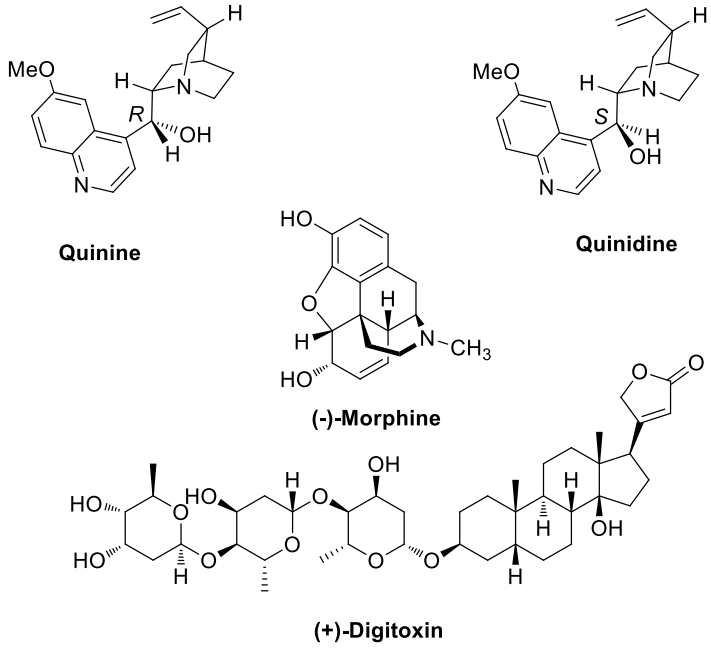

Figure 4 Structures of some naturally occurring medicinal agents.

Malaria disease can be given as an illustrative example to emphasize the importance of asymmetric synthesis on human health. The third world countries have been still exposed to unfortunate consequences of malaria. According to the report of World Health Organization published in 2017, the scenario is so drastic that there were an estimated 445,000 deaths globally. Also an independent study claims that the number is twice when undiagnosed and untreated cases are included.[12] *Plasmodium falciparum* is one of the species causing malaria in humans and recently tetrahydropyridines **12** have been synthesized and screened for this parasite (Scheme 1).[13] From cheap starting materials, β-ketoester **10**, aromatic aldehydes and anilines, asymmetric organocatalytic one-pot

multicomponent reaction in the presence of L-proline (**11**) afforded *trans*-aryl-substituted tetrahydropyridines **12**. In the first step, enamine **13** formed by organocatalyst **11** and β-ketoester attacks to the aldehyde and subsequent dehydration leads to Knoevenagel condensation product **14**. Meanwhile, condensation of aniline with both **14** and aldehyde afforded imine and 2-aza-diene **15**, respectively. Aza-Diels-Alder reaction of **15** gives the target molecules **12** (Scheme 1) which were later assayed for their blood schizonticidal activity against *P. falciparum* 3D/ strain. Even in very low concentrations, one of the derivatives of **12** provided 91% inhibition of the parasite. With countless studies similar to this example, the field of asymmetric synthesis is hope for humanity which has always been in fight for mortal diseases for ages.

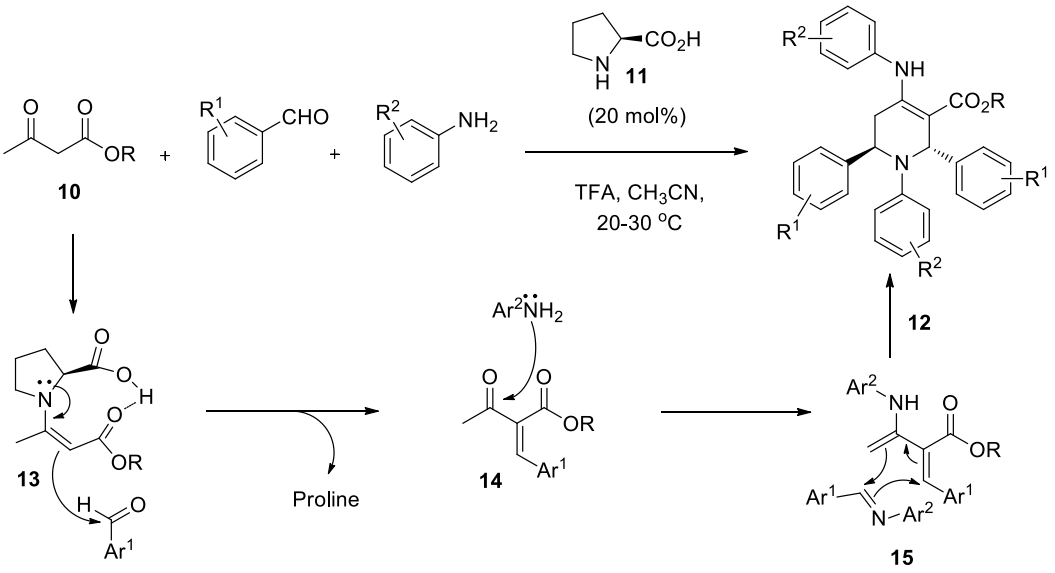

Scheme 1 Synthesis of tetrahydropyridines against *Plasmodium falciparum*.

1.2.2 The Market of Chiral Drugs

In 2015, 45 new drugs were approved by the US Food and Drug Administration (FDA) and 44% of these drugs are small molecule active pharmaceutical ingredients (APIs) with at least one or more chirality centers.[14] Therefore, the

current drug industry has tendency to either exploit chiral switching or establish *de novo* synthesis of enantiomerically pure compounds for chiral drugs. The term "chiral switching" goes back to 1997 which is accepted as the adolescence of the field of chiral drugs. The first definition of "chiral switching" was given by Agranat and Caner in 1999[15a] and later clarified as the replacement of a chiral drug that has been developed initially as a racemate or mixture of diastereomers (usually marketed but not necessarily) with its single enantiomer.[15b] That is to say, the fundamental criterion for "chiral switching" is the alteration in the status of chirality.

The first drug switched to single enantiomer was a non-steroidal anti-inflammatory drug ibuprofen in 1994 (Figure 5). The reason for this change was the fact that inhibition activity of the (*S*)-enantiomer toward cyclooxygenase 1 (COX-1) was over 100-fold more than that of (*R*)-isomer.[16] As a result, by reducing the source of configurational diversity, application of enantiopure (*S*)-ibuprofen would lead a rapid onset of action with a lower dosage.[17] Besides a faster onset of action and patient's being exposed to a lower dosage, other potential advantages of chiral switching comprise an enhanced therapeutic index by increased selectivity, decreased side-effects and a reduced liability for drug-drug interactions.[14]

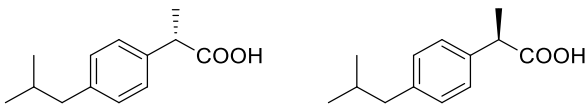

(*S*)-(+)-Ibuprofen (*R*)-(-)-Ibuprofen

Figure 5 Structure of ibuprofen enantiomers.

Instead of putting many efforts into separation and purification of two enantiomers from a mixture, *de novo* induction of stereochemistry is the second alternative applied by the drug industry. For the development of enantiopure drug,

there are three methods: (i) to start from an enantiomerically pure natural product (chiral pool); (ii) to employ asymmetric synthesis; (iii) to resolve the racemate obtained by a non-stereoselective synthetic protocol. In each case, in order to specify the identity, stereochemistry, purity and quality of the drug, various instrumental and experimental methods must be strictly applied.[14]

1.2.3 Isomers and Odor or Nose as Stereochemist

Smell is one of the ways to perceive the world around us. Fragrant objects have influence on human well-being. However, we usually do not realize that organ which can even distinguish trace amount of impurities in the sample. Functioning as an extremely sensitive analytical machine, our olfactory receptors can identify even minor spatial differences (i.e. configuration of the double bonds and chiral centers) in the structure of a related aroma.[18]

One of the most frequently used compounds is rose oxide **16** for the creation of rose notes. The two diastereomeric form of rose oxide (2*R*,4*R*)-*trans*-**16b** and (2*S*,4*R*)-*cis*-**16a** were encountered in geranium oil and rose oil. Taking place of each isomer on the shelves of perfumery became possible after the asymmetric synthesis of them starting from (*S*)-citronellol (Scheme 2).[19] In general, rose oxide has a refreshing, floral, green note. However, characteristics of odor vary from isomer to isomer so that *cis*-rose oxide has geranium and peppermint like note, while *trans*-rose oxide has much more intense fragrance. In 1972, Ohloff synthesized and evaluated the enantiomers of *cis*-rose oxide (**16a**, **16c**). Isomer **16a** was found to have a sweet fragrance; however, **16c** have somewhat spicy. Later the threshold of each enantiomer was found to be different by 100 times so that while 0.5 ppb is enough to perceive (2*S*, 4*R*)-**16a**, for (2*R*, 4*S*)-**16c** 50 ppb is required.[20] It is noteworthy to indicate that reliable data can be obtained only for highly pure compounds. Therefore, necessity of asymmetric methods is not surprising in the field of perfumery.

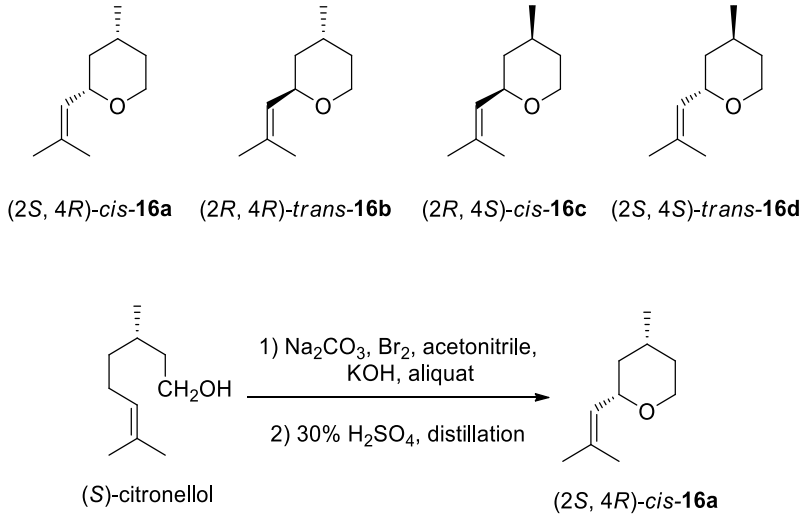

Scheme 2 Stereoselective synthesis of rose oxide.

1.3 Asymmetric Organocatalysis

Since the turn of the century, a profound interest raised for the development of new asymmetric catalysts using organic molecules to attain optically active organic molecules. Although the first utility of such metal-free organic molecules as catalyst dates back to 1971 with proline-catalyzed intermolecular asymmetric aldol reactions established by two independent industrial groups (Scheme 3),[21] recognition of asymmetric organocatalysis as a research field came true after the conceptualization and description of the generic activation modes. In this reaction, a triketone **17** generates an enamine with the (*S*)-proline (**11**) than the neutral enamine attacks to the carbonyl group activated by H-bonding with a facial selectivity to afford cyclic aldol product **18**.

Discovery of transition-metal catalysis with tunable activity and selectivity with different ligands has offered a powerful tool for the construction of C-H and C-C bonds. But still organic chemists have a consensus on the drawbacks of transition-metal catalysis. These are the high cost and effort for the preparation of catalysts,

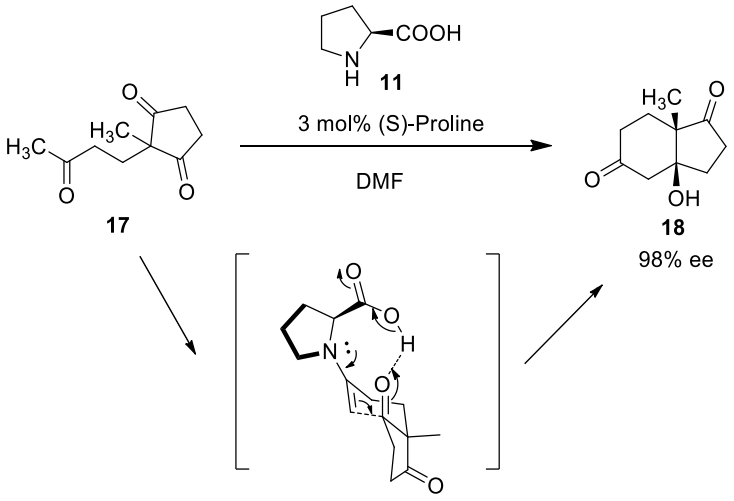

Scheme 3 The first asymmetric organocatalytic reaction.

toxicity carried forward to final product and lack of orthogonality with different functional groups.[22] However, after a series of primary studies, organocatalysis appear to solve these problems with better tolerance to moisture, air and various functional groups. In combination with other synthetic tools and concepts, organocatalysis have altered the map of catalysis. Nevertheless, these achievements are insufficient in terms of efficiency to meet the industrial needs. [23]

1.3.1 Bond Formation Methodologies and Activation Modes

Along with the structural simplicity of the organocatalysts, asymmetric organocatalysis is notable for a variety of activation modes which are fundamental for establishing mechanistic working models and the prediction of the stereochemical outcome. Modes of activation can be classified according to two perspectives. From a mechanistic point of view, activation mode can be categorized as either covalent or noncovalent with respect to substrate-catalyst interaction. In the second perspective, the chemical nature is considered and Lewis base, Lewis acid, Brønsted base and Brønsted acid assortment is used.[24] However, it is important to note that many organocatalysts (e.g. amino acids, phosphoric acids) act by both covalent and noncovalent interaction or have dual

acid-base nature (bifunctional catalysts) (Figure 6). Aiming the synthesis and application of new Brønsted base/H-bond donor bifunctional organocatalysts in this thesis, preferentially more detailed literature will be presented on this subdivision.

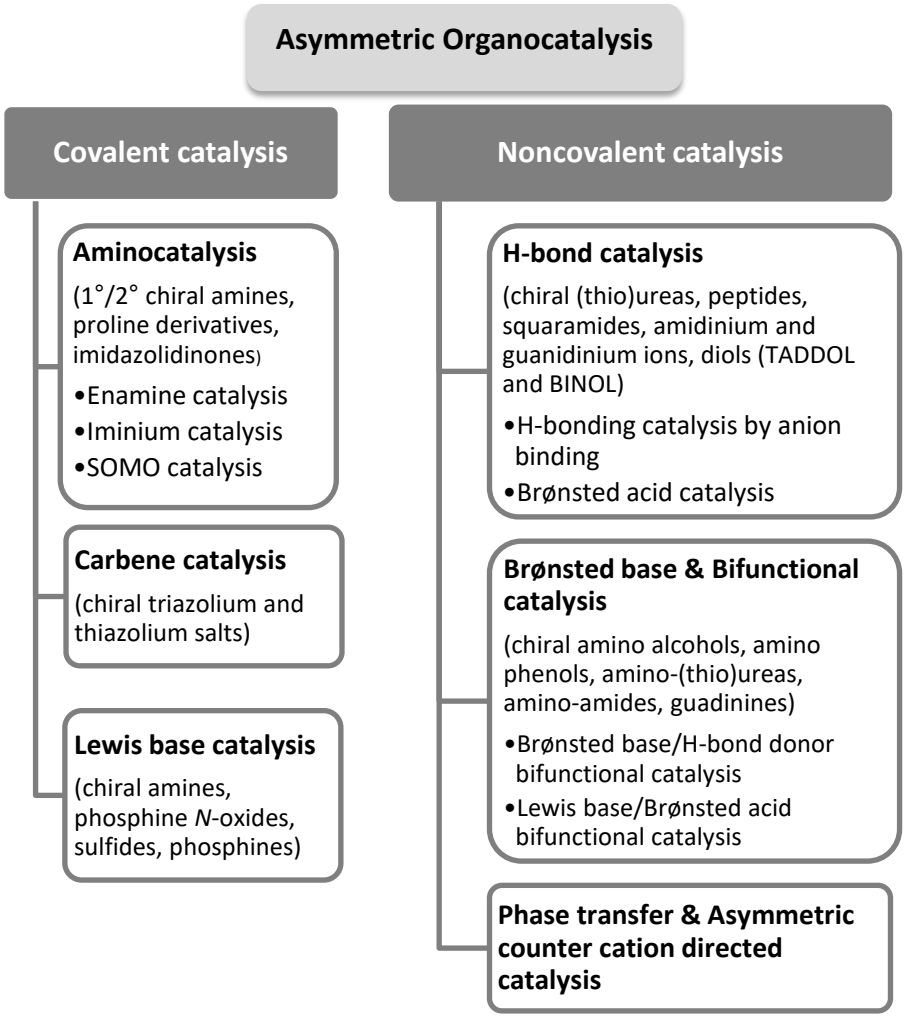

Figure 6 Classification of asymmetric organocatalysis according to activation modes.

1.3.1.1 Brønsted Base/H-Bond Donor Bifunctional Catalysis

Multifunctional asymmetric catalysis, targeting the synergistic activation of both reactants by dual organocatalysts bearing acidic and basic sites, has attracted considerable interest in modern synthetic chemistry. Until being introduced by Takemoto and co-workers as a consistent and general strategy in 2003,[25] previous reports of Riant and Kagan (1989)[26] on quinidine catalyzed Diels-Alder reaction of anthrones **19** and Morita-Baylis-Hillman reaction of Hatakeyama and co-workers[27] had already indicated the future of bifunctional organocatalysis (Scheme 4).

In the first example, while tertiary amine of the quinidine (**21**) was responsible for the enolate formation from **19**, presence of a free –OH group was essential for a better yield since its assumed to activate dienophile **20** through H-bonding (Scheme 4).[26] In the second report, phenolic hydroxy group of the catalyst **24** plays a key role for the stereochemistry of the major and minor products (**25** and **26**). Enolate, generated by Michael addition of catalyst to acrylate **23**, stereoselectively attacks to aldehyde to form an oxyanion intermediate stabilized by the H-bonding interaction of the phenolic hydroxyl of the catalyst **24**.[27] Later, the concept of "bifunctional organocatalysis" was first introduced by Takemoto's catalyst **29** in which thiourea moiety (H-bond donor) was combined with tertiary amine (Brønsted base) with (*R*,*R*)-1,2-cyclohexyldiamine as a chiral scaffold (Scheme 4). Michael addition of malonates **28** to nitroolefins **27** occurred highly stereoselectively to afford (*S*)-**30** with high yields and enantiopurities.[25]

Although, (thio)ureas had been formerly used for molecular recognition, their mode of action in catalysis was investigated after the interpretation of dual H-bonding nature of enzymes activating Lewis basic compounds (e.g. nitroaromatic compounds, ketones, sulfoxides, imines). H-Bond donor associated with other complementary

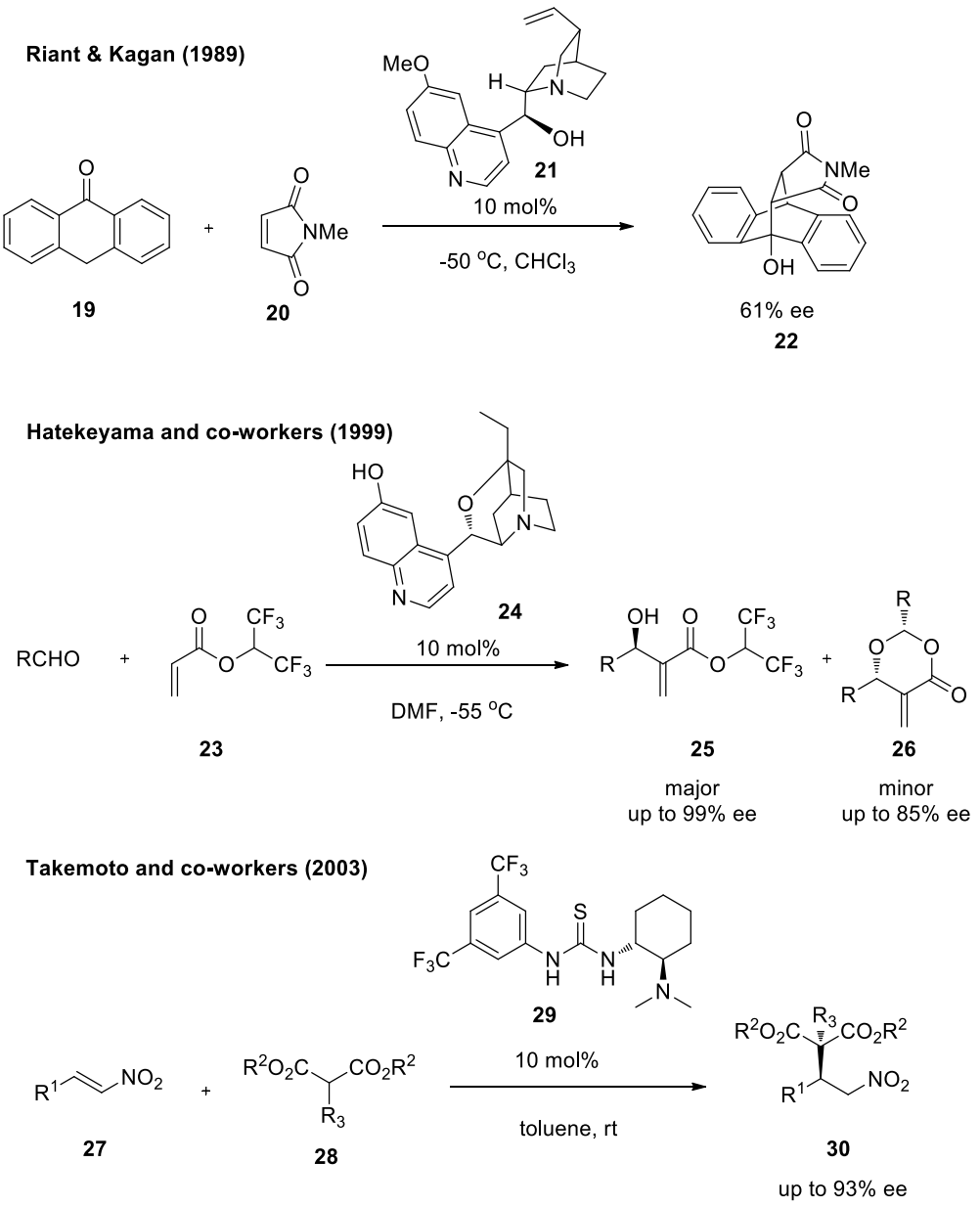

Scheme 4 Pioneering examples of asymmetric bifunctional organocatalysis.

and structural frameworks directs the spatial arrangement of both nucleophile and electrophile with as much control as covalent catalysis (Figure 7). However, since there is no covalent intermediate between the substrate and the catalyst, isolation and characterization of the reactive intermediates to enlighten the mechanism is difficult. But still, bifunctional organocatalysis disclosed many C-C and C-

heteroatom bond formation reactions with a wide spectrum of substrates.[28] In Figure 7, different combinations of mainly noted Brønsted basic simple tertiary amines **31**, quinine derivatives **32** and 2-aminoDMAP units **33** and H-bond donors ((thio)ureas **34** and squaramides **35**) reported hitherto are represented with their first developers.

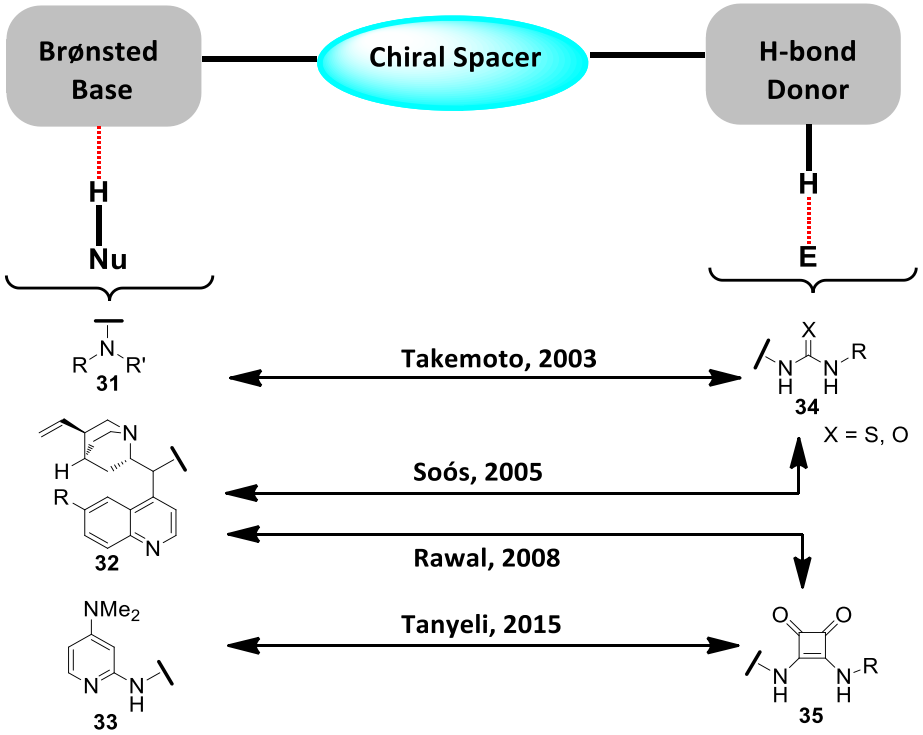

Figure 7 Brønsted basic moieties with H-bond donors.

1.3.1.2 Superior Performance of Squaramides

Squaramides, nitrogenated squaric acid derivatives, were initially designed for the molecular recognition of negatively charged carboxylates and nitrates. Later they entered organocatalysis as their urea and thiourea analogues. However, with its conformationally rigid square-shaped structure, squaramido functionality differs significantly in five aspects; (i) duality in binding, (ii) H-bond spacing, (iii) H-bond angle, (iv) rigidity and (v) acidity.[29]

While urea and thiourea reveal excellent anion-binding ability, their capability to bind cations is limited. On the contrary, recognizing both anions and cations, squaramides exhibit duality in binding. As a result of this ambivalent nature, squaramides possess three different H-bonding patterns (Figure 8) which makes them much more bifunctional. Calculated H-bond spacing in *N*,*N*′-dimethylthiourea and *N*,*N*′-dimethylsquaramide is aproximately 2.13 Å and 2.72 Å, respectively (Figure 8).[30] With a larger space, squramides have a wider substrate scope. Furthermore, square geometry of cyclobutenedione ring induces convergent orientation of the N-H groups (α-β≈6°) (Figure 8). This deviation brings about a greater linearity in H-bonding for some substrates.

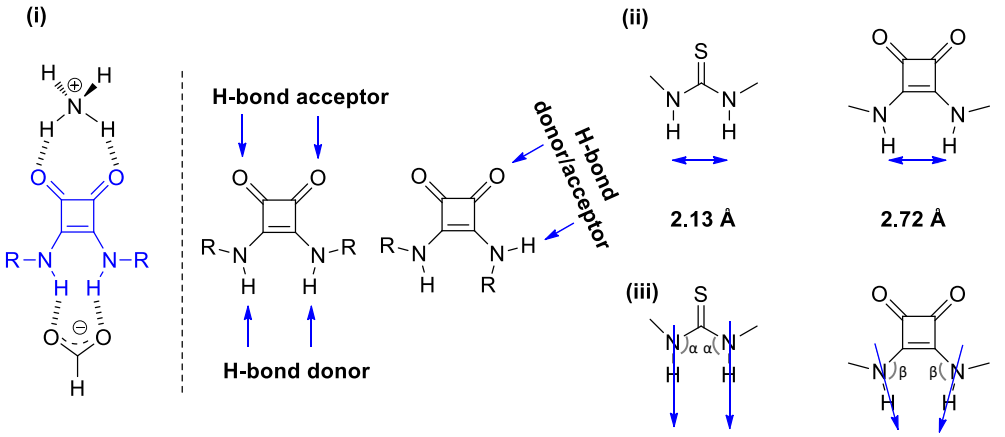

Figure 8 (i) Duality in binding, (ii) H-bond spacing, (iii) H-bond angle.

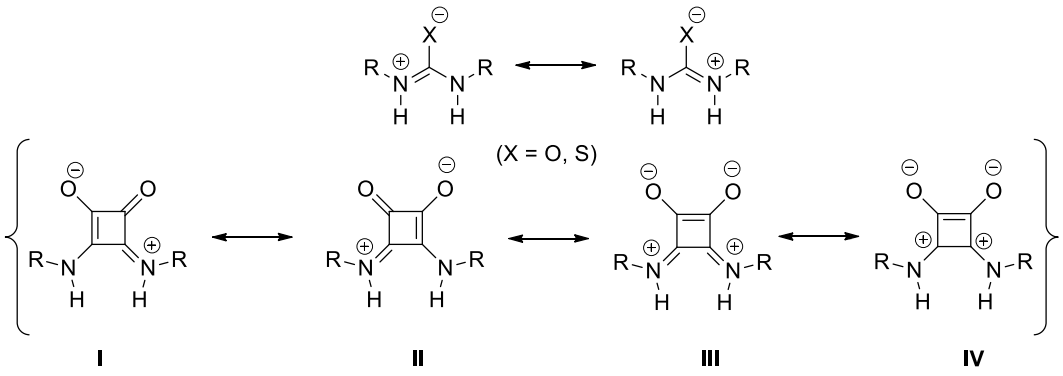

Figure 9 Resonance structures of (thio)urea and squaramide.

Both (thio)urea and squaramide functionalities have the ability to delocalize the nitrogen lone pair through carbonyl or thiocarbonyl groups, thereby they restrict the rotation of C-N bond. However, squaramides undergo further delocalization to give the cyclobutene ring with two positive charges on the ring **IV** (Figure 9). By computational methods, this structure is known to fulfill the energetic, geometric and magnetic criteria of aromaticity which brings about rigidity for the catalyst. Finally, acidities of urea and squaramide were compared by analogy with carbonic acid (pK_{a1} :3.6; pK_{a2} :10.3) and squaric acid (pK_{a1} :1.5; pK_{a2} :3.4) from which a higher acidity is inferred for squaramides.[29]

1.4 α-Chiral Amines

A nitrogen atom bearing an adjacent carbon atom with at least three different substituents are named as "α-chiral amine". Due to their inherited H-bond ability, abundance in vast majority of natural products as building element and resolving agent potency they are powerful pharmacophores. However, their synthesis faces some challenges such as functional group interconversion and industrial feasibility.[31] When regio-, chemo- and stereocontrol are added to these challenges, development of single step strategies inducing heteroatom gains more importance.[32]

1.4.1 Organocatalytic Strategies for α-Chiral Amine Synthesis

There are various metal mediated, Brønsted acid and chiral tertiary amine catalyzed strategies hitherto reported for α-chiral amine synthesis. Among them chiral Brønsted base/H-bond donor (thio)urea and squaramides are mostly utilized in asymmetric organocatalytic direct addition of carbanions to imines or conjugate addition of nitrogen nucleophiles with high levels of enantiofacial discrimination. Namely, enantioselective aza-Henry, aza-Friedel-Crafts, Strecker, Mannich and

aza-Michael reactions are efficient synthetic tools for the synthesis of secondary and tertiary α-chiral amines (Scheme 5).

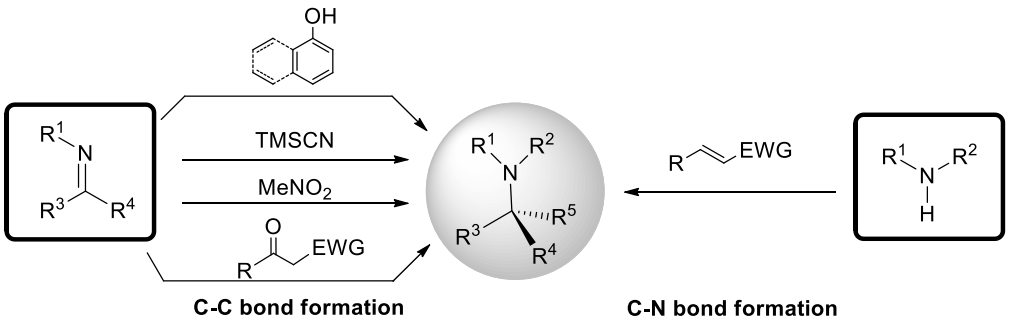

Scheme 5 Common strategies for α-chiral amine synthesis.

1.4.1.1 Aza-Friedel-Crafts Reaction

1,2-Addition of naphthols, activated phenols, benzenes and heteroaromatic compounds (indole, pyrrole, furan etc.) to imines are known as aza-Friedel-Crafts reaction. The seminal study on asymmetric aza-Friedel-Crafts reaction was a chiral copper (I)-Tol-BINAP catalyzed addition of indole (**37**) to imino esters **38** affording chiral α-amino acid derivatives **39** (Scheme 6).[33] Later, many chiral phosphoric acid, thiourea and cupreine-catalyzed asymmetric aza-Friedel-Crafts reactions have been reported.[34] However, bifunctional squaramides have been implemented in aza-Friedel-Crafts reactions very recently.

Even though aza-Friedel-Crafts reactions of indoles and pyrroles have been examined extensively, examples with naphthols and phenols were very elusive. Furthermore, due to low reactivity and difficult face selectivity of ketimines, this type was limited to aldimines. In 2015, the first quinine squaramide catalyzed aza-Friedel-Crafts reaction of cyclic trifluoromethyl ketimines **41** and naphthols/phenols **42** were reported (Scheme 7).[35] The fluorenyl substituted organocatalyst **40** afforded trifluoromethyl bearing dihydroquinazolinones **43**,

which are prominently known as potential HIV nonnucleoside reverse transcriptase inhibitor, in excellent yield and enantiopurity.

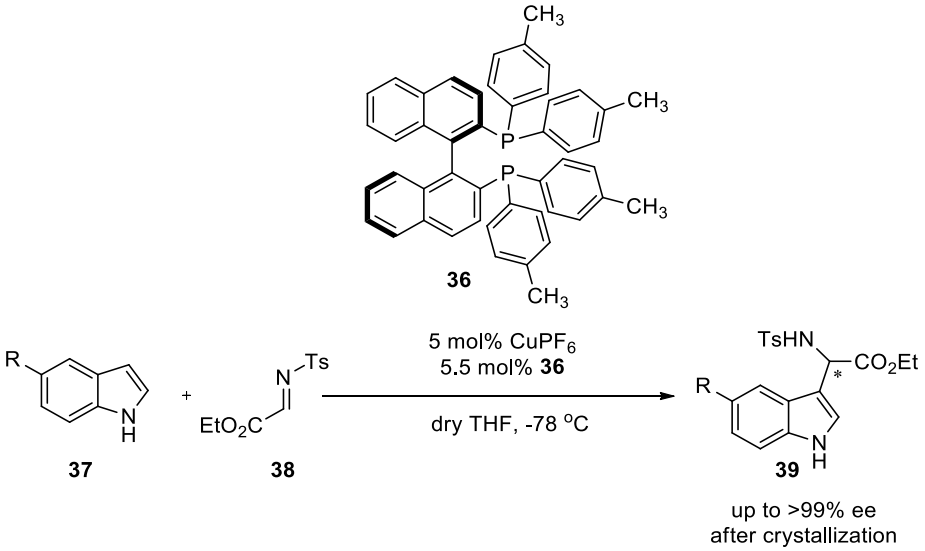

Scheme 6 The first asymmetric aza-Friedel-Crafts reaction.

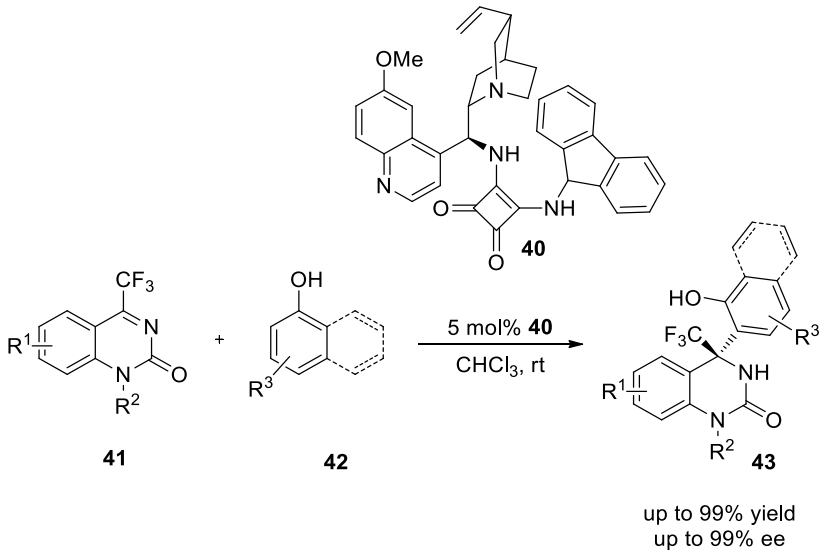

Scheme 7 Bifunctional squaramide catalyzed aza-Friedel-Crafts reaction of trifluoromethyl ketimines.

In 2017, Enders group[36] developed a domino protocol utilizing *N*-Boc ketimines derived from pyrazolin-5-ones **46** possessing two electrophilic centers (Scheme 8). Subsequent to aza-Friedel-Crafts reaction, adduct of 2-naphthols **47** underwent further *N*,*O*-acetalization to give dihydronaphtofurans **48** with two vicinal tetrasubstituted stereogenic centers. However, reaction with 1-naphthols terminates at the first step with the formation of 1,3-aminonaphthols **45** (Scheme 8). With the well-established milestones of squaramides and familiar electrophilicity of isatin, aza-Friedel-Crafts reaction of isatin ketimines was worth to investigate as a part of this thesis study.[37]

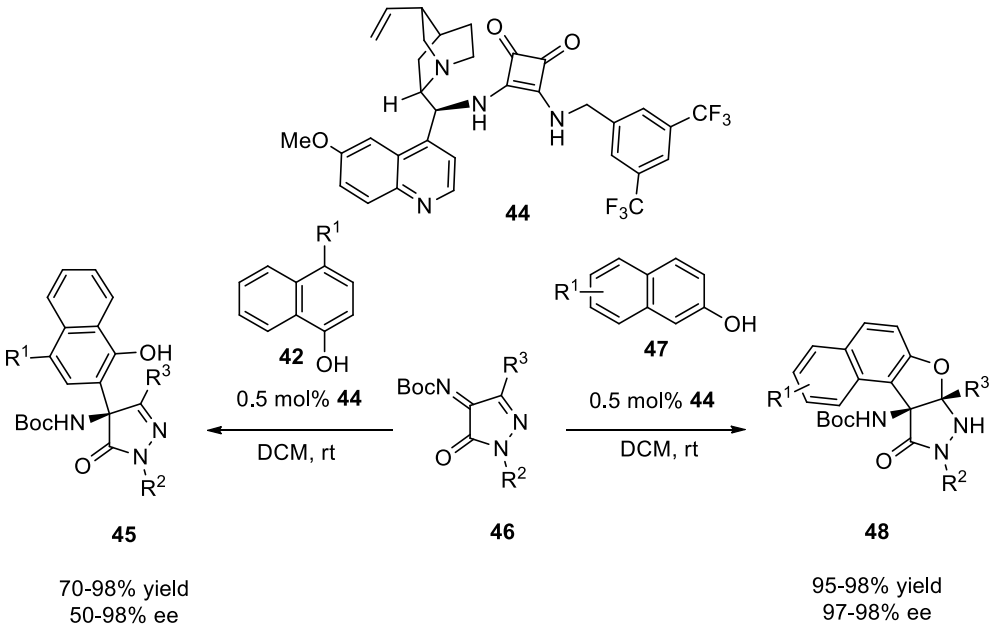

Scheme 8 Bifunctional squaramide catalyzed aza-Friedel-Crafts reaction of pyrazoline-5-one ketimines.

1.4.1.2 Mannich Reaction

Mannich reaction is a useful tool for the construction of β-aminoketones via multi-component C-C bond formation between an aldehyde, an enolisable ketone or equivalent and a primary or secondary amine. The key element of this reaction

is the formation of an imine or iminium intermediate. The products are called as Mannich bases and valuable for the synthesis of alkaloids.[38]

The first example of catalytic asymmetric Mannich reaction emerged as a result of List's interest on whether chiral amines or amino acids would catalyze the Mannich reactions as they did in the direct asymmetric aldol reactions.[39] Three-component Mannich reaction of acetone, an aliphatic or aromatic aldehyde and *p*-anisidine (**49**) in the presence of L-proline (**11**) as the organocatalyst afforded PMP (*p*-methoxyphenyl) protected amines **50** with moderate yields due to the formation of aldol addition and condensation side products (Scheme 9). But still obtained enantioselectivities was high (70-96% ee).

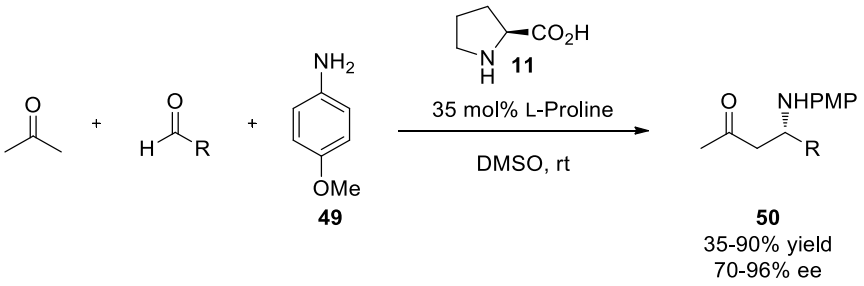

Scheme 9 The first asymmetric organocatalytic Mannich reaction.

Subsequent to pioneering work of List,[39] diverse organocatalytic approaches have been developed utilizing enamine catalysis, chiral Brønsted bases and chiral Brønsted acids. β-Dicarbonyl compounds (symmetrical and unsymmetrical diketones, malonates, dithiomalonates, 3-oxobutanoates etc.), isocyanoacetates, pyrazolones etc. have been examined as nucleophile in the Mannich reaction.

After transformation to their carbamate protected ketimines **55**, potential of isatin has been benefited in Mannich reactions as well. Examples of Mannich, vinylogous Mannich and domino Mannich/cyclization reactions utilizing squaramides **51**-**54** are given in Scheme 10. In 2014, dihydrofurans **61** were synthesized by the Mannich reaction of 4-bromo-3-oxobutanoates **60** with

ketimines **55** in the presence of only 1 mol% bifunctional squaramide **52**.[40] Although the reaction yield was low when organocatalyst was used solely, additive base sodium carbonate as HBr scavenger triggered cyclization step to afford products in high yield and excellent enantioselectivity (90-97% yield, 92-98% ee).

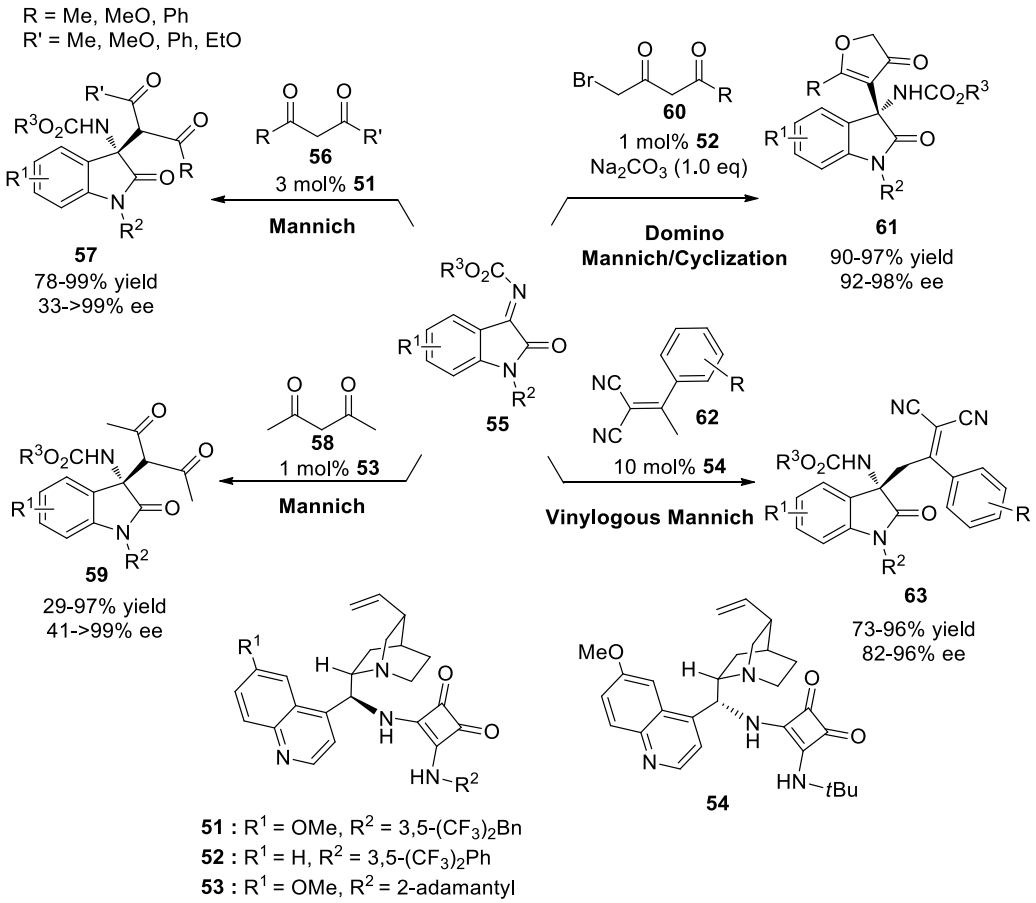

Scheme 10 Asymmetric organocatalytic Mannich reactions of isatin-derived ketimines.

Later, Zhu et al. demonstrated the vinylogous Mannich reaction of α,α-dicyanoolefins **62** with the same electrophile.[41] Cinchona alkaloid-derived *tert*-butyl substituted organocatalyst **54** lead to 3,3'-substituted oxindoles **63** again in high yields (73-96%) and enantiopurity (82-96% ee) (Scheme 10).

Then Trivedi[42] and our group[43] examined the squaramide catalyzed Mannich reaction of isatin ketimines with 1,3-dicarbonyls **56**. Although the substrate scope of the former study was limited to *N*-Boc protected ketimines, different *N*-alkoxycarbonyl protecting groups have been tolerated by sterically hindered 2-adamantyl substituted squaramide **53** with very low (1 mol%) catalyst loading. Reaction proceeded smoothly with acetylacetone (**58**) and stereoselectivity up to greater than 99% ee was attained in adducts **59** (Scheme 10).

Besides synthetically valuable properties of organic azides, α-azido ketones, special subclass within the azides, have enhanced acidity which offers C-C bond forming potential. To the best of our knowledge, since α-azido ketones have not been explored in Mannich reaction previously, their reactivity with isatin-derived ketimines has been investigated as a part of this thesis study.

1.5 α-Chiral Azides

Organic azides are valuable synthons in organic synthesis. Due to their different mesomeric structures, they reveal diverse chemical reactivity. Their facile decomposition to nitrene and nitrogen can be attributed to the dipolar structure **II** given in Figure 10. Moreover, whereby resonance structure **III**, their regioselective 1,3-dipolar cycloaddition with both nucleophiles and electrophiles is not surprising (nucleophiles attack on N3, while electrophiles are attacked by N1).[44]

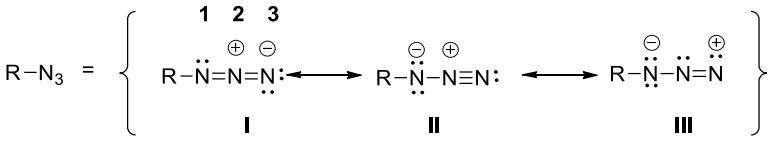

Figure 10 Resonance structures of azido group.

Among organic azides, α-chiral azides constitute a special subclass with a mask of chiral amino functionality. Furthermore, they undergo various synthetic transformations such as reduction, aza-ylide formation, cycloaddition and so on (Figure 11).[44] Nitrenes, generated from azides by thermolysis or photolysis, are uncharged, monovalent carbene analogues presenting similar reaction patterns such as C-H insertion, cycloaddition, Curtis and Hoffmann rearrangements. Staudinger reaction of organic azides with phosphines is a mild tool for the synthesis of aza-ylides which are reactive through carbonyl compounds to enable imine synthesis (aza-Wittig reaction).[45]

Among the reactions of organic azides as being good 1,3-dipoles, especially metal catalyzed azide-alkyne coupling leading to 1,2,3-triazoles have great importance in medicinal chemistry. Due to their strong dipole moments, these motifs are effective amide surrogates. Their physical properties such as hydrogen bond formation, dipole-dipole and π-stacking interactions makes triazoles important in medicinal chemistry as they readily bind with biological target.[46]

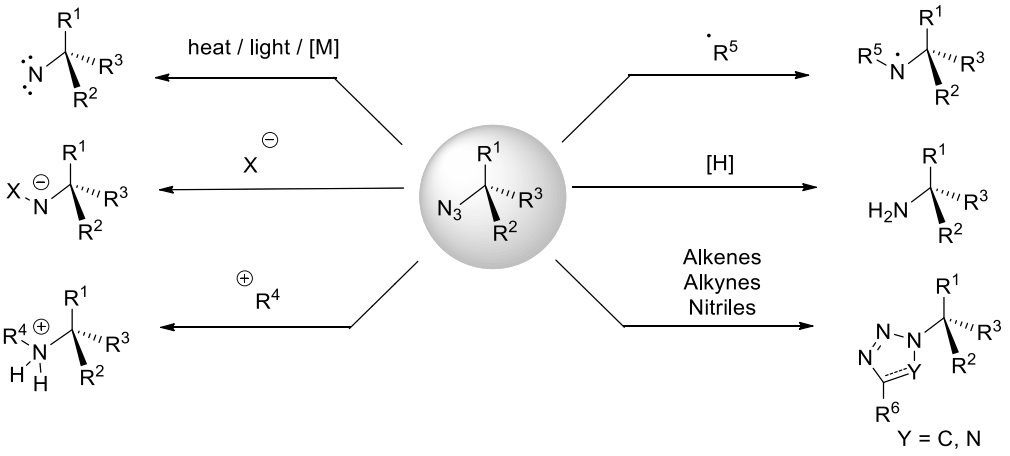

Figure 11 Synthetic transformations of α-chiral azides.

1.5.1 Strategies for α-Chiral Azide Synthesis

Even though α-chiral azides have already been efficiently used for the total synthesis of natural products and pharmacophores for years, generally chiral starting materials are chosen as precursor. Therefore, development of new asymmetric methodologies is still in demand. There are three major strategies furnishing α-chiral azides as given in Figure 12: (a) nucleophilic azidation, (b) electrophilic azidation and (c) functionalization. As a result of small size of the azido group, ensuring enantiofacial discrimination becomes difficult in nucleophilic and electrophilic azidation.[44] In organocatalytic approaches, functionalization of achiral azides is much more preferable mainly due to three reasons: (i) with azido moiety introduced in advance, improvement of stereocontrol might be more attainable; (ii) diversity of organic azides expands the limits of reaction types as well; (iii) mild reaction conditions of asymmetric organocatalysis reduces the decomposition of unstable azido group.

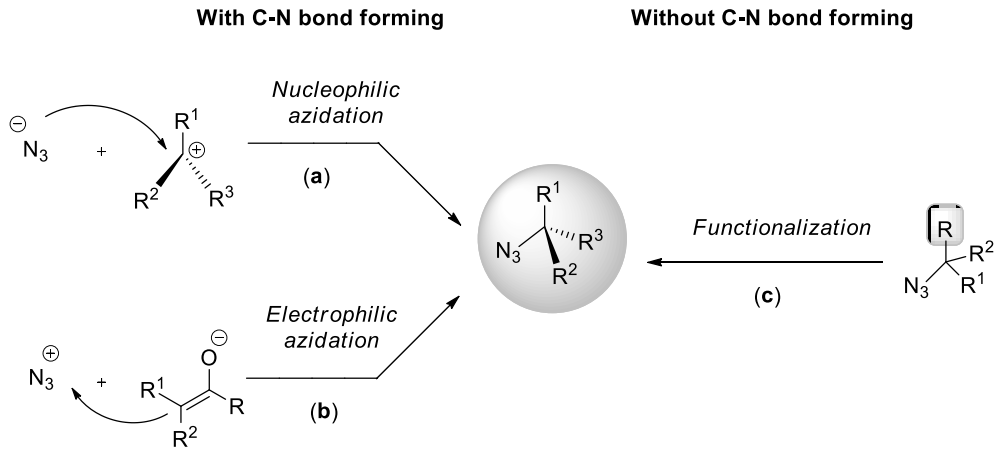

Figure 12 Current strategies furnishing α-chiral azides.

1.6 Aim of the Study

The main objective of this thesis study is enantioselective synthesis of 2-oxindole derived α-tertiary amines having wide applicability in medicinal chemistry and total synthesis of natural products. As being encouraging synthons for the generation of stereochemically and architecturally complex 2-oxindole fused spiro-heterocycles, development of new stereoselective approaches for 2-oxindole derived α-chiral amines was aimed. For both activation of the substrates and chiral induction, chiral bifunctional organocatalysts were preferred. After a careful examination of the literature, it was discovered that steric influence of the substituents on squaramides, a special class of H-bond donor organocatalysts, had been underestimated because mostly the acidity of N-H protons was focus of interest. Therefore, initially, new quinine-based squaramides **64** with bulky hydrocarbon substituents were designed in order to examine their potential in the subsequent asymmetric transformation of isatin ketimines (Figure 13).

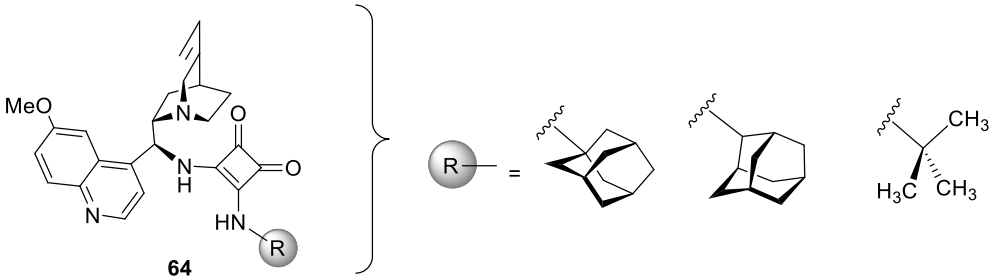

Figure 13 Targeted new bulky hydrocarbon substituted quinine-derived squaramides.

In the second part of the study, besides the known H-bond donor/Brønsted base bifunctional organocatalysts, newly synthesized derivatives would be utilized in the asymmetric organocatalytic aza-Friedel-Crafts reaction of *N*-protected isatin ketimines **65** with 1-naphthol (**42**). Among diverse synthetic transformations that ketimines show reactivity, aza-Friedel-Crafts reaction was preferred with the anticipation of converting the resulting 1,3-aminonaphthols **66** to aforementioned

spiro-heterocycles bearing 2-oxindole unit **67**. In continuation of this strategy, adduct **66** would be transformed into representative 1,4-naphthoxazepine **67** (Scheme 11).

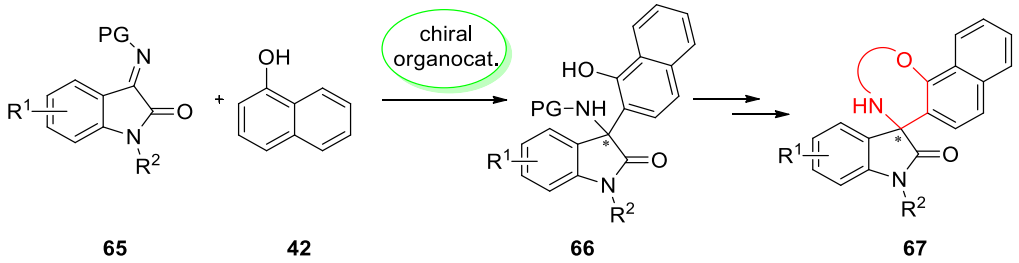

Scheme 11 Synthetic route for asymmetric aza-Friedel-Crafts reaction.

In the last part, aiming the stereoselective synthesis of alternative precursor for 2-oxindole fused spirocycles, a new strategy based on 2-azido ethanamine functionality was implemented. Inspired from the results of our preliminary study[47] on the asymmetric aldol addition of α-azido ketones **68**, whose asymmetric organocatalytic reactions had not been discovered previously, we would like to investigate their Mannich reaction with isatin ketimines **65**, as well (Scheme 12). In addition to generation of α-chiral azido ketones **69** by functionalization of achiral starting materials, these enantioenriched α-chiral azides would bring about a masked amino functionality. With two contiguous stereogenic centers in hand, compound **69** would be converted to spiro-cyclic urea as an illustrative of target compound **71**. Moreover, the 1,3-dipolar potency of azido functionality was going to be evaluated to obtain 1,2,3-triazole **70** (Scheme 12).

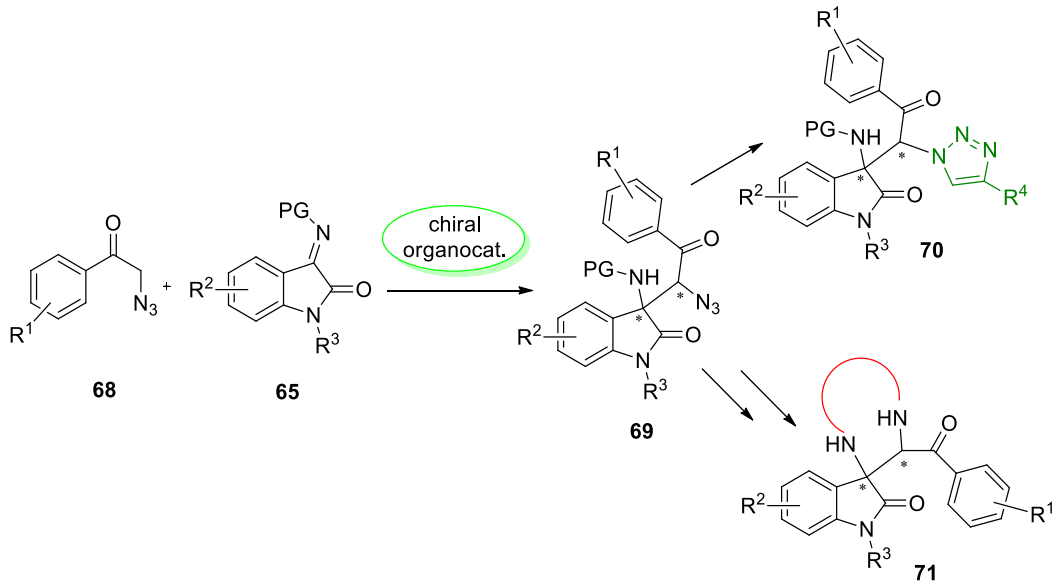

Scheme 12 Synthetic route for asymmetric Mannich reaction.

CHAPTER 2

RESULTS AND DISCUSSION

2.1 Synthesis of Bifunctional Squaramides

Literature survey on quinine-derived squaramides showed that mainly CF_3-substituted aryl squaramides endowed with high N-H acidity had been widely utilized in asymmetric organocatalytic applications.[48]

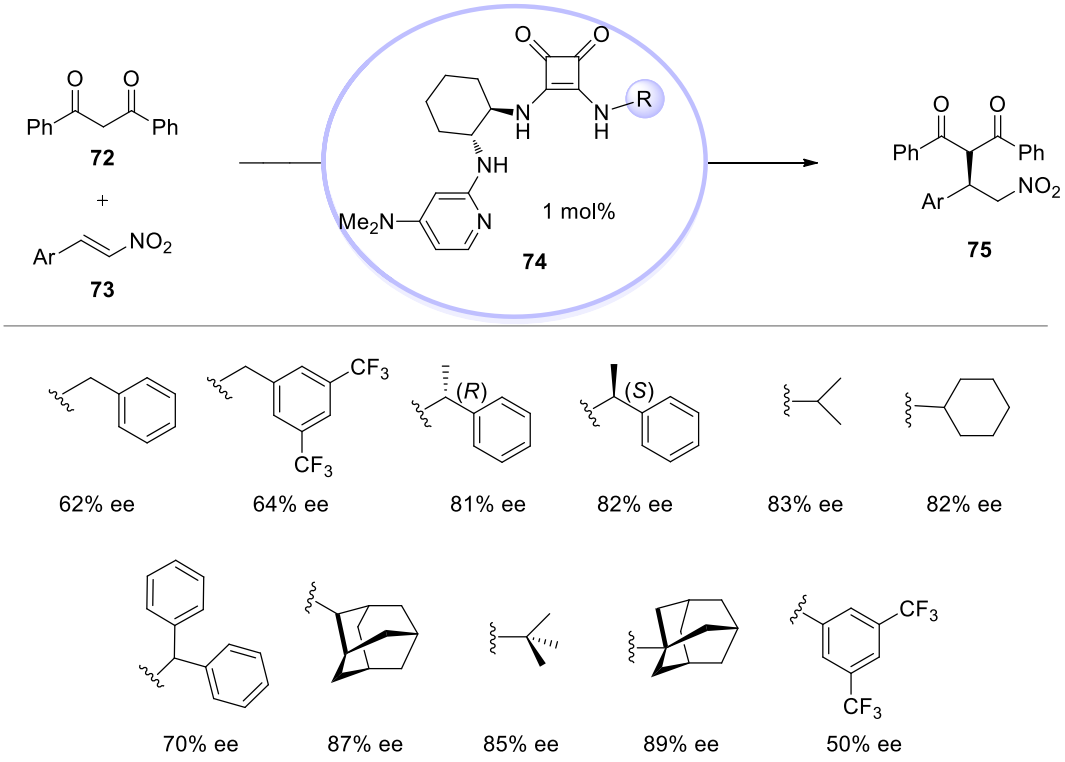

Scheme 13 Catalyst tunning on squaramido moiety.

Previously, our group had reported a study examining the effects of different aryl and alkyl substituents of 2-aminoDMAP based squaramide organocatalyst **74** on dibenzoylmethane (**72**) addition to trans-β-nitroalkenes **73**.[49] Set by set modulation of R-substituent through electronic and steric factors brought about diverse outcomes in the enantioselectivity and highest results were attained with 1-adamantyl and 2-adamantyl substituents (89% and 87% ee, respectively) (Scheme 13). Inspiring from this study and the lack of sterically bulky hydrocarbon units for squaramides, we decided to synthesize 1-adamantyl, 2-adamantyl and *t*-butyl substituted quinine derived squaramides **64** according to synthetic route depicted in Scheme 14.

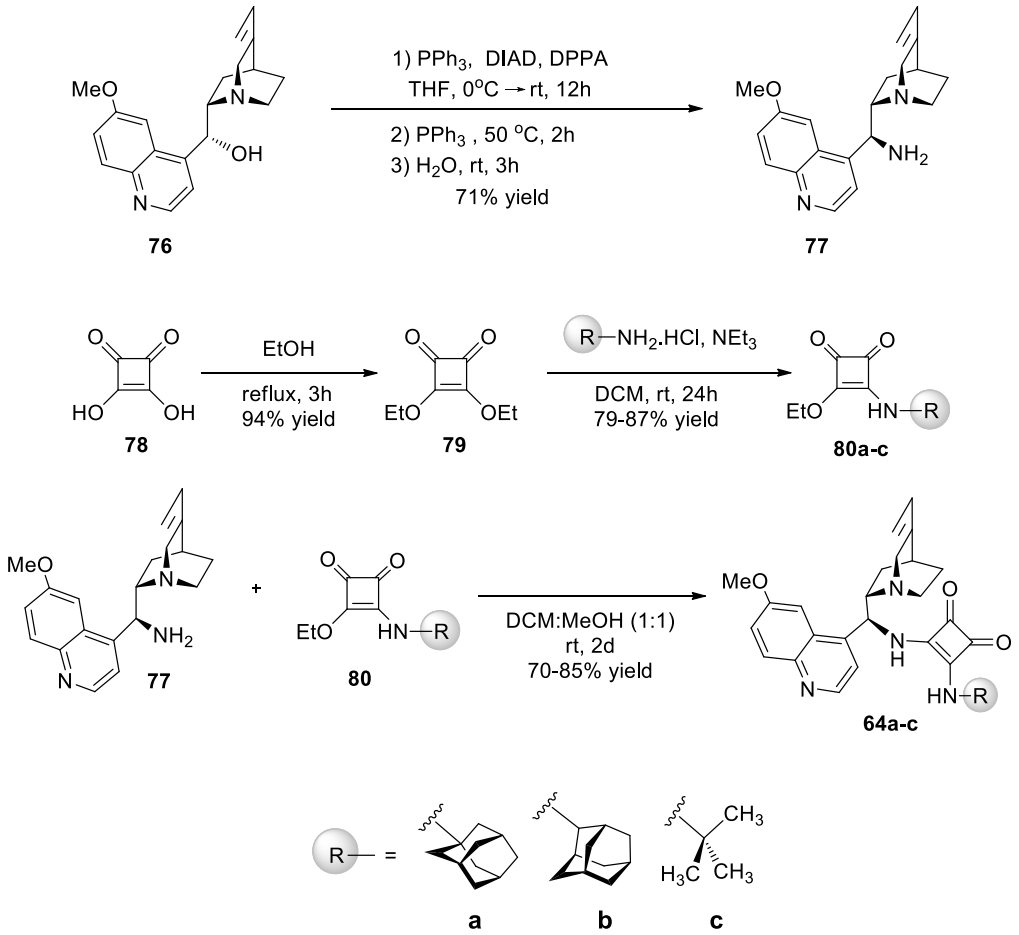

Scheme 14 Synthetic route for quinine-derived bifunctional squaramides.

In the first step, quinine (**76**) was converted into amine **77** according to Soós's one-pot procedure.[50] Upon the addition of triphenylphosphine, diisopropyl azadicarboxylate (DIAD) and diphenylphosphoryl azide (DPPA), by Mitsunobu reaction, azide intermediate formed in situ with inversion of configuration on reaction center. Later, treatment of the intermediate with triphenylphosphine generated an iminophosphane by evolution of nitrogen gas. Hydrolysis of iminophosphane afforded quinine-derived amine **77** in 71% yield (Scheme 14).

Meanwhile, for the synthesis of monosquaramide **80**, squaric acid (**78**) was converted into diethyl squarate (**79**) by refluxing in absolute ethanol for 3 hours.[51] Then adapting the procedure of Rawal and co-workers,[30b] stirring the related alkylamine (or hydrochloride salt of the amine in the presence of stoichiometric triethylamine base) with **79** at room temperature afforded monosquaramide **80**. Repeating the similar process with the amine **77** in DCM/MeOH (1:1) mixture at room temperature yielded in our quinine-derived squaramides **64** with 70-85% isolated yield for the final step (Scheme 14).

2.2 Synthesis of Starting Materials

2.2.1 Synthesis of *N*-Carbamate Protected Ketimines

Due to known facile deprotection procedures, *N*-alkoxycarbonyl moiety was preferred as protecting groups. At first, iminophosphane **83** was synthesized starting from carbazate in the presence of sodium nitrite and glacial acetic acid. After basic work-up, highly reactive acyl azide **82** was treated with triphenylphosphine which leads to formation of iminophosphane through nitrogen loss from phosphazide intermediate according to literature procedure (Scheme 15).[52] *t*-Butyl, ethyl and benzyl triphenyliminophosphane **83** were synthesized to establish the tolerance of our organocatalysts **64** toward various carbamate protecting groups. Synthesis of isatin ketimines **55** could be achieved by aza-

Wittig reaction of commercially available isatins **84** with iminophosphane reagent **83** according to literature[53] (Scheme 16).

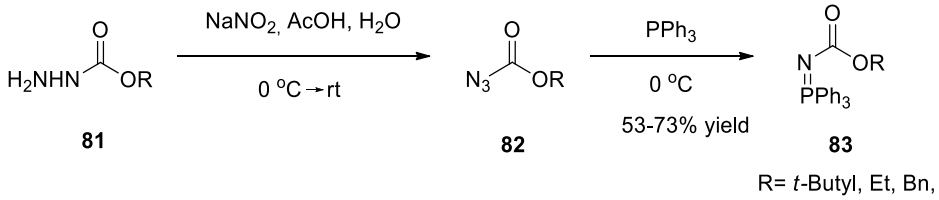

Scheme 15 Synthesis of triphenyliminophosphane reagent.

Commercially available isatin derivatives **84**, were further derivatized through by *N*-substitution of amide moiety. *N*-Alkylation, alkenylation and benzylation were achieved by using corresponding alkyl, alkenyl and benzyl halide (X = Br, I) in the presence of potassium carbonate as base. *N*-Acetylisatin **85e** was attained upon the reflux of isatin **84** in acetic anhydride. For the synthesis of *N*-Boc isatin **85f**, isatin was treated with di-*tert*-butyl dicarbonate (Boc_2O) and 4-dimethylaminopyridine (DMAP). Later aza-Wittig reaction of all *N*-substituted and unsubstituted isatin derivatives **84** with triphenyliminophosphane reagent **83** yielded in isatin derived ketimines **55** (70-95% yield) (Scheme 16).

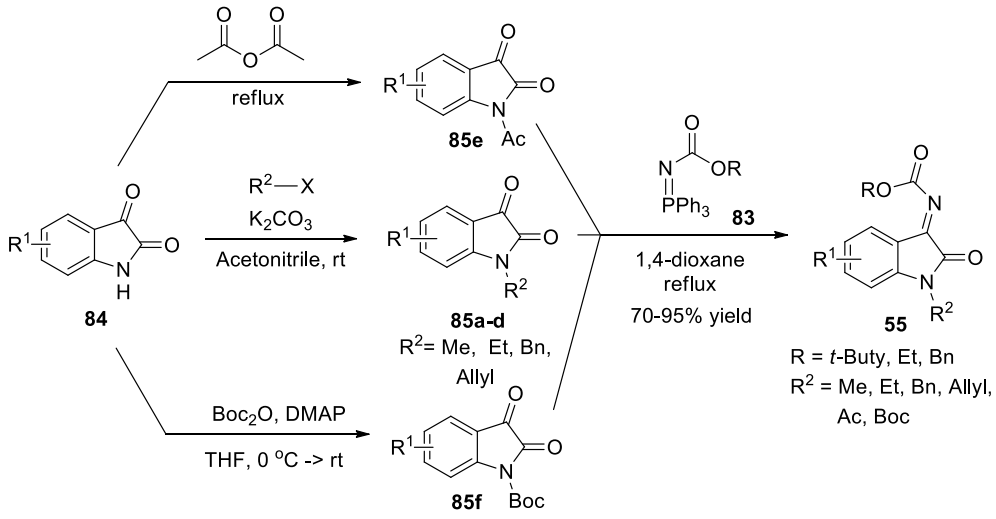

Scheme 16 *N*-Substitution of isatin and subsequent ketimine synthesis**.**

20 Derivatives of isatin ketimine with different substituents on amide nitrogen, aromatic ring and carbamate protecting groups (Boc, Cbz and ethoxycarbonyl) were synthesized according to above mentioned protocol. Isolated yields of 20 isatin-derived ketimines **55a-t** are depicted in Table 1.

Table 1 Synthesized *N*-carbamate protected ketimines.[a]

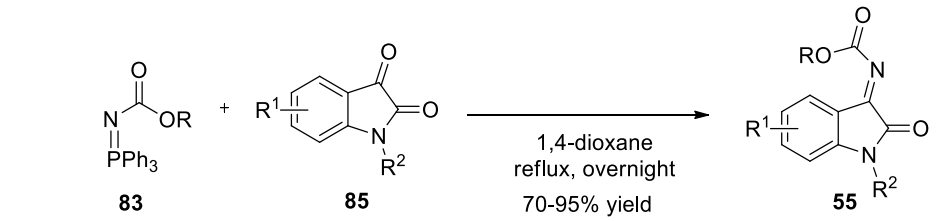

83 **85** **55**

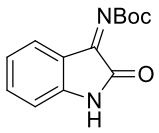	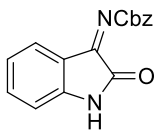	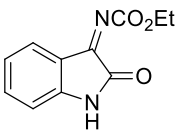	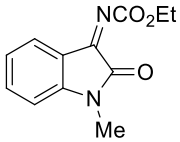	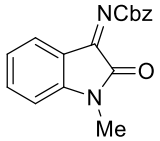
55a 80% yield	**55b** 70% yield	**55c** 85% yield	**55d** 78% yield	**55e** 70% yield
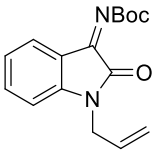	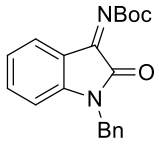	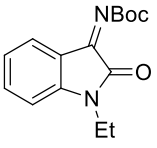	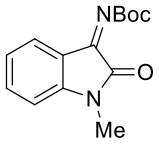	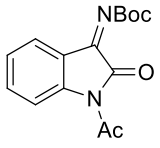
55f 90% yield	**55g** 93% yield	**55h** 90% yield	**55i** 95% yield	**55j** 80% yield
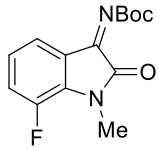	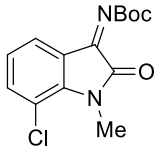	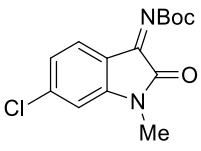	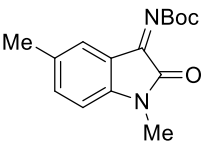	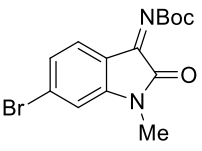
55k 93% yield	**55l** 91% yield	**55m** 95% yield	**55n** 93% yield	**55o** 93% yield
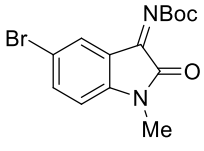	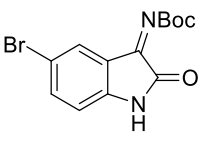	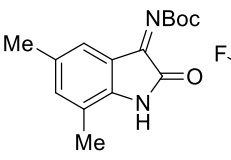	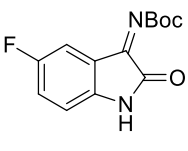	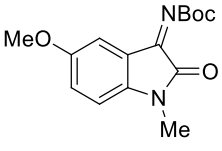
55p 78% yield	**55q** 83% yield	**55r** 70% yield	**55s** 87% yield	**55t** 90% yield

[a]Isolated yields.

2.2.2 Synthesis of α-Azido Ketones

Initially, cyclic α-bromo chromanone, thiochromanone, indanone and tetralone (**87a**,**b** and **90a**,**b**) could be obtained by bromination of chromanone (**86a**), thiochromanone (**86b**), indanone (**89a**) and tetralone (**89b**) prior to azidation. Although stoichiometric amount of bromine was used in bromination step at decreased reaction temperature, formation of α,α-dibromoketone (**88** and **91**) could be avoided only to some extent (Scheme 17).

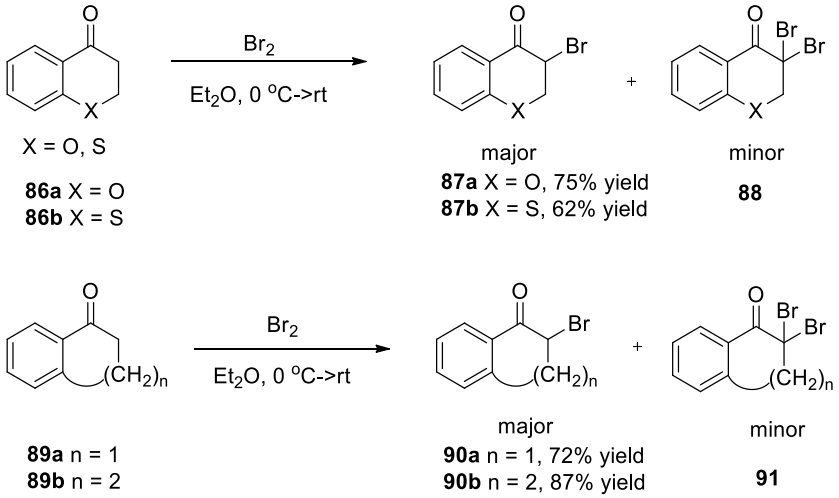

Scheme 17 Synthesis of α-bromo ketones as α-azido ketone precursors.

In order to synthesize α-azido ketones **93**, nucleophilic substitution of α-bromo ketone precursors **92** was utilized. Acyclic α-azido ketones **93a-j** were synthesized from commercially available 2-bromoacetophenones **92** (Table 2). Following the general procedure given in the experimental part, 2-bromoketones **92** were treated with excess sodium azide in acetone to obtain α-azido ketones **93** as nucleophile of the further Mannich reaction. To the best of our knowledge, synthesis of **90a** and **90b** from their brominated precursors had not been reported so far. Synthesized α-azido ketones **93** are shown in Table 2. Except for **93k** and **93m**, as long as they are stored at cold and in amber bottles, they can be used for months without decomposition.

Table 2 Synthesized α-azido ketones.

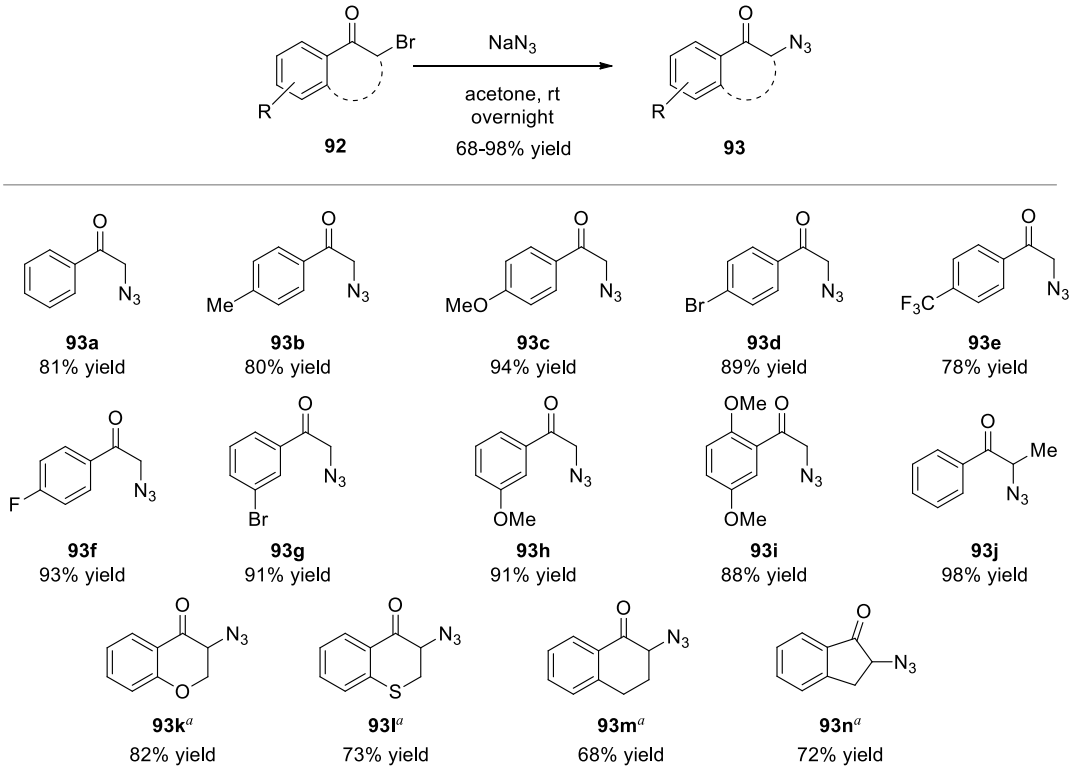

[a]Additional to the given reaction conditions, 18-crown-6 (20 mol%) was used.

Besides the chromatographic indicators, chemical shifts of α-proton on ^{1}H NMR spectra were decisive on the substitution of bromine with azide. As an illustrative example, ^{1}H NMR spectrum of **90a** and **93n** were depicted in Figure 14. Apparently, while the α-proton of bromo substituted ketone **90a** resonates at lower field with 4.58 ppm as doublet of doublet, upon the replacement with azido group, that signal of **93n** shifts to higher magnetic field (4.25 ppm).

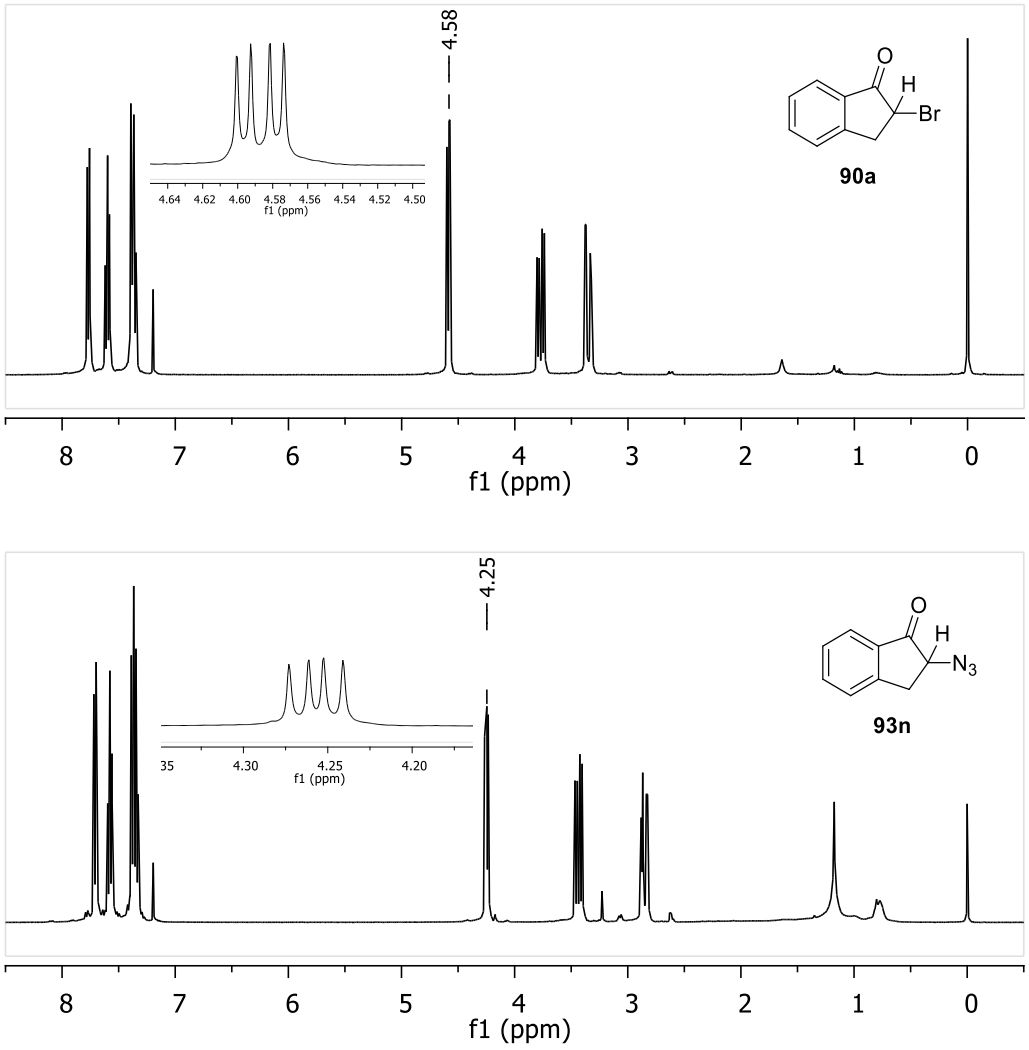

Figure 14 ^{1}H NMR spectrum of α-bromo and α-azido indanone.

2.3 Asymmetric Aza-Friedel-Crafts Reaction

2.3.1 Optimization of Reaction Parameters for Aza-Friedel-Crafts Reaction

In order to achieve our goal on the asymmetric synthesis of 2-oxindole bearing 1,3-aminonaphthols, we firstly surveyed squaramides **74a**, **74b**, **64a-d**, as well as quinine-based (thio)urea bifunctional organocatalysts **94a** and **94b**, respectively in the model reaction (Table 3). Although aza-Friedel-

Crafts reaction of isatin-derived ketimine **55a** (1 eq) with 1-naphthol (**42**) (1.1 eq) afforded adduct **95a** in good yield with 2-aminoDMAP cored squaramides **74a** and **74b**, it was almost racemate (Table 3, entries 1 and 2). When quinine-derived squaramides **64a-d** were compared with thiourea and urea counterparts (**94a** and **94b)**, the former category revealed superior performance in terms of stereoselectivity (entries 3-8). It is important to note that CF_3-substituted aryl quinine-derived squaramide catalyst **64d**, which has been commonly utilized in the literature, dragged behind our newly introduced organocatalyst **64b** in terms of enantiopurity (70% ee, 90% ee, respectively, entries 4 and 6). Background reaction with no catalyst led to adduct *rac*-**95a** with 61% yield in 24 hours (entry 9). Considering the reaction duration and chemical yields obtained by catalysts **64a-d** and **94a**,**b** (entries 3-8) it can be claimed that bifunctional H-bond donor/Brønsted base catalysts activate the substrates so that higher amount of adducts was handled in a shorter time than the background reaction, in overall (entry 9). Furthermore, ending up with racemic mixture of **95a** in the uncatalyzed reaction is indicative of organocatalysts' being the sole chiral induction source. Among the quinine-derived squaramides **64a-d**, as the most encouraging class of organocatalysts, **64b** would be organocatalyst of choice with 90% ee and excellent yield.

Table 3 Optimization studies for asymmetric aza-Friedel-Crafts reaction.

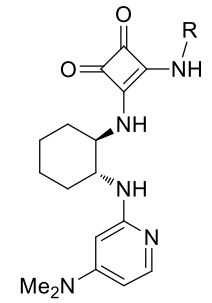

R = 1-adamantyl (**74a**)
2-adamantyl (**74b**)

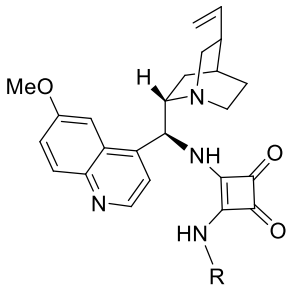

R = 1-adamantyl (**64a**)
2-adamantyl (**64b**)
t-butyl (**64c**)
3,5-bis(trifluoromethyl)phenyl (**64d**)

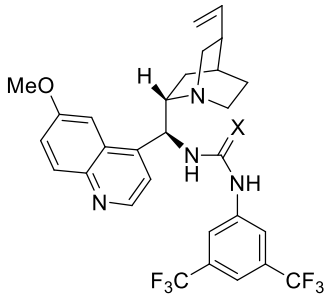

X = S (**94a**)
O (**94b**)

Table 3 Continued.[a]

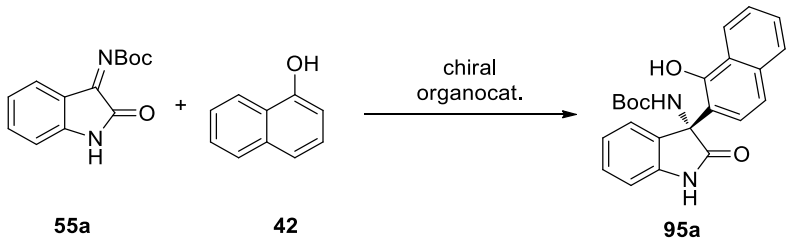

55a **42** **95a**

Entry	Catalyst	Solvent	Cat. loading (mol%)	T (°C)	Time (h)	Yield (%)[c]	ee (%)[d]
1[b]	**74a**	DCM	5	r.t.	60	68	8
2[b]	**74b**	DCM	5	r.t.	60	94	7
3	**64a**	DCM	5	r.t.	19	71	60
4	**64b**	DCM	5	r.t.	16	99	90
5	**64c**	DCM	5	r.t.	19	60	60
6	**64d**	DCM	5	r.t.	13	98	70
7	**94a**	DCM	5	r.t.	19	71	44
8	**94b**	DCM	5	r.t.	19	81	21
9	No cat.	DCM	-	r.t.	24	61	rac
10	**64b**	DCM	2	r.t.	18	99	89
11	**64b**	DCM	1	r.t.	19	40	6
12	**64b**	$CHCl_3$	2	r.t.	26	90	20
13	**64b**	THF	2	r.t.	46	43	70
14	**64b**	CH_3CN	2	r.t.	26	70	47
15	**64b**	Dioxane	2	r.t.	46	32	52
16	**64b**	DCM	2	0	26	97	86
17	**64b**	DCM	2	-20	18	98	97
18	**64b**	DCM	2	-40	46	75	89

[a]Reaction conditions: 1-naphthol (**42**) (0.055 mmol, 1.1 eq), isatin ketimine **55a** (0.050 mmol, 1 eq), catalyst, solvent (0.5 mL), 25mg 4Å molecular sieve. [b]Opposite enantiomer. [c]Isolated yields. [d]Determined by HPLC with chiral stationary phase.

Decrement of catalyst loading from 5 mol% to 2 mol% lead to no explicit change in yield, stereoselectivity and reaction time as well (Table 3, entries 4 and 10). Hence, for the sake of atom economy, 2 mol% of **64b** was preferred for the further trials. Neither yields nor enantiopurity increased upon examination of other solvents (chloroform, THF, acetonitrile and dioxane) (entries 12-15).

Among the decreased reaction temperatures (entries 16-18), -20 ˚C brought about **95a** in excellent yield and satisfactorily high enantioselectivity (97% ee) with no significant elongation in reaction time. Consequently, as the optimal condition, 1 eq of ketimine **55**, 1.1 eq of 1-naphthol (**42**), 2 mol% organocatalyst **64b** and 25 mg 4Å molecular sieve were used in DCM (0.5 mL) at -20 °C.

2.3.2 Scope of Aza-Friedel-Crafts Reaction

In order to investigate the scope of the reaction, various *N*-carbamate protected ketimines **55** were treated with 1-naphtol (**42**) under optimized condition. Initially, protecting group tolerance of the catalysts was tested by using Cbz and $–CO_2Et$ alkoxycarbonyl units additional to *tert*-butoxycarbonyl (Boc) (Table 4, **95a-c**). It is obvious that the catalyst **64b** is compatible with other carbamate protective groups so that high enantioselectivities (97-99% ee) could be obtained in **95b** and **95c**. Additionally, *p*-methoxyphenyl (PMP) protected isatin ketimine was also tested in the reaction; however, no product was attained in this situation. It can be inferred that carbamate group is crucial in the activation mode of the squaramide **64b**. Later, reactivity of *N*-substituted isatin-derived ketimines with Boc protecting group were investigated (Table 4, **95d-g**). Good to excellent enantioselectivity was obtained with ethyl, methyl and benzyl substituents (94-99% ee) whereas, *N*-acetyl substituted adduct **95g** was almost racemic mixture. Presumably, coordination of the squaramide protons with the carbonyl moiety of the acetyl part overrides desired selective substrate binding through imine moiety. Next, various isatin-derived 1,3-aminonaphthols (**95h-j**, **95m-t**) with electron donating and withdrawing groups on the benzene ring and the naphthol were synthesized similarly. Except for **95h**, excellent outcomes in terms of enantiomeric excess (92->99%) and yield (67-98%) were attained. According to the results, electronic character of the substituents do not have significant role on stereoselectivity. In the scale up study of **95e**, 3 mmol isatin-derived ketimine **55g** afforded product in 85% yield with the same enantiomeric excess (99%).

Table 4 Scope of aza-Friedel-Crafts reaction with 1-naphthols **42**.[a]

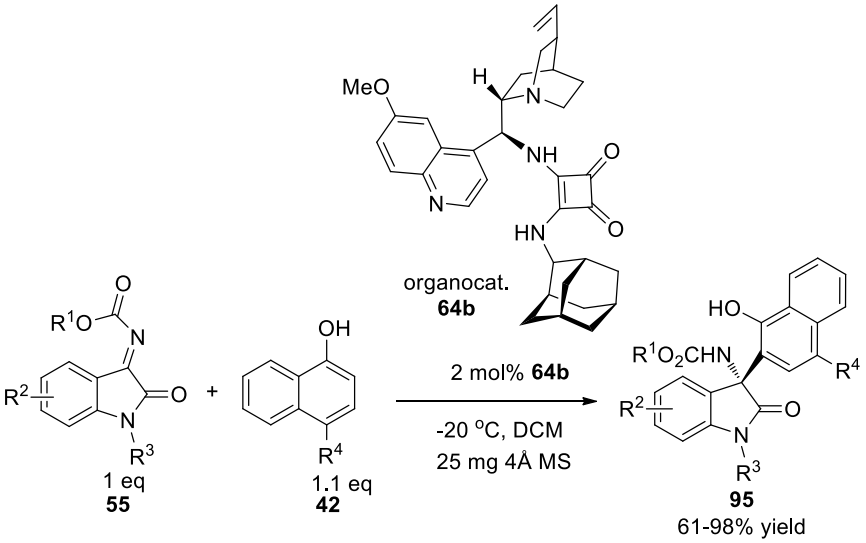

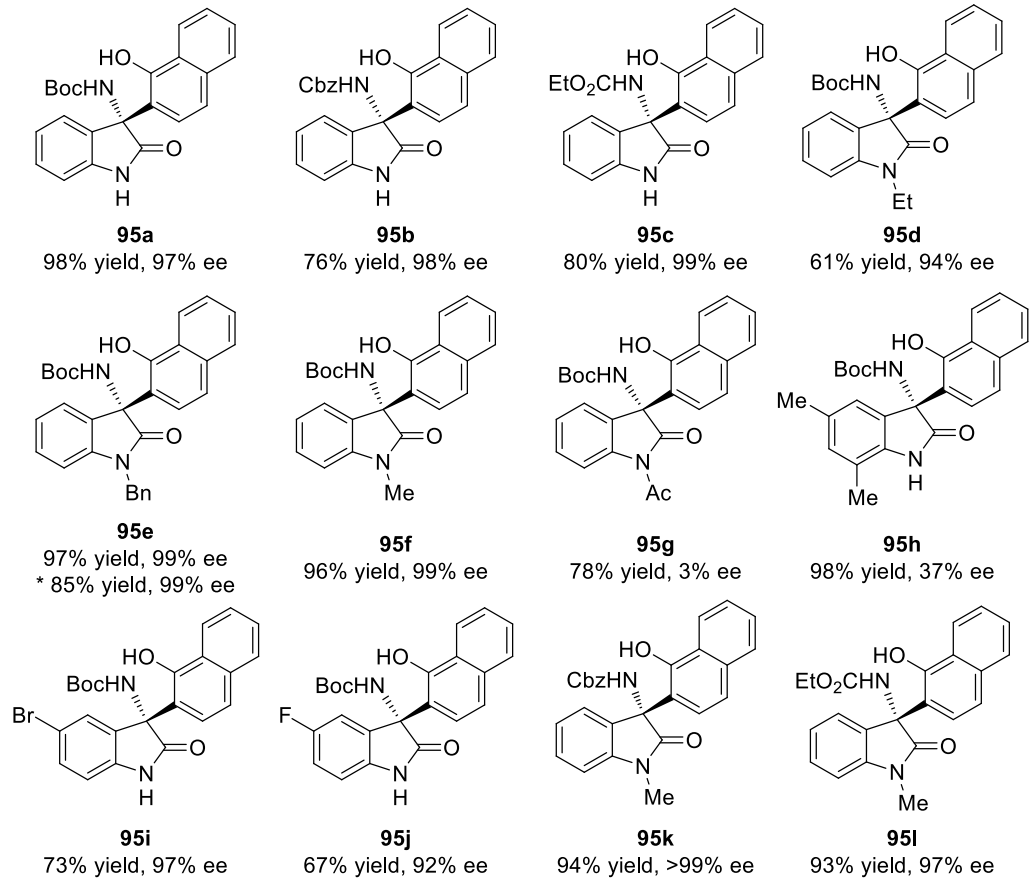

[a]Reaction conditions: **42** (0.11 mmol), isatin ketimine **55** (0.1 mmol), catalyst **64b** (2 mol%), DCM (1.0 mL), 25 mg 4Å molecular sieve, -20˚C. *Reaction was carried out with 3 mmol isatin ketimine.

Table 4 Continued.[a]

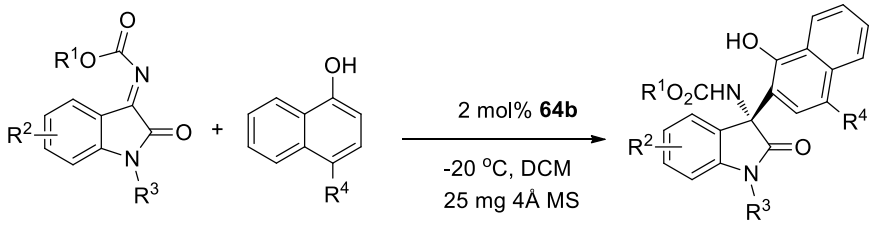

55
1 eq

42
1.1 eq

95
61-98% yield
up to >99% ee

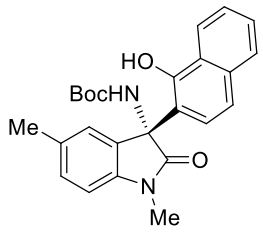

95m
98% yield, 97% ee

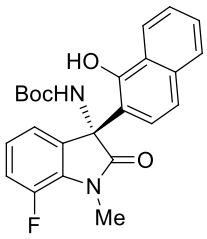

95n
94% yield, >99% ee

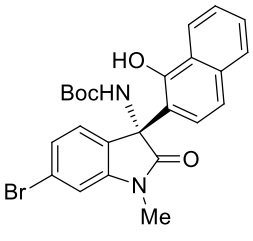

95o
70% yield, 99% ee

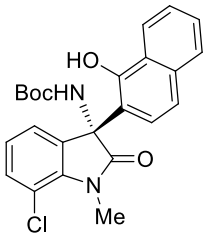

95p
90% yield, 99% ee

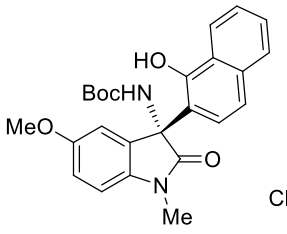

95q
96% yield, 98% ee

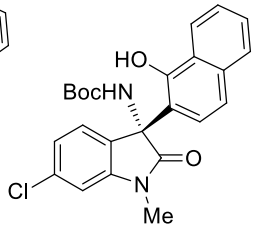

95r
90% yield, 99% ee

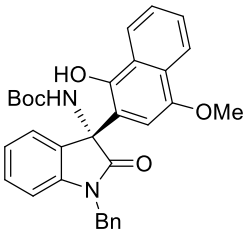

95s
96% yield, 91% ee

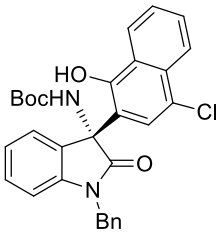

95t
74% yield, 99% ee

[a]Reaction conditions: **42** (0.11 mmol), isatin ketimine **55** (0.1 mmol), catalyst **64b** (2 mol%), DCM (1.0 mL), 25 mg 4Å molecular sieve, -20˚C.

As an illustrative example; ^{1}H and ^{13}C NMR spectra of compound **95f** are given in Figures 15 and 16, respectively. The most decisive signal in ^{1}H NMR spectrum belongs to –NH proton resonating as broad singlet at 5.66 ppm and newly formed quaternary carbon atom resonating at 66.0 ppm in ^{13}C NMR spectrum. Additionally, phenolic hydroxyl proton appears as broad singlet at 10.78 ppm. *N*-Me and *t*-butoxy methyl protons give singlet at 3.14 and 1.19 ppm, respectively. Also 10 aromatic protons are observed in the range of 6.60-8.60 ppm. Amide (-N-

C=O) and carbamate (-N-CO-O-) carbonyls resonate at 179.5 and 154.1 ppm, respectively in ^{13}C NMR spectrum (Figure 16). While aliphatic carbon atoms of methyl groups resonate at 26.7 and 28.0 ppm, ipso carbon of *t*-butoxy group at 80.5 ppm. Phenolic ipso carbon atom is observed at the lowermost field of the aromatic region with chemical shift 153.9 ppm. Other ipso aromatic carbons are at 143.4, 134.7, 129.3 and 126.9 ppm. Also there are 10 aromatic CH- carbon atoms.

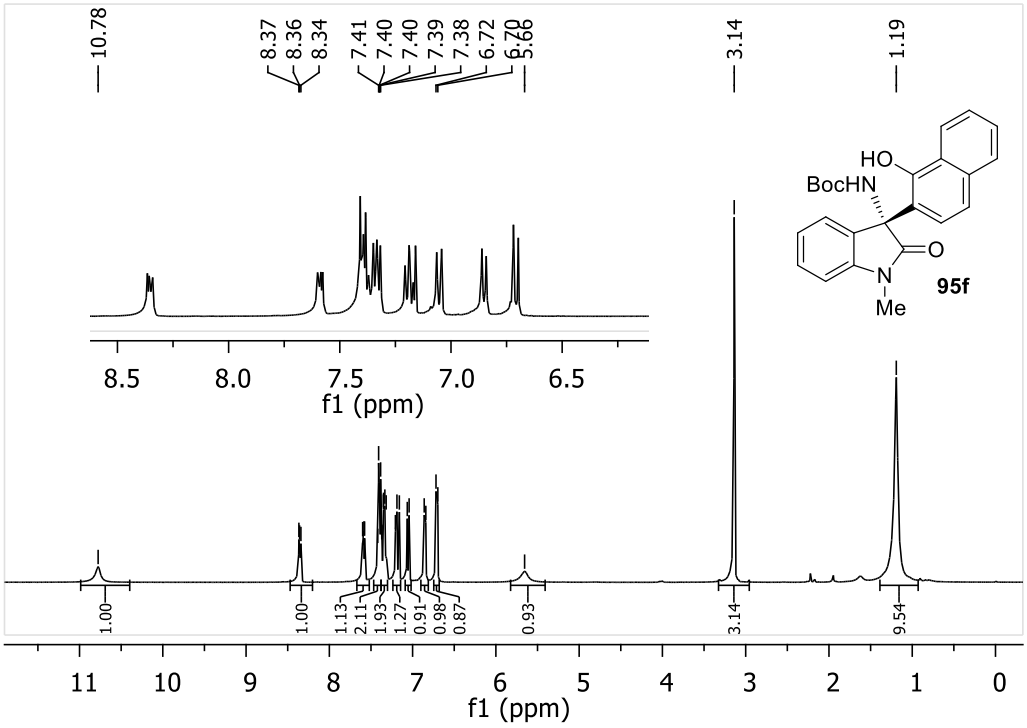

Figure 15 ^{1}H NMR spectrum of **95f**.

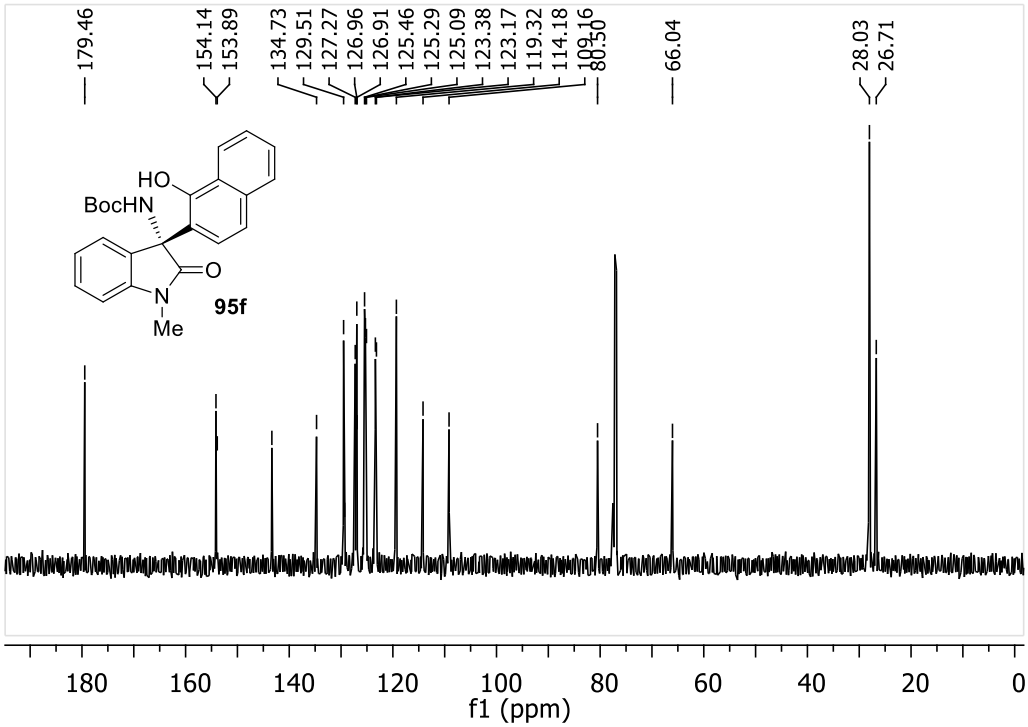

Figure 16 ^{13}C NMR spectrum of **95f**.

Hereafter, scope of the reaction with 2-naphthol (**47**) was explored (Table 5). Reaction proceeded also well with 2-naphthols **47** in the presence of 2 mol% bifunctional squaramide **64b** to give 1,3-aminonaphthols **96** in good yields (76-99%) and moderate to high enantioselectivity (54-97% ee).

Table 5 Scope of aza-Friedel-Crafts reaction with 2-naphthols **47**.[a]

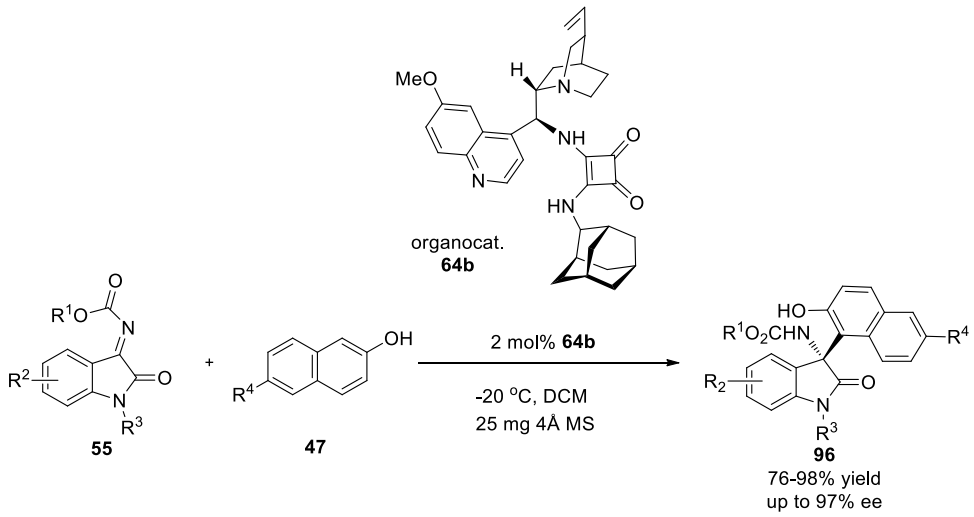

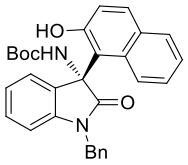

96a
98% yield, 97% ee

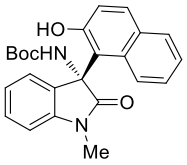

96b
85% yield, 79% ee

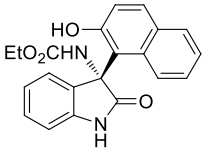

96c
76% yield, 73% ee

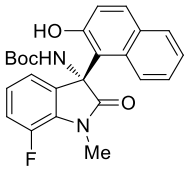

96d
95%yield, 95% ee

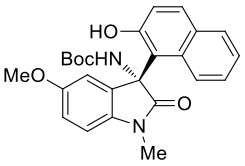

96e
86% yield, 85% ee

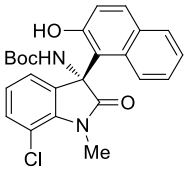

96f
97% yield, 91% ee

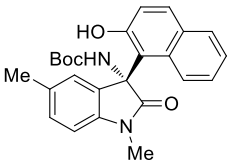

96g
98% yield, 54% ee

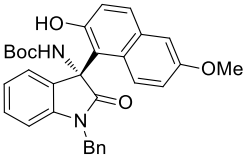

96h
97% yield, 97% ee

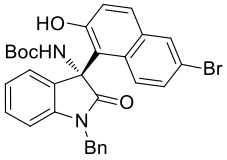

96i
98% yield, 93% ee

[a]Reaction conditions: **47** (0.11 mmol), isatin ketimine **55** (0.1 mmol), catalyst **64b** (2 mol%), DCM (1.0 mL), 25 mg 4Å molecular sieve, -20˚C.

To increase the synthetic efficacy, aza-Wittig and aza-Friedel-Crafts reactions were merged in one-pot-sequential protocol. After the formation of the ketimine **55g** in 1,4-dioxane, without any work-up procedure, the reaction conditions of aza-Friedel-Crafts reaction was ensured (Scheme 18). Although there was a small decrease by 5% in enantiomeric excess, this protocol was still practical and applicable.

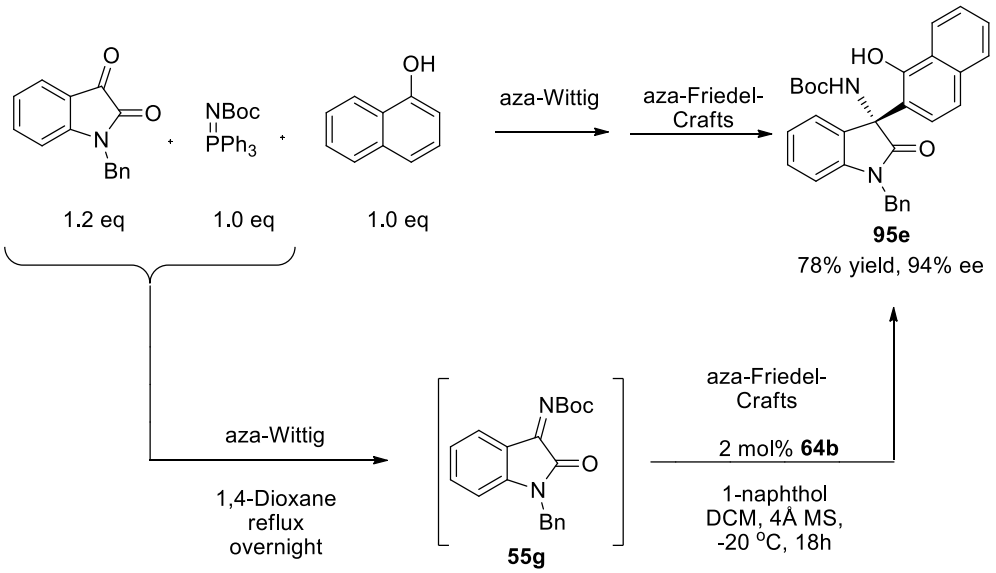

Scheme 18 One-pot sequential aza-Wittig/aza-Friedel-Crafts reaction.

Further scope of our methodology was tested with phenols **97** (Table 6). In addition to parent phenol (**97a**), activated phenols with electron donating groups were preferred due to noted lower nucleophilicity of *ortho*- carbon of phenoxide ion compared to naphthoxide. Only the trial with 4-methoxyresorcinol **97b** resulted with the desired product **98b** in 70% yield and 84% ee.

Table 6 Scope of aza-Friedel-Crafts reaction with phenols **97**.[a]

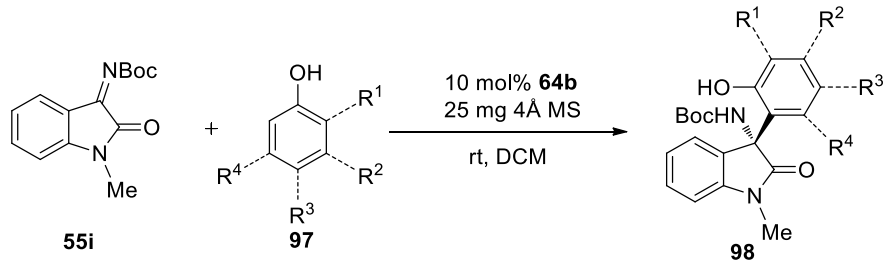

Entry	Phenol	Product	Time (h)	Yield (%)	ee (%)
1	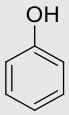 **97a**	-	72	NR	-
2	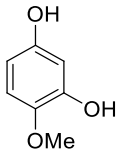 **97b**	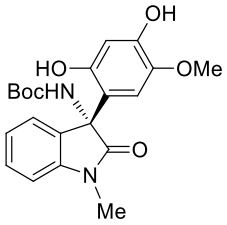 **98b**	48	70	84
3	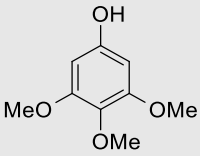 **97c**	-	72	NR	-
4	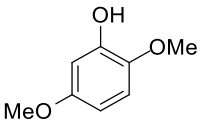 **97d**	-	72	NR	-

[a]Reaction conditions: Phenol **97** (0.11 mmol), ketimine **55l** (0.1 mmol), catalyst **64b** (10 mol%), DCM (1.0 mL), 25 mg 4Å molecular sieve, room temperature.

In this case, aza-Friedel-Crafts reaction regioselectively occurs from one of the available *ortho*- positions with reference to phenolic hydroxyl groups. The preference for **98b** was elucidated by ^{1}H NMR spectrum (Figure 15). Two singlets (H2 = 6.19 ppm, and H5 = 6.54 ppm) resonating at the upper field of the aromatic region indicates that aromatic protons of phenol are

para- to each other. Therefore, substitution occurs at sterically more available 6-position. This situation can be used to interpret the lack of any product from **97c** and **97d** having sterically more crowded *ortho*-carbons (Table 6).

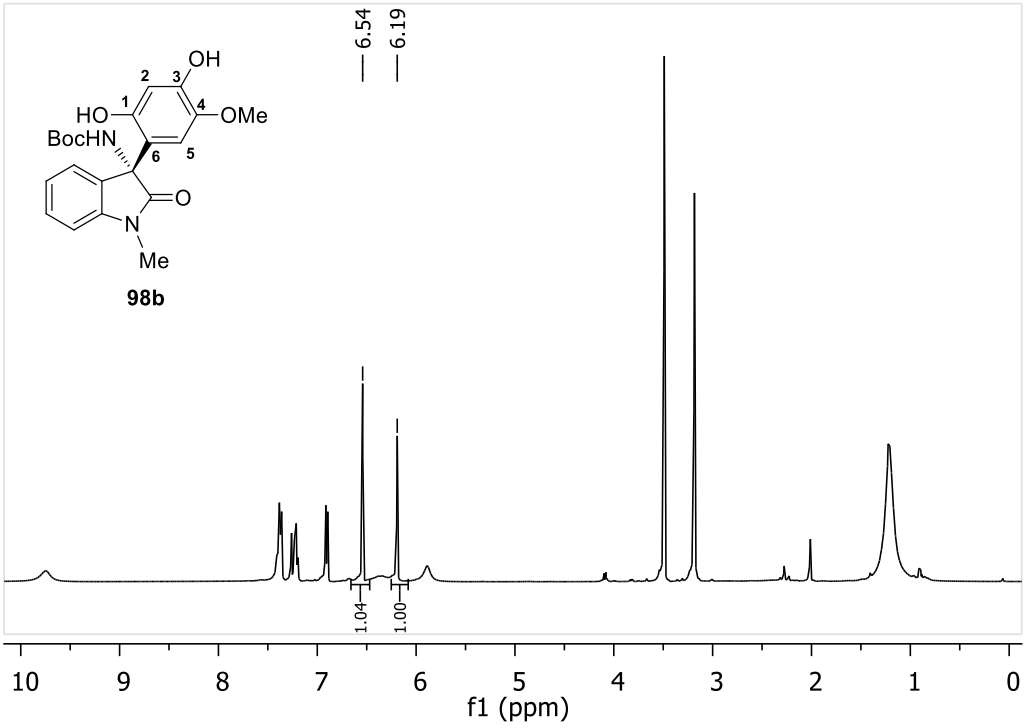

Figure 17 ^{1}H NMR spectrum of **98b**.

Absolute configuration of adduct **95e** was decided as (*R*) by comparing the retention times of the enantiomers with the literature and generalized for the others.[54] To interpret the *R*-selectivity, we proposed a transition state model shown in Figure 18. While isatin-ketimine is activated through the dual H-bonding by squaramide functionality, 1-naphthol (**42**) coordinates similarly after deprotonation by the quinuclidine ring. In such a transition state, *Si*-face of the ketimine is hindered by the sterically bulky adamantyl unit so that of the naphthoxide selectively attacks from *Re*-face to afford (*R*)-isomer exclusively.

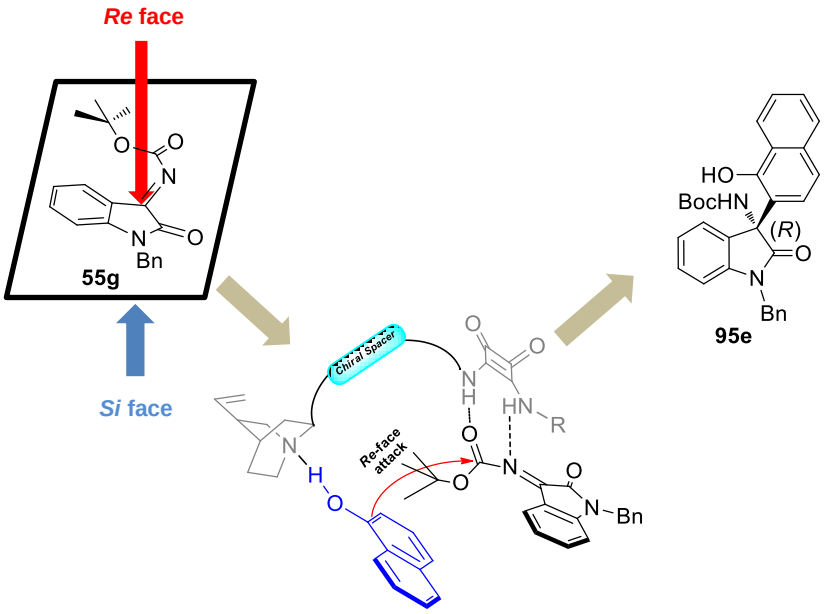

Figure 18 Proposed transition state model for aza-Friedel-Crafts reaction.

2.3.3 Representative Transformation of Enantioenriched 1,3-Aminonaphthols to Spirocycles

To demonstrate the synthetic potential of enantioenriched 3-amino-2-oxindoles as synthons for spirocycles, we used the methodology of Aggarwal and co-workers reported for annulation of 1,3-aminoalcohols to afford more challenging 7-membered heterocycles (Scheme 19).[55] By treating 1,3-aminonaphthol **95e** with 4M HCl solution in acetonitrile, free amine functionality regained with almost quantitative yield. After the formation of deprotection product **99**, reaction with bromoethylsulfonium salt **101** in the presence of sodium hydride resulted in 1,4-naphthoxazepine **100** with the conservation of the inherited enantiopurity (99% ee). Naphthoxazepine derivatives are known to have medicinal importance especially in nervous system as antidepressant[56a,b] and antipsychotics.[56c]

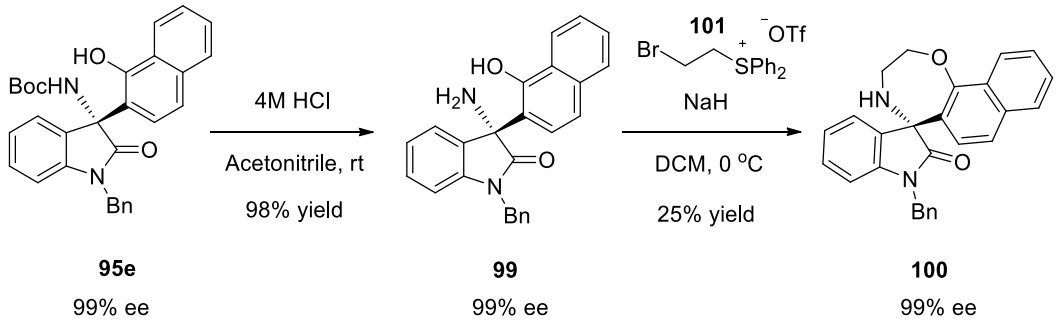

95e
99% ee

99
99% ee

100
99% ee

Scheme 19 Transformation of 1,3-aminonaphthol **95e** to 1,4-naphthoxazepine **100**.

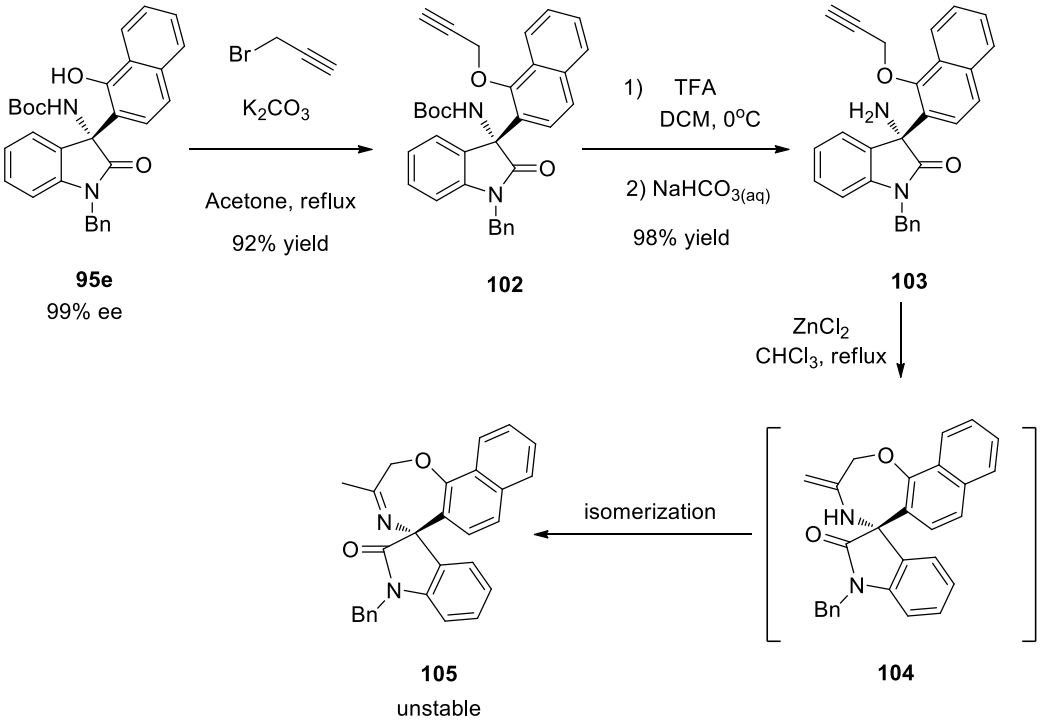

95e
99% ee

102

103

105
unstable

104

Scheme 20 $ZnCl_2$ promoted intramolecular cyclization.

Also we would like to run metal-mediated intramolecular cyclization through alkyne activation to obtain 2-oxindole fused spiro-heterocycle (Scheme 20). Therefore, initially *O*-propargylation of **95e** by using propargyl bromide and potassium carbonate was performed to obtain compound **102** in good yield. After

the deprotection of Boc-group by trifluoroacetic acid and subsequent basic work-up afforded amine **103**. Zinc chloride promoted cyclization, under reflux in chloroform, leading to compound **104** followed by isomerization yielded in cyclic imine **105**. However, 7-membered cyclic imine **105** was so unstable in solution that we could not get ^{13}C NMR spectrum which requires elongated data collection process compared to ^{1}H NMR spectroscopy. Therefore, the structure given in **105** was proposed according to ^{1}H NMR spectrum. Similarly, due to lack of stability in solution, enantiopurity of **105** could not be determined by HPLC analysis.

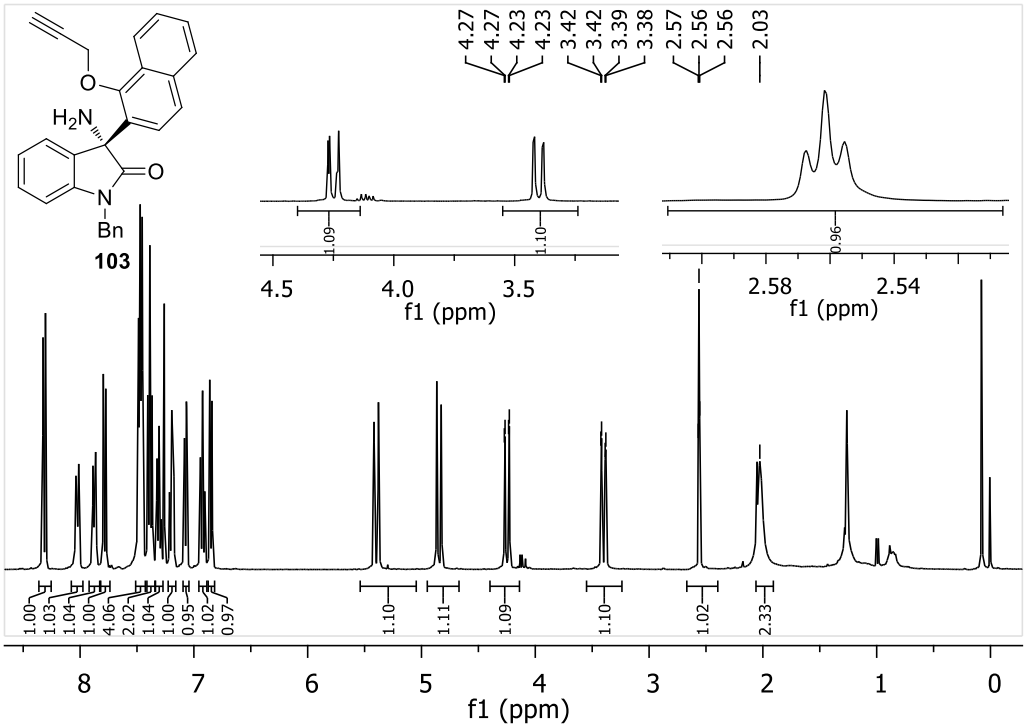

Figure 19 ^{1}H NMR spectrum of **103**.

Upon the cyclization, the triplet of propargylic –CH proton at 2.56 ppm and broad singlet of $–NH_2$ protons (2.03 ppm) observed in the ^{1}H NMR spectrum of compound **103** (Figure 19) disappears in Figure 20. Similarly, two doublet of doublets (4.25 and 3.40 ppm, Figure 19) corresponding to propargylic methylene protons and observed as a result of both geminal and allylic coupling with terminal –CH, change pattern to give two doublets at 4.99 and 4.69 ppm in

cyclized product **105** (Figure 20). Also, in the ^{1}H NMR spectrum shown in Figure 20, singlet resonating at 2.00 ppm belongs to methyl protons adjacent to sp^2 hybridized imine carbon.

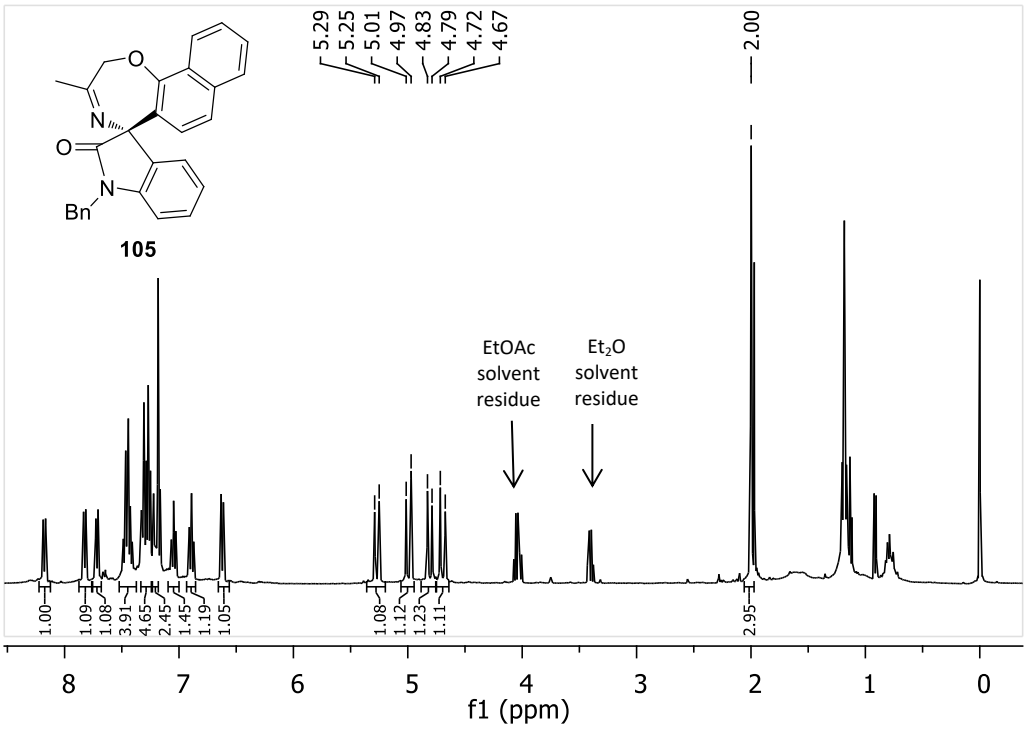

Figure 20 ^{1}H NMR spectrum of **105**.

2.4 Asymmetric Mannich Reaction

Asymmetric Mannich reaction is a useful tool for the synthesis of α-chiral amines. With enolizable α-azido carbonyl compounds, reaction delivers α-chiral azides bearing two contiguous stereogenic centers by single carbon-carbon bond formation. Both the amine functionality of the Mannich base adduct and azide moiety with masked amino nature are crucial synthons in heterocyclic chemistry.

Although, carbanion intermediates generated from α-azido ketones in the presence of base had been trapped by carbon electrophiles such as aldehydes, ketones,[57] α-

oxo aldehydes and α-keto esters,[58] there was a few L-proline derivative catalyzed asymmetric reports[59] with those. In 2014, we reported the first enantioselective aldol reaction of α-azido ketones **93** with ethyl pyruvate (**107**) with 2 mol% cinchona-based bifunctional urea catalyst *epi*-**94b** (Scheme 21). Aldol adducts **107** were obtained with diastereoselectivity up to 19:1 and enantioselectivity up to 82% ee.

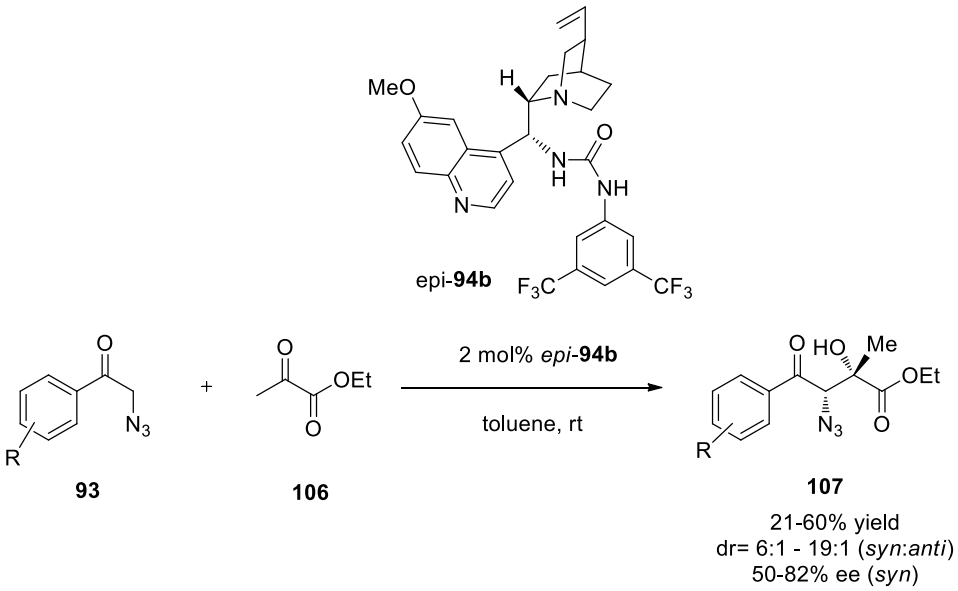

Scheme 21 Asymmetric organocatalytic aldol reaction of α-azido ketones.

Moderate stereoselectivity obtained in the former study, directed us to improve and expand the utility of α-azido ketones in asymmetric transformations. Consequently, as a part of this thesis study aiming the synthesis of α-chiral amines bearing 2-oxindole scaffold, we examined the Mannich reaction of **93**, with isatin-derived ketimines **55**.

2.4.1 Optimization of Reaction Parameters for Mannich Reaction

In order to initiate the study on the asymmetric Mannich reaction of α-azido ketones **93**, various organocatalysts have been examined in the model reaction of

2-azido-1-phenylethanone (**93a**) and isatin ketimine **55i** (Table 7). Firstly, 10 mol% of organocatalysts were screened at room temperature in DCM (Table 7, entries 1-12). Among 2-aminoDMAP based squaramides **74c** was better in terms of reaction rate (Table 7, entry 2), it afforded desired product in low yield due to formation of side products. High yield (90%) and good diastereoselectivity with 9:1 diastereomeric ratio were obtained in case of 2-adamantyl substituted quinine-based squaramide **64b** (entry 4). Although the highest enantioselectivity with 87% ee was attained by the catalyst **64d**, it brought about poorer diastereoselectivity with 4:1 dr (entry 6). Trials with bifunctional (thio)urea organocatalysts (**108** and **94**), quinidine (**21**) and quinine-9-epiamine (**109**) resulted in lack of enantiopurity (entries 7-12). Eventually, prior to optimization of catalyst loading, we decided to examine potentially promising catalysts **74c** and **64a-d**.

Table 7 Catalyst screening.[a]

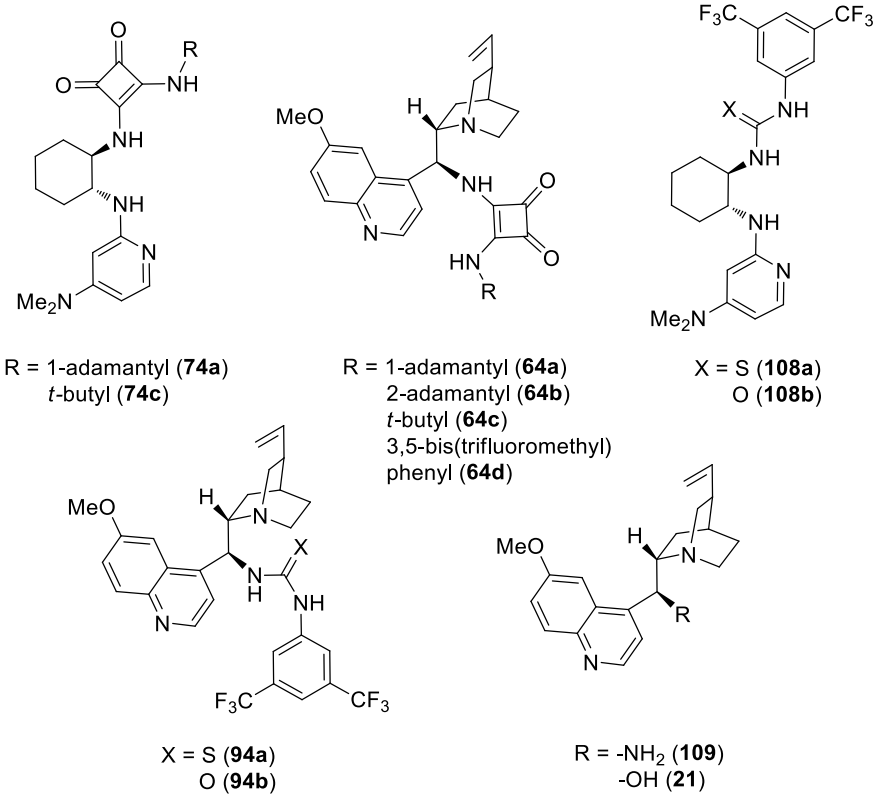

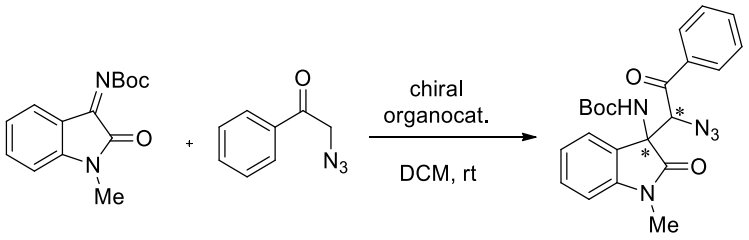

55i **93a** **107a**

Table 7 Continued.

Entry	Catalyst	Cat. loading (mol%)	Time (h)	Yield (%)	dr	ee (%)
1	**74a**	10	16	75	3:1	60
2	**74c**	10	2	41	2:1	68
3	**64a**	10	20	68	2:1	70
4	**64b**	10	16	90	9:1	56
5	**64c**	10	24	62	3:1	70
6	**64d**	10	3	94	4:1	87
7	**108a**	10	16	85	2:1	rac
8	**108b**	10	16	60	2:1	30
9	**94a**	10	6	71	10:1	10
10	**94b**	10	16	64	2:1	rac
11	**109**	10	48	20	nd	5
12	**21**	10	24	30	2:1	17

[a]Reaction condition: 0.05 mmol (1 eq) ketimine **55i**, 1.1 eq α-azido ketone **93a**, 10 mol% organocatalyst, DCM (0.5 mL), room temperature.

Decrement of catalyst loading from 10 mol% to 5 mol% raised the enantioselectivity of **64b** from 56% ee (Table 7, entry 4) to 77% ee and diastereoselectivity from 9:1 to 12:1 dr (Table 8, entry 3). Therefore, for the solvent screening study, we have focused on organocatalyst **64b**.

Table 8 Screning of 5 mol% catalyst loading with catalysts **74c** and **64a-d**.[a]

Entry	Catalyst	Cat. loading (mol%)	Time (h)	Yield (%)	dr	ee (%)
1	**74c**	5	24	63	8:1	67
2	**64a**	5	24	43	7:1	70
3	**64b**	5	24	70	12:1	77
4	**64c**	5	24	59	10:1	65
5	**64d**	5	24	86	3:1	77

[a]Reaction condition: 0.05 mmol (1 eq) ketimine **55i**, 1.1 eq. α-azido ketone **93a**, 5 mol% organocatalyst, DCM (0.5 mL), room temperature.

Later, examination of other solvents in the presence of 5 mol% **64b** at room temperature in the presence of 1 eq of ketimine **55i** and 1.1 eq of α-azido ketone **93a** did not furnish the enantioselectivity (Table 9, entries 1-5). Hereafter, with DCM as the solvent of choice, we progressed to determine the optimal reaction temperature and substrate equivalency.

Table 9 Solvent screening for organocatalyst **64b**.[a]

Entry	Catalyst	Solvent	Time (h)	Yield (%)	ee (%)
1	**64b**	$CHCl_3$	24	76	49
2	**64b**	CH_3CN	24	50	8
3	**64b**	THF	24	43	36
4	**64b**	Toluene	24	35	31
5	**64b**	1,2-DCE	25	45	37

[a]Reaction condition: 0.05 mmol (1 eq) ketimine **55i**, 1.1 eq. α-azido ketone **93a**, 5 mol% **64b**, solvent (0.5 mL), room temperature. Due to low enantiopurity, diastereomeric ratios were not determined.

Instead of performing the reaction at fluctuant ambient temperature, it was fixed at 22 °C for the sake of reproducibility and precision (Table 10). When the temperature was 22°C, enantioselectivity of **64b** increased to 81% ee in DCM with 1.1 eq of α-azido ketone **93a** (Table 10, entry 1). When the equivalency was

2, small increase was attained both in yield and enantioselectivity (78% yield and 83% ee, entry 4).

Table 10 Screening of α-azido ketone **93a** equivalency.[a]

Entry	Catalyst	α-Azido ketone eq.	T (^{o}C)	Time (h)	Yield (%)	dr	ee (%)
1	**64b**	1.1	22	24	73	10:1	81
2	**64b**	1.5	22	21	70	11:1	82
3	**64b**	3	22	21	78	9:1	75
4	**64b**	2	22	24	78	12:1	83

[a]Reaction condition: 0.05 mmol (1 eq) ketimine **55i**, α-azido ketone **93a**, 5 mol% **64b**, DCM (0.5 mL), 22 °C.

Finally, lower temperatures (0 °C and -20 °C) were screened for the catalyst **64b**. However, a decrement both in yield and ee was detected (Table 11, entries 1, 2). Although leading lower diastereoselectivity and similar enantioselectivity (4:1 dr, 87% ee, Table 7 entry 6) with the optimal outcome reached for **64b** (12:1 dr, 83% ee), the potential of **64d** was reconsidered. However, examination of 0 °C and 22°C for **64d** did not raise stereoselectivity (Table 11, entries 3 and 4).

Table 11 Temperature screening for **64b** and **64d**.

Entry	Catalyst	Cat. loading (% mol)	Solvent	T (^{o}C)	Time (h)	Yield (%)	dr	ee (%)
1	**64b**	5	DCM	0	41	63	nd	70
2	**64b**	5	DCM	-20	46	53	nd	48
3	**64d**	10	DCM	0	24	95	7:1	77
4	**64d**	10	DCM	22	24	90	6:1	74

[a]Reaction condition: 0.05 mmol (1 eq) ketimine **55i**, α-azido ketone **93a** (2 eq for **64b**, 1.1 eq for **64d)**, DCM (0.5 mL).

Eventually, optimum conditions were determined for both **64b** as 2 eq of α-azido ketone **93**, 5 mol% catalyst, DCM as reaction solvent and reaction temperature as

22 °C. For the organocatalyst **64d**; 1.1 eq of α-azido ketone **93**, 10 mol% catalyst, reaction solvent DCM and room temperature.

2.4.2 Scope of Mannich Reaction

Although derivatization studies had been initiated by quinine derived 2-adamantyl substituted squaramide **64b**, due to leading better enantioselectivities with some substrates organocatalyst **64d** was also investigated in asymmetric Mannich reaction. In general, squaramide **64b** afforded better diastereoselectivity with higher diastereomeric ratio than **64d** (Table 12). However, higher enantiomeric excesses were attained for the derivatives **107a-c**, **107f**, **107i**, **107j** and **107n** by organocatalyst **64d**. Furthermore it was investigated that organocatalyst **64b**, which has relatively less acidic squaramide protons, distinctively lead to higher enantioselectivities for isatin ketimines bearing no substituent on indoline nitrogen (Table 12, **107m-p**). It can be inferred from this outcome that in the presence of substrates having H-bonding potential, 3,5-bis(trifluoromethyl)aniline substituted organocatalyst **64d** fails to coordinate to *N*-carbamate ketimine to some extent. To conclude, two organocatalysts are supplementary to each other for the asymmetric organocatalytic Mannich reaction of α-azido ketones and isatin ketimines. Among sixteen derivatives high enantioselectivities up to 96% ee and 20:1 diastereomeric ratio were obtained. The highest enantioselectivity (96% ee) belongs to chromanone bearing derivatives **107g** and **107l**.

Table 12 Scope of Mannich reaction.[a]

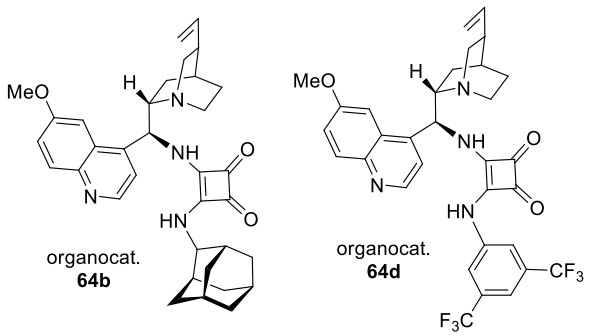

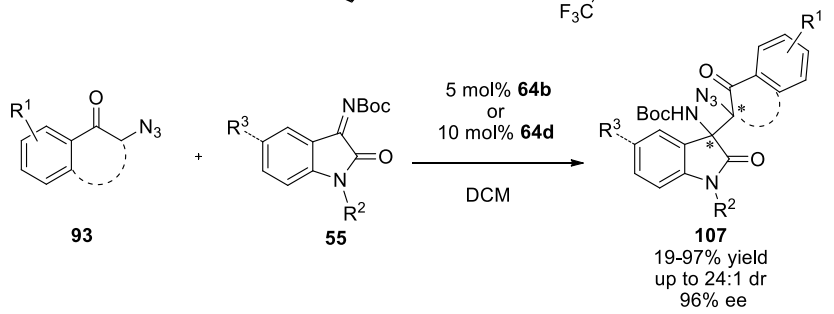

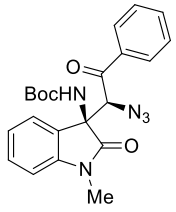

107a

cat. **64b**:
78% yield,12:1 dr, 83% ee

cat. **64d**:
95% yield, 4:1 dr, 86% ee

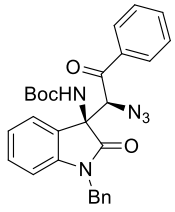

107b

cat. **64b**:
75% yield,14:1 dr, 69% ee

cat. **64d**:
96% yield, 4:1 dr, 84% ee

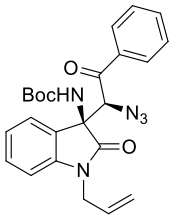

107c

cat. **64b**:
70% yield, 4:1 dr, 70% ee

cat. **64d**:
80% yield, 9:1 dr, 82% ee

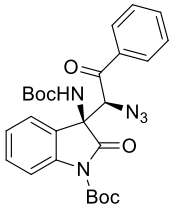

107d

cat. **64b**:
19% yield, 20:1 dr, *rac*

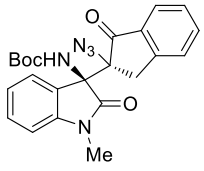

107e

cat. **64b**:
97% yield,18:1 dr, 88% ee

cat. **64d**:
72% yield,15:1 dr, 86% ee

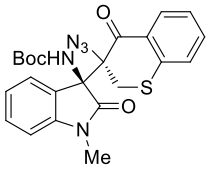

107f

cat. **64b**:
29% yield,14:1 dr, 26% ee

cat. **64d**:
89% yield, 6:1 dr, 90% ee

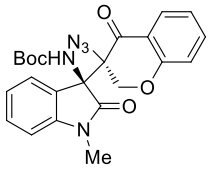

107g

cat. **64b**:
85% yield, 20:1 dr, 96% ee

cat. **64d**:
59% yield, 5:1 dr, 95% ee

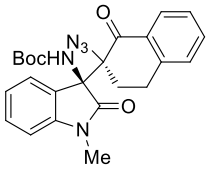

107h

cat. **64b**:
26% yield, 8:1 dr, 83% ee

cat. **64d**:
22% yield, 3:1 dr, 62% ee

[a]Reaction condition for cat. **64b**: isatin ketimine **55** (0.1 mmol), α-azido ketone **93** (0.2 mmol), 5 mol% cat., DCM (1.0 mL), 22 °C. Reaction condition for cat. **64d**: isatin ketimine **55** (0.1 mmol), α-azido ketone **93** (0.11 mmol), 10 mol% cat., DCM (1.0 mL), rt.

Table 12 Continued.[a]

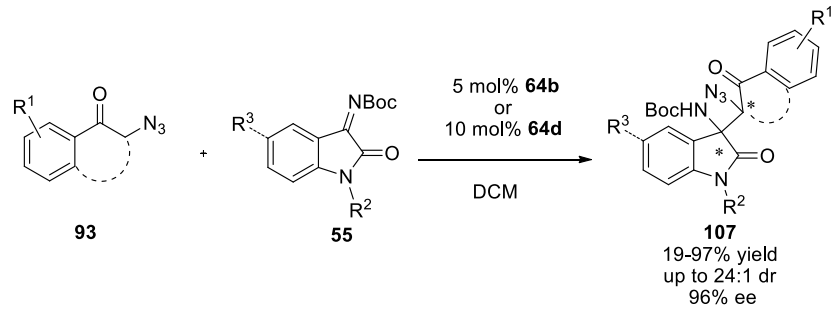

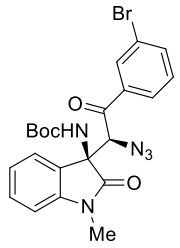

107i

cat. **64b**:
76% yield,14:1 dr, 84% ee

cat. **64d**:
97% yield, 11:1 dr, 90% ee

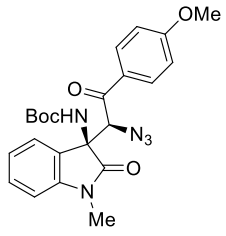

107j

cat. **64b**:
71% yield,8:1 dr, 64% ee

cat. **64d**:
80% yield, 4:1 dr, 75% ee

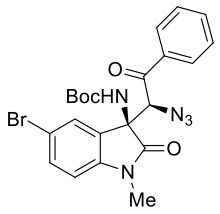

107k

cat. **64b**:
60% yield,11:1 dr, 70% ee

cat. **64d**:
85% yield, 20:1 dr, 53% ee

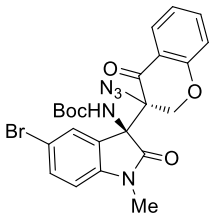

107l

cat. **64b**:
78% yield,15:1 dr, 96% ee

cat. **64d**:
76% yield, 13:1 dr, 96% ee

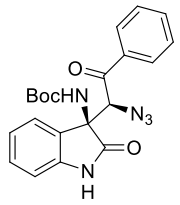

107m

cat. **64b**:
49% yield, 9:1 dr, 93% ee

cat. **64d**:
38% yield, 10:1 dr, 58% ee

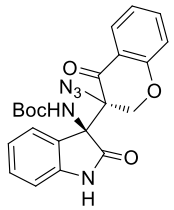

107n

cat. **64b**:
28% yield, 5:1 dr, 89% ee

cat. **64d**:
59% yield, 9:1 dr, 16% ee

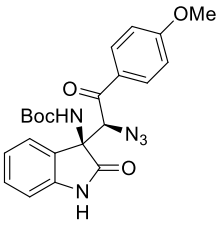

107o

cat. **64b**:
64% yield,15:1 dr, 80% ee

cat. **64d**:
66% yield, 6:1 dr, 68% ee

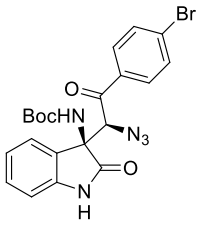

107p

cat. **64b**:
68% yield, 24:1 dr, 80% ee

cat. **64d**:
40% yield, 19:1 dr, 23% ee

[a]Reaction condition for cat. **64b**: isatin ketimine **55** (0.1 mmol), α-azido ketone **93** (0.2 mmol), 5 mol% cat., DCM (1.0 mL), 22 °C. Reaction condition for cat. **64d**: isatin ketimine **55** (0.1 mmol), α-azido ketone **93** (0.11 mmol), 10 mol% cat., DCM (1.0 mL), rt.

Representative ^{1}H and ^{13}C NMR spectra of **107a** are depicted in Figure 21 and Figure 22. Signals indicating the bond formation are observed as singlets at 5.86 ppm for –NH and 5.28 ppm for methine proton adjacent to azido moiety (Figure

21). Interestingly, instead of carbamate –NH proton, methine proton appears as broad singlet. These two protons were precisely designated according to 2D HSQC and DEPT 90 NMR spectra. Methyl protons resonate at 3.27 ppm (N-CH_3) and 1.30 ppm (-O-*t*Bu) as strong singlets. Among the aromatic methine protons, doublet at the highest field of the aromatic region (6.81 ppm) belongs to the *ortho*-CH with respect to indoline nitrogen.

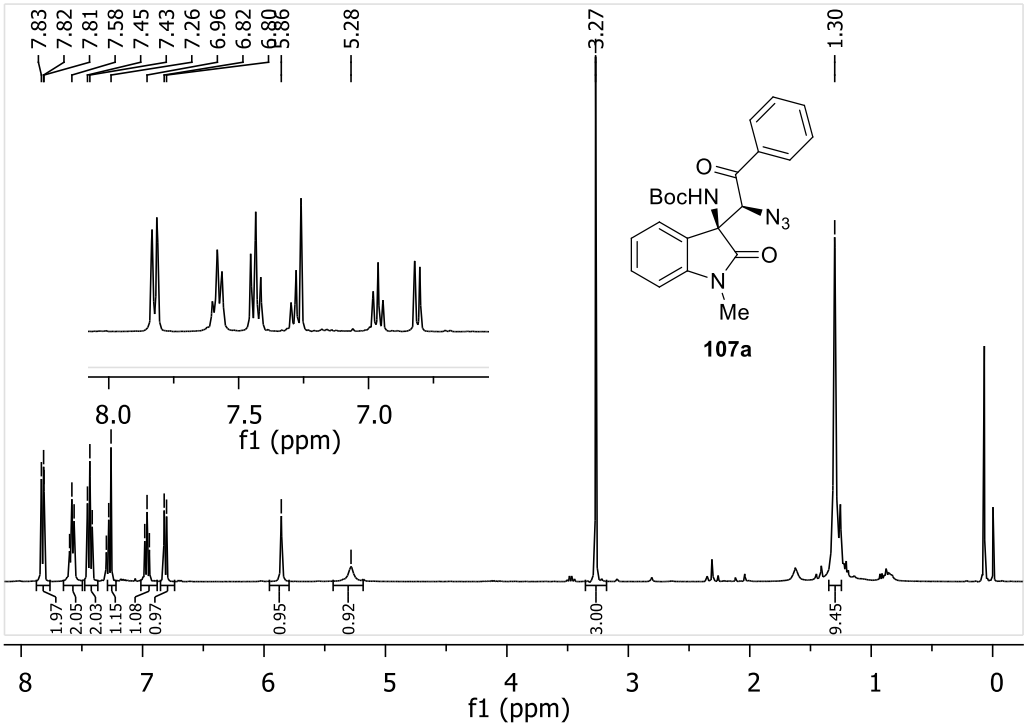

Figure 21 ^{1}H NMR spectrum of **107a**.

In ^{13}C NMR spectrum of **107a** (Figure 22), different types of carbonyl carbons are observed at 193.7 ppm (ketone), 173.9 ppm (amide) and 154.2 ppm (carbamate). Aromatic -CH carbons resonates at 135.5, 134.3, 130.1, 128.9, 128.8, 122.7, 108.4 ppm. Aromatic ipso-carbons resonate at 144.2, 126.5 and 125.8 ppm. Aliphatic methine carbon at 64.0 ppm and quaternary stereogenic carbon atom at 62.9 ppm proves the suggested structure. Moreover, the strong peak at ~2100 cm^{-1} at IR spectrum indicates the presence of azido moiety.

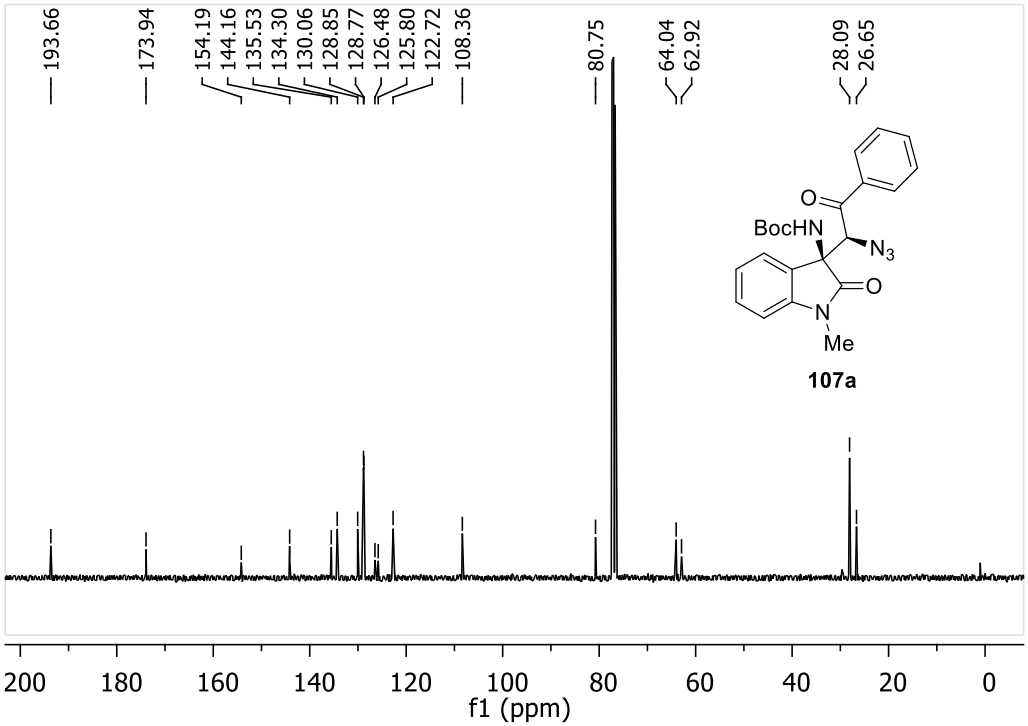

Figure 22 ^{13}C NMR spectrum of **107a**.

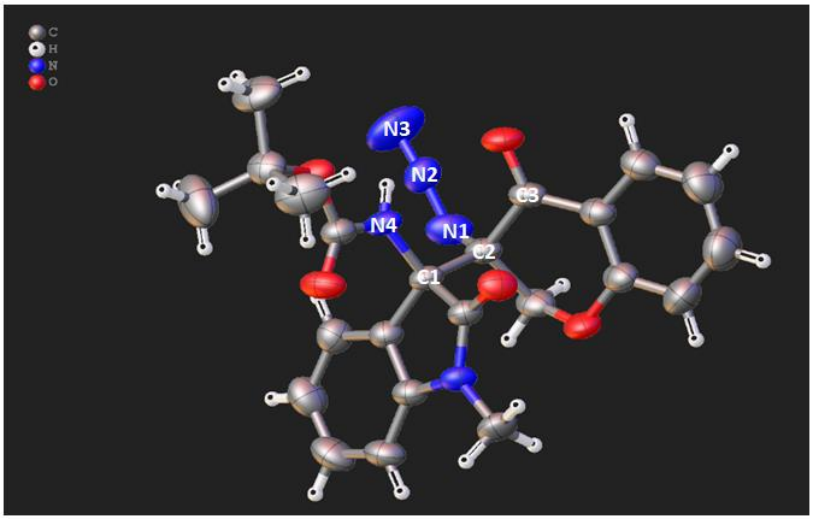

Figure 23 X-ray crystall structure of **107g**.

Absolute configuration of enantioenriched **107g** was determined by single crystal X-ray diffraction analysis. According to this crystal image, *C1* and *C2* asymmetric

centers have *S*-configuration (Figure 23). The relative conformation of -NHBoc and $-N_3$ moieties are observed as *syn*-clinal (Figure 23 and 24). This *syn*-conformation and absolute configuration were generalized for the other derivatives as well.

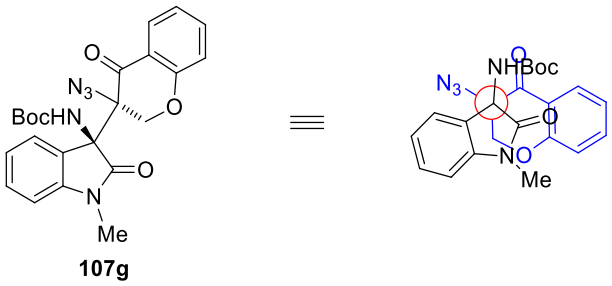

107g

Figure 24 Newman projection of **107g**.

By analogy to Zimmerman-Traxler model, which explains the diastereofacial selectivity in aldol reactions through a chair-like transition state, we tried to interpret the *syn*-selectivity determined by the single crystal XRD analysis. In Figure 25, all possible interactions between the (*Z*)- and (*E*)-enolates and the ketimine were considered in a chair-like transition state. In the model given as (i) (*Z*)-enolate interacts with the ketimine from its *Si*-face so that the steric repulsions are minimized. However, the transition state in which *Re*-face of isatin ketimine interacts with both (*Z*)- and (*E*)-enolate (ii and iv, Figure 25) are disfavored due to both the 1,3-diaxial interactions and the steric hindrance caused by Boc-group. Because of the electron repulsion between the azido and carbonyl groups, model (iii) is also disfavored. Even though the role of the bifunctional organocatalyst is excluded, Zimmerman-Traxler model is useful to describe the *syn*-preference of the asymmetric Mannich reaction.

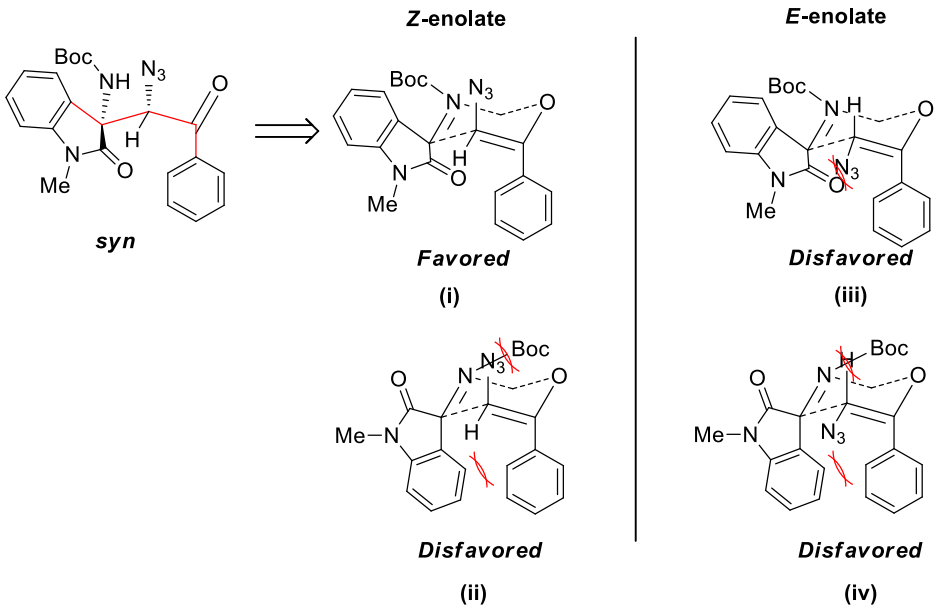

Figure 25 Zimmerman-Traxler approach for diastereofacial selectivity.

To explain the stereoselectivity observed in **107g**, transition state model given in Figure 26 was suggested. Isatin-derived ketimine **55i** coordinates to squaramide moiety through double H-bonding while the quinuclidine base enhances the enolate formation. Similar to the face selectivity estimated in Figure 25, (*Z*)-enolate attacks to ketimine selectively from the *Si*-face to afford two contiguous stereogenic carbon atoms with (*S*)-configuration.

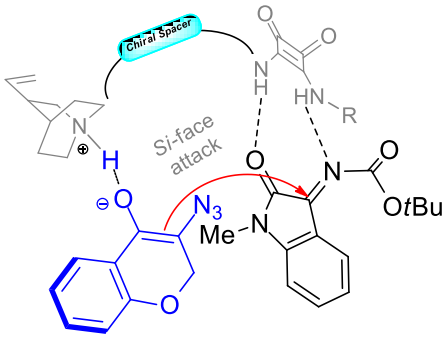

Figure 26 Proposed transition state for asymmetric Mannich reaction.

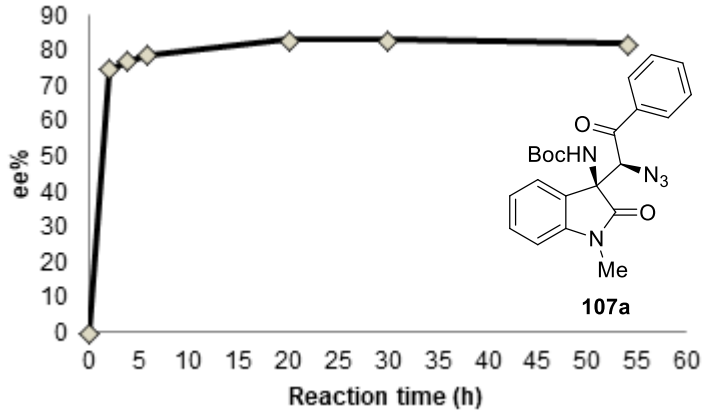

Graph 1 Reaction time vs ee% graph for compound **107a**.

In order to determine whether the Mannich adducts **107** (**a**-**d**, **i**-**k**, **m**, **o**, **p**) obtained from acyclic α-azido ketones undergo any epimerization under reaction conditions due to enolisation, change in enantiomeric excess by reaction time was monitored. Graph shown above belongs to compound **107a**, obtained by 2-adamantyl substituted quinine-derived squaramide **64b**. Accordingly, in the first 6 hours there is a drastic increase in enantiopurity and it reaches equilibrium by 83% ee after 20 hours (Graph 1). Although the reaction had already been complete in 24 hours, elongation of reaction duration to 54 hours did not cause any distinguished decrease in enantiopurity.

2.4.3 Representative Transformation of Mannich Adducts to 1,2,3-Triazole and Spiro-cyclic Urea.

In order to show the versatility of the enantioselectively synthesized 3-amino-3-(1-azido-2-oxo)indolin-2-one skeleton, we wanted to transform the azide moiety into 1,4-disubstituted triazole via copper (I) catalyzed azide-alkyne cycloaddition (CuAAC). For this purpose, initially catalytic amount of $CuSO_4.5H_2O$ together with sodium L-ascorbate as reducing agent were used in *t*-BuOH:H_2O solvent mixture. However, the yield obtained in the catalytic reaction with substrate **107a**

was lower than expected from a "click reaction". Then tris(triazolyl)methanol−Cu(I) salt **108** (Figure 27) known as highly active Huisgen 1,3-dipolar cycloaddition catalyst was also examined in 2 mol% in EtOH:H_2O solvent mixture according to literature.[60] However, presumably due to high sterical hindrance around our azide compound **107a** this catalyst was inefficient for our substrate.

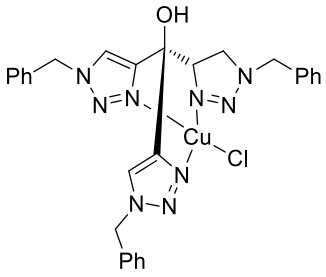

108

Figure 27 Tris(triazolyl)methanol−Cu(I) salt **108.**

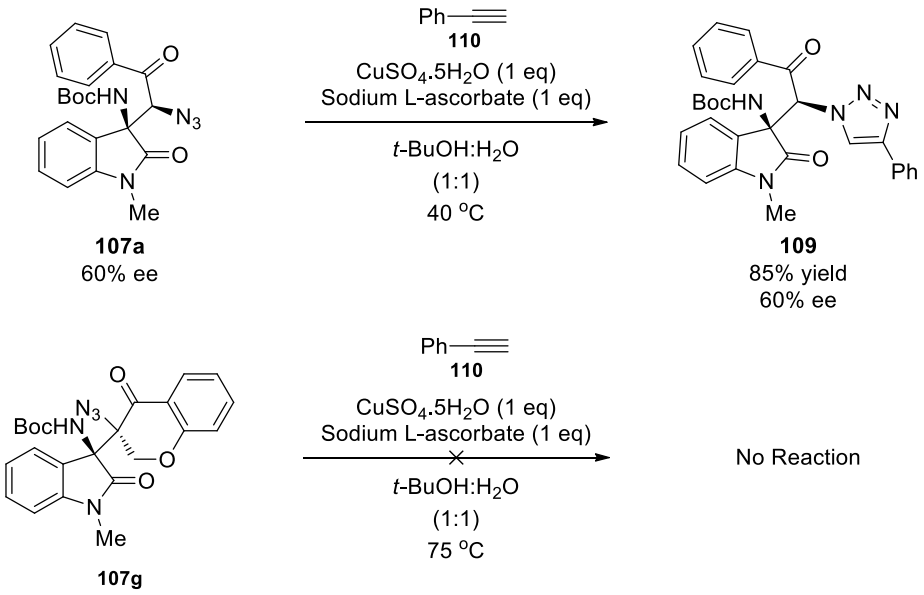

Scheme 22 Copper (I) catalyzed azide-alkyne cycloaddition reaction of Mannich adduct.

Later, it was decided to use stoichiometric amount of $CuSO_4.5H_2O$ (1 eq) and reducing agent with excess phenylacetylene (**110**). Reaction proceed smoothly and all the starting azide was consumed in 3 hours to give yellow precipitate **109**. After purification by column chromatography, 1,2,3-triazole **109** was obtained as white solid in 85% yield with the conservation of previously inhereted enantiopurity. However, same procedure with chiral azide **107g** at increased reaction temperature resulted in no product (Scheme 22). Triazole structure was proven by ^{1}H NMR spectroscopy. The characteristic signal of triazole –CH proton is detected as singlet at 8.11 ppm (Figure 28).

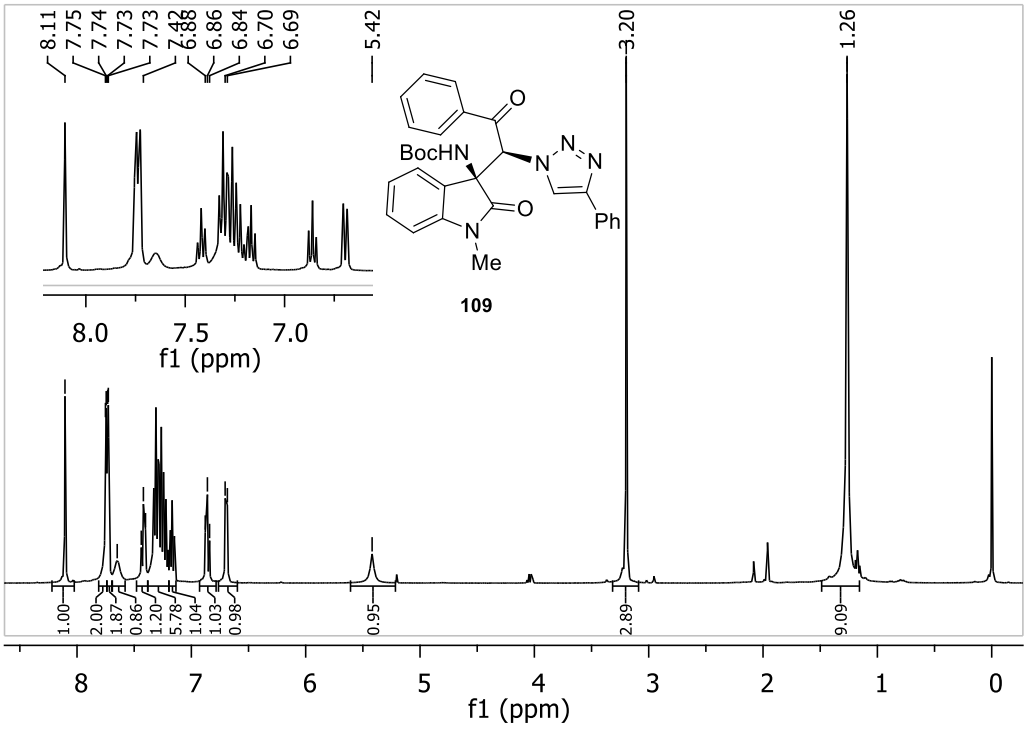

Figure 28 ^{1}H NMR spectrum of triazole **109**.

Additionally, in order to use the 1,2-ethanamine functionality of **107a**, azido moiety was reduced to amine by using both Pd-catalyzed hydrogenation at atmospheric pressure and Staudinger reduction (Scheme 23). The former afforded compound **111a** in high yield (94%) and with almost full conservation of

enantiopurity (85% ee). The similar enantiomeric excess obtained in amine product and the formation of no diastereomer ensures that there is no epimerization due to nitrogen inversion and enolisation of **111a**. However, Staudinger reduction of azide afforded **111a** in only 30% yield. After the deprotection of Boc-group with TFA, without isolation, 1,1'-carbonyldiimidazole (**113**) was added to the reaction medium in the presence of triethylamine. This reaction pathway brought about spiro-cyclic urea **112a** with 85% ee (Scheme 23).

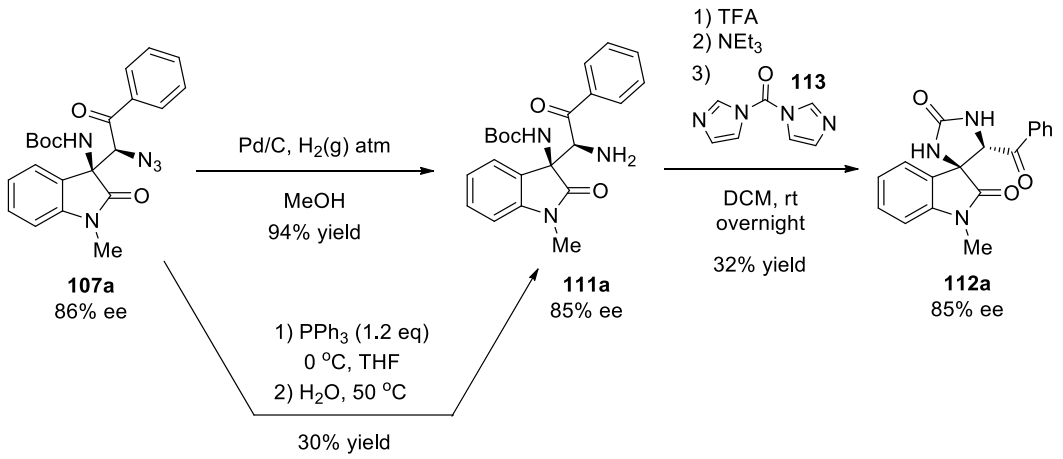

Scheme 23 Synthetic route for spiro-cyclic urea **112a**.

In the ^{1}H NMR spectrum of urea **112a** (Figure 29), one of the urea –NH proton and aliphatic methine proton coupled with each other by J = 9.3 Hz are depicted. The other –NH proton overlaps with aromatic protons. In ^{13}C NMR spectrum, urea carbonyl resonates at 158.1 ppm as expected along with other carbonyls at 193.4 and 172.4 ppm (Figure 30). Accordingly, here 10 aromatic and 3 aliphatic carbon atoms are clearly shown on the spectrum.

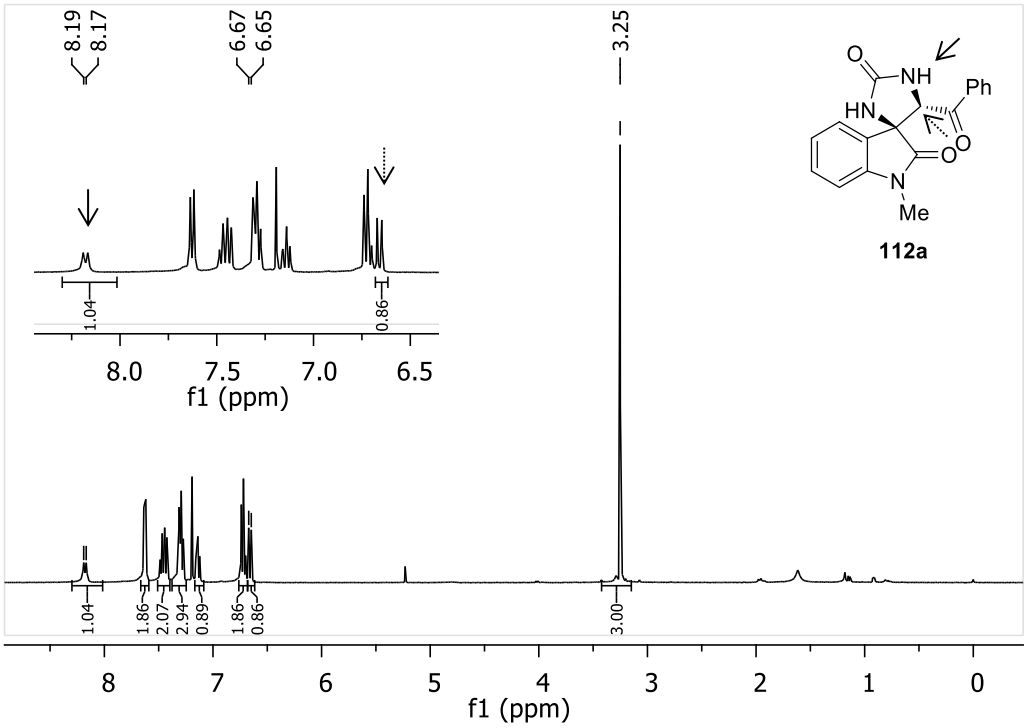

Figure 29 [1]H NMR spectrum of spiro-cyclic urea **112a**.

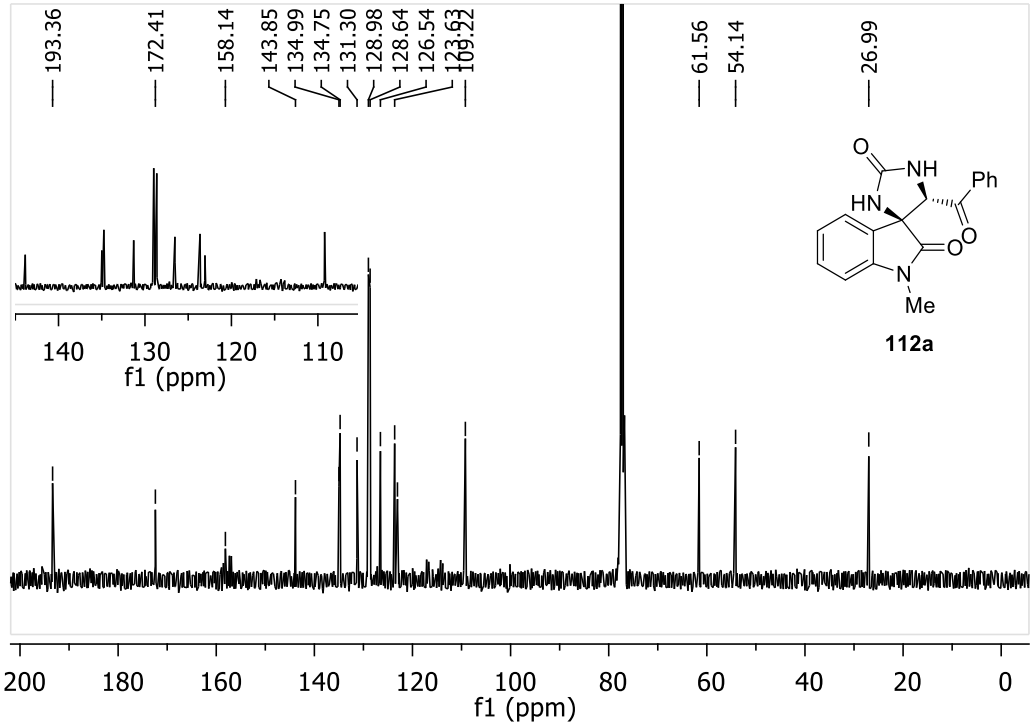

Figure 30 [13]C NMR spectrum of spiro-cyclic urea **112a**.

CHAPTER 3

EXPERIMENTAL

3.1 Materials and Methods

^{1}H NMR and ^{13}C NMR spectra were recorded at 400 MHz and 100 MHz in $CDCl_3$ or DMSO-d_6 with TMS as internal standard with residual nondeuterated solvent peaks at δ 7.26 and 77.0 ppm, or 2.50 and 39.5 ppm, respectively. Chemical shifts are given in ppm, and coupling constants (*J*) are given in Hertz (Hz). ^{1}H and ^{13}C NMR spectra of products which are unknown in literature are given in appendix A. All reactions were monitored by thin layer chromatography (TLC) on Merck silica gel 60, F-254 TLC. Plates were visualized by UV light and *p*-anisaldehyde stain. Flash column chromatography was performed by using glass columns with a flash grade silica gel (230-400 mesh). Melting points were measured by capillary tubes. Optical rotations were made by the sodium D-line (589 nm) and reported as $[\alpha]_D^T$ (c in g mL^{-1}, solvent). HPLC chromatograms were recorded with Daicel AD-H, AS-H, OD-H, and IA chiral column (0.46 cm ϕ x 25 cm) and with indicated hexane : i-PrOH eluent. HPLC chromatograms of chiral products and racemic forms of them were given in appendix B. High resolution mass (HRMS) data were acquired on a time of flight (TOF) mass spectrometer with electrospray ionization (ESI) method. Infrared radiation (IR) spectra of all new compounds were recorded on ATR spectrometer. The compounds were named by using ChemDraw Ultra 12.0. All glassware was dried in oven prior to use.

3.2 General Procedure A: Synthesis of Bifunctional Squaramides

3.2.1 (8*S*,9*S*)-9-Amino-9-deoxyepiquinine (77)

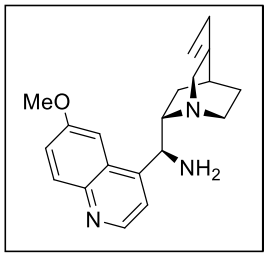

According to literature procedure,[50] quinine (**76**) (10.0 mmol, 3.2 g) and triphenylphosphine (12.0 mmol, 3.1 g) were dissolved in 50 mL of dry THF (dried over sodium metal and benzophenone) and the solution was cooled to 0 °C. Diisopropyl azodicarboxylate (DIAD) (12.0 mmol, 2.4 g) was added all at once to the cooled solution. Diphenyl phosphoryl azide (DPPA) (12.0 mmol, 3.3 g) was dissolved in 20 mL dry THF in another flask and cooled to 0 °C in ice bath. DPPA solution was added to the quinine mixture dropwise and after the complete addition mixture was allowed to reach to ambient temperature. After 12 h, the solution was heated to 50 °C for 2 h. For the reduction of azide intermediate, a second portion of triphenylphosphine (13.0 mmol, 3.4 g) was added and stirred at 50 °C until the gas evolution has finished. After cooling the solution to room temperature, deionized water (1 mL) was added and stirred for 3 h. Upon the removal of solvent in vacuo, the residue was dissolved in 1:1 mixture of DCM and 10% HCl (100 mL) and layers are separated. The aqueous phase was washed with DCM (4 x 50 mL). Later, the acidic solution was made alkaline with 30% aqueous NH_3 solution and aqueous phase washed with DCM (4 x 50 mL). The combined organic layers was dried over $MgSO_4$ and concentrated. The residue was purified by silica gel column chromatography initially with ethyl acetate and gradual increase of methanol until EtOAc : MeOH : TEA = 50 : 50 : 1 ratio. The title amine **77** was obtained as colorless viscous oil in 71% yield. The spectral data was in accordance with literature.[50]

3.2.2 Synthesis of Monosquaramides 80a-c

Monosquaramides **80a-c** were synthesized according to literature procedure,[51] by stirring diethyl squarate (**79**) (1.0 mmol, 170.2 mg) with the corresponding commercially available amines (1.0 mmol) in DCM (4 mL) at room temperature. In case amines are in the form of hydrochloride salt, triethylamine (1.1 mmol, 165.4 μL) was added. The mixture was concentrated and 15:1 (pentane : ether) was added, the solid was filtered and dried for use in the further step. Spectroscopic data for 3-(*tert*-butylamino)-4-ethoxycyclobut-3-ene-1,2-dione (**80c**) was in accordance with literature[61] and for adamantane derivatives are given below.

The acidic part 3-((3,5-bis(trifluoromethyl)phenyl)amino)-4-ethoxycyclobut-3-ene-1,2-dione, required for organocatalyst **64d** was synthesized according to literature procedure.[62] Diethyl squarate (**79)** (1.5 mmol, 255.2 mg) and zinc triflate (0.2 mmol, 72.7 mg) was dissolved in EtOH (5 mL) at room temperature. 3,5-bis(trifluoromethyl)aniline (1.2 mmol, 187.4 μL) was added dropwise and stirred overnight. The precipitate was filtered and washed with ethanol. The filtrate was recrystallized from ethanol/hexane to afford yellow solid. Spectral data was in accordance with the literature.[62]

3.2.2.1 3-(Adamantan-2-ylamino)-4-ethoxycyclobut-3-ene-1,2-dione (80b)

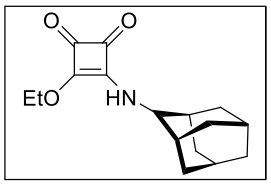

Major rotamer: ^{1}H NMR (400 MHz, $CDCl_3$) δ 6.19 (bs, 1H), 4.70 (q, *J* = 6.6 Hz, 2H), 3.77 (d, *J* = 6.6 Hz, 1H), 1.93 (s, 2H), 1.89 – 1.66 (m, 10H), 1.60 (d, *J* = 12.7 Hz, 2H), 1.39 (t, *J* = 7.1 Hz, 3H). ^{13}C NMR (100 MHz, $CDCl_3$) δ 189.3, 183.2, 177.2, 171.6, 69.3, 58.8, 36.7, 32.7, 30.7, 26.6, 15.7.

Minor rotamer: ^{1}H NMR (400 MHz, $CDCl_3$) δ 5.71 (bs, 1H), 4.70 (q, *J* = 6.6 Hz, 2H), 4.21 (d, *J* = 6.2 Hz, 1H), 1.93 (s, 2H), 1.89 – 1.66 (m, 10H), 1.60 (d, *J* = 12.7

Hz, 2H), 1.39 (t, J = 7.1 Hz, 3H). ^{13}C NMR (100 MHz, $CDCl_3$) δ 189.3, 183.2, 177.2, 171.6, 69.3, 58.8, 37.1, 32.7, 30.7, 26.8, 15.7.

3.2.3 Synthesis of Quinine-Based Bifunctional Squaramides (64a-d)

(8*S*,9*S*)-9-Amino-9-deoxyepiquinine (**77**) (1.0 mmol, 323.4 mg) was dissolved in MeOH (2 mL). In another vessel, corresponding monosquaramide **80** (1.2 mmol) was dissolved in DCM and added to the amine solution. Mixture was stirred at room temperature for 3-4 days. Reaction mixture was directly loaded onto silica gel column for chromatography by 3:1 (EtOAc : MeOH) eluent. Quinine-based squaramides **64a-d** were obtained as white solid in good yields (70-85%). Spectral data for **64a**[51] and **64c**[63] was in accordance with literature. Spectral data of **64b** and **64d** are given below.

3.2.3.1 3-((1*R*,3*S*,5*S*,7*S*)-Adamantan-2-ylamino)-4-(((*S*)-(6-methoxyquinolin-4-yl)((1*S*,2*S*,4*S*,5*R*)-5-vinylquinuclidin-2-yl)methyl)amino)cyclobut-3-ene-1,2-dione (64b)

The use of 2-adamantylamine hydrochloride in general procedure afforded squaramide **64b** as white solid in 87% yield. mp 200-208 °C (decomposed); $[\alpha]_D^{20}$= 376.0° (*c* 0.25, CH_2Cl_2).

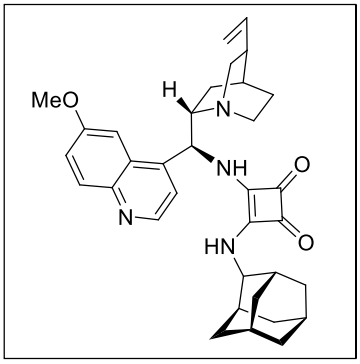

^{1}H NMR (400 MHz, $CDCl_3$) δ 8.66 (d, J = 3.2 Hz, 1H), 8.01 (d, J = 9.2 Hz, 1H), 7.78 (s, 1H), 7.51 (d, J = 4.1 Hz, 1H), 7.39 (d, J = 9.2 Hz, 1H), 6.12 (bs, 1H), 5.84 – 5.62 (m, 1H), 5.14 – 4.85 (m, 2H), 4.02 (bs, 1H), 3.97 (s, 3H), 3.69 (s, 1H), 3.46 (s, 2H), 3.16 (t, J = 10.5 Hz, 1H), 2.83 – 2.52 (m, 2H), 2.30 (bs, 1H), 1.85 – 1.40 (m, 15H), 1.38 – 1.17 (m, 3H), 1.00 – 0.65 (bs, 2H). ^{13}C NMR (100 MHz, $CDCl_3$) δ 182.8, 182.7, 167.7, 167.4, 158.9, 147.9, 145.0, 144.0, 140.8, 131.9, 128.0, 125.8, 122.6, 115.3, 101.5, 58.5,

56.2, 56.0, 41.0, 39.3, 37.3, 36.9, 36.8, 33.4, 33.2, 30.7, 27.5, 27.1, 26.8. IR (neat): 3226, 2905, 2853, 2359, 1792, 1660, 1620, 1574, 1506, 1455, 1363, 1339, 1228, 1100, 1026, 977, 909, 847, 727, 691 cm^{-1}. HRMS (ESI) m/z: calcd. for $C_{34}H_{41}N_4O_3$ $[M+H]^+$: 553.3179; found 553.3173.^{13}C NMR spectrum was in accordance with literature.[48j]

3.2.3.2 3-3-((3,5-bis(trifluoromethyl)phenyl)amino)-4-(((*S*)-(6-methoxy quinolin-4-yl)((1*S*,2*S*,4*S*,5*R*)-5-vinylquinuclidin-2-yl)methyl)amino) cyclobut-3-ene-1,2-dione (64d)

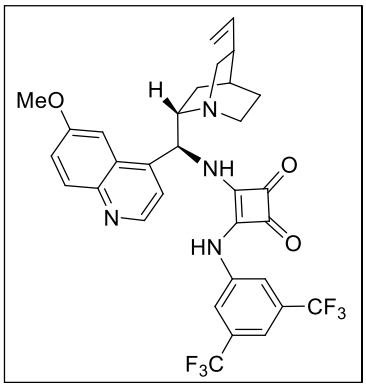

The use of 3,5-bis(trifluoromethyl)aniline in general procedure afforded squaramide **64d** as white solid in 87% yield. mp 227-229 °C (decomposed).

^1H NMR (400 MHz, $CDCl_3$) δ 8.61 (s, 1H), 7.99 (d, *J* = 9.0 Hz, 1H), 7.81 – 7.41 (m, 4H), 7.35 (d, *J* = 9.0 Hz, 1H), 7.29 (s, 1H), 6.15 (bs, 1H), 5.70 (dd, *J* = 16.1, 8.4 Hz, 1H), 5.13 – 4.60 (m, 2H), 3.86 (s, 3H), 3.50 (s, 1H), 3.27 (bs, 1H), 3.01 (bs, 1H), 2.69 (bs, 1H), 2.53 (bs, 1H), 2.22 (bs, 1H), 1.67 (s, 1H), 1.63 – 1.35 (m, 3H), 0.95 – 0.65 (m, 1H). (Two aliphatic protons overlap with others)

3.3 General Procedure B: Synthesis of *N*-Substituted Isatin Derivatives

3.3.1 *N*-Alkylation of Isatin:

According to literature procedure,[64] isatin (1*H*-indole-2,3-dione) (**84**) (30.0 mmol, 4.4 g) and potassium carbonate (60.0 mmol, 8.3 g) was dissolved in 100 mL of acetonitrile at room temperature. Corresponding alkyl halide (33.0 mmol) was added to the suspension and reaction was stirred overnight at room temperature. Upon the monitoring of reaction progress by TLC, reaction was quenched with

distilled water. After the evaporation of reaction solvent, content was dissolved in ethyl acetate and organic phase extracted with 5% (w/v) aqueous $NaHCO_3$ solution three times and brine for compounds **85a**, **85c**, **85d**. For **85b**, extraction was done only with water and brine. Organic phase was dried over anhydrous $MgSO_4$ and concentrated in vacuo. Multiple recrystallization of the crude product from ethyl acetate and hexane at room temperature afforded compounds **85a-d** in good yields (80-92%) as needle-like crystals. The spectral data was in accordance with literature.[64-65]

3.3.2 *N*-Benzylation of Isatin

Isatin (1*H*-indole-2,3-dione) (**84**) (30.0 mmol, 4.4 g), potassium carbonate (60.0 mmol, 8.3 g) and potassium iodide (3.0 mmol, 0.5 g) was suspended in 100 mL of acetonitrile. After benzyl bromide (33.0 mmol, 3.92 mL) was added and stirred at room temperature overnight. Upon the completion, solvent was evaporated under vacuum and work-up procedure was performed with aqueous $NaHCO_3$ in analogy with *N*-alkylation procedure. The spectral data of the recrystallized orange needle-like solid (88% yield) was in accordance with literature.[64]

3.3.3 *N*-Acetylation of Isatin

Adapted from the literature,[66] a mixture of isatin (3.4 mmol, 0.5 g) and acetic anhydride (20 mL) was refluxed for 6 h. After cooling, the solution was poured into cold water and filtration of the precipitate afforded *N*-acetylisatin **85e** as yellow powder with 90% yield. The crude product was used without further purification in later steps.

3.3.4 *N*-Boc Isatin Synthesis

According to literature procedure,[67] dry THF (38 mL) was added to an oven-dried Schlenk charged with isatin (**84**) (6.3 mmol, 926.9 mg) and DMAP (0.6 mmol, 73.3 mg) at 0 °C under inert atmosphere. A solution of di-*tert*-butyldicarbonate (Boc_2O) (7.6 mmol, 1.6 g) in THF (20 mL) was slowly added to the solution at 0 °C and resulting solution was stirred at room temperature for 4 h. After monitoring consumption of the starting material by TLC, reaction mixture was quenched with water. Standard work-up with ethyl acetate and recrystallization via EtOAc : hexane yielded in yellow solid with 63% yield. The spectral data was in agreement with literature.[67]

3.4 General Procedure C: Synthesis of Triphenyliminophosphane 83

According to literature procedure,[52] sodium nitrite (66.6 mmol, 4.6 g) was added in small portions to a solution of corresponding carbazate **81** (60.5 mmol) in water (40 mL) and glacial acetic acid (20 mL) stirred at 0 °C. Solution was stirred for 30 min, and then extracted into ether (2 x 40 mL). The combined organics were washed with water (40 mL) and then $NaHCO_3$ (1M, 2 x 40 mL). Organic layers were combined and dried over $MgSO_4$, filtered and used for the next step without evaporation of the solvent. (CAUTION: Acyl azides **82** are highly explosive in case of concentration to dryness!)

The ether solution of crude azide **82** obtained in the previous step was added dropwise to a stirring suspension of triphenylphosphine (47.5 mmol, 11.2 g) in ether (40 mL) at 0 °C. After the completion of the addition, insoluble white precipitate was filtered and recrystallized over ethyl acetate to afford iminophosphane **83** (53-73% yield). Spectral data of *t*-butyl,[52] ethyl[68] and benzyl[69] triphenyliminophosphanes was in accordance with the literature.

3.5 General Procedure D: Synthesis of Isatin-Derived Ketimines

According to literature procedure,[53] in an oven-dried Schlenk flask related triphenyliminophosphane **83** (2.9 mmol) and isatin derivative **84** (2.6 mmol) were dissolved in 4 mL of dry 1,4-dioxane and refluxed under argon atmosphere until completion of the reaction. After evaporation of the organic solvent, the mixture was purified by flash column chromatography over silica gel column and EtOAc : hexane (1:3) eluent. Characterization of compounds **55a-t** was done by comparing with previously reported ^{1}H and ^{13}C NMR spectra.

3.6 General Procedure E: Racemic Synthesis of Aza-Friedel-Crafts Adducts

To a solution isatin ketimine **55** (0.1 mmol) and 1-naphthol (**42**) (1.1 eq, 15.9 mg) in CH_2Cl_2 (1 mL), triethylamine (0.10 mL) was added at room temperature. In the case of 2-naphthol (**47**) addition, to a solution of ketimine **55** (0.1 mmol), 2-naphthol (1.1 eq) in 1 mL of CH_2Cl_2, 5 mol% TEA and Schreiner's thiourea (10.0 mg) were added at room temperature. In each case, reaction progress was monitored by TLC and purified by silica gel column chromatography as described for asymmetric synthesis.

3.7 General Procedure F: Asymmetric Synthesis of Aza-Friedel-Crafts Adducts

To a test tube charged with 0.1 mmol of related ketimine **55**, 1.1 eq naphthol **42** or **47**, 25.0 mg 4Å molecular sieve and 2 mol% catalyst **64b**, 1 mL of CH_2Cl_2 was added at -20 °C. Reaction was monitored by TLC. Being colored by *p*-anisaldehyde stain, products on TLC plate were observed as blue spots. Upon completion, reaction content was directly loaded on silica

gel column chromatography. 1:5 (EtOAc : hexane) to 1:3 (EtOAc : hexane) gradient eluent afforded products **95a-t**, **96a-i**.

3.7.1 (*R*)-*tert*-Butyl (3-(1-hydroxynaphthalen-2-yl)-2-oxoindolin-3-yl)carbamate (95a)

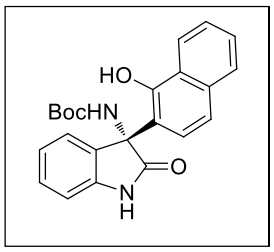

The use of (*E*)-*tert*-butyl (2-oxoindolin-3-ylidene)carbamate (**55a**) and 1-naphthol (**42**) in general procedure afforded chiral adduct **95a** as white solid in 18 h in 99% yield. mp 213-215 °C; $[\alpha]_D^{25}$= +352.1° (*c* 0.66, $CHCl_3$). Enantiomeric excess was determined by Chiralpak OD-H column, 90:10 (hexane : i-PrOH), 254 nm, 1 mL/min, t_{minor} = 7.48 min, t_{major} = 21.95 min, (97% ee). ^{1}H NMR ($CDCl_3$, 400 MHz) δ 10.79 (s, 1H), 8.95 (s, 1H), 8.46-8.42 (m, 1H), 7.71-7.65 (m, 1H), 7.52-7.46 (m, 2H), 7.39 (d, *J* = 7.3 Hz, 1H), 7.28-7.19 (m, 2H), 7.14 (d, *J* = 8.7 Hz, 1H), 6.82 (d, *J* = 8.7 Hz, 1H), 6.70 (bs, 1H), 6,02 (bs, 1H), 1.36 (s, 9H). ^{13}C NMR ($CDCl_3$, 100 MHz) δ 181.3, 154.5, 154.3, 141.2, 134.9, 129.6, 127.5, 127.1, 125.7, 125.5, 125.3, 123.3, 123.1, 119.6, 114.2, 111.6, 81.3, 66.4, 28.3. IR (neat): 3270, 3058, 2922, 2852, 1702, 1622, 1471, 1367, 1255, 1158, 808, 747 cm^{-1}. HRMS (ESI) m/z: calcd. for $C_{23}H_{22}N_2O_4Na$ $[M+Na]^+$: 413.1477; found 413.1480.

3.7.2 (*R*)-Benzyl (3-(1-hydroxynaphthalen-2-yl)-2-oxoindolin-3-yl)carbamate (95b)

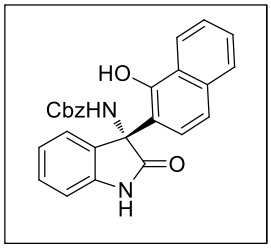

The use of (*E*)-benzyl (2-oxoindolin-3-ylidene)carbamate (**55b**) and 1-naphthol (**42**) in general procedure afforded chiral adduct **95b** as white solid in 48 h in 76% yield. mp 194-197 °C; $[\alpha]_D^{28}$=

+306.5° (*c* 0.57, $CHCl_3$). Enantiomeric excess was determined by Chiralpak OD-H column, 80:20 (hexane : i-PrOH), 254 nm, 1 mL/min, t_{minor} = 8.58 min, t_{major} = 20.03 min, (98% ee). ^{1}H NMR (400 MHz, $CDCl_3$) δ 10.71 (s, 1H), 8.63 (s, 1H), 8.44-8.38 (m, 1H), 7.71-7.64 (m, 1H), 7.54-7.44 (m, 2H), 7.38 (d, *J*= 7.1 Hz, 1H), 7.35-7.17 (m, 7H), 7.15 (d, *J* = 8.9 Hz, 1H), 6.81 (d, *J* = 8.8 Hz, 1H), 6.71 (d, *J* = 7.5 Hz, 1H), 6.29 (bs, 1H), 5.03 (s, 2H). ^{13}C NMR ($CDCl_3$, 100 MHz) δ 180.8, 154.9, 154.2, 141.0, 135.7, 135.0, 129.8, 128.5, 128.2, 127.9, 127.5, 127.1, 127.0, 125.75, 125.69, 125.1, 123.3, 123.2, 119.7, 119.5, 113.8, 111.5, 67.5, 66.5. IR (neat): 3248, 3034, 2921, 2852, 1704, 1682, 1525, 1460, 1383, 1259, 1058, 803, 747 cm^{-1}. HRMS (ESI) m/z: calcd. for $C_{26}H_{20}N_2O_4Na$ $[M+Na]^+$: 447.1321; found 447.1329.

3.7.3 (*R*)-Ethyl (3-(1-hydroxynaphthalen-2-yl)-2-oxoindolin-3-yl)carbamate (95c)

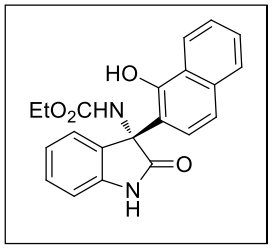

The use of (*E*)-ethyl (2-oxoindolin-3-ylidene)carbamate (**55c**) and 1-naphthol (**42**) in general procedure afforded chiral adduct **95c** as white solid in 48 h in 80% yield. mp 103-107 °C; $[\alpha]_D^{28}$= +353.9° (*c* 0.38, $CHCl_3$). Enantiomeric excess was determined by Chiralpak OD-H column, 90:10 (hexane : i-PrOH), 254 nm, 1 mL/min, t_{minor} = 12.73 min, t_{major} = 32.60 min, (99% ee). ^{1}H NMR (400 MHz, $CDCl_3$) δ 10.53 (s, 1H), 8.44 (dd, *J* = 6.1, 3.7 Hz, 1H), 7.76-7.68 (m, 1H), 7.65 (s, 1H), 7.51 (dd, *J* = 6.2, 3.4 Hz, 2H), 7.44-7.33 (m, 2H), 7.28-7.21 (m, 1H), 7.22 (d, *J* = 8.8 Hz, 1H), 6.95 (d, *J* = 7.8 Hz, 1H), 6.85 (d, *J* = 8.8 Hz, 1H), 5.94 (s, 1H), 4.05 (m, 2H), 1.23-1.12 (m, 3H). ^{13}C NMR ($CDCl_3$, 100 MHz) δ 181.0, 155.2, 154.3, 140.9, 135.1, 129.9, 129.2, 127.7, 127.2, 127.16, 126.0, 125.8, 125.3, 123.5, 123.4, 119.9, 114.0, 111.4, 66.5, 61.9, 14.4. IR (neat): 3286, 3060, 2958, 2922, 2853, 1694, 1621, 1471,

1256, 1059, 805, 748 cm^{-1}. HRMS (ESI) m/z: calcd. for $C_{21}H_{18}N_2O_4Na$ $[M+Na]^+$: 385.1164; found 385.1163.

3.7.4 (*R*)-*tert*-Butyl (1-ethyl-3-(1-hydroxynaphthalen-2-yl)-2-oxoindolin-3-yl)carbamate (95d)

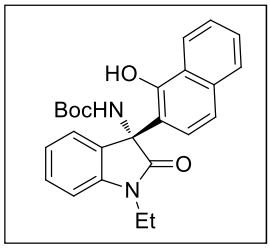

The use of (*E*)-*tert*-butyl (1-ethyl-2-oxoindolin-3-ylidene)carbamate (**55h**) and 1-naphthol (**42**) in general procedure afforded chiral adduct **95d** as white solid in 21 h in 61% yield. mp 93-95 °C; $[\alpha]_D^{22}$= +273.8° (*c* 0.57, $CHCl_3$). Enantiomeric excess was determined by Chiralpak OD-H column, 90:10 (hexane : i-PrOH), 254 nm, 1 mL/min, t_{major} = 5.05 min, t_{minor} = 6.28 min, (94% ee). ^{1}H NMR (400 MHz, $CDCl_3$) δ 10.92 (s, 1H), 8.45 (dd, *J* = 6.6, 3.1 Hz, 1H), 7.76 – 7.64 (m, 1H), 7.55 – 7.47 (m, 2H), 7.44 (d, *J* = 7.4 Hz, 2H), 7.31 – 7.22 (m, 1H), 7.18 (d, *J* = 8.8 Hz, 1H), 6.98 (d, *J* = 7.5 Hz, 1H), 6.82 (d, *J* = 8.8 Hz, 1H), 5.69 (s, 1H), 3.87 (dd, *J* = 14.1, 7.0 Hz, 1H), 3.71 (s, 1H), 1.29 (s, 9H), 1.26 (t, *J* = 7.3 Hz, 3H). ^{13}C NMR (100 MHz, $CDCl_3$) δ 178.3, 153.7, 153.5, 142.3, 134.9, 130.5, 130.1, 127.3, 127.2, 126.7, 126.3, 125.7, 124.1, 123.9, 122.9, 119.9, 117.6, 109.5, 80.2, 77.4, 35.4, 29.8, 12.6. IR (neat): 3286, 3058, 2922, 2852, 1693, 1619, 1470, 1383, 1256, 1088, 1059, 804, 749 cm^{-1}. HRMS (ESI) m/z: calcd. for $C_{25}H_{26}N_2O_4Na$ $[M+Na]^+$: 441.1790; found 441.1792.

3.7.5 (*R*)-*tert*-Butyl (1-benzyl-3-(1-hydroxynaphthalen-2-yl)-2-oxoindolin-3-yl)carbamate (95e)

The use of (*E*)-*tert*-butyl (1-benzyl-2-oxoindolin-3-ylidene)carbamate (**55g**) and 1-naphthol (**42**) in general procedure afforded chiral adduct **95e** as white solid in 12 h in 99% yield. mp 97-100 °C; $[\alpha]_D^{25}$= +317.6° (*c* 1.48,

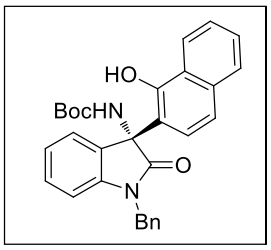

$CHCl_3$). Enantiomeric excess was determined by Chiralpak IA column, 80:20 (hexane : i-PrOH), 254 nm, 1 mL/min, t_{minor} = 12.00 min, t_{major} = 44.74 min, (99% ee). ^{1}H NMR (400 MHz, $CDCl_3$) δ 10.75 (s, 1H), 8.36 (dd, *J* = 5.4, 4.3 Hz, 1H), 7.66 – 7.53 (m, 1H), 7.46–7.35 (m, 2H), 7.31 (d, *J* = 7.1 Hz, 1H), 7.25–7.07 (m, 7H), 7.05 (d, *J* = 8.8 Hz, 1H), 6.70 (d, *J* = 8.8 Hz, 1H), 6.66 (d, *J* = 7.7 Hz, 1H), 5.79 (s, 1H), 4.94 (d, *J* = 14.6 Hz, 1H), 4.73 (d, *J* = 5.1 Hz, 1H), 1.23 (s, 9H). ^{13}C NMR (100 MHz, $CDCl_3$) δ 179.9, 154.2, 154.0, 142.7, 135.02, 134.97, 129.5, 128.90, 128.88, 127.7, 127.5, 127.1, 125.7, 125.5, 125.2, 123.6, 123.3, 119.7, 114.6, 110.4, 80.8, 66.3, 44.5, 28.2. IR (neat): 3324, 2972, 2923, 1686, 1614, 1466, 1366, 1257, 1157, 1072, 807, 746 cm^{-1}. HRMS (ESI) m/z: calcd. for $C_{30}H_{28}N_2O_4Na$ $[M+Na]^+$: 503.1947; found 503.1953.

3.7.6 (*R*)-*tert*-Butyl (3-(1-hydroxynaphthalen-2-yl)-1-methyl-2-oxoindolin-3-yl)carbamate (95f)

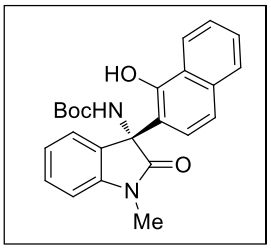

The use of (*E*)-*tert*-butyl (1-methyl-2-oxoindolin-3-ylidene)carbamate (**55i**) and 1-naphthol (**42**) in general procedure afforded chiral adduct **95f** as white solid in 21 h in 99% yield. mp 112-115 °C; $[\alpha]_D^{26}$= +391.4° (*c* 0.75, $CHCl_3$). Enantiomeric excess was determined by Chiralpak OD-H column, 95:5 (hexane : i-PrOH), 1 mL/min, 254 nm, t_{major} = 8.08 min, t_{minor} = 11.46 min, (99% ee). ^{1}H NMR (400 MHz, $CDCl_3$) δ 10.78 (s, 1H), 8.55 – 8.19 (m, 1H), 7.59 (dd, *J* = 6.6, 2.8 Hz, 1H), 7.48 – 7.38 (m, 2H), 7.38 – 7.30 (m, 2H), 7.18 (dd, *J* = 13.2, 5.7 Hz, 1H), 7.05 (d, *J* = 8.8 Hz, 1H), 6.85 (d, *J* = 7.8 Hz, 1H), 6.71 (d, *J* = 8.8 Hz, 1H), 5.66 (s, 1H), 3.14 (s, 3H), 1.19 (s, 9H). ^{13}C NMR (100 MHz, $CDCl_3$) δ 179.5, 154.1, 153.9, 143.3, 134.7, 129.5, 129.3, 127.3, 127.0, 126.9, 125.5, 125.3, 125.1, 123.4, 123.2, 119.3, 114.2, 109.2, 80.5, 66.0, 28.0, 26.7. IR (neat): 3322,

3057, 2974, 2923, 1688, 1613, 1570, 1470, 1366, 1253, 1159, 1075, 808, 747 cm^{-1}. HRMS (ESI) m/z: calcd. for $C_{24}H_{24}N_2O_4Na$ $[M+Na]^+$: 427.1634; found 427.1639.

3.7.7 (*R*)-*tert*-Butyl (1-acetyl-3-(1-hydroxynaphthalen-2-yl)-2-oxoindolin-3-yl)carbamate (95g)

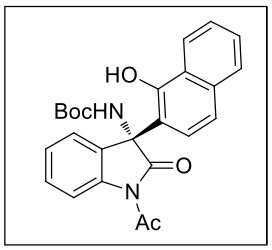

The use of (*E*)-*ter*t-butyl (1-acetyl-2-oxoindolin-3-ylidene)carbamate (**55j**) and 1-naphthol (**42**) in general procedure afforded adduct **95g** as white solid in 18 h in 78% yield. mp 188-191 °C; $[\alpha]_D^{28}$= +3.1° (*c* 1.05, $CHCl_3$). Enantiomeric excess was determined by Chiralpak OD-H column, 95:5 (hexane : i-PrOH), 254 nm, 1 mL/min, t_{major} = 9.39 min, t_{minor} = 12.24 min, (3% ee). ^{1}H NMR (400 MHz, $CDCl_3$) δ 9.58 (s, 1H), 8.43 (dd, *J* = 6.0, 3.4 Hz, 1H), 8.33 (d, *J* = 7.9 Hz, 1H), 7.70 (dd, *J* = 6.0, 3.2 Hz, 1H), 7.56 – 7.43 (m, 3H), 7.40 (t, *J* = 6.8 Hz, 2H), 7.18 (d, *J* = 8.8 Hz, 1H), 6.62 (d, *J* = 8.8 Hz, 1H), 5.87 (s, 1H), 2.64 (s, 3H), 1.28 (s, 9H). ^{13}C NMR (100 MHz, $CDCl_3$) δ 180.3, 170.6, 154.0, 153.7, 140.4, 135.2, 130.1, 127.9, 127.3, 126.8, 126.1, 126.0, 125.2, 124.84, 124.77, 123.2, 120.2, 117.3, 113.7, 81.7, 66.6, 28.1, 26.7. IR (neat): 33450, 3211, 2973, 2921, 2852, 1708, 1464, 1370, 1253, 1161, 1015, 754 cm^{-1}. HRMS (ESI) m/z: calcd. for $C_{25}H_{24}N_2O_5Na$ $[M+Na]^+$: 455.1583; found 455.1589.

3.7.8 (*R*)-*tert*-Butyl (3-(1-hydroxynaphthalen-2-yl)-5,7-dimethyl-2-oxoindolin-3-yl)carbamate (95h)

The use of (*E*)-*tert*-butyl (5,7-dimethyl-2-oxoindolin-3-ylidene)carbamate (**55r**) and 1-naphthol (**42**) in general procedure afforded chiral adduct **95h** as white solid in 18 h in 98% yield. mp 139-143 °C; $[\alpha]_D^{28}$= +70.6° (*c* 0.92, $CHCl_3$). Enantiomeric excess was determined by Chiralpak IA column,

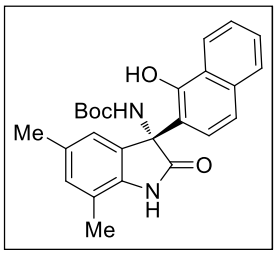

80:20 (hexane : i-PrOH), 254 nm, 1 mL/min, t_{minor} = 8.24 min, t_{major} = 10.88 min, (37% ee). ^{1}H NMR (400 MHz, $CDCl_3$) δ 10.65 (s, 1H), 9.89 (s, 1H), 8.60 – 8.29 (m, 1H), 7.71 (d, *J* = 4.8 Hz, 1H), 7.50 (dd, *J* = 5.7, 3.6 Hz, 2H), 7.17 (d, *J* = 8.8 Hz, 1H), 7.03 (s, 1H), 6.96 (s, 1H), 6.85 (d, *J* = 8.8 Hz, 1H), 5.95 (s, 1H), 2.41 (s, 3H), 2.20 (s, 3H), 1.26 (s, 9H). ^{13}C NMR (100 MHz, $CDCl_3$) δ 182.4, 154.2, 137.2, 134.9, 132.9, 131.5, 129.5, 127.3, 127.1, 125.5, 123.6, 123.3, 120.6, 119.5, 114.4, 81.1, 67.1, 28.0, 21.3, 16.1. IR (neat): 3322, 3056, 2973, 2923, 1688, 1613, 1470, 1378, 1253, 1159, 1057, 808, 747 cm^{-1}. HRMS (ESI) m/z: calcd. for $C_{25}H_{26}N_2O_4Na$ $[M+Na]^+$: 441.1790; found 441.1798.

3.7.9 (*R*)-*tert*-Butyl (5-bromo-3-(1-hydroxynaphthalen-2-yl)-2-oxoindolin-3-yl)carbamate (95i)

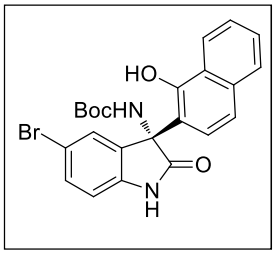

The use of (*E*)-*tert*-butyl (5-bromo-2-oxoindolin-3-ylidene)carbamate (**55q**) and 1-naphthol (**42**) in general procedure afforded chiral adduct **95i** as white solid in 21 h in 73% yield. mp 169-173 °C; $[\alpha]_D^{25}$= +223.3° (*c* 0.46, $CHCl_3$). Enantiomeric excess was determined by Chiralpak OD-H column, 90:10 (hexane : i-PrOH), 254 nm, 1 mL/min, t_{minor} = 7.27 min, t_{major} = 18.09 min, (97% ee). ^{1}H NMR (400 MHz, DMSO-d_6) δ 11.03 (s, 1H), 10.46 (s, 1H), 8.30–8.20 (m, 1H), 8.10 (s, 1H), 7.86–7.73 (m, 1H), 7.54-7.48 (m, 4H), 7.32 (d, *J* = 8.8 Hz, 1H), 6.90 (dd, *J* = 10.9, 8.5 Hz, 2H), 1.27 (s, 9H). ^{13}C NMR (100 MHz, DMSO-d_6) δ 179.7, 154.1, 152.9, 141.3, 134.1, 133.6, 131.7, 127.3, 127.2, 127.0, 125.9, 125.4, 124.9, 122.4, 119.1, 115.2, 113.9, 112.4, 79.3, 65.8, 27.8. IR (neat): 3288, 3060, 2924, 2853, 1741, 1671, 1517, 1474, 1382, 1283, 1155, 808, 604 cm^{-1}. HRMS (ESI) m/z: calcd. for $C_{23}H_{21}BrN_2O_4Na$ $[M+Na]^+$: 491.0582; found 491.0584.

3.7.10 (*R*)-*tert*-Butyl (5-fluoro-3-(1-hydroxynaphthalen-2-yl)-2-oxoindolin-3-yl)carbamate (95j)

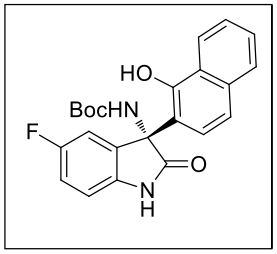

The use of (*E*)-*tert*-butyl (5-fluoro-2-oxoindolin-3-ylidene)carbamate (**55s**) and 1-naphthol (**42**) in general procedure afforded chiral adduct **95j** as white solid in 18 h in 67% yield. mp 125-127 °C; $[\alpha]_D^{26}$= +221.3° (*c* 0.74, $CHCl_3$). Enantiomeric excess was determined by Chiralpak OD-H column, 90:10 (hexane : i-PrOH), 254 nm, 1 mL/min, t_{minor} = 10.49 min, t_{major} = 18.01 min, (92% ee). ^{1}H NMR (400 MHz, DMSO-d_6) δ 10.97 (s, 1H), 10.65 (s, 1H), 8.29 (dd, *J* = 5.4, 4.4 Hz, 1H), 8.11 (s, 1H), 7.79 (dd, *J* = 6.3, 3.1 Hz, 1H), 7.61 – 7.44 (m, 2H), 7.29 (d, *J* = 8.8 Hz, 1H), 7.24 – 7.11 (m, 2H), 6.96 (dd, *J* = 8.4, 4.3 Hz, 1H), 6.87 (d, *J* = 8.8 Hz, 1H), 1.27 (s, 9H). ^{13}C NMR (100 MHz, $CDCl_3$) δ 180.5, 158.4 (d, *J* = 238.3 Hz), 156.3, 154.1, 153.3, 138.1, 134.2, 132.8 (d, *J* = 8.3 Hz), 127.1, 127.0, 126.1, 125.3, 125.1, 122.5, 119.0, 115.4 (d, *J* = 23.3 Hz), 114.8, 112.5 (d, *J* = 25.1 Hz), 111.4 (d, *J* = 7.9 Hz), 79.19, 77.0, 66.3, 28.3. IR (neat): 3269, 2956, 2922, 2853, 1704, 1487, 1367, 1259, 1160, 1078, 798, 748 cm^{-1}. HRMS (ESI) m/z: calcd. for $C_{23}H_{21}FN_2O_4Na$ $[M+Na]^+$: 431.1383; found 431.1388.

3.7.11 (*R*)-Benzyl (3-(1-hydroxynaphthalen-2-yl)-1-methyl-2-oxoindolin-3-yl)carbamate (95k)

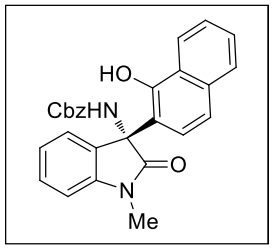

The use of (*E*)-benzyl (1-methyl-2-oxoindolin-3-ylidene)carbamate (**55e**) and 1-naphthol (**42**) in general procedure afforded chiral adduct **95k** as white solid in 18 h in 94% yield. mp 90-92 °C; $[\alpha]_D^{28}$= +341.2° (*c* 0.85, $CHCl_3$). Enantiomeric excess was determined by Chiralpak AD-H column, 80:20 (hexane : i-PrOH), 254 nm,

1 mL/min, t_{minor} = 17.30 min, t_{major} = 19.96 min, (>99% ee). ^{1}H NMR (400 MHz, $CDCl_3$) δ 10.90 (s, 1H), 8.43 (dd, *J* = 6.2, 3.5 Hz, 1H), 7.75–7.60 (m, 1H), 7.49 (dd, *J* = 6.3, 3.4 Hz, 2H), 7.47–7.39 (m, 2H), 7.31-7.26 (m, 5H), 7.17 (d, *J* = 8.8 Hz, 2H), 6.95 (s, 1H), 6.83 (d, *J* = 8.8 Hz, 1H), 6.14 (s, 1H), 4.99 (s, 2H), 3.25 (s, 3H). ^{13}C NMR (100 MHz, $CDCl_3$) δ 179.3, 154.7, 154.4, 143.7, 135.0, 130.0, 128.8, 128.6, 128.3, 128.2, 127.6, 127.2, 127.1, 125.8, 125.7, 125.2, 123.7, 123.4, 119.7, 114.0, 109.5, 67.3, 64.5, 25.5. IR (neat): 3391, 3305, 3059, 2918, 2850, 1686, 1612, 1494, 1469, 1253, 1073, 747 cm^{-1}. HRMS (ESI) m/z: calcd. for $C_{27}H_{22}N_2O_4Na$ $[M+Na]^+$: 461.1477; found 461.1484.

3.7.12 (*R*)-Ethyl (3-(1-hydroxynaphthalen-2-yl)-1-methyl-2-oxoindolin-3-yl)carbamate (95l)

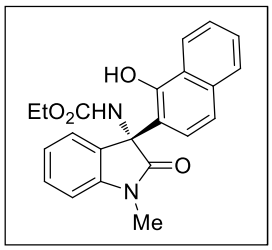

The use of (*E*)-ethyl (1-methyl-2-oxoindolin-3-ylidene)carbamate (**55d**) and 1-naphthol (**42**) in general procedure afforded chiral adduct **95l** as white solid in 15 h in 99% yield. mp 89-91°C; $[\alpha]_D^{26}$= +391.7° (c 1.00, $CHCl_3$). Enantiomeric excess was determined by Chiralpak AD-H column, 90:10 (hexane : i-PrOH), 254 nm, 1 mL/min, t_{major} = 26.12 min, t_{minor} = 27.76 min, (97% ee). ^{1}H NMR (400 MHz, $CDCl_3$) δ 10.93 (s, 1H), 8.61 – 8.16 (m, 1H), 7.63 (dd, *J* = 12.3, 9.0 Hz, 1H), 7.51 – 7.36 (m, 4H), 7.25 (dd, *J* = 15.1, 7.6 Hz, 1H), 7.09 (d, *J* = 8.8 Hz, 1H), 6.93 (d, *J* = 7.8 Hz, 1H), 6.79 (d, *J* = 8.8 Hz, 1H), 6.13 (s, 1H), 4.08 – 3.91 (m, 2H), 3.21 (s, 3H), 1.31 – 1.19 (m, 3H). ^{13}C NMR (100 MHz, $CDCl_3$) δ 179.5, 155.0, 154.3, 143.8, 135.0, 129.9, 128.8, 127.5, 127.2, 127.1, 125.72, 125.67, 125.2, 123.6, 123.3, 119.7, 114.1, 109.4, 66.2, 61.6, 27.0, 14.4. IR (neat): 3306, 3058, 2918, 2850, 1717, 1686, 1613, 1379, 1253, 1074, 806, 747 cm^{-1}. HRMS (ESI) m/z: calcd. for $C_{22}H_{20}N_2O_4Na$ $[M+Na]^+$: 399.1321; found 399.1322.

3.7.13 (*R*)-*tert*-Butyl (3-(1-hydroxynaphthalen-2-yl)-1,5-dimethyl-2-oxoindolin-3-yl)carbamate (95m)

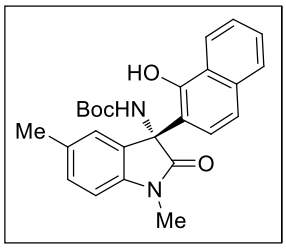

The use of (*E*)-*tert*-butyl (1,5-dimethyl-2-oxoindolin-3-ylidene)carbamate (**55n**) and 1-naphthol (**42**) in general procedure afforded chiral adduct **95m** as white solid in 15 h in 98% yield. mp 119-121 °C; $[\alpha]_D^{26}$= +336.0° (*c* 1.05, $CHCl_3$). Enantiomeric excess was determined by Chiralpak OD-H column, 90:10 (hexane : i-PrOH), 254 nm, 1 mL/min, t_{major} = 6.63 min, t_{minor} = 8.84 min, (97% ee). ^{1}H NMR (400 MHz, $CDCl_3$) δ 10.84 (s, 1H), 8.53 – 8.15 (m, 1H), 7.55 – 7.46 (m, 1H), 7.40 – 7.28 (m, 2H), 7.16 – 7.01 (m, 2H), 6.89 (d, *J* = 8.7 Hz, 1H), 6.65 (dd, *J* = 8.3, 2.9 Hz, 2H), 5.79 (s, 1H), 3.02 (s, 3H), 2.33 (s, 3H), 1.15 (s, 9H). ^{13}C NMR (100 MHz, $CDCl_3$) δ 179.4, 154.2, 154.0, 141.0, 134.8, 133.0, 129.8, 129.3, 127.3, 127.0, 126.1, 125.5, 125.2, 123.2, 119.3, 114.4, 108.9, 80.5, 66.2, 28.1, 26.8, 21.3. IR (neat): 3307, 2918, 2850, 1687, 1496, 1378, 1253, 1074, 807, 748 cm^{-1}. HRMS (ESI) m/z: calcd. for $C_{25}H_{26}N_2O_4Na$ $[M+Na]^+$: 441.1790; found 441.1798.

3.7.14 (*R*)-*tert*-Butyl (7-fluoro-3-(1-hydroxynaphthalen-2-yl)-1-methyl-2-oxoindolin-3-yl)carbamate (95n)

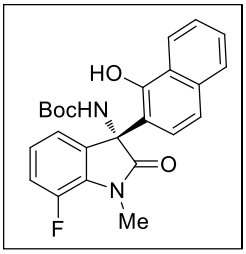

The use of (*E*)-*tert*-butyl (7-fluoro-1-methyl-2-oxoindolin-3-ylidene)carbamate (**55k**) and 1-naphthol (**42**) in general procedure afforded chiral adduct **95n** as white solid in 15 h in 94% yield. mp 192-195 °C; $[\alpha]_D^{20}$= +395.8° (*c* 1.01, $CHCl_3$). Enantiomeric excess was determined by Chiralpak IA column, 90:10 (hexane : i-PrOH), 254 nm, 1 mL/min, t_{major} = 10.98 min, t_{minor} = 12.32 min, (>99% ee). ^{1}H NMR (400 MHz, $CDCl_3$) δ 10.70 (s, 1H), 8.44 (dd, *J* = 6.2, 3.5 Hz, 1H), 7.70 (dd, *J* =

6.2, 3.2 Hz, 1H), 7.51 (dd, *J* = 6.3, 3.3 Hz, 2H), 7.23 – 7.14 (m, 4H), 6.73 (d, *J* = 8.8 Hz, 1H), 5.75 (s, 1H), 3.45 (d, *J* = 2.5 Hz, 3H), 1.32 (s, 9H). ^{13}C NMR (100 MHz, $CDCl_3$) δ 179.4, 154.4, 154.0, 148.6 (d, *J* = 245.2 Hz), 135.0, 132.4, 130.2 (d, *J* = 8.7 Hz), 127.7, 127.2, 127.1, 125.9, 125.0, 124.2 (d, *J* = 6.3 Hz), 123.4, 121.3 (d, *J* = 3.2 Hz), 119.8, 117.8 (d, *J* = 19.4 Hz), 113.9, 81.1, 66.3, 29.8, 28.2. IR (neat): 3311, 2919, 2851, 1691, 1471, 1375, 1254, 1074, 806, 752 cm^{-1}. HRMS (ESI) m/z: calcd. for $C_{24}H_{23}FN_2O_4Na$ $[M+Na]^+$: 445.1540; found 445.1547.

3.7.15 (*R*)-*tert*-Butyl (6-bromo-3-(1-hydroxynaphthalen-2-yl)-1-methyl-2-oxoindolin-3-yl)carbamate (95o)

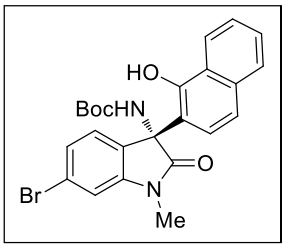

The use of (*E*)-*tert*-butyl (6-bromo-1-methyl-2-oxoindolin-3-ylidene)carbamate (**55o**) and 1-naphthol (**42**) in general procedure afforded chiral adduct **95o** as white solid in 24 h in 70% yield. mp 112-115 °C; $[\alpha]_D^{20}$= +341.9° (*c* 0.86, $CHCl_3$). Enantiomeric excess was determined by Chiralpak AD-H column, 80:20 (hexane : i-PrOH), 254 nm, 1 mL/min, t_{major} = 7.35 min, t_{minor} = 10.53 min, (99% ee). ^{1}H NMR (400 MHz, $CDCl_3$) δ 10.65 (s, 1H), 8.43 (dd, *J* = 6.2, 3.5 Hz, 1H), 7.70 (dd, *J* = 6.1, 3.3 Hz, 1H), 7.55 – 7.47 (m, 2H), 7.42 (dd, *J* = 7.9, 1.6 Hz, 1H), 7.28 (d, *J* = 7.9 Hz, 2H), 7.18 (d, *J* = 8.8 Hz, 1H), 7.11 (d, *J* = 1.6 Hz, 1H), 6.76 (d, *J* = 8.8 Hz, 1H), 5.75 (s, 1H), 3.23 (s, 3H), 1.32 (s, 9H). ^{13}C NMR (100 MHz, $CDCl_3$) δ 179.6, 154.3, 153.9, 144.9, 135.1, 128.4, 127.7, 127.19, 127.16, 126.7, 126.5, 125.9, 124.9, 123.4, 123.3, 119.8, 113.8, 113.0, 81.1, 65.9, 28.3, 27.1. IR (neat): 3317, 2926, 1693, 1606, 1366, 1161, 805, 759 cm^{-1}. HRMS (ESI) m/z: calcd. for $C_{24}H_{24}N_2O_4Br$ $[M+H]^+$: 483.0919; found 483.0941.

3.7.16 (*R*)-*tert*-Butyl (7-chloro-3-(1-hydroxynaphthalen-2-yl)-1-methyl-2-oxoindolin-3-yl)carbamate (95p)

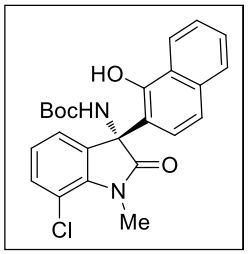

The use of (*E*)-*tert*-butyl (7-chloro-1-methyl-2-oxoindolin-3-ylidene)carbamate (**55l**) and 1-naphthol (**42**) in general procedure afforded chiral adduct **95p** as white solid in 15 h in 90% yield. mp 87-90 °C; $[\alpha]_D^{20}$= +409.0° (*c* 1.01, $CHCl_3$). Enantiomeric excess was determined by Chiralpak IA column, 85:15 (hexane : i-PrOH), 254 nm, 1 mL/min, t_{major} = 9.02 min, t_{minor} = 14.77 min, (99% ee). ^{1}H NMR (400 MHz, $CDCl_3$) δ 10.68 (s, 1H), 8.44 (dd, *J* = 6.3, 3.5 Hz, 1H), 7.70 (dd, *J* = 6.1, 3.3 Hz, 1H), 7.55 - 7.48 (m, 2H), 7.37 (d, *J* = 8.1 Hz, 1H), 7.30 (dd, *J* = 7.3, 1.2 Hz, 1H), 7.20 - 7.16 (m, 2H), 6.69 (d, *J* = 8.8 Hz, 1H), 5.75 (s, 1H), 3.60 (s, 3H), 1.32 (s, 9H). ^{13}C NMR (100 MHz, $CDCl_3$) δ 180.0, 154.4, 153.9, 139.4, 135.1, 132.1, 127.8, 127.7, 127.17, 127.16, 125.9, 124.9, 124.3, 124.0, 123.4, 119.8, 116.9, 114.0, 81.2, 65.7, 30.5, 28.3. IR (neat): 3324, 3055, 2975, 2924, 1693, 1463, 1366, 1256, 1114, 802, 737 cm^{-1}. HRMS (ESI) m/z: calcd. for $C_{24}H_{23}ClN_2O_4Na$ $[M+Na]^+$: 461.1244; found 461.1252.

3.7.17 (*R*)-*tert*-Butyl (3-(1-hydroxynaphthalen-2-yl)-5-methoxy-1-methyl-2-oxoindolin-3-yl)carbamate (95q)

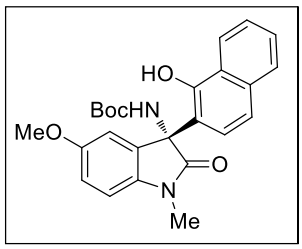

The use of (*E*)-*tert*-butyl (5-methoxy-1-methyl-2-oxoindolin-3-ylidene)carbamate (**55t**) and 1-naphthol (**42**) in general procedure afforded chiral adduct **95q** as white solid in 12 h in 99% yield. mp 97-101 °C; $[\alpha]_D^{20}$= +376.8° (*c* 0.91, $CHCl_3$). Enantiomeric excess was determined by Chiralpak IA column, 80:20 (hexane : i-PrOH), 254 nm, 1 mL/min, t_{major} = 10.91 min, t_{minor} = 14.05 min,

(98% ee). ^{1}H NMR (400 MHz, $CDCl_3$) δ 10.96 (s, 1H), 8.45 (dd, *J* = 6.2, 3.6 Hz, 1H), 7.74 – 7.61 (m, 1H), 7.49 (dd, *J* = 6.3, 3.3 Hz, 2H), 7.17 (d, *J* = 8.7 Hz, 1H), 7.04 (d, *J* = 2.5 Hz, 1H), 6.95 (dd, *J* = 8.5, 2.6 Hz, 1H), 6.85 (dd, *J* = 8.6, 2.3 Hz, 2H), 5.74 (s, 1H), 3.87 (s, 3H), 3.21 (s, 3H), 1.31 (s, 9H). ^{13}C NMR (100 MHz, $CDCl_3$) δ 179.3, 156.8, 154.4, 154.0, 137.0, 135.0, 130.8, 127.5, 127.2, 127.1, 125.7, 125.2, 123.4, 119.6, 114.5, 113.9, 112.9, 109.8, 80.9, 66.5, 56.1, 28.3, 27.1. IR (neat): 3319, 2924, 1682, 1497, 1366, 1286, 1161, 1031, 808, 736 cm^{-1}. HRMS (ESI) m/z: calcd. for $C_{25}H_{26}N_2O_5Na$ $[M+Na]^+$: 457.1739; found 457.1746.

3.7.18 (*R*)-*tert*-Butyl (6-chloro-3-(1-hydroxynaphthalen-2-yl)-1-methyl-2-oxoindolin-3-yl)carbamate (95r)

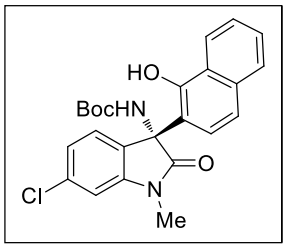

The use of (*E*)-*tert*-butyl (6-chloro-1-methyl-2-oxoindolin-3-ylidene)carbamate (**55m**) and 1-naphthol (**42**) in general procedure afforded chiral adduct **95r** as white solid in 24 h in 90% yield. mp 184-187 °C; $[\alpha]_D^{20}$= +356.8° (*c* 0.99, $CHCl_3$). Enantiomeric excess was determined by Chiralpak AD-H column, 80:20 (hexane : i-PrOH), 254 nm, 1 mL/min, t_{major} = 7.22 min, t_{minor} = 10.29 min, (99% ee). ^{1}H NMR (400 MHz, $CDCl_3$) δ 10.65 (s, 1H), 8.43 (dd, *J* = 6.3, 3.5 Hz, 1H), 7.69 (dd, *J* = 6.1, 3.3 Hz, 1H), 7.55 – 7.45 (m, 2H), 7.34 (d, *J* = 7.9 Hz, 1H), 7.26 (dd, *J* = 7.9, 1.8 Hz, 1H), 7.16 (d, *J* = 8.8 Hz, 1H), 6.96 (d, *J* = 1.7 Hz, 1H), 6.76 (d, *J* = 8.8 Hz, 1H), 5.77 (s, 1H), 3.22 (s, 3H), 1.32 (s, 9H). ^{13}C NMR (100 MHz, $CDCl_3$) δ 179.7, 154.3, 153.9, 144.8, 135.5, 135.0, 127.8, 127.7, 127.16, 127.15, 126.4, 125.9, 124.9, 123.5, 123.3, 119.8, 113.9, 110.2, 81.1, 65.9, 28.3, 27.1. IR (neat): 3320, 2977, 1694, 1609, 1367, 1251, 1162, 1069, 806, 751 cm^{-1}. HRMS (ESI) m/z: calcd. for $C_{24}H_{24}ClN_2O_4$ $[M+H]^+$: 439.1425; found 439.1423.

3.7.19 (*R*)-*tert*-Butyl(1-benzyl-3-(1-hydroxy-4-methoxynaphthalen-2-yl)-2-oxoindolin-3-yl)carbamate (95s)

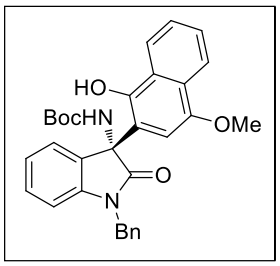

The use of (*E*)-*tert*-butyl (1-benzyl-2-oxoindolin-3-ylidene)carbamate (**55g**) and 4-methoxy-1-naphthol in general procedure afforded chiral adduct **95s** as white solid in 20 h in 96% yield. mp 155-157 °C; $[\alpha]_D^{20}$= +329.6° (*c* 1.00, $CHCl_3$). Enantiomeric excess was determined by Chiralpak IA column, 80:20 (hexane : i-PrOH), 254 nm, 1 mL/min, t_{minor} = 10.38 min, t_{major} = 25.96 min, (91% ee). ^{1}H NMR (400 MHz, $CDCl_3$) δ 10.25 (s, 1H), 8.33 (dd, *J* = 7.2, 2.1 Hz, 1H), 8.01 (dd, *J* = 7.1, 2.1 Hz, 1H), 7.50 – 7.39 (m, 2H), 7.36 (dd, *J* = 7.2, 0.8 Hz, 1H), 7.26 – 7.18 (m, 2H), 7.18 – 7.09 (m, 5H), 6.69 (d, *J* = 7.7 Hz, 1H), 6.05 (s, 1H), 5.87 (s, 1H), 4.94 (d, *J* = 15.5 Hz, 1H), 4.80 (s, 1H).), 3.52 (s, 3H), 1.25 (s, 9H). ^{13}C NMR (100 MHz, $CDCl_3$) δ 179.8, 154.1, 149.0, 147.8, 142.7, 135.0, 129.6, 129.5, 128.9, 127.9, 127.7, 127.2, 126.9, 126.7, 126.4, 125.2, 123.3, 123.2, 121.5, 113.8, 110.5, 103.6, 80.8, 66.3, 55.5, 44.5, 28.3. IR (neat): 3370, 2973, 1710, 1687, 1491, 1451, 1242, 1154, 1005, 846, 764 cm^{-1}. HRMS (ESI) m/z: calcd. for $C_{31}H_{30}N_2O_5Na$ $[M+Na]^+$: 533.2052; found 533.2029.

3.7.20 (*R*)-*tert*-Butyl(1-benzyl-3-(4-chloro-1-hydroxynaphthalen-2-yl)-2-oxoindolin-3-yl)carbamate (95t)

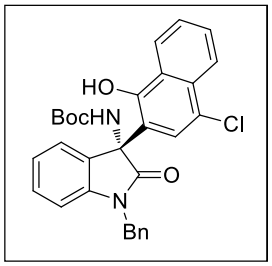

The use of (*E*)-*tert*-butyl (1-benzyl-2-oxoindolin-3-ylidene)carbamate (**55g**) and 4-chloro-1-naphthol in general procedure afforded chiral adduct **95t** as white solid in 20 h in 74% yield. mp 201-203 °C (decomposed); $[\alpha]_D^{20}$= +338.3° (*c* 0.98, $CHCl_3$). Enantiomeric excess was determined by Chiralpak IA column, 80:20 (hexane : i-PrOH), 254 nm, 1 mL/min, t_{minor} = 10.35 min, t_{major} = 18.27 min, (99% ee). ^{1}H NMR (400 MHz, $CDCl_3$) δ

10.99 (s, 1H), 8.48 (d, *J* = 8.1 Hz, 1H), 8.09 (d, *J* = 8.2 Hz, 1H), 7.63 (ddd, *J* = 8.3, 6.9, 1.3 Hz, 1H), 7.59 – 7.53 (m, 1H), 7.43 (dd, *J* = 7.2, 1.0 Hz, 1H), 7.35 – 7.20 (m, 7H), 6.93 (s, 1H), 6.80 (d, *J* = 7.7 Hz, 1H), 5.80 (s, 1H), 5.03 (d, *J* = 15.7 Hz, 1H), 4.86 (d, *J* = 14.1 Hz, 1H), 1.31 (s, 9H). ^{13}C NMR (100 MHz, $CDCl_3$) δ 179.7, 153.9, 153.6, 142.7, 134.9, 131.9, 129.9, 129.0, 128.8, 128.7, 128.2, 127.9, 127.3, 126.5, 125.4, 125.1, 124.05, 123.98, 123.9, 122.9, 114.9, 110.7, 81.1, 65.9, 44.7, 28.3. IR (neat): 3242, 2971, 1707, 1686, 1613, 1352, 1156, 1018, 757, cm^{-1}. HRMS (ESI) m/z: calcd. for $C_{30}H_{27}ClN_2O_4Na$ $[M+Na]^+$: 537.1557; found 537.1533.

3.7.21 (*R*)-*tert*-Butyl (1-benzyl-3-(2-hydroxynaphthalen-1-yl)-2-oxoindolin-3-yl)carbamate (96a)

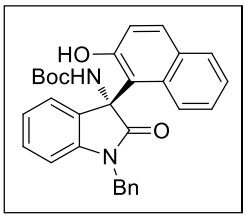

The use of (*E*)-*tert*-butyl (1-benzyl-2-oxoindolin-3-ylidene)carbamate (**55g**) and 2-naphthol (**47**) in general procedure afforded chiral adduct **96a** as white solid in 18 h in 99% yield. mp 89-91 °C; $[\alpha]_D^{25}$= +55.0° (*c* 0.57, $CHCl_3$). Enantiomeric excess was determined by Chiralpak IA column, 80:20 (hexane : i-PrOH), 254 nm, 1 mL/min, t_{minor} = 15.39 min, t_{major} = 34.72 min, (97% ee). ^{1}H NMR (400 MHz, DMSO-d_6) δ 10.19 (s, 1H), 8.93 (d, *J* = 8.6 Hz, 1H), 7.81 (d, *J* = 8.2 Hz, 2H), 7.70 (d, *J* = 8.8 Hz, 1H), 7.57 (d, *J* = 7.4 Hz, 2H), 7.51 – 7.45 (m, 1H), 7.43 (d, *J* = 7.5 Hz, 1H), 7.39 – 7.25 (m, 4H), 7.11 (t, *J* = 7.7 Hz, 1H), 7.04 (d, *J* = 8.8 Hz, 1H), 6.81 (t, *J* = 7.5 Hz, 1H), 6.74 (d, *J* = 7.8 Hz, 1H), 5.76 (s, 1H), 4.01 (d, *J* = 16.0 Hz, 1H), 4.93 (d, *J* = 16.0 Hz, 1H) 1.20 (s, 9H). ^{13}C NMR (100 MHz, DMSO-d_6) δ 176.4, 154.0, 152.0, 143.6, 136.8, 132.8, 131.0, 129.6, 129.4, 128.8, 128.3, 128.1, 127.5, 127.0, 125.6, 125.4, 123.4, 122.3, 121.6, 118.7, 116.5, 108.5, 78.3, 63.6, 55.1, 43.7, 39.5, 27.9. IR (neat): 3217, 2973, 1693, 1609, 1466, 1347, 1156, 815, 749 cm^{-1}. HRMS (ESI) m/z: calcd. for $C_{30}H_{28}N_2O_4Na$ $[M+Na]^+$: 503.1947; found 503.1955.

3.7.22 (*R*)-*tert*-Butyl (3-(2-hydroxynaphthalen-1-yl)-1-methyl-2-oxoindolin-3-yl)carbamate (96b)

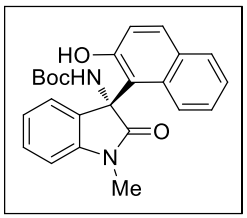

The use of (*E*)-*tert*-butyl (1-methyl-2-oxoindolin-3-ylidene)carbamate (**55i**) and 2-naphthol (**47**) in general procedure afforded chiral adduct **96b** as white solid in 18 h in 85% yield. mp 117-119 °C; $[\alpha]_D^{25}$= +84.37˚ (*c* 0.98, $CHCl_3$). Enantiomeric excess was determined by Chiralpak AD-H column, 80:20 (hexane : i-PrOH), 254 nm, 1 mL/min, t_{minor} = 6.83 min, t_{major} = 30.74 min, (79% ee). ^{1}H NMR (400 MHz, $CDCl_3$) δ 9.82 (s, 1H), 7.67 (d, *J* = 7.8 Hz, 1H), 7.55 (d, *J* = 8.8 Hz, 1H), 7.47 – 7.27 (m, 3H), 7.20 (q, *J* = 7.3 Hz, 1H), 7.15 – 7.04 (m, 3H), 6.97 (d, *J* = 7.8 Hz, 1H), 5.87 (s, 1H), 3.32 (s, 3H), 1.28 (s, 9H). ^{13}C NMR (100 MHz, $CDCl_3$) δ 179.7, 155.2, 154.1, 143.9, 132.0, 131.5, 130.8, 130.4, 129.6, 129.1, 125.8, 125.3, 124.6, 123.5, 122.9, 121.1, 114.7, 108.9, 80.7, 65.4, 28.3, 27.0. IR (neat): 3368, 2970, 1703, 1607, 1470, 1348, 1243, 1157, 1055, 826, 754 cm^{-1}. HRMS (ESI) m/z: calcd. for $C_{24}H_{24}N_2O_4Na$ $[M+Na]^+$: 427.1637; found 427.1640.

3.7.23 (*R*)-Ethyl (3-(2-hydroxynaphthalen-1-yl)-2-oxoindolin-3-yl)carbamate (96c)

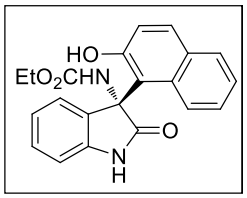

The use of (*E*)-ethyl (2-oxoindolin-3-ylidene)carbamate (**55c**) and 2-naphthol (**47**) in general procedure afforded chiral adduct **96c** as white solid in 36 h in 76% yield. mp 98-100 °C; $[\alpha]_D^{36}$= -154.0° (*c* 0.92, $CHCl_3$). Enantiomeric excess was determined by Chiralpak IA column, 80:20 (hexane : i-PrOH), 254 nm, 1 mL/min, t_{minor} = 17.85 min, t_{major} = 35.80 min, (73% ee). ^{1}H NMR (400 MHz, $CDCl_3$) δ 9.36 (s, 1H), 9.08 (s, 1H), 8.03 – 7.89 (m, 1H), 7.70 (d, *J* = 7.9 Hz, 1H), 7.48 – 7.36 (m, 2H), 7.32 – 7.21 (m, 2H), 7.09 (s, 1H), 6.97 – 6.79 (m, 2H), 6.72 (s, 1H), 6.22 (d, *J* = 4.6 Hz,

1H), 4.01 (q, *J* = 6.9 Hz, 2H), 1.10 (t, *J* = 6.9 Hz, 3H). ^{13}C NMR (100 MHz, $CDCl_3$) δ 181.2, 154.9, 141.5, 132.1, 131.9, 131.5, 131.2, 131.1, 130.8, 130.4, 130.4, 129.6, 129.3, 126.2, 125.1, 124.7, 123.1, 111.1, 65.4, 61.6, 14.4. IR (neat): 3250, 2988, 1698, 1619, 1507, 1471, 1228, 1054, 815, 725 cm^{-1}. HRMS (ESI) m/z: calcd. for $C_{21}H_{18}N_2O_4Na$ $[M+Na]^+$: 385.1164; found 385.1171.

3.7.24 (*R*)-*tert*-butyl (7-fluoro-3-(2-hydroxynaphthalen-1-yl)-1-methyl-2-oxoindolin-3-yl)carbamate (96d)

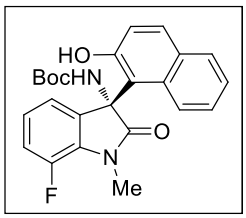

The use of (*E*)-*tert*-butyl (7-fluoro-1-methyl-2-oxoindolin-3-ylidene)carbamate (**55k**) and 2-naphthol (**47**) in general procedure afforded chiral adduct **96d** as white solid in 42 h in 95% yield. mp 137-139 °C; $[\alpha]_D^{37}$= +41.4° (*c* 1.00, $CHCl_3$). Enantiomeric excess was determined by Chiralpak IA column, 80:20 (hexane : i-PrOH), 254 nm, 1 mL/min, t_{minor} = 6.33 min, t_{major} = 34.93 min, (95% ee). ^{1}H NMR (400 MHz, $CDCl_3$) δ 9.67 (s, 1H), 7.68 (d, *J*= 8.0 Hz, 1H), 7.55 (d, *J* = 8.8 Hz, 1H), 7.30 (d, *J* = 4.6 Hz, 1H), 7.26 – 7.20 (m, 1H), 7.19-7.12 (m, 3H), 7.09 (d, *J* = 8.8 Hz, 1H), 7.02 – 6.93 (m, 1H), 5.88 (s, 1H), 3.55 (d, *J*= 2.6 Hz, 3H), 1.31 (s, 9H). ^{13}C NMR (100 MHz, $CDCl_3$) δ 179.5, 155.3, 154.0, 148.2 (d, *J* = 244.6 Hz), 133.7, 131.8 (d, *J* = 2.0 Hz), 130.7 (d, *J* = 8.3 Hz), 130.4, 129.2, 126.5, 126.0, 124.4, 124.0 (d, *J* = 6.4 Hz), 123.1, 121.3, 121.1, 117.7 (d, *J* = 19.4 Hz), 114.3, 81.0, 65.4, 29.7 (d, *J* = 5.9 Hz), 28.3. IR (neat): 3243, 2975, 2926, 1698, 1626, 1480, 1345, 1236, 1158, 855, 730 cm^{-1}. HRMS (ESI) m/z: calcd. for $C_{24}H_{23}FN_2O_4Na$ $[M+Na]^+$: 445.1540; found 445.1535.

3.7.25 (*R*)-*tert*-Butyl (3-(2-hydroxynaphthalen-1-yl)-5-methoxy-1-methyl-2-oxoindolin-3-yl)carbamate (96e)

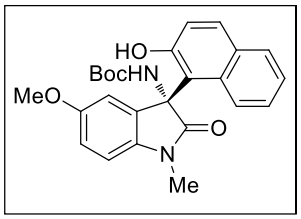

The use of (*E*)-*tert*-butyl (5-methoxy-1-methyl-2-oxoindolin-3-ylidene)carbamate (**55t**) and 2-naphthol (**47**) in general procedure afforded chiral adduct **96e** as white solid in 42 h in 86% yield. mp 112-115 °C; $[\alpha]_D^{37}$= +180.3° (*c* 0.93, $CHCl_3$). Enantiomeric excess was determined by Chiralpak IA column, 80:20 (hexane : i-PrOH), 254 nm, 1 mL/min, t_{minor} = 8.83 min, t_{major} = 37.33 min, (85% ee). ^{1}H NMR (400 MHz, $CDCl_3$) δ 10.11 (s, 1H), 7.66 (d, *J* = 8.0 Hz, 2H), 7.57 (d, *J* = 8.8 Hz, 1H), 7.20 (t, *J* = 7.9 Hz, 1H), 7.12 (d, *J* = 8.8 Hz, 3H), 7.00-6.85 (m, 3H), 5.85 (s, 1H), 3.70 (s, 3H), 3.30 (s, 3H), 1.30 (s, 9H). ^{13}C NMR (100 MHz, $CDCl_3$) δ 179.5, 156.9, 155.8, 154.0, 137.6, 132.1, 132.0, 131.7, 130.4, 129.0, 125.8, 124.5, 122.9, 121.4, 114.6, 114.4, 112.8, 109.4, 80.7, 65.8, 56.1, 28.3, 27.1. IR (neat): 3247, 2981, 2923, 1688, 1497, 1366, 1275, 1158, 1040, 815, 750 cm^{-1}. HRMS (ESI) m/z: calcd. for $C_{25}H_{26}N_2O_5Na$ $[M+Na]^+$: 457.1739; found 457.1736.

3.7.26 (*R*)-*tert*-Butyl (7-chloro-3-(2-hydroxynaphthalen-1-yl)-1-methyl-2-oxoindolin-3-yl)carbamate (96f)

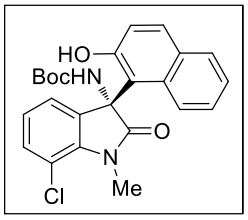

The use of (*E*)-*tert*-butyl (7-chloro-1-methyl-2-oxoindolin-3-ylidene)carbamate (**55l**) and 2-naphthol (**47**) in general procedure afforded chiral adduct **96f** as white solid in 24 h in 97% yield. mp 169-171 °C; $[\alpha]_D^{29}$= +12.7° (*c* 0.91, $CHCl_3$). Enantiomeric excess was determined by Chiralpak IA column, 80:20 (hexane : i-PrOH), 254 nm, 1 mL/min, t_{minor} = 6.93 min, t_{major} = 42.63 min, (91% ee). ^{1}H NMR (400 MHz, $CDCl_3$) δ 9.72 (s, 1H), 7.67 (d, *J* = 7.7 Hz, 1H), 7.55 (d, *J* = 8.8 Hz, 1H), 7.34 (d, *J* = 8.2 Hz, 1H),

7.30 – 7.11 (m, 4H), 7.08 (d, *J* = 8.8 Hz, 1H), 6.96 (t, *J* = 7.8 Hz, 1H), 5.84 (s, 1H), 3.70 (s, 3H), 1.31 (s, 9H). ^{13}C NMR (100 MHz, $CDCl_3$) δ 179.0, 154.3, 152.8, 138.8, 132.7, 130.8, 130.75, 130.67, 129.3, 128.1, 124.8, 123.3, 123.0, 122.9, 121.9, 120.0, 115.2, 113.1, 79.9, 64.8, 29.4, 27.1. IR (neat): 3228, 2979, 1721, 1690, 1469, 1366, 1164, 1020, 823, 736 cm^{-1}. HRMS (ESI) m/z: calcd. for $C_{24}H_{23}ClN_2O_4Na$ $[M+Na]^+$: 461.1244; found 461.1241.

3.7.27 (*R*)-*tert*-Butyl (3-(2-hydroxynaphthalen-1-yl)-1,5-dimethyl-2-oxoindolin-3-yl)carbamate (96g)

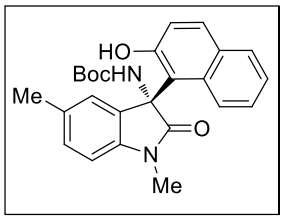

The use of (*E*)-*tert*-butyl (1,5-dimethyl-2-oxoindolin-3-ylidene)carbamate (**55n**) and 2-naphthol (**47**) in general procedure afforded chiral adduct **96g** as white solid in 24 h in 98% yield. mp 101-103 °C; $[\alpha]_D^{29}$= +65.7° (*c* 1.00, $CHCl_3$). Enantiomeric excess was determined by Chiralpak IA column, 80:20 (hexane : i-PrOH), 254 nm, 1 mL/min, t_{minor} = 7.00 min, t_{major} = 38.45 min, (54% ee). ^{1}H NMR (400 MHz, $CDCl_3$) δ 9.54 (s, 1H), 7.66 (s, 1H), 7.58 – 7.48 (m, 1H), 7.36 (dd, *J* = 17.0, 8.8 Hz, 1H), 7.12 (t, *J* = 6.2 Hz, 3H), 7.02 (d, *J* = 7.8 Hz, 1H), 6.93 (dd, *J* = 12.5, 8.9 Hz, 1H), 6.69 (d, *J* = 7.9 Hz, 1H), 5.84 (s, 1H), 3.17 (s, 3H), 2.12 (s, 3H), 1.17 (s, 9H). ^{13}C NMR (100 MHz, $CDCl_3$) δ 179.3, 154.1, 141.5, 132.8, 132.0, 131.2, 131.1, 130.5, 130.2, 129.7, 129.7, 129.1, 125.8, 124.7, 122.8, 120.6, 115.1, 108.5, 80.5, 65.2, 28.2, 26.9, 21.2. IR (neat): 3227, 2975, 1690, 1500, 1432, 1348, 1247, 1160, 813, 747 cm^{-1}. HRMS (ESI) m/z: calcd. for $C_{25}H_{26}N_2O_4Na$ $[M+Na]^+$: 441.1790; found 441.1782.

3.7.28 (*R*)-*tert*-Butyl(1-benzyl-3-(2-hydroxy-6-methoxynaphthalen-1-yl)-2-oxoindolin-3-yl)carbamate (96h)

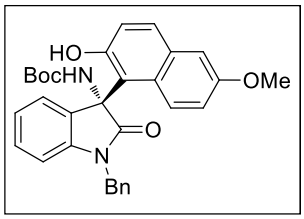

The use of (*E*)-*tert*-butyl (1-benzyl-2-oxoindolin-3-ylidene)carbamate (**55g**) and 6-methoxy-2-naphthol in general procedure afforded chiral adduct **96h** as white solid in 24 h in 97% yield. mp 189-191 °C (decomposed); $[\alpha]_D^{29}$= +65.52° (*c* 1.00, $CHCl_3$). Enantiomeric excess was determined by Chiralpak AD-H column, 90:10 (hexane : i-PrOH), 254 nm, 1 mL/min, t_{major} = 35.86 min, t_{minor} = 39.75 min, (97% ee). ^{1}H NMR (400 MHz, DMSO) δ 9.89 (s, 1H), 8.79 (d, *J* = 8.7 Hz, 1H), 7.83 (s, 1H), 7.59 (d, *J* = 8.8 Hz, 1H), 7.54 (d, *J* = 7.2 Hz, 2H), 7.39 – 7.24 (m, 4H), 7.22 (d, *J* = 2.8 Hz, 1H), 7.14 (dd, *J* = 9.4, 2.2 Hz, 1H), 7.08 (t, *J* = 7.7 Hz, 1H), 6.95 (d, *J* = 8.8 Hz, 1H), 6.78 (t, *J* = 7.6 Hz, 1H), 6.70 (d, *J* = 7.8 Hz, 1H), 5.75 (s, 1H), 4.97 (d, *J* = 16.1 Hz, 1H), 4.89 (d, *J* = 16.0 Hz, 1H), 3.83 (s, 3H), 1.18 (s, 9H). ^{13}C NMR (100 MHz, DMSO) δ 176.5, 154.4, 154.0, 150.2, 143.6, 136.8, 131.1, 130.6, 128.4, 128.3, 128.1, 127.7, 127.6, 127.0, 123.4, 121.6, 119.1, 117.5, 116.8, 108.5, 107.5, 78.3, 63.6, 55.0, 54.9, 43.7, 28.0. IR (neat): 3313, 2974, 1698, 1609, 1515, 1346, 1251, 1157, 1010, 867, 729 cm^{-1}. HRMS (ESI) m/z: calcd. for $C_{31}H_{30}N_2O_5Na$ $[M+Na]^+$: 533.2052; found 533.2032.

3.7.29 (*R*)-*tert*-Butyl(1-benzyl-3-(6-bromo-2-hydroxynaphthalen-1-yl)-2-oxoindolin-3-yl)carbamate (96i)

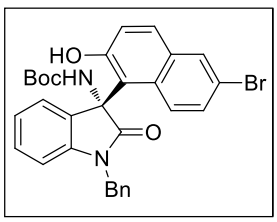

The use of (*E*)-*tert*-butyl (1-benzyl-2-oxoindolin-3-ylidene)carbamate (**55g**) and 6-bromo-2-naphthol in general procedure afforded chiral adduct **96i** as white solid in 48 h in 98% yield. mp 137-139 °C (decomposed); [α]29= +61.02° (*c* 1.00, $CHCl_3$). Enantiomeric excess was determined by Chiralpak IA column, 80:20 (hexane : i-PrOH), 254 nm, 1 mL/min,

t_{major} = 8.23 min, t_{minor} = 13.64 min, (93% ee). ^{1}H NMR (400 MHz, $CDCl_3$) δ 10.02 (s, 1H), 7.84 (d, *J* = 2.0 Hz, 1H), 7.53 (d, *J* = 8.8 Hz, 1H), 7.41 – 7.18 (m, 8H), 7.13 (d, *J* = 9.1 Hz, 1H), 7.05 (t, *J* = 7.5 Hz, 1H), 6.98 (s, 1H), 6.81 (d, *J* = 7.8 Hz, 1H), 5.86 (s, 1H), 5.15 (d, *J* = 15.9 Hz, 1H), 4.87 (d, *J* = 16.0 Hz, 1H), 1.33 (s, 9H). ^{13}C NMR (100 MHz, $CDCl_3$) δ 180.2, 156.5, 154.5, 143.7, 135.7, 132.3, 131.4, 131.32, 131.26, 131.0, 130.4, 129.5, 129.4, 128.3, 127.8, 126.7, 126.0, 124.3, 123.1, 117.2, 115.4, 110.8, 81.5, 66.0, 45.4, 28.9. IR (neat): 3168, 2977, 1692, 1608, 1465, 1335, 1152, 1009, 874, 731 cm^{-1}. HRMS (ESI) m/z: calcd. for $C_{30}H_{27}BrN_2O_4Na$ $[M+Na]^+$: 581.1052; found 581.1052.

3.7.30 (*R*)-*tert*-Butyl (3-(2,4-dihydroxy-5-methoxyphenyl)-1-methyl-2-oxoindolin-3-yl)carbamate (98b)

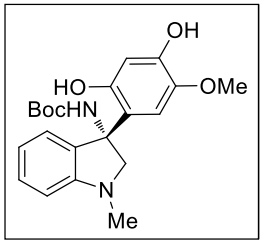

The reaction of 0.1 mmol (*E*)-tert-butyl (1-methyl-2-oxoindolin-3-ylidene)carbamate (**55i**) and 4-methoxybenzene-1,3-diol (1.1 eq) (**97b**) with 10 mol% **64b** in 1 mL DCM, at room temperature afforded chiral adduct **98b** as pale yellow solid in 67 h in 70% yield. mp 97-99 °C; $[\alpha]_D^{24}$= +239.1° (*c* 1.00, $CHCl_3$). Enantiomeric excess was determined by Chiralpak IA column, 80:20 (hexane : i-PrOH), 254 nm, 1 mL/min, t_{major} = 13.55 min, t_{minor} = 22.27 min, (84% ee). ^{1}H NMR (400 MHz, $CDCl_3$) δ 9.75 (s, 1H), 7.38 (t, *J* = 8.7 Hz, 2H), 7.21 (t, *J* = 7.5 Hz, 1H), 6.90 (d, *J* = 7.7 Hz, 1H), 6.54 (s, 1H), 6.39 (bs, 1H), 6.19 (s, 1H), 5.89 (bs, 1H), 3.49 (s, 3H), 3.18 (s, 3H), 1.21 (s, 9H). ^{13}C NMR (100 MHz, $CDCl_3$) δ 179.2, 154.0, 152.2, 147.9, 143.3, 140.4, 129.6, 124.8, 123.3, 112.0, 111.9, 109.3, 107.1, 80.7, 65.6, 56.4, 28.0, 26.8. IR (neat): 3324, 2976, 2871, 1687, 1611, 1505, 1367, 1278, 1156, 807, 754 cm^{-1}. HRMS (ESI) m/z: calcd. for $C_{21}H_{24}N_2O_6Na$ $[M+Na]^+$: 423.1527; found 423.1533.

3.8 Procedure for the Synthesis of 95e by One-pot Sequential aza-Wittig/aza-Friedel-Crafts Reaction

To a schlenk tube filled with *N*-benzyl isatin **97** (1.2 eq, 28.5 mg) and 0.1 mmol *t*-butyl triphenylphosphoranylidenecarbamate **83**, 1 mL of dry 1,4-dioxane was added and reaction was refluxed overnight under argon atmosphere. Upon the consumption of limiting reagent, solvent was evaporated. Then reaction mixture was dissolved with DCM (2 mL) 2-3 times and concentrated in vacuo. Then, 0.1 mmol 1-naphthol (**42**), 2 mol% **64b**, molecular sieve (25.0 mg) and 1 mL DCM were added and reaction was stirred at -20 °C for 18 hours. Product is purified with silica gel column chromatography with hexane : ethyl acetate eluent. The product **95e** was isolated as white solid with 78% yield and 94% ee. Enantiomeric excess was determined by Chiralpak IA column, 80:20 (hexane : i-PrOH), 254 nm, 1 mL/min, t_{minor} = 13.31 min, t_{major} = 54.00 min, (94% ee).

3.9 Procedure for Deprotection of 95e

Adduct **95e** (336.4 mg, 0.7 mmol) was dissolved in 4M HCl in acetonitrile (15 mL) and stirred at r.t. for 30 min. Reaction was monitored by TLC. After all starting compound finished reaction content was concentrated by vacuo. Then, reaction mixture diluted with DCM was quenched with 30 mL of 10% (w/w) $K_2CO_{3(aq)}$ and aqueous phase was washed with DCM (3 x 20 mL). Organic phase dried over $MgSO_4$ and solvent was evaporated.

3.9.1 (*R*)-3-Amino-1-benzyl-3-(1-hydroxynaphthalen-2-yl)indolin-2-one (99)

Compound **99** was obtained according to given deprotection procedure of **95e** with 98% yield as white solid and it is used without further purification.

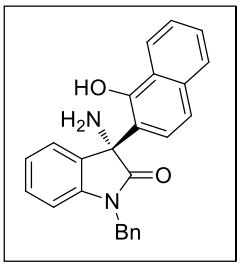

mp 131-133 °C (decomposed); $[\alpha]_D^{20}$= -655.1° (*c* 0.64, $CHCl_3$) Enantiomeric excess was determined by Chiralpak AD-H column, 70:30 (hexane : i-PrOH), 254 nm, 1 mL/min, t_{minor} = 17.98, t_{major} = 20.64 min (99% ee). ^{1}H NMR (400 MHz, $CDCl_3$) δ 8.56 – 8.25 (m, 1H), 7.69 (dd, *J* = 6.8, 3.1 Hz, 2H), 7.55 – 7.27 (m, 7H), 7.23-7.13 (m, 2H), 6.98 (t, *J* = 7.5 Hz, 1H), 6.87 – 6.71 (m, 2H), 5.12 (d, *J* = 15.5 Hz, 1H), 4.94 (d, *J* = 15.5 Hz, 1H). ^{13}C NMR (100 MHz, $CDCl_3$) δ 178.3, 155.0, 141.3, 135.6, 134.4, 129.8, 129.1, 128.1, 127.6, 127.3, 126.8, 126.3, 125.3, 124.7, 123.9, 123.8, 122.6, 119.1, 116.1, 110.0, 65.3, 44.4. IR (neat): 3343, 3280, 3060, 1710, 1604, 1486, 1364, 1190, 1062, 796, 727 cm^{-1}.

3.10 Procedure for the Synthesis of 1,4-Naphthoxazepine 100

According to literature procedure,[55] (*R*)-3-amino-1-benzyl-3-(1-hydroxynaphthalen-2-yl)indolin-2-one (**99**) (266.3 mg, 0.7 mmol) and NaH (60.0 mg, 2.5 mmol) were dissolved in 5 mL DCM at 0 °C for 5 minutes. Bromoethyldiphenylsulfonium salt **101** (1.2 eq, 372.4 mg), synthesized according to ref. 55, was added and reaction was stirred at 0 °C for 2 hours. Progress was monitored by TLC. Reaction content was quenched with saturated $NH_4Cl_{(aq)}$ and extracted with DCM (3 x 20 mL), washed with brine and dried over $MgSO_4$. After concentration under reduced pressure, the product was purified by column chromatography on silica gel with 1:3 (EtOAc : hexane) as eluent.

3.10.1 (*R*)-1-Benzyl-3',4'-dihydro-2'H-spiro[indoline-3,5'-naphtho[2,1-f][1,4]oxazepin]-2-one (100)

Compound **100** was obtained according to given procedure with 25% yield as white solid. mp 143-145 °C (decomposed); $[\alpha]_D^{19}$= -327.4° (*c* 0.21,

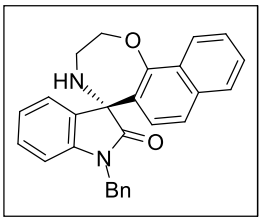

$CHCl_3$). Enantiomeric excess was determined by Chiralpak AD-H column, 70:30 (hexane : i-PrOH), 1 mL/min, t_{major} = 14.47 min, t_{minor} = 19.33 min, (99% ee). ^{1}H NMR (400 MHz, $CDCl_3$) δ 8.03 – 7.94 (m, 1H), 7.81 – 7.67 (m, 1H), 7.55-7.26 (m, 10H), 7.09 (t, *J* = 8.3 Hz, 1H), 6.93 (d, *J* = 7.9 Hz, 1H), 6.61 (d, *J* = 8.7 Hz, 1H), 5.13 (d, *J* = 15.3 Hz, 1H), 4.98 (d, *J* = 15.3 Hz, 1H), 4.56 (dt, *J* = 14.6, 8.1 Hz, 2H), 3.06 – 2.90 (m, 1H), 2.76 (bs, 1H), 1.63 (bs, 1H). ^{13}C NMR (100 MHz, $CDCl_3$) δ 178.8, 154.4, 143.4, 136.4, 134.6, 132.7, 129.4, 129.0, 128.9, 128.1, 128.0, 127.9, 127.7, 126.5, 126.1, 125.9, 124.4, 123.8, 122.9, 109.4, 100.1, 72.6, 45.2, 44.4, 29.8. IR (neat): 3050, 2936, 1717, 1609, 1466, 1332, 1173, 1081, 809, 698 cm^{-1}. HRMS (ESI) m/z: calcd. for $C_{27}H_{23}N_2O_2$ $[M+H]^+$: 407.1760; found 407.1761.

3.11 Procedure for *O*-Propargylation of 95e

In an oven-dried round bottom flask 1,3-aminonaphthol compound **95e** (0.8 mmol, 384.4 mg,) and anhydrous potassium carbonate (1.2 mmol, 165.8 mg) was dissolved in 15 mL of acetone. To this suspension, propargyl bromide (80 wt. % in toluene, 0.9 mmol, 97.16 μL) was added and reaction was refluxed for 6 h. Monitoring the consumption of starting compound by TLC, reaction content was concentrated by evaporation and directly loaded to a silica gel column. Column chromatography with 1:5 (EtOAc : hexane) as the eluent afforded *O*-propargyl naphthol derivative **102** as white solid.

3.11.1 (*R*)-*tert*-Butyl (1-benzyl-2-oxo-3-(1-(prop-2-yn-1-yloxy)naphthalen-2-yl)indolin-3-yl)carbamate (102)

Compound **102** was obtained according to given procedure in 92% yield as white solid. mp 77-79 °C ^{1}H NMR (400 MHz, $CDCl_3$) δ 8.14 (d, *J* = 8.3 Hz,

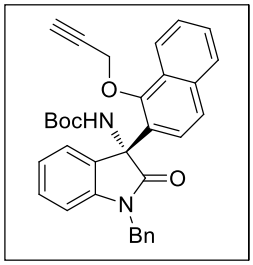

1H), 7.70 (d, *J* = 7.6 Hz, 1H), 7.61 (s, 1H), 7.49 (ddd, *J* = 8.4, 6.9, 1.3 Hz, 1H), 7.46 – 7.38 (m, 2H), 7.32 (d, *J* = 7.0 Hz, 2H), 7.28 – 7.21 (m, 2H), 7.21 – 7.16 (m, 1H), 7.16 – 7.10 (m, 2H), 6.94 (t, *J* = 7.2 Hz, 1H), 6.74 (dd, *J* = 16.7, 8.3 Hz, 2H), 5.01 (d, *J* = 15.7, 1H), 4.99 (dd, *J* = 14.9, 2.4, 1H), 4.86 (d, *J* = 15.8 Hz, 1H), 4.64 (dd, *J* = 15.0, 2.4 Hz, 1H), 2.61 (t, *J* = 2.4 Hz, 1H), 1.32 (s, 9H). ^{13}C NMR (100 MHz, $CDCl_3$) δ 176.8, 154.5, 152.7, 143.6, 136.0, 134.8, 132.4, 129.2, 128.9, 128.8, 128.0, 127.7, 127.6, 127.2, 126.9, 126.2, 125.5, 124.9, 124.5, 123.4, 122.7, 109.4, 80.3, 79.1, 76.1, 65.9, 64.3, 44.6, 28.4. IR (neat): 3389, 3290, 2975, 1714, 1612, 1486, 1352, 1160, 749 cm^{-1}. HRMS (ESI) m/z: calcd. for $C_{33}H_{30}N_2O_4Na$ $[M+Na]^+$: 541.2103; found 541.2098.

3.12 Procedure for Deprotection of compound 102

In an oven-dried Schlenk tube compound **102** (0.8 mmol, 414.9 mg) was dissolved in 20 mL of DCM under argon atmosphere at 0 °C. Trifluoroacetic acid (32.0 mmol, 2.43 mL) was added via syringe at the same temperature. The reaction mixture was allowed to reach ambient temperature through the overnight. Upon the completion of the reaction, all volatiles were evaporated. Extraction of the mixture with DCM and saturated $NaHCO_{3(aq)}$ followed by drying over anhydrous $MgSO_4$ afforded crude product. Column chromatography with silica gel and 1:2 (EtOAc:DCM) afforded amine **103** as white solid.

3.12.1 (*R*)-3-Amino-1-benzyl-3-(1-(prop-2-yn-1-yloxy)naphthalen-2-yl)indolin-2-one (103)

Compound **103** was obtained according to given procedure in 98% yield as white solid. mp 99-102°C. ^{1}H NMR (400 MHz, $CDCl_3$) δ 8.31 (d, *J* = 8.7 Hz, 1H), 8.03 (dd, *J* = 5.4, 4.2 Hz, 1H), 7.91 – 7.82 (m, 1H), 7.78 (d, *J* = 8.7 Hz, 1H), 7.51 –

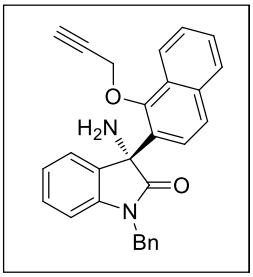

7.43 (m, 4H), 7.39 (t, *J* = 7.5 Hz, 2H), 7.31 (t, *J* = 7.3 Hz, 1H), 7.20 (dt, *J* = 7.8, 1.1 Hz, 1H), 7.07 (d, *J* = 7.3 Hz, 1H), 6.92 (t, *J* = 7.4 Hz, 1H), 6.85 (d, *J* = 7.9 Hz, 1H), 5.40 (d, *J* = 15.7 Hz, 1H), 4.85 (d, *J* = 15.7 Hz, 1H), 4.25 (dd, *J* = 15.0, 2.4 Hz, 1H), 3.40 (dd, *J* = 15.0, 2.4 Hz, 1H), 2.56 (t, *J* = 2.4 Hz, 1H), 2.03 (bs, 2H). ^{13}C NMR (100 MHz, $CDCl_3$) δ 180.7, 151.2, 143.1, 136.4, 135.2, 133.2, 130.5, 129.3, 129.0, 128.3, 127.73, 127.68, 127.4, 126.4, 126.3, 125.0, 124.7, 124.5, 123.0, 122.4, 109.8, 79.4, 75.4, 61.7, 61.4, 44.3. IR (neat): 3337, 2920, 1712, 1610, 1465, 1351, 726, 682 cm^{-1}. HRMS (ESI) m/z: calcd. for $C_{28}H_{22}N_2O_2Na$ $[M+Na]^+$: 441.1579; found 441.1574.

3.13 $ZnCl_2$ Mediated Cyclization of 103

Compound **103** (0.6 mmol, 251.1 mg) and $ZnCl_2$ (1.2 mmol, 163.6 mg) was dissolved in 6 mL of chloroform in an flame-dried two-neck round-bottom flask. The resulting solution was refluxed under argon atmosphere for 12 h. Initially, pale yellow solution turned into deep red color. After the evaporation of the solvent, purification of the product by silica gel column chromatography with 1:20 (EtOAc:DCM) afforded compound **105** as unstable pale yellow oil.

3.13.1 (*R*)-1-Benzyl-3'-methyl-2'H-spiro[indoline-3,5'-naphtho[2,1-f][1,4]oxazepin]-2-one (105)

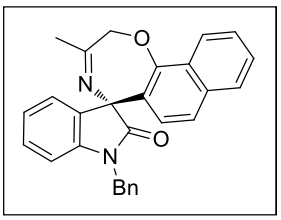

Compound **105** was obtained according to given procedure in 46% yield as unstable (decomposes in DCM, i-propanol and ethyl acetate) pale yellow oil. ^{1}H NMR (400 MHz, $CDCl_3$) δ 8.18 (d, *J* = 8.2 Hz, 1H), 7.82 (d, *J* = 7.6 Hz, 1H), 7.72 (d, *J* = 7.6 Hz, 1H), 7.56 – 7.38 (m, 4H), 7.36 – 7.23 (m, 4H), 7.20 (dd, *J* = 12.8, 10.5 Hz, 1H), 7.05 (t, *J* = 7.2 Hz, 1H), 6.89 (t, *J* = 7.6 Hz, 1H), 6.62 (d, *J* = 7.8 Hz, 1H), 5.27 (d, *J* = 15.9 Hz, 1H), 4.99 (d, *J* = 17.2 Hz, 1H), 4.81

(d, *J* = 15.9 Hz, 1H), 4.69 (d, *J* = 17.2 Hz, 1H), 2.00 (s, 3H). IR (neat): 2923, 2351, 1723, 1609, 1467, 1259, 1028, 799 cm^{-1}. HRMS (ESI) m/z: calcd. for $C_{28}H_{23}N_2O_2$ $[M+H]^+$: 419.1759; found 419.1774.

3.14 General Procedure G: Synthesis of α-Azido Ketones

Synthesis of Acyclic α-Azido Ketones (93a-j)

According to literature procedure,[57] to a stirred solution of appropriate 2-bromo-1-phenylethanone **92** (5.0 mmol) in 40 mL acetone, sodium azide (975.0 mg, 15.0 mmol) was added at room temperature. The resulting solution was stirred overnight at room temperature. The reaction was checked by TLC. After the completion of reaction, the solvent was evaporated. Then the mixture was poured into water and extracted with ethyl acetate (3 x 50 mL). The organic layer was dried over $MgSO_4$, and concentrated in vacuo. After the evaporation of solvent the crude product was purified by column chromatography eluting with ethyl acetate: hexane (1:5) to give 2-azido-1-phenylethanones **93a-j**. Spectral data was in accordance with literature.[70]

Synthesis of Cyclic α-Azido Ketones (93k-n)

In accordance with literature procedure,[71a] to a stirred solution of α-bromo chromanone, thiochromanone, indanone or tetralone (**87a**, **87b**, **90a**, **90b**) (4.0 mmol) in acetone (20 mL) sodium azide (8.0 mmol, 520.0 mg) and 18-crown-6 (0.8 mmol, 211.5 mg) was added. The reaction content was stirred at room temperature. Monitoring by TLC, the reaction solvent was evaporated and residue was dissolved in ethyl acetate and extracted with water and brine, respectively. Being dried over $MgSO_4$, organic phase was concentrated in vacuo. Silica gel column eluted with ethyl acetate:hexane (1:10) yielded in corresponding azido ketones **93k-n**. Compound **93k** and **93l** were characterized by comparing ^1H and

^{13}C NMR spectra with literature.[57,71] Spectroscopic data of **93m** and **93n** are given below.

3.14.1 2-Azido-3,4-dihydronaphthalen-1(2*H*)-one (93m)

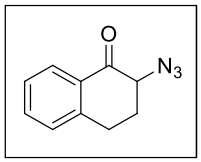

General procedure given for cyclic α-azido ketones afforded compound **93m** as dark green oil in 68% yield. ^{1}H NMR (400 MHz, $CDCl_3$) δ 7.96 (d, *J* = 7.8 Hz, 1H), 7.41 (t, *J* = 7.5 Hz, 1H), 7.23 (t, *J* = 7.4 Hz, 1H), 7.17 – 7.05 (m, 1H), 4.33 – 3.91 (m, 1H), 2.94 (d, *J* = 4.3 Hz, 2H), 2.23 (ddd, *J* = 9.0, 7.4, 4.4 Hz, 1H), 1.99 (tdd, *J* = 8.9, 8.0, 4.4 Hz, 1H).^{13}C NMR (100 MHz, $CDCl_3$) δ 194.3, 143.6, 134.4, 131.2, 128.9, 128.1, 127.3, 64.5, 29.4, 27.7.

3.14.2 2-Azido-2,3-dihydro-1*H*-inden-1-one (93n)

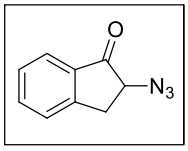

General procedure given for cyclic α-azido ketones afforded compound **93n** as white crystals in 72% yield. mp. 45-47 °C; ^{1}H NMR (400 MHz, $CDCl_3$) δ 7.79 (d, *J* = 7.7 Hz, 1H), 7.65 (td, *J* = 7.6, 1.1 Hz, 1H), 7.51 – 7.34 (m, 2H), 4.32 (dd, *J* = 8.2, 4.6 Hz, 1H), 3.51 (dd, *J* = 17.1, 8.1 Hz, 1H), 2.93 (dd, *J* = 17.1, 4.6 Hz, 1H). ^{13}C NMR (100 MHz, $CDCl_3$) δ 201.9, 151.3, 136.2, 134.3, 128.3, 126.7, 124.7, 62.1, 33.1.

3.15 General Procedure H: Racemic Synthesis of Mannich Adducts

In an oven-dried test tube with screw cap isatin ketimine **55** (0.4 mmol), α-azido ketone **93** (1.1 eq) and 5 mol% 1:1 mixture of quinine-derived urea catalysts **94b** and *epi*-**94b** were dissolved in 3 mL of DCM at room temperature. Upon the completion, reaction mixture was directly loaded to glass column for purification. Racemates of each isomer were isolated by silica gel column chromatography with a gradient solvent system of ethyl acetate:hexane from (1:5) to (1:3) ratio.

3.16 General Procedure I: Asymmetric Synthesis of Mannich Adducts

Experimental procedures for the asymmetric organocatalytic synthesis of Mannich bases **107a-p** with two different organocatalysts **64b** and **64d** were given below.

With organocatalyst 64b: In an oven-dried test tube with screw cap isatin ketimine **55** (0.1 mmol), α-azido ketone **93** (0.2 mmol) and 5 mol% quinine-derived squaramide **64b** were dissolved in 1 mL of DCM at 22 °C. Reaction progress was monitored by TLC and purified by silica gel column chromatography as described for racemic synthesis in general procedure H.

With organocatalyst 64d: In an oven-dried test tube with screw cap isatin ketimine **55** (0.1 mmol), α-azido ketone **93** (1.1 eq) and 10 mol% quinine-derived squaramide **64d** were dissolved in 1 mL of DCM at 22 °C. Reaction progress was monitored by TLC and purified by silica gel column chromatography as described for racemic synthesis in general procedure H.

3.16.1 *tert*-Butyl ((*S*)-3-((*S*)-1-azido-2-oxo-2-phenylethyl)-1-methyl-2-oxoindolin-3-yl)carbamate (107a)

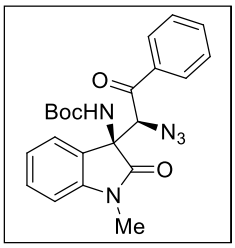

The use of **64d** with (*E*)-*tert*-butyl (1-methyl-2-oxoindolin-3-ylidene)carbamate (**55i**) and 2-azido-1-phenylethanone (**93a**) in general procedure afforded chiral adduct **107a** as white solid in 3 h in 95% yield with diastereomeric ratio 4:1 (syn:anti). mp. 65-67 °C; $[\alpha]_D^{30}$ = -18.7° (*c* 0.5, $CHCl_3$). Enantiomeric excess was determined by Chiralpak AD-H column, 85:15 (hexane : i-PrOH), 254 nm, 1 mL/min, t_{minor} = 12.14 min, t_{major} = 15.74 min, (86% ee). ^{1}H NMR (400 MHz, $CDCl_3$) δ 7.90 – 7.75 (m, 2H), 7.58 (t, *J* = 7.4 Hz, 2H), 7.43 (t, *J* = 7.8 Hz, 2H), 7.33 – 7.22 (m, 1H), 6.96 (t, *J* = 7.6 Hz, 1H), 6.81 (d, *J* = 7.8 Hz, 1H), 5.86 (s, 1H),

5.28 (s, 1H), 3.27 (s, 3H), 1.30 (s, 9H). ^{13}C NMR (100 MHz, $CDCl_3$) δ 193.7, 173.9, 154.2, 144.2, 135.5, 134.3, 130.1, 128.8, 128.8, 126.5, 125.8, 122.7, 108.4, 80.7, 64.0, 62.9, 28.1, 26.6. IR (neat): 3312, 2976, 2102, 1710, 1612, 1470, 1249, 1158, 752, 687 cm^{-1}. HRMS (ESI) m/z: calcd. for $C_{22}H_{23}N_5O_4Na$ $[M+Na]^+$: 444.1648; found 444.1634.

3.16.2 *tert*-Butyl ((*S*)-3-((*S*)-1-azido-2-oxo-2-phenylethyl)-1-benzyl-2-oxoindolin-3-yl)carbamate (107b)

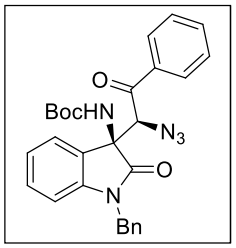

The use of **64d** with (*E*)-*tert*-butyl (1-benzyl-2-oxoindolin-3-ylidene)carbamate (**55g**) and 2-azido-1-phenylethanone (**93a**) in general procedure afforded chiral adduct **107b** as white solid in 18 h in 96% yield with diastereomeric ratio 4:1 (syn:anti). mp. 72-74 °C; $[\alpha]_D^{30}$= -0.3° (*c* 0.95, $CHCl_3$). Enantiomeric excess was determined by Chiralpak AD-H column, 80:20 (hexane : i-PrOH), 254 nm, 1 mL/min, t_{minor} = 15.32 min, t_{major} = 21.46 min, (84% ee). ^{1}H NMR (400 MHz, $CDCl_3$) δ 7.73 (d, *J* = 7.7 Hz, 2H), 7.48 (dd, *J* = 15.2, 7.5 Hz, 2H), 7.39 – 7.11 (m, 7H), 7.06 (t, *J* = 7.6 Hz, 1H), 6.85 (dd, *J* = 14.1, 6.8 Hz, 1H), 6.61 (d, *J* = 7.8 Hz, 1H), 6.01 (s, 1H), 5.16 (s, 1H), 4.98 (d, *J* = 14.6 Hz, 1H), 4.72 (d, *J* = 14.6 Hz, 1H), 1.21 (s, 9H). ^{13}C NMR (100 MHz, $CDCl_3$) δ 194.0, 174.2, 154.2, 143.3, 135.6, 134.4, 130.0, 128.9, 128.82, 128.79, 128.7, 127.7, 127.6, 126.6, 125.8, 122.8, 109.5, 80.8, 63.8, 63.3, 44.5, 28.1. IR (neat): 3300, 2977, 2103, 1714, 1613, 1486, 1248, 1157, 751, 694 cm^{-1}. HRMS (ESI) m/z: calcd. for $C_{28}H_{27}N_5O_4Na$ $[M+Na]^+$: 520.1961; found 520.1944.

3.16.3 *tert*-Butyl ((*S*)-1-allyl-3-((*S*)-1-azido-2-oxo-2-phenylethyl)-2-oxoindolin-3-yl)carbamate (107c)

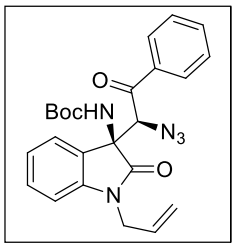

The use of **64d** with (*E*)-*tert*-butyl (1-allyl-2-oxoindolin-3-ylidene)carbamate (**55f**) and 2-azido-1-phenylethanone (**93a**) in general procedure afforded chiral adduct **107c** as white solid in 18 h in 80% yield with diastereomeric ratio 9:1 (syn:anti). mp 55-57 °C; $[\alpha]_D^{17}$= -22.6° (*c* 0.92, $CHCl_3$). Enantiomeric excess was determined by Chiralpak AD-H column, 85:15 (hexane : i-PrOH), 254 nm, 1 mL/min, t_{minor} = 13.12 min, t_{major} = 17.92 min, (82% ee). ^{1}H NMR (400 MHz, $CDCl_3$) δ 7.85 (d, *J* = 8.0 Hz, 2H), 7.59 (m, 2H), 7.44 (t, *J* = 7.5 Hz, 2H), 7.26 (dd, *J* = 13.7, 6.0 Hz, 1H), 6.97 (t, *J* = 7.6 Hz, 1H), 6.83 (d, *J* = 7.8 Hz, 1H), 5.96 (s, 1H), 5.94 – 5.80 (m, 1H), 5.40 (d, *J* = 17.2 Hz, 1H), 5.32 (s, 1H), 5.28 (d, *J* = 17.2 Hz, 1H), 4.55 (d, *J* = 13.4 Hz, 1H), 4.26 (d, *J* = 13.4 Hz, 1H), 1.32 (s, 9H). ^{13}C NMR (100 MHz, $CDCl_3$) δ 193.8, 173.8, 154.2, 143.4, 135.6, 134.4, 131.3, 130.0, 128.9, 128.8, 126.5, 125.9, 122.7, 118.0, 109.4, 80.8, 64.0, 63.0, 43.0, 28.2. IR (neat): 3420, 2977, 2102, 1716, 1611, 1484, 1365, 1156, 754, 695 cm^{-1}. HRMS (ESI) m/z: calcd. for $C_{24}H_{25}N_5O_4Na$ $[M+Na]^+$: 470.1804; found 470.1796.

3.16.4 *tert*-Butyl 3-(1-azido-2-oxo-2-phenylethyl)-3-((tert-butoxycarbonyl)amino)-2-oxoindoline-1-carboxylate (107d)

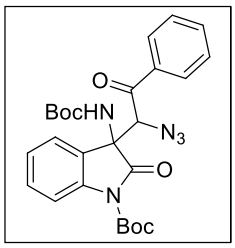

The use of **64b** with (*E*)-*tert*-butyl 3-((tert-butoxycarbonyl)imino)-2-oxoindoline-1-carboxylate and 2-azido-1-phenylethanone (**93a**) in general procedure afforded chiral adduct **107d** as white solid in 48 h in 19% yield with diastereomeric ratio 20:1 (syn:anti). mp 56-58 °C; $[\alpha]_D^{31}$= -0.5° (*c* 0.5, $CHCl_3$). Enantiomeric excess was determined by

Chiralpak AD-H column, 85:15 (hexane : i-PrOH), 254 nm, 1 mL/min, t = 9.37, 10.60 min, *rac*. ^{1}H NMR (400 MHz, $CDCl_3$) δ 8.00 – 7.74 (m, 3H), 7.69 – 7.52 (m, 1H), 7.53 – 7.37 (m, 3H), 7.31 (t, *J* = 7.9 Hz, 1H), 7.07 (t, *J* = 7.6 Hz, 1H), 6.00 (s, 1H), 5.11 (s, 1H), 1.63 (s, 9H), 1.25 (s, 9H). ^{13}C NMR (100 MHz, $CDCl_3$) δ 193.4, 172.5, 153.9, 148.9, 140.3, 135.2, 134.5, 130.3, 130.2, 128.9, 125.7, 124.7, 124.5, 115.3, 84.5, 81.3, 65.1, 63.3, 28.1, 27.9. IR (neat): 3370, 2924, 2105, 1777, 1709, 1597, 1477, 1343, 1248, 1145, 753 cm^{-1}. HRMS (ESI) m/z: calcd. for $C_{26}H_{29}N_5O_6Na$ $[M+Na]^+$: 530.2016; found 530.1995.

3.16.5 *tert*-Butyl ((*S*)-3-((*R*)-2-azido-1-oxo-2,3-dihydro-1H-inden-2-yl)-1-methyl-2-oxoindolin-3-yl)carbamate (107e)

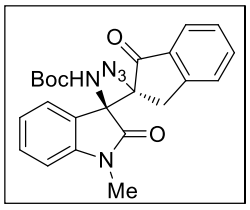

The use of **64b** with (*E*)-*tert*-butyl (1-methyl-2-oxoindolin-3-ylidene)carbamate (**55i**) and 2-azido-2,3-dihydro-1*H*-inden-1-one (**93n**) in general procedure afforded chiral adduct **107e** as white solid in 24 h in 97% yield with diastereomeric ratio 18:1 (syn:anti). mp 92-94 °C; $[\alpha]_D^{19}$= +93.4° (*c* 0.50, $CHCl_3$). Enantiomeric excess was determined by Chiralpak AD-H column, 80:20 (hexane : i-PrOH), 254 nm, 1 mL/min, t_{minor} = 7.80 min, t_{major} = 10.78 min, (88% ee). ^{1}H NMR (400 MHz, $CDCl_3$) δ 7.81 (d, *J* = 7.6 Hz, 1H), 7.64 – 7.58 (m, 1H), 7.57 (d, *J* = 8.6 Hz, 1H), 7.44 – 7.36 (m, 1H), 7.34 (d, *J* = 7.7 Hz, 1H), 7.28 (d, *J* = 7.6 Hz, 1H), 7.09 (t, *J* = 7.4 Hz, 1H), 6.85 (d, *J* = 7.8 Hz, 1H), 6.82 (s, 1H), 3.10 (s, 3H), 3.00 (d, *J* = 18.0 Hz, 1H), 2.81 (d, *J* = 18.0 Hz, 1H), 1.23 (s, 9H). ^{13}C NMR (100 MHz, $CDCl_3$) δ 199.4, 173.3, 154.0, 149.8, 144.1, 136.6, 134.7, 129.9, 128.7, 126.7, 126.0, 125.3, 125.2, 123.1, 108.4, 80.5, 69.0, 66.8, 36.3, 28.1, 26.5. IR (neat): 3348, 2976, 2104, 1710, 1610, 1469, 1367, 1249, 1159, 750 cm^{-1}. HRMS (ESI) m/z: calcd. for $C_{23}H_{23}N_5O_4Na$ $[M+Na]^+$: 456.1647; found 456.1657.

3.16.6 *tert*-Butyl ((*S*)-3-((*R*)-3-azido-4-oxothiochroman-3-yl)-1-methyl-2-oxoindolin-3-yl)carbamate (107f)

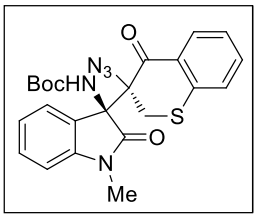

The use of **64d** with (*E*)-*tert*-butyl (1-methyl-2-oxoindolin-3-ylidene)carbamate (**55i**) and 3-azidothiochroman-4-one (**93l**) in general procedure afforded chiral adduct **107f** as white solid in 18 h in 89% yield with diastereomeric ratio 6:1 (syn:anti). mp 78-81 °C; $[\alpha]_D^{18}$= +10.4° (*c* 0.50, $CHCl_3$). Enantiomeric excess was determined by Chiralpak AD-H column, 90:10 (hexane : i-PrOH), 254 nm, 1 mL/min, t_{minor} = 14.58 min, t_{major} = 19.64 min, (90% ee). ^{1}H NMR (400 MHz, $CDCl_3$) δ 8.11 (d, *J* = 7.9 Hz, 1H), 7.49 (d, *J* = 7.5 Hz, 1H), 7.40-7.25 (m, 2H), 7.22 (d, *J* = 7.8 Hz, 1H), 7.13 (d, *J* = 7.9 Hz, 1H), 7.03 (t, *J* = 7.6 Hz, 1H), 6.76 (d, *J* = 7.7 Hz, 1H), 6.76 (s, 1H), 3.08 (s, 3H), 3.00 (d, *J* = 14.2 Hz, 1H), 2.91 (d, *J* = 14.1 Hz, 1H), 1.17 (s, 9H). ^{13}C NMR (100 MHz, $CDCl_3$) δ 190.7, 173.0, 153.8, 144.8, 140.7, 133.9, 132.7, 131.01, 130.3, 127.6, 126.6, 125.8, 125.5, 123.1, 108.5, 80.5, 69.7, 67.2, 29.8, 28.2, 26.8. IR (neat): 3398, 2924, 2109, 1713, 1610, 1469, 1249, 1159, 750 cm^{-1}. HRMS (ESI) m/z: calcd. for $C_{23}H_{23}N_5O_4SNa$ $[M+Na]^+$: 488.1368; found 488.1343.

3.16.7 *tert*-Butyl ((*S*)-3-((*S*)-3-azido-4-oxochroman-3-yl)-1-methyl-2-oxoindolin-3-yl)carbamate (107g)

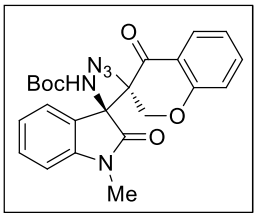

The use of **64b** with (*E*)-*tert*-butyl (1-methyl-2-oxoindolin-3-ylidene)carbamate (**55i**) and 3-azidochroman-4-one (**93k**) in general procedure afforded chiral adduct **107g** as white solid in 48 h in 85% yield with diastereomeric ratio 20:1 (syn:anti). mp 173-175 °C (decomposed); $[\alpha]_D^{30}$= +15.3° (*c* 1.00, $CHCl_3$). Enantiomeric excess was determined by Chiralpak AD-H column, 90:10 (hexane : i-PrOH), 254 nm,

1 mL/min, t_{minor} = 9.36 min, t_{major} = 11.21 min, (96% ee). ^{1}H NMR (400 MHz, DMSO) δ 7.85 (dd, *J* = 7.9, 1.6 Hz, 1H), 7.62 (ddd, *J* = 8.7, 7.3, 1.7 Hz, 1H), 7.58 (d, *J* = 7.4 Hz, 1H), 7.36 (td, *J* = 7.7, 1.0 Hz, 1H), 7.17 (s, 1H), 7.17 – 7.10 (m, 1H), 7.09 – 6.98 (m, *J* = 13.0, 7.7 Hz, 3H), 4.61 (d, *J* = 12.5 Hz, 1H), 4.23 (d, *J* = 12.5 Hz, 1H), 3.07 (s, 3H), 1.14 (s, 9H). ^{13}C NMR (100 MHz, DMSO) δ 186.2, 172.5, 160.7, 153.0, 144.7, 137.2, 129.9, 127.3, 125.6, 122.3, 122.1, 120.7, 117.6, 108.3, 79.5, 69.0, 67.4, 65.1, 27.7, 26.3. IR (neat): 3429, 2982, 2101, 1717, 1673, 1490, 1254, 1145, 754 cm^{-1}. HRMS (ESI) m/z: calcd. for $C_{23}H_{23}N_5O_5Na$ $[M+Na]^+$: 472.1596; found 472.1592. See Appendix C for crystallographic data.

3.16.8 *tert*-Butyl ((*S*)-3-((*R*)-2-azido-1-oxo-1,2,3,4-tetrahydronaphthalen-2-yl)-1-methyl-2-oxoindolin-3-yl)carbamate (107h)

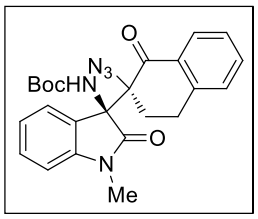

The use of **64b** with (*E*)-*tert*-butyl (1-methyl-2-oxoindolin-3-ylidene)carbamate (**55i**) and 2-azido-3,4-dihydronaphthalen-1(2*H*)-one (**93m**) in general procedure afforded chiral adduct **107h** as white solid in 60 h in 26% yield with diastereomeric ratio 8:1 (syn:anti). mp 92-95 °C; $[\alpha]_D^{20}$= +35.8° (*c* 0.13, $CHCl_3$). Enantiomeric excess was determined by Chiralpak AD-H column, 90:10 (hexane : i-PrOH), 254 nm, 1 mL/min, t_{minor} = 9.52 min, t_{major} = 14.61 min, (83% ee). ^{1}H NMR (400 MHz, $CDCl_3$) δ 8.12 (d, *J* = 7.9 Hz, 1H), 7.58 – 7.45 (m, 3H), 7.41 – 7.31 (m, 2H), 7.19 – 7.08 (m, 2H), 6.82 (d, *J* = 7.7 Hz, 1H), 3.15 (s, 3H), 2.93 (ddd, *J* = 15.7, 11.1, 4.3 Hz, 1H), 2.61 (dt, *J* = 16.7, 4.4 Hz, 1H), 1.84 (ddd, *J* = 14.7, 11.0, 4.1 Hz, 1H), 1.68 (dt, *J* = 14.0, 4.5 Hz, 1H), 1.26 (s, 9H). ^{13}C NMR (100 MHz, $CDCl_3$) δ 193.1, 174.2, 154.3, 144.6, 143.2, 134.6, 132.4, 129.8, 129.0, 128.1, 127.7, 126.8, 125.1, 123.0, 108.2, 80.3, 68.6, 67.7, 29.3, 28.2, 26.6, 24.8. IR (neat): 3342, 2976, 2102, 1713, 1612, 1470, 1249, 1158, 751 cm^{-1}.

HRMS (ESI) m/z: calcd. for $C_{24}H_{25}N_5O_4Na$ $[M+Na]^+$: 470.1804; found 470.1788.

3.16.9 *tert*-Butyl ((*S*)-3-((*S*)-1-azido-2-(3-bromophenyl)-2-oxoethyl)-1-methyl-2-oxoindolin-3-yl)carbamate (107i)

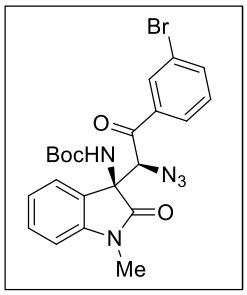

The use of **64d** with (*E*)-*tert*-butyl (1-methyl-2-oxoindolin-3-ylidene)carbamate (**55i**) and 2-azido-1-(3-bromophenyl)ethanone (**93g**) in general procedure afforded chiral adduct **107i** as white solid in 19 h in 97% yield with diastereomeric ratio 11:1 (syn:anti). mp 69-71 °C; $[\alpha]_D^{28}$= -224.4° (*c* 0.37, $CHCl_3$). Enantiomeric excess was determined by Chiralpak AD-H column, 85:15 (hexane : i-PrOH), 254 nm, 1 mL/min, t_{minor} = 13.46 min, t_{major} = 21.86 min, (90% ee). ^{1}H NMR (400 MHz, $CDCl_3$) δ 7.88 (t, *J* = 1.7 Hz, 1H), 7.73 (d, *J* = 7.9 Hz, 1H), 7.67 (d, *J* = 7.3 Hz, 1H), 7.57 (d, *J* = 7.3 Hz, 1H), 7.31 (d, *J* = 7.9 Hz, 1H), 7.27 (d, *J* = 6.8 Hz, 1H), 6.96 (t, *J* = 7.6 Hz, 1H), 6.81 (d, *J* = 7.8 Hz, 1H), 5.89 (s, 1H), 5.24 (s, 1H), 3.25 (s, 3H), 1.29 (s, 9H). ^{13}C NMR (100 MHz, $CDCl_3$) δ 192.6, 173.8, 154.3, 144.1, 137.3, 137.1, 131.7, 130.4, 130.3, 127.3, 126.4, 125.9, 123.2, 122.9, 108.6, 80.9, 64.2, 63.0, 28.1, 26.7. IR (neat): 3320, 2977, 2104, 1709, 1612, 1470, 1366, 1248, 1158, 752 cm^{-1}. HRMS (ESI) m/z: calcd. for $C_{22}H_{22}BrN_5O_4Na$ $[M+Na]^+$: 522.0753; found 522.0763.

3.16.10 *tert*-Butyl ((*S*)-3-((*S*)-1-azido-2-(4-methoxyphenyl)-2-oxoethyl)-1-methyl-2-oxoindolin-3-yl)carbamate (107j)

The use of **64d** with (*E*)-*tert*-butyl (1-methyl-2-oxoindolin-3-ylidene)carbamate (**55i**) and 2-azido-1-(4-methoxyphenyl)ethanone (**93c**) in general procedure afforded chiral adduct **107j** as white solid in 18 h in 80%

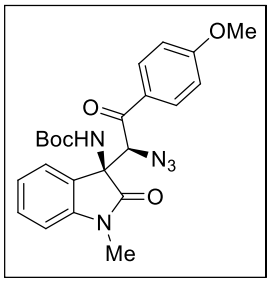

yield with diastereomeric ratio 4:1 (syn:anti). mp 79-82 °C; $[\alpha]_D^{19}$= -12.6° (*c* 1.00, $CHCl_3$). Enantiomeric excess was determined by Chiralpak AD-H column, 75:25 (hexane : i-PrOH), 254 nm, 1 mL/min, t_{minor} = 13.34 min, t_{major} = 15.66 min, (75% ee). ^{1}H NMR (400 MHz, $CDCl_3$) δ 7.83 (d, *J* = 8.9 Hz, 2H), 7.54 (d, *J* = 6.9 Hz, 1H), 7.26 (dd, *J* = 9.8, 5.2 Hz, 1H), 6.95 (t, *J* = 7.6 Hz, 1H), 6.87 (d, *J* = 8.9 Hz, 2H), 6.80 (d, *J* = 7.8 Hz, 1H), 6.00 (s, 1H), 5.17 (s, 1H), 3.82 (s, 3H), 3.24 (s, 3H), 1.26 (s, 9H). ^{13}C NMR (100 MHz, $CDCl_3$) δ 191.7, 174.1, 164.6, 154.1, 144.2, 131.4, 130.0, 128.2, 126.6, 125.6, 122.6, 114.1, 108.3, 80.6, 63.8, 63.0, 55.6, 28.1, 26.6. IR (neat): 3322, 2976, 2102, 1713, 1597, 1470, 1248, 1162, 1022, 752 cm^{-1}. HRMS (ESI) m/z: calcd. for $C_{23}H_{25}N_5O_5Na$ $[M+Na]^+$: 474.1753; found 474.1757.

3.16.11 *tert*-Butyl ((*S*)-3-((*S*)-1-azido-2-oxo-2-phenylethyl)-5-bromo-1-methyl-2-oxoindolin-3-yl)carbamate (107k)

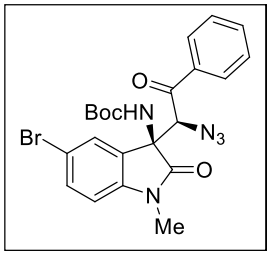

The use of **64b** with (*E*)-*tert*-butyl (5-bromo-1-methyl-2-oxoindolin-3-ylidene)carbamate (**55p**) and 2-azido-1-phenylethanone general procedure afforded chiral adduct **107k** as white solid in 24 h in 60% yield with diastereomeric ratio 11:1 (syn:anti). mp 71-73 °C; $[\alpha]_D^{20}$= +3.8° (*c* 1.00, $CHCl_3$). Enantiomeric excess was determined by Chiralpak AS-H column, 97:3 (hexane : i-PrOH), 254 nm, 1 mL/min, t_{major} = 21.49 min, t_{minor} = 28.35 min, (70% ee). ^{1}H NMR (400 MHz, $CDCl_3$) δ 7.91 – 7.78 (m, 2H), 7.69 (s, 1H), 7.60 (t, *J* = 7.4 Hz, 1H), 7.45 (t, *J* = 7.8 Hz, 2H), 7.38 (dd, *J* = 8.3, 2.0 Hz, 1H), 6.68 (d, *J* = 8.3 Hz, 1H), 5.90 (s, 1H), 5.24 (s, 1H), 3.24 (s, 3H), 1.32 (s, 9H). ^{13}C NMR (100 MHz, $CDCl_3$) δ 193.5, 173.6, 154.2, 143.4, 135.4, 134.7, 132.9, 129.1, 129.0, 128.9, 128.6, 115.5, 109.9, 81.2, 64.2, 63.0, 28.2, 26.9. IR (neat): 3343, 2976, 2103, 1710, 1608, 1486, 1365, 1248,

1158, 777 cm^{-1}. HRMS (ESI) m/z: calcd. for $C_{22}H_{22}BrN_5O_4Na$ $[M+Na]^+$: 522.0753; found 522.0747.

3.16.12 *tert*-Butyl ((*S*)-3-((*S*)-3-azido-4-oxochroman-3-yl)-5-bromo-1-methyl-2-oxoindolin-3-yl)carbamate (107l)

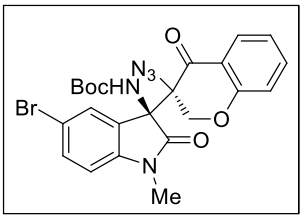

The use of **64b** with (*E*)-*tert*-butyl (5-bromo-1-methyl-2-oxoindolin-3-ylidene)carbamate (**55p**) and 3-azidochroman-4-one (**93k**) in general procedure afforded chiral adduct **107l** as white solid in 48 h in 78% yield with diastereomeric ratio 15:1 (syn:anti). mp 198-201 °C (decomposed); $[\alpha]_D^{21}$= +15.8° (*c* 1.00, $CHCl_3$). Enantiomeric excess was determined by Chiralpak AD-H column, 90:10 (hexane : i-PrOH), 254 nm, 1 mL/min, t_{minor} = 7.33 min, t_{major} = 9.43 min, (96% ee). ^{1}H NMR (400 MHz, $CDCl_3$) δ 8.05 (dd, *J* = 7.9, 1.5 Hz, 1H), 7.63 (d, *J* = 1.9 Hz, 1H), 7.57 – 7.52 (m, 1H), 7.51 (dd, *J* = 8.3, 1.8 Hz, 1H), 7.14 (t, *J* = 7.5 Hz, 1H), 6.88 (d, *J* = 8.3 Hz, 1H), 6.74 (d, *J* = 8.3 Hz, 1H), 6.39 (s, 1H), 4.02 (d, *J* = 12.5 Hz, 1H), 3.89 (d, *J* = 12.5 Hz, 1H), 3.12 (s, 3H), 1.25 (s, 9H). ^{13}C NMR (100 MHz, $CDCl_3$) δ 187.7, 171.9, 161.5, 153.5, 143.8, 137.2, 133.0, 128.5, 128.1, 127.3, 123.0, 121.7, 117.5, 115.3, 109.5, 80.9, 70.0, 67.3, 65.7, 28.1, 26.6. IR (neat): 3369, 2975, 2108, 1670, 1477, 1269, 1150, 720 cm^{-1}. HRMS (ESI) m/z: calcd. for $C_{23}H_{22}BrN_5O_5Na$ $[M+Na]^+$: 550.0702; found 550.0687.

3.16.13 *tert*-Butyl ((*S*)-3-((*S*)-1-azido-2-oxo-2-phenylethyl)-2-oxoindolin-3-yl)carbamate (107m)

The use of **64b** with (*E*)-*tert*-butyl (2-oxoindolin-3-ylidene)carbamate (**55a**) and 2-azido-1-phenylethanone (**93a**) in general procedure afforded chiral adduct **107m** as white solid in 24 h in 49% yield with diastereomeric ratio

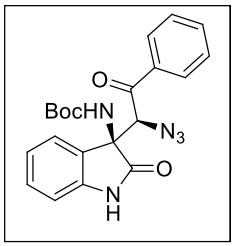

9:1 (syn:anti) . mp 169-171 °C (decomposed); $[\alpha]_D^{30}$= -13.0° (*c* 0.5, $CHCl_3$). Enantiomeric excess was determined by Chiralpak AS-H column, 80:20 (hexane : i-PrOH), 254 nm, 1 mL/min, t_{minor} = 7.24 min, t_{major} = 23.89 min, (93% ee). ^{1}H NMR (400 MHz, $CDCl_3$) δ 8.46 (s, 1H), 7.94 – 7.84 (m, 2H), 7.60 (t, *J* = 7.4 Hz, 1H), 7.55 (d, *J* = 7.4 Hz, 1H), 7.46 (t, *J* = 7.8 Hz, 2H), 7.23 (td, *J* = 7.7, 1.1 Hz, 1H), 6.98 (dd, *J* = 11.1, 4.0 Hz, 1H), 6.83 (d, *J* = 7.7 Hz, 1H), 6.09 (s, 1H), 5.22 (s, 1H), 1.34 (s, 9H). ^{13}C NMR (100 MHz, $CDCl_3$) δ 194.0, 175.7, 154.2, 141.1, 135.5, 134.5, 130.0, 128.9, 128.8, 127.0, 125.9, 122.8, 110.5, 81.1, 63.8, 63.6, 28.1. IR (neat): 3342, 2977, 2114, 1730, 1693, 1516, 1170, 759 cm^{-1}. HRMS (ESI) m/z: calcd. for $C_{21}H_{21}N_5O_4Na$ $[M+Na]^+$: 430.1491; found 430.1479.

3.16.14 *tert*-Butyl ((*S*)-3-((*S*)-3-azido-4-oxochroman-3-yl)-2-oxoindolin-3-yl)carbamate (107n)

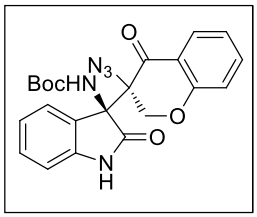

The use of **64d** with (*E*)-*tert*-butyl (2-oxoindolin-3-ylidene)carbamate (**55a**) and 3-azidochroman-4-one (**93k**) in general procedure afforded chiral adduct **107n** as white solid in 20 h in 28% yield with diastereomeric ratio 5:1 (syn:anti). mp 184-186 °C (decomposed); $[\alpha]_D^{17}$= -21.7° (*c* 0.20, $CHCl_3$). Enantiomeric excess was determined by Chiralpak AD-H column, 80:20 (hexane : i-PrOH), 254 nm, 1 mL/min, t_{minor} = 6.89 min, t_{major} = 8.18 min, (89% ee). ^{1}H NMR (400 MHz, DMSO) δ 10.63 (s, 1H), 7.86 (d, *J* = 8.0 Hz, 1H), 7.61 (dd, *J* = 12.0, 4.8 Hz, 1H), 7.54 (t, *J* = 8.1 Hz, 1H), 7.25 (t, *J* = 7.7 Hz, 1H), 7.19 – 7.09 (m, 1H), 7.08 – 6.90 (m, 3H), 6.80 (d, *J* = 7.8 Hz, 1H), 4.60 (d, *J* = 12.5 Hz, 1H), 4.28 (d, *J* = 11.7 Hz, 1H), 1.18 (s, 9H). ^{13}C NMR (100 MHz, DMSO) δ 184.6, 172.2, 158.7, 151.1, 141.6, 135.1, 127.7, 125.3, 124.2, 120.3, 119.4, 118.8, 115.7, 107.5, 77.5, 67.0,

65.2, 63.5, 25.7. IR (neat): 3267, 2924, 2108, 1721, 1606, 1466, 1250, 1154, 751 cm^{-1}. HRMS (ESI) m/z: calcd. for $C_{22}H_{21}N_5O_5Na$ $[M+Na]^+$: 458.1440; found 458.1440.

3.16.15 *tert*-Butyl ((*S*)-3-((*S*)-1-azido-2-(4-methoxyphenyl)-2-oxoethyl)-2-oxoindolin-3-yl)carbamate (107o)

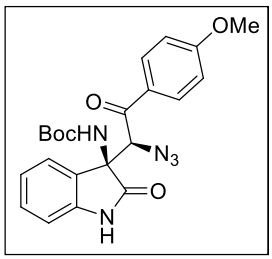

The use of **64b** with (*E*)-*tert*-butyl (2-oxoindolin-3-ylidene)carbamate (**55a**) and 2-azido-1-(4-methoxyphenyl)ethanone (**93c**) in general procedure afforded chiral adduct **107o** as white solid in 44 h in 64% yield with diastereomeric ratio 15:1 (syn:anti). mp 195-197 °C (decomposed); $[\alpha]_D^{24}$= -5.0° (*c* 1.00, $CHCl_3$). Enantiomeric excess was determined by Chiralpak AS-H column, 70:30 (hexane : i-PrOH), 254 nm, 1 mL/min, t_{minor} = 7.80 min, t_{major} = 27.32 min, (80% ee). ^{1}H NMR (400 MHz, DMSO) δ 10.53 (s, 1H), 7.83 (d, *J* = 8.8 Hz, 2H), 7.41 (s, 1H), 7.38 (d, *J* = 7.4 Hz, 1H), 7.12 (t, *J* = 7.6 Hz, 1H), 7.03 (d, *J* = 8.8 Hz, 2H), 6.80 (t, *J* = 7.5 Hz, 1H), 6.72 (d, *J* = 7.7 Hz, 1H), 5.38 (s, 1H), 3.84 (s, 3H), 1.23 (s, 9H). ^{13}C NMR (100 MHz, DMSO) δ 190.4, 175.0, 163.9, 153.5, 143.0, 131.0, 129.3, 128.0, 127.5, 124.8, 121.1, 114.2, 109.5, 79.1, 62.4, 62.3, 55.7, 27.8. IR (neat): 3142, 2978, 2099, 1713, 1659, 1595, 1468, 1219, 1152, 851, 752 cm^{-1}. HRMS (ESI) m/z: calcd. for $C_{22}H_{23}N_5O_5Na$ $[M+Na]^+$: 460.1597; found 460.1580.

3.16.16 *tert*-Butyl ((*S*)-3-((*S*)-1-azido-2-(4-bromophenyl)-2-oxoethyl)-2-oxoindolin-3-yl)carbamate (107p)

The use of **64b** with (*E*)-*tert*-butyl (2-oxoindolin-3-ylidene)carbamate (**55a**) and 2-azido-1-(4-bromophenyl)ethanone (**93d**) in general procedure afforded chiral adduct **107p** as white solid in 24 h in 68% yield with

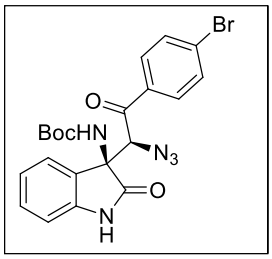

diastereomeric ratio 24:1 (syn:anti). mp 79-81 °C; $[\alpha]_D^{24}$= -8.66° (*c* 2.27, $CHCl_3$). Enantiomeric excess was determined by Chiralpak AS-H column, 80:20 (hexane : i-PrOH), 254 nm, 1 mL/min, t_{minor} = 7.45 min, t_{major} = 20.14 min, (80% ee). ^{1}H NMR (400 MHz, $CDCl_3$) δ 9.24 (s, 1H), 7.70 (d, *J* = 8.4 Hz, 2H), 7.53 (d, *J* = 8.4 Hz, 3H), 7.19 (t, *J* = 7.6 Hz, 1H), 6.95 (t, *J* = 7.6 Hz, 1H), 6.79 (d, *J* = 7.7 Hz, 1H), 6.16 (s, 1H), 5.19 (s, 1H), 1.31 (s, 9H). ^{13}C NMR (100 MHz, $CDCl_3$) δ 193.2, 176.2, 154.3, 141.4, 134.3, 132.2, 130.3, 130.2, 129.9, 127.0, 125.8, 122.8, 110.8, 81.1, 63.84, 63.78, 28.1. IR (neat): 3170, 2981, 2111, 1731, 1667, 1396, 1162, 1070, 749 cm^{-1}. HRMS (ESI) m/z: calcd. for $C_{21}H_{20}BrN_5O_4Na$ $[M+Na]^+$: 508.0596; found 508.0598.

3.17 Copper (I) Catalyzed Azide-Alkyne Cycloaddition

A flame-dried Schlenk tube was charged with **107a** (86% ee) (0.12 mmol, 50.6 mg), phenylacetylene (**110**) (0.59 mmol, 64.79 μL), *t*-BuOH (2 mL), water (2 mL) and sodium L-ascorbate (0.12 mmol, 23.8 mg) under argon. $CuSO_4.5H_2O$ (0.12 mmol, 30.0 mg) was added and reaction mixture was stirred at 40 °C for 4h. After the consumption of **107a**, mixture was diluted with diethyl ether followed by extraction with water dried over $NaSO_4$. Column chromatography with ethyl acetate:hexane (1:2) afforded triazole **109**.

3.17.1 *tert*-Butyl ((*S*)-1-methyl-2-oxo-3-((*S*)-2-oxo-2-phenyl-1-(4-phenyl-1H-1,2,3-triazol-1-yl)ethyl)indolin-3-yl)carbamate (109)

Given procedure starting from **107a** (60% ee) and phenylacetylene (**110**) general afforded **109** as white solid in 8h in 85% yield. mp 227-229 °C; $[\alpha]_D^{29}$= -10.32° (*c* 0.37, $CHCl_3$). Enantiomeric excess was determined by Chiralpak IA column, 80:20 (hexane : i-PrOH), 254 nm, 1 mL/min, t_{minor} = 14.12 min, t_{major} = 33.57 min,

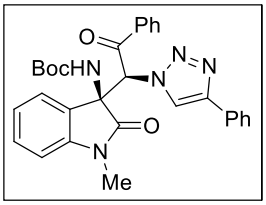

(60% ee). ^{1}H NMR (400 MHz, $CDCl_3$) δ 8.11 (s, 1H), 7.75 (d, *J* = 2.7 Hz, 2H), 7.73 (d, *J* = 2.2 Hz, 2H), 7.65 (s, 1H), 7.42 (t, *J* = 7.4 Hz, 1H), 7.37 – 7.20 (m, 6H), 7.19 – 7.11 (m, 1H), 6.86 (t, *J* = 7.6 Hz, 1H), 6.69 (d, *J* = 7.8 Hz, 1H), 5.42 (s, 1H), 3.20 (s, 3H), 1.26 (s, 9H). ^{13}C NMR (100 MHz, $CDCl_3$) δ 189.4, 171.5, 152.0, 145.4, 141.8, 132.5, 132.4, 128.2, 126.7, 126.6, 126.0, 123.8, 123.7, 120.8, 119.2, 106.3, 78.9, 62.1, 59.4, 26.0, 24.5 (3 overlapping signals). IR (neat): 3298, 2924, 1692, 1613, 1246, 1158, 1021, 754, 689 cm^{-1}. HRMS (ESI) m/z: calcd. for $C_{30}H_{30}N_5O_4$ $[M+H]^+$: 524.2298; found 524.2317.

3.18 Reduction of Azides

Method A: Catalytic Hydrogenation

Adapted from the literature procedure,[72] to a solution of **107a** or **107g** (100 mg) in MeOH (3 mL) Pd/C (10 mol%) was added at room temperature. The suspension was stirred under hydrogen gas at atmospheric pressure for 12 h. The reaction mixture was filtered and washed with MeOH (20 mL). The filtrate was concentrated in vacuo and loaded to silica gel column eluted with ethyl acetate: DCM (1:3) to afford corresponding amine.

Method B: Staudinger Reduction

Compound **107a** (0.7 mmol, 295.0 mg) was dissolved in THF (5 mL) in a Schlenk tube at 0 °C. Triphenylphosphine (0.7 mmol, 183.6 mg) was added in small portions and mixture was allowed to reach room temperature. Upon the consumption of the starting material, distilled water (321.8 μL) was added and stirred at 50 °C until the gas evolution ceases. After the reaction mixture was concentrated, residue was diluted with ethyl acetate and extracted with water and brine, respectively. Organic phase was dried over $MgSO_4$, filtered and condensed.

Silica gel column chromatography with ethyl acetate : DCM (1:3) afforded compound **111** as white solid in 30% yield.

3.18.1 *tert*-Butyl ((S)-3-((S)-1-amino-2-oxo-2-phenylethyl)-1-methyl-2-oxoindolin-3-yl)carbamate (111a)

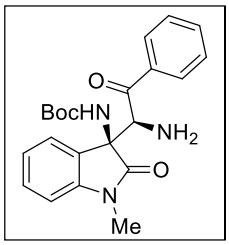

Reduction of **107a** (86% ee) according to procedures given as method A and B afforded chiral **111** as white solid in 94% and 30% yield, respectively. mp 75-77 °C; $[\alpha]_D^{29}$= -17.0° (*c* 0.50, $CHCl_3$). Enantiomeric excess was determined by Chiralpak AD-H column, 70:30 (hexane : i-PrOH), 254 nm, 1 mL/min, t_{minor} = 14.29 min, t_{major} = 19.71 min, (85% ee). ^{1}H NMR (400 MHz, $CDCl_3$) δ 7.66 (d, *J* = 7.3 Hz, 2H), 7.46 (t, *J* = 7.4 Hz, 1H), 7.40 - 7.26 (m, 3H), 7.12 (td, *J* = 7.7, 1.0 Hz, 1H), 6.84 (t, *J* = 7.5 Hz, 1H), 6.67 (d, *J* = 7.8 Hz, 1H), 6.33 (s, 1H), 4.99 (s, 1H), 3.22 (s, 3H), 2.44 (s, 2H), 1.24 (s, 9H). ^{13}C NMR (100 MHz, $CDCl_3$) δ 199.0, 175.4, 154.6, 144.2, 136.2, 133.5, 129.5, 128.6, 128.3, 127.8, 124.1, 122.4, 108.2, 80.5, 62.4, 59.3, 28.2, 26.5. IR (neat): 3325, 2976, 2927, 1707, 1613, 1469, 1366, 1248, 1160, 733 cm^{-1}. HRMS (ESI) m/z: calcd. for $C_{22}H_{25}N_3O_4Na$ $[M+Na]^+$: 418.1743; found 418.1721.

3.18.2 *rac-tert*-Butyl (3-(3-amino-4-oxochroman-3-yl)-1-methyl-2-oxoindolin-3-yl)carbamate (111g)

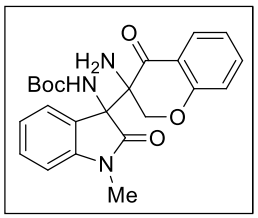

Reduction of r*ac*-**107g** according to method A afforded amine as white solid in 8h in 90% yield. mp 89-91 °C; ^{1}H NMR (400 MHz, $CDCl_3$) δ 7.78 (d, *J* = 7.8 Hz, 1H), 7.41 (t, *J* = 7.6 Hz, 1H), 7.32 (d, *J* = 7.4 Hz, 1H), 7.25 (t, *J* = 7.7 Hz, 1H), 6.98 (d, *J* = 7.5 Hz, 1H), 6.94 (d, *J* = 7.5 Hz, 1H), 6.86 (d, *J* = 8.4 Hz, 1H), 6.78 (d, *J* = 7.8 Hz, 1H), 6.52 (s, 1H), 4.43 (d, *J* = 11.9

Hz, 1H), 4.29 (d, *J* = 11.9 Hz, 1H), 3.21 (s, 3H), 2.36 (s, 2H), 1.18 (s, 9H).^{13}C NMR (100 MHz, $CDCl_3$) δ 191.6, 175.4, 160.7, 154.5, 145.2, 136.2, 129.7, 127.9, 126.0, 124.8, 122.2, 121.9, 120.3, 117.5, 108.2, 80.3, 72.1, 63.6, 61.5, 28.0, 26.5. IR (neat): 3375, 2930, 1707, 1612, 1469, 1366, 1248, 1160, 1020, 751 cm^{-1}.

3.19 Synthesis of Cyclic Urea (112a)

In an oven-dried round bottom flask **111a** (0.25 mmol, 98.9 mg) was dissolved in DCM (5 mL) at room temperature. Trifluoroacetic acid (10.00 mmol, 765.75 μL) was added all in once and reaction progress was monitored by TLC. After the consumption of the starting, all volatiles were evaporated in vacuum. The residue again dissolved in DCM (5 mL) and 1,1'-carbonyldiimidazole (**113**) (1.25 mmol, 202.7 mg) and triethylamine (1.25 mmol, 173.96 μL) was added at room temperature, sequentially. After overnight reaction, reaction mixture was directly loaded to silica gel column and elution with ethyl acetat:hexane (1:5) afforded cyclic urea **112a**.

3.19.1 (3'*S*,5*S*)-5-Benzoyl-1'-methylspiro[imidazolidine-4,3'-indoline]-2,2'-dione (112a)

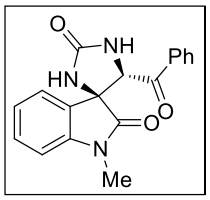

Given procedure starting from **107a** (85% ee) afforded **112a** as colorless crystals in 12h in 32% yield. mp 164-166 °C; $[\alpha]_D^{29}$= -51.51° (*c* 0.37, $CHCl_3$). Enantiomeric excess was determined by Chiralpak IA column, 90:10 (hexane : i-PrOH), 254 nm, 1 mL/min, t_{minor} = 8.50 min, t_{major} = 10.50 min, (85% ee). ^{1}H NMR (400 MHz, $CDCl_3$) δ 8.18 (d, *J* = 9.3 Hz, 1H), 7.62 (dd, *J* = 7.3, 1.2 Hz, 2H), 7.46 (dd, *J* = 16.7, 7.7 Hz, 2H), 7.35-7.25 (m, 3H), 7.14 (dt, *J* = 7.8, 1.1 Hz, 1H), 6.71 (t, *J* = 11.9, 2H), 6.66 (d, *J* = 9.3 Hz, 1H), 3.25 (s, 3H). ^{13}C NMR (100 MHz, $CDCl_3$) δ 193.4, 172.4, 158.1, 143.8, 135.0, 134.7, 131.3, 129.0, 128.6, 126.5, 123.6, 123.1,

109.2, 61.6, 54.1, 27.0. IR (neat): 3260, 3069, 2922, 1670, 1548, 1220, 1160, 752, 627 cm^{-1}.

CHAPTER 4

CONCLUSION

In brief, a wide variety 2-oxindole fused spiro-heterocycle precursors were synthesized through bifunctional squaramide catalyzed aza-Friedel-Crafts and Mannich reactions of isatin-derived ketimines **55** in high yield and stereoselectivity (Scheme 24). In the first part of this thesis study, quinine-derived bifunctional squaramides with bulky hydrocarbon units (1-adamantyl, 2-adamantyl and *t*-butyl) were synthesized. Synthesized organocatalysts were examined in the asymmetric transformations of isatin-derived ketimines and facile methodologies with optimized reaction conditions were determined for the synthesis of α-chiral amines.

In the first part, 1,3-aminonaphthols **95** merged with 2-oxindole scaffold were obtained by very low (2 mol%) 2-adamantyl substituted squaramide **64b** via aza-Friedel-Crafts reaction of isatin ketimines and 1-naphthol, 2-naphthol and activated phenols (Scheme 24). The reaction proceeded smoothly to afford excellent yield (up to 98%) and enantioselectivity (>99% ee) for the large majority of various substrates. To the best of our knowledge, squaramide **64b** was examined in an asymmetric reaction for the first time. It was also discovered that besides being compatible with different *N*-alkoxycarbonyl protecting groups, squaramide **64b** surpasses previously known quinine-derived squaramides in terms of stereoselectivity. In representative examples, the resulting carbamate protected aminonaphthols were converted into 1,4-naphthoxazepine **100** through bromoethylsulfonium triflate as annulation reagent and 7-membered spirocyclic imine via $ZnCl_2$ promoted intramolecular cyclization (Scheme 24).

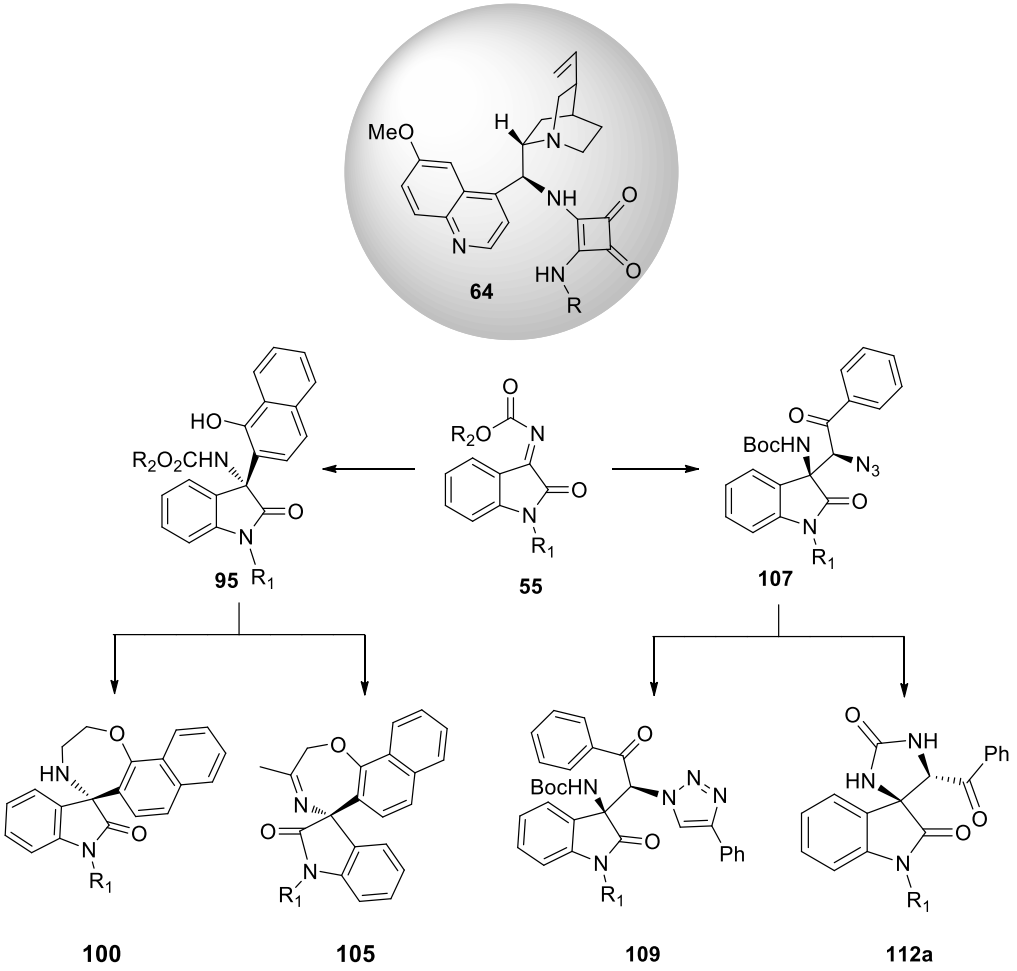

Scheme 24 General synthetic pathway for target compounds.

In the second part of the study, asymmetric Mannich reactions α-azido ketones possessing masked amino functionality were investigated (Scheme 24). After a careful optimization study 2-adamantyl substituted squaramide **64b** and 3,5-bis(trifluoromethyl)aniline substituted squaramide **64d** were decided to be the most promising organocatalysts and optimum reaction conditions were determined for both. Several cyclic and acylic α-azido ketones reacted with isatin-derived ketimines **55** in the presence of each catalyst. Satisfactory results with high yields (up to 97%) and stereoselectivity (up to dr = 24:1 *syn*:*anti* and 96% ee) were attained in the corresponding Mannich bases **107** with two contiguous stereogenic centers. Absolute configuration of adducts were determined by X-ray

crystallography and stereochemical outcome were supported by proposed transition state models taking account of steric interactions. In order to exhibit the synthetic potential of the 2-azidoethaneamine functionality, enantioenriched products were converted into 1,2,3-triazole **109** via Copper (I) catalyzed azide-alkyne cycloaddition and spirocyclic urea **112a** after the reduction of azide moiety by Pd-catalyzed hydrogenation (Scheme 24).

REFERENCES

1. Singh, G. S.; Desta, Z. Y. *Chem. Rev*. **2012**, *112*, 6104-6155.

2. Erdmann, O. L. *J. Prakt. Chem.* **1840**, *19*, 321–362.

3. Laurent, A. *Ann. Chim. Phys*. **1840**, *3*, 393-434.

4. Kekule, A. *Chem. Ber*. **1869**, *2*, 748-749.

5. (a) Kitamura, H.; Kato, A.; Esaki, T.; *Eur. J. Pharmacol*. **2001**, *418*, 225-230; (b) Crosignani, S.; Jorand-Lebrun, C.; Grippi-Vallotton, T. U.S. Patent 20120115895, **2012**; (c) Griebel, G.; Simiand, J.; Gal, C. S-L.; Wagnon, J.; Pascal, M.; Scatton, B.; Maffrand, J-P.; Soubrié, P. *PNAS*, **2002**, *99*, 6370-6375; (d) Yeung, B. K. S.; Zou, B.; Rottmann, M.; Lakshminarayana, S. B., Ang, S. H.; Leong, S. Y.; Tan, J.; Wong, J.; Keller-Maerki, S.; Fischli, C.; Goh, A.; Schmitt, E. K.; Krastel, P.; Francotte, E.; Kuhen, K.; Plouffe, D.; Henson, K.; Wagner, T.; Winzeler, E. A.; Petersen, F.; Brun, R.; Dartois, V.; Diagana, T. T.; Keller, T. H. *J. Med. Chem*. **2010**, *53*, 5155–5164; (e) Ghosh, A. K.; Schiltz, G.; Perali, R. S.; Leshchenko, S.; Kay, S.; Walters, D. E.; Koh, Y.; Maeda, K.; Mitsuya, H. *Bioorg. Med. Chem. Lett.* **2006**, *16*, 1869–1873; (f) Kumar, R. S.; Rajesh, S. M.; Perumal, S.; Debjani, B.; Yogeeswari, P.; Sriram, D. *Eur. J. Med. Chem.* **2010**, *45*, 411-422.

6. Mei, G-J.; Shi, F. *Chem. Commun*. **2018**, *54*, 6607-6621.

7. Pavlovska, T. L.; Redkin, R. G.; Lipson, V. V.; Atamanuk, D. V. *Mol. Diversity* **2016**, *20*, 299-344.

8. Cheng, D.; Ishihara, Y.; Tan, B.; Barbas, C. F. III. *ACS Catal.* **2014**, *4*, 743-762.

9. Mei, G.-J.; Shi, F. *J. Org. Chem.***2017**, *82*, 7695-7707.

10. (a) Dalko, P. I. *Chimia* **2007**, *61*, 213-218; (b) Kolodiazhnyi, O. I. *Tetrahedron:Asymmetry* **1998**, *9*, 1279-1332; (c) Farina, V.; Reeves, J. T.; Senanayake, C. H.; Song, J. J. *Chem Rev.* **2006**, *106*, 2734-2793; (d) Ghislieri, D.; Green, A. P.; Pontini, M.; Willies, S. C.; Rowles, I.; Frank, A.; Grogan, G.; Turner, N. J. *J Am Chem Soc.* **2013**, *135*, 10863-10869.

11. Hyneck, M.; Dent, J.; Hook, J. B. In *Chirality in Drug Design an Synthesis*. Brown C. Ed.; Elsevier, **1990**; Vol. 1, pp 1-28.

12. Murray, C. J.; Rosenfeld, L. C.; Lim, S. S.; Andrew, K. G.; Foreman, K. J.; Haring, D.; Fullman, N.; Naghavi, M.; Lozano, R.; Lopez, A. D. *Lancet* **2012**, *379*, 413-431.

13. Misra, M.; Pandey, S. K.; Pandey, V. P.; Pandey, J.; Tripathi, R.; Tripathi, R. P. *Bioorg. Med. Chem*. **2009**, *17*, 625-633.

14. Calcaterra, A.; D'Acquarica, I. *J. Pharmaceut. Biomed.* **2018**, *147*, 323-340.

15. (a) Agranat, I.; Caner, H. *Drug Discovery Today* **1999**, *4*, 313-321; (b) Agranat, I.; Wainschtein, S. R. *Drug Discovery Today* **2010**, *15*, 163-170.

16. Mayer, J. M.; Testa, B. *Drugs Future* **1997**, *22*, 1347-1366.

17. (a) Hutt, A. J.; Caldwell, J. T. *J. Pharm. Pharmacol.* **1983**, *35*, 693-704; (b) Hao, H.; Wang, G.; Sun, J. *Drug Metab. Rev.* **2005**, *37*, 215-234.

18. Wínska, K.; Potaniec, B.; Maczka, W.; Grabarczyk, M.; Anioł, M.; Wawrzeńczyk, C. *Chemik* **2014**, *68*, 83-90.

19. (a) Ohloff, G.; Klein, E.; Schenck, G. O. *Angew. Chem.* **1961**, *73*, 578; (b) Ohloff, G. *Pure Appl. Chem*. **1975**, *43*, 481.

20. Brenna, E.; Fuganti, C.; Serra, S. *Tetrahedron:Asymmetry* **2013**, *14*, 1-42.

21. (a) Hajos, Z. G.; Parrish, D. R. *J. Org. Chem*. **1974**, *39*, 1615-1621; (b) Eder, U.; Sauer, G.; Wiechert R. *Angew. Chem*. **1971**, *83*, 492-493.

22. Dondoni, A.; Massi, A. *Angew. Chem. Int. Ed*. **2008**, *47*, 4638-4660.

23. Zhou, Q-L. *Angew. Chem. Int. Ed*. **2016**, *55*, 5352-5353.

24. Moyano, A. In *Stereoselective Organocatalysis: Bond Formation Methodologies and Activation Modes*. Torres, R. R. Ed.; Wiley: New Jersey, **2013**; Vol. 2, pp 11-81.

25. Okino, T.; Hoashi, Y.; Takemoto, Y. *J. Am. Chem. Soc*. **2003**, *125*, 12672-12673.

26. Riant, O.; Kagan, H. B. *Tetrahedron Lett*. **1989**, *30*, 7403-7406.

27. Iwabuchi, Y.; Nakatani, M.; Yokoyama, N.; Hatakeyama, S. *J. Am. Chem. Soc*. **1999**, *121*, 10219-10220.

28. Doyle, A. G.; Jacobsen, E. N. *Chem. Rev*. **2007**, *107*, 5713-5743.

29. Alemán, J.; Parra, A.; Jiang, H.; Jørgensen, K. A. *Chem. Eur. J*. **2011**, *17*, 6890-6899.

30. (a) Okino, T.; Hoashi, Y.; Furukawa, T.; Xu, X. N.; Takemoto, Y. *J. Am. Chem. Soc.* **2005**, *127*, 119-125; (b) Malerich, J. P.; Hagihara, K.; Rawal, V. H. *J. Am. Chem. Soc*. **2008**, *130*, 14416-14417.

31. Nugent, T. C. In *Process Chemistry in the Pharmaceutical Industry*. Gadamasetti, K.; Braish, T. Ed.; Taylor & Francis: Baco Raton, **2008**; Vol. 2, pp 137-156.

32. Charette, A. B. In *Chiral Amine Synthesis*. Nugent, T. C. Ed.; Wiley: Weinheim, **2010**; pp 1-43.

33. Johannsen, M. *Chem. Commun.* **1999**, 2233-2234.

34. (a) Chauhan, P.; Chimni, S. S. *Eur. J. Org. Chem*. **2011**, *9*, 1636-1640; (b) Uraguchi, D.; Sorimachi, K.; Terada, M. *J. Am. Chem. Soc.* **2004**, *126*, 11804-11805; (c) Feng, J.; Yan, W.; Wang, D.; Li, P.; Sun, Q.; Wang, R. *Chem. Commun*. **2012**, *48*, 8003-8005; (d) Yarlagadda, S.; Sridhar, B.; Reddy, B. V. S. *Chem. Asian J.* **2018**, *13*, 1327-1334; (e) Zhang, K-F.; Nie, J.; Guo, R.; Zheng, Y.; Ma, J-A. *Adv. Synth. Catal*. **2013**, *355*, 3497-3502.

35. Zhou, D.; Huang, Z.; Yu, X.; Wang, Y.; Li, J.; Wang, W.; Xie, H. *Org. Lett*. **2015**, *17*, 5554-5557.

36. Kaya, U.; Chauhan, P.; Mahajan, S.; Deckers, K.; Valkonen, A.; Rissanen, K.; Enders D. *Angew. Chem. Int. Ed.* **2017**, *56*, 15358-15362.

37. Karahan, S.; Tanyeli, C. *New J. Chem*. **2017**, *41*, 9192-9202.

38. Verkade, J. M. M.; van Hemert, L. J. C.; Quaedflieg, P. J. L. M.; Rutjies, F. P. J. T. *Chem. Soc. Rev.* **2008**, *37*, 29-41.

39. List, B. *J. Am. Chem. Soc.* **2000**, *122*, 9336- 9337.

40. Wang X-B.; Li T-Z.; Sha, F.; Wu, X-Y. *Eur. J. Org. Chem*. **2014**, *4*, 739-744.

41. Zhu, Y.; Meng, Q.; Li, X. *Org. Chem. Front*. **2016**, *3*, 709-713.

42. Rao, K. S.; Ramesh, P.; Chowhan, L. R. Trivedi, R. *RSC Adv*. **2016**, *6*, 8242-8247.

43. İşibol, D.; Karahan, S.; Tanyeli, C. *Tetrahedron Lett*. **2018**, *59*, 541-545.

44. Ding, P-G.; Hu, X-S.; Zhou, F.; Zhou, J. *Org. Chem. Front.* **2018**, *5*, 1542-1559.

45. Palacios, F.; Alonso, C.; Aparicio, D.; Rubiales, G.; de los Santos, J. M. In *Organic Azides: Syntheses and Applications*. Bräse, S.; Banert, K. Wiley: Chippenham, **2010**; pp 439-467.

46. Dheer, D.; Singh, V.; Shankar, R. *Bioorg. Chem.* **2017**, *71*, 30-54.

47. Okumuş, S.; Tanyeli, C.; Demir, A. S. *Tetrahedron Lett*. **2014**, *55*, 4302-4305.

48. For selected examples of organocatalytic reactions catalyzed by $-CF_3$ substituted aryl squaramides, see: (a) Parhi, B.; Maity, S.; Ghorai, P. *Org. Lett.* **2016**, *18*, 5220-5223; (b) Cosimi, E.; Engl, O. D.; Saadi, J.; Ebert, M.; Wennemers, H. *Angew. Chem. Int. Ed*. **2016**, *55*, 13127-13131; (c) Chauhan, P.; Mahajan, S.; Kaya, U.; Valkonen, A.; Rissanen, K.; Enders, D. *Adv. Synth. Catal*. **2016**, *358*, 3173-3178; (d) Iriarte, I.; Vera, S.; Badiola, E.; Mielgo, A.; Oiarbide, M.; Garcia, J. M.; Odriozola, J. M.; Palomo, C. *Chem. Eur. J.* **2016**, *22*, 13690-13696; (e) Veverkova, E.; Bilka, S.; Baran, R.; Sebesta, R. *Synthesis* **2016**, *48*, 1474-1482; (f) Chen, L.; Wu, Z-J.; Zhang, M-L.; Yue, D-F.; Zhang, X-M.; Xu X-Y.; Yuan, W-C. *J. Org. Chem.* **2015**, *80*, 12668–12675; (g) Zhao, M-X.; Zhu, H-K.; Dai, T-L.; Shi, M. *J. Org. Chem.* **2015**, *80*, 11330–11338; (h) Sun, W.; Hong, L.; Zhu, G.; Wang, Z.; Wei, X.; Ni, J.; Wang, R. *Org. Lett.* **2014**, *16*, 544–547; (i) Zhao, M-X.; Bi, H-L.; Zhou, H.; Yang, H.; Shi, M. *J. Org. Chem*. **2013**, *78*, 9377–9382; (j) Yang, W.; Du, D-M. *Org*. *Lett*. **2010**, *12*, 5450-5453; (k) He, H-X.; Du, D-M. *RSC Adv*. **2013**, *3*, 16349-16358; *Tetrahedron* **2014**, *25*, 637-643; *Eur*. *J*. *Org*. *Chem*. **2014**, *28*, 6190-6199; (l) Zhao B-L.; Du, D-M. *Org*. *Biomol*. *Chem*. **2014**, *12*, 1585-1594; *Adv*. *Synth*. *Catal*. **2016**, *358*, 3992-3998; *Chem*. *Commun*. **2016**, *52*, 6162-6165; (m) Peng, J.; Zhao, B-L.; Du, D-M. *Adv. Synth. Catal*. **2015**, *357*, 3639-3647; (n) Zhao, B-L.; Zhang, D.; Liu, L.; Du, D-M. *Org*. *Biomol*. *Chem*. **2016**, *14*, 6337-6345;

(o) Li, J. H.; Wen, H.; Liu, L.; Du, D. M. *Eur. J. Org. Chem.* **2016**, *14*, 2492-2499; (p) Alemán, J.; Parra, A.; Jiang, H.; Jørgensen, K. A. *Chem. Eur. J.* **2011**, *17*, 6890-6899.

49. Işık, M.; Ünver, M. Y.; Tanyeli, C. *J. Org. Chem.* **2015**, *80*, 828-835.

50. Vakulya, B.; Varga, S.; Csampai, A.; Soós, T. *Org. Lett.* **2005**, *7*, 1967-1969.

51. Kanberoğlu, E.; Tanyeli, C. *Asian J. Org. Chem.* **2016**, *5*, 114-119.

52. Cali, P.; Begtrup, M. *Synthesis* **2002**, *1*, 63-66.

53. Yan, W.; Wang, D.; Feng, J.; Li, P.; Zhao, D.; Wang, R. *Org. Lett.* **2013**, *14*, 2512-2515.

54. Montesinos-Magraner, M.; Vila, C.; Cantón, R.; Blay, G.; Fernández, I.; Muñoz, M. C.; Pedro, J. R. *Angew. Chem. Int. Ed.* **2015**, *54*, 6320-6324.

55. Yar, M.; McGarrigle, E. M.; Aggarwal, V. K. *Org. Lett.* **2009**, *11*, 257-260.

56. (a) Nagarajan, K.; Venkateswarlu, A.; Kulkarni, C. L.; Nagana, G. A.; Shah, R. K. *Indian J. Chem.* **1974**, *12*, 236-238; (b) Nagarajan, K.; David, J.; Kulkarn, Y. S.; Hendi, S. B.; Shenoy, S.; Upadhyaya, J. P. *Eur. J. Med. Chem.* **1986**, *21*, 21-22; (c) Liao, Y.; Venhuis, B. J.; Rodenhuis, N.; Timmerman, W.; Wikström, H.; Meier, E.; Bartoszyk, G. D.; Böttcher, H.; Seyfried, C. A.; Sundell, S. *J. Med. Chem.* **1999**, *42*, 2235-2244.

57. Patonay, T.; Hoffman, R. V. *J. Org. Chem.* **1994**, *59*, 2902-2905.

58. Juhász-Tóth, E.; Patonay, T. *Eur. J. Org. Chem.* **2002**, *67*, 3055-3064.

59. (a) Martínez-Castañeda, Á.; Kędziora, K.; Lavandera, I.; Rodríguez-Solla, H.; Concellón, C.; del Amo, V. *Chem. Commun.* **2014**, *50*, 2598–2600. (b) Chowdari, N. S.; Ahmad, M.; Albertshofer, K.; Tanaka, F.; Barbas, C. F. III. *Org. Lett.* **2006**, *8*, 2839–2842.

60. Özçubukçu, S.; Ozkal, E.; Jimeno, C.; Pericás, M. A. *Org. Lett.* **2009**, *11*, 4680-4683.

61. Bobcheva, Z.; Zhiryakova, D.; Guncheva, M. *J. Enzyme Inhib. Med. Chem.* **2011**, *26*, 587-591.

62. Busschaert, N.; Park, S-H.; Baek, K-H.; Choi, Y. P.; Park, J.; Howe, E. N. W.; Hiscock, J. R.; Karagiannidis, L. E.; Marques, I.; Félix, V.; Namkung, W.; Sessler, J. L.; Gale, P. A.; Shin, I. *Nat. Chem*. **2017**, *9*, 667-675.

63. Manoni, F.; Connon, S. J. *Angew. Chem. Int. Ed.* **2014**, *53*, 2628-2632.

64. Furdas, S. D.; Shekfeh, S; Kannan, S.; Sippl W.; Jung, M. *Med. Chem. Commun.* **2012**, *3*, 305-311.

65. Tang, B-X.; Song, R-J.; Wu, C-Y.; Liu, Y.; Zhou M-B.; Wei, W-T.; Deng, G-B.; Yin, D-L.; Li J-H. *J. Am. Chem. Soc.* **2010**, *132*, 8900-8902.

66. Boraei, A. T.; El Tamany, E. S. H.; Ali, I. A. I.; Gebriel, S. M. *J. Heterocyclic Chem.* **2017**, *54*, 2881-2888.

67. Vyas, D. J.; Fröhlich, R.; Oestreich, M. *J. Org. Chem*. **2010**, *75*, 6720-6723.

68. Bittner, S.; Assaf, Y.; Krief, P.; Pomerantz, M.; Ziemnicka, B. T.; Smith, C. G. *J. Org. Chem.* **1985**, *50*, 1712-1718.

69. Urban, M.; Franc, M.; Hofmanová, C.; Veselý, J. *Org. Biomol. Chem.* **2017**, *15*, 9071-9076.

70. (a) Lourenço, N. M. T.; Afonso, C. A. M. *Tetrahedron* **2003**, *59*, 789-794; (b) Gong, P. K.; Blough, B. E.; Brieaddy, L. E.; Huang, X.; Kuhar, M. J.; Navarro, H. A.; Carroll, F. I. *J. Med. Chem.* **2007**, *50*, 3686-3695.

71. (a) Patonay, T.; Juhász-Tóth, E.; Bényei, A. *Eur. J. Org. Chem.* **2002**, *2002*, 285-295; (b) Vita, M. V.; Waser, J. *Org. Lett*. **2013**, *15*, 3246-3249.

72. Johannes, J.W.; Almeida, L.; Daly, K.; Ferguson, A. D.; Grosskurth, S. E.; Guan, H.; Howard, T.; Ioannidis, S.; Kazmirski, S.; Lamb, M. L.; Larsen, N. A.; Lyne, P. D.; Mikule, K.; Ogoe, C.; Peng, B.; Petteruti, P.; Read, J. A.; Su, N.; Sylvester, M.; Throner, S.; Wang, W.; Wang, X.; Wu, J.; Ye, Q.; Yu, Y.; Zheng, X; Scott, D. A. *Bioorg. Med. Chem. Lett.* **2015**, *25*, 5743-5747.

APPENDIX A

NMR SPECTRA

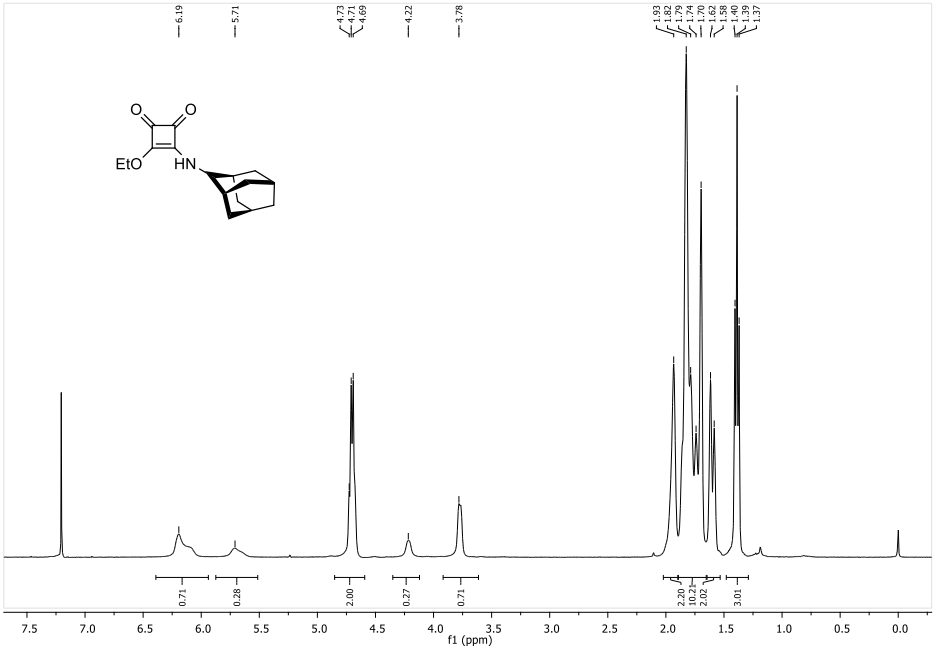

Figure A. 1 ^{1}H NMR spectrum of **80b**.

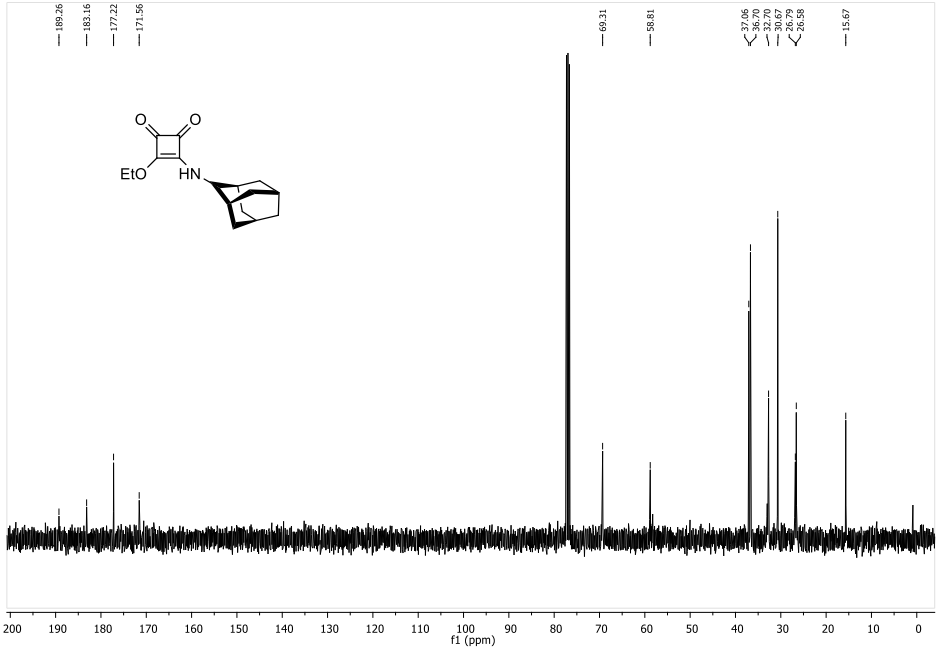

Figure A. 2 ^{13}C NMR spectrum of **80b**.

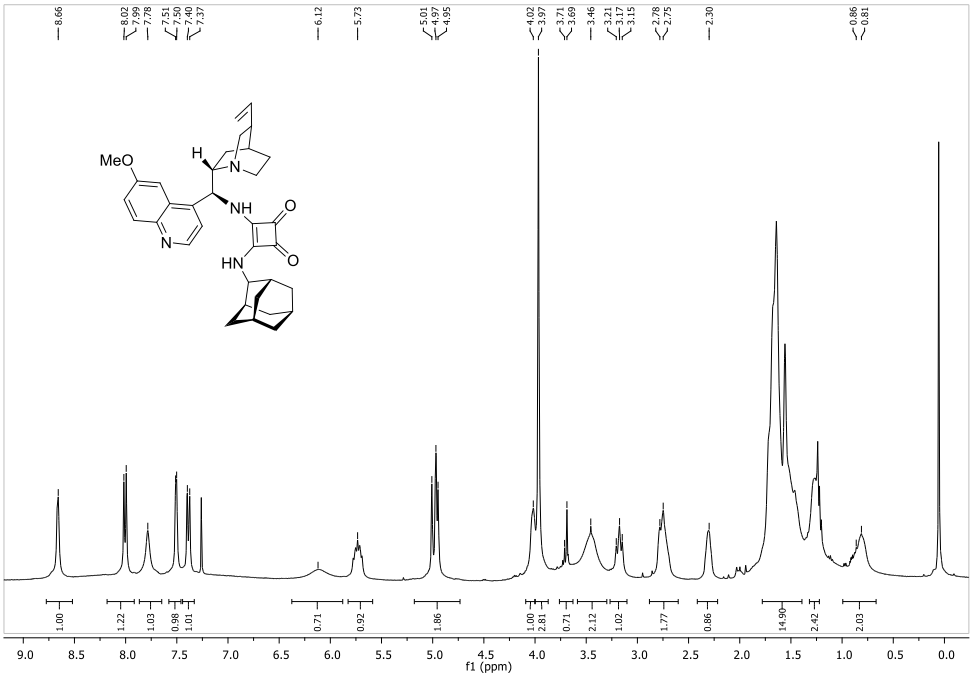

Figure A. 3 ^{1}H NMR spectrum of **64b**.

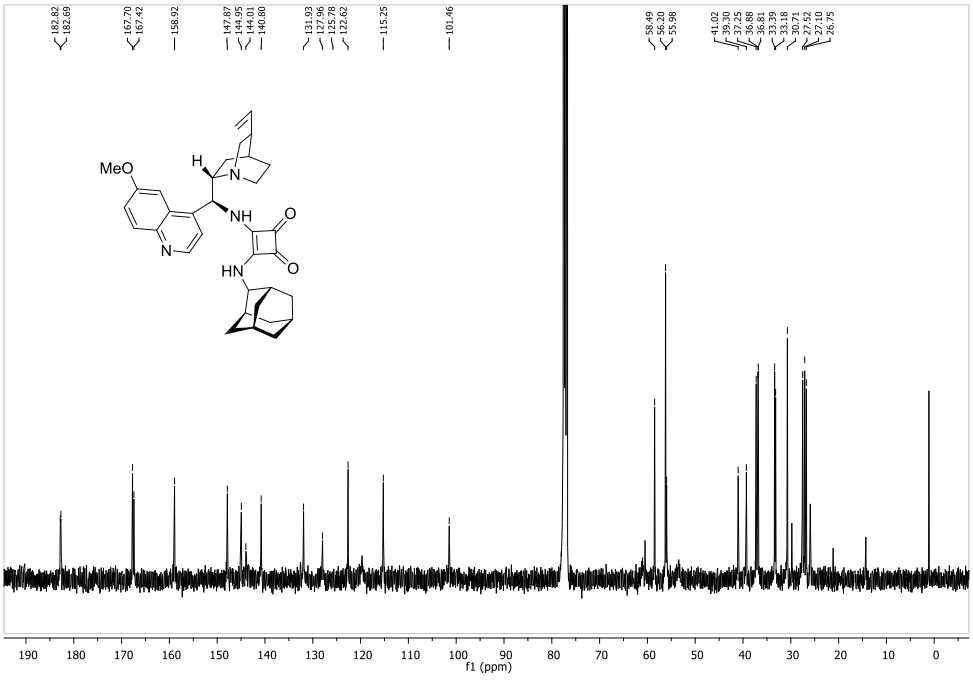

Figure A. 4 ^{13}C NMR spectrum of **64b**.

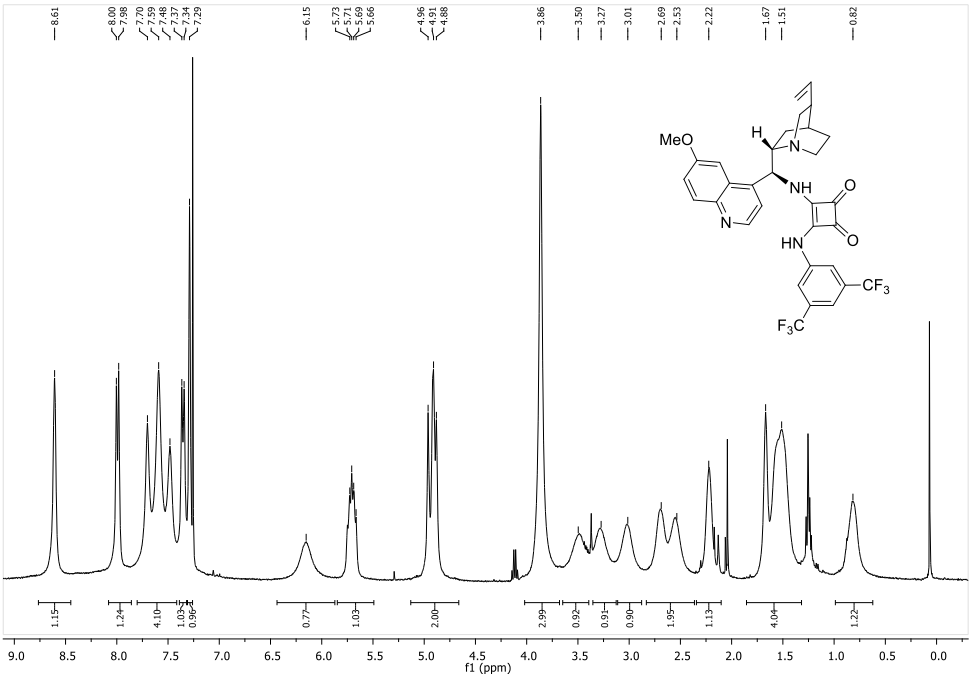

Figure A. 5 ^{1}H NMR spectrum of **64d**.

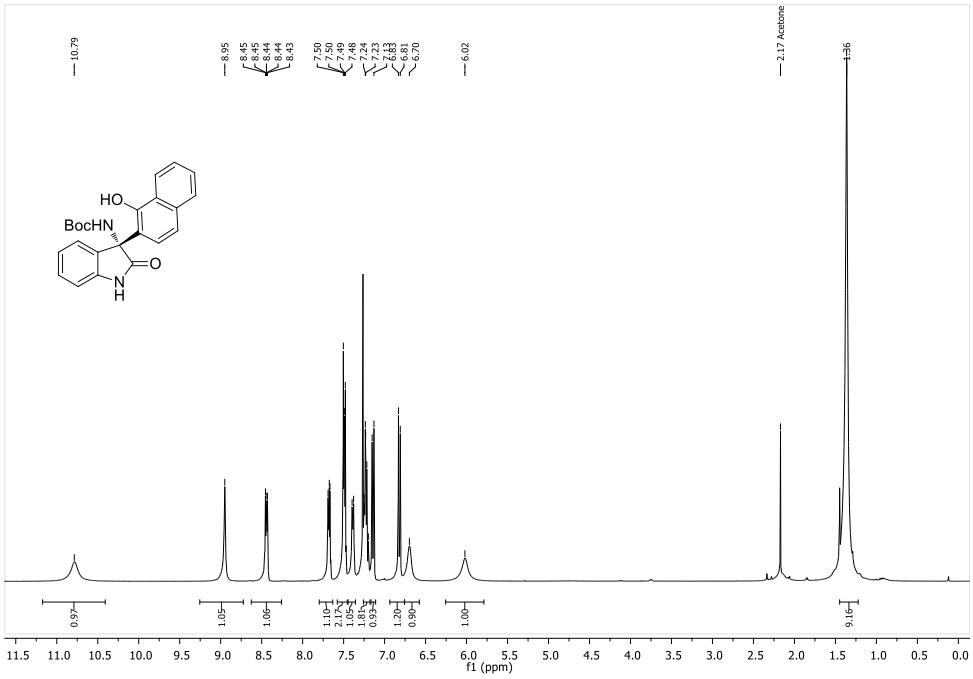

Figure A. 6 ^{1}H NMR spectrum of **95a**.

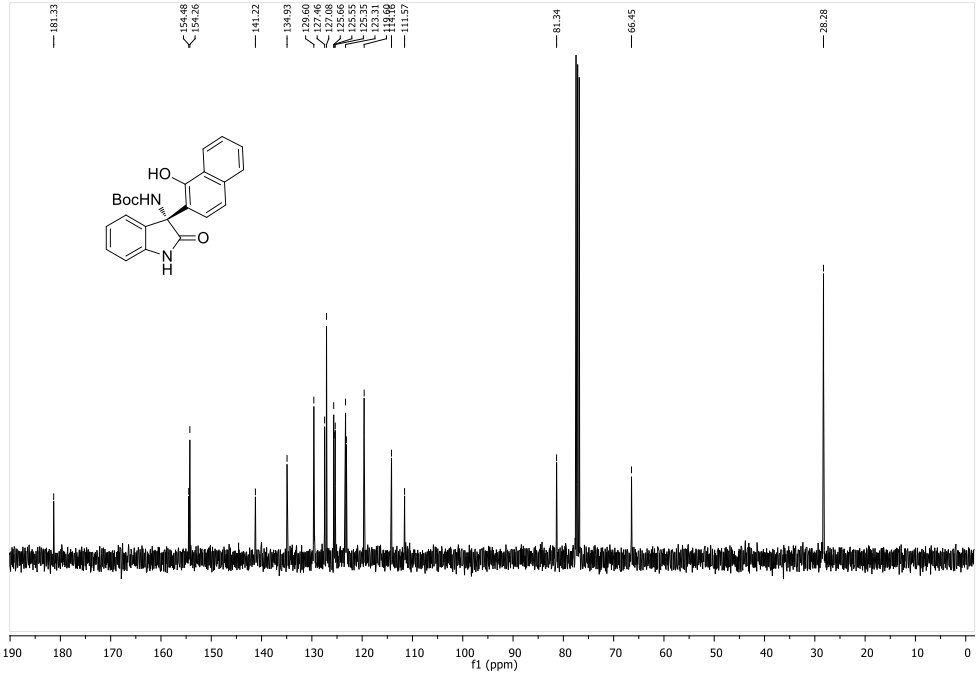

Figure A. 7 ^{13}C NMR spectrum of **95a**.

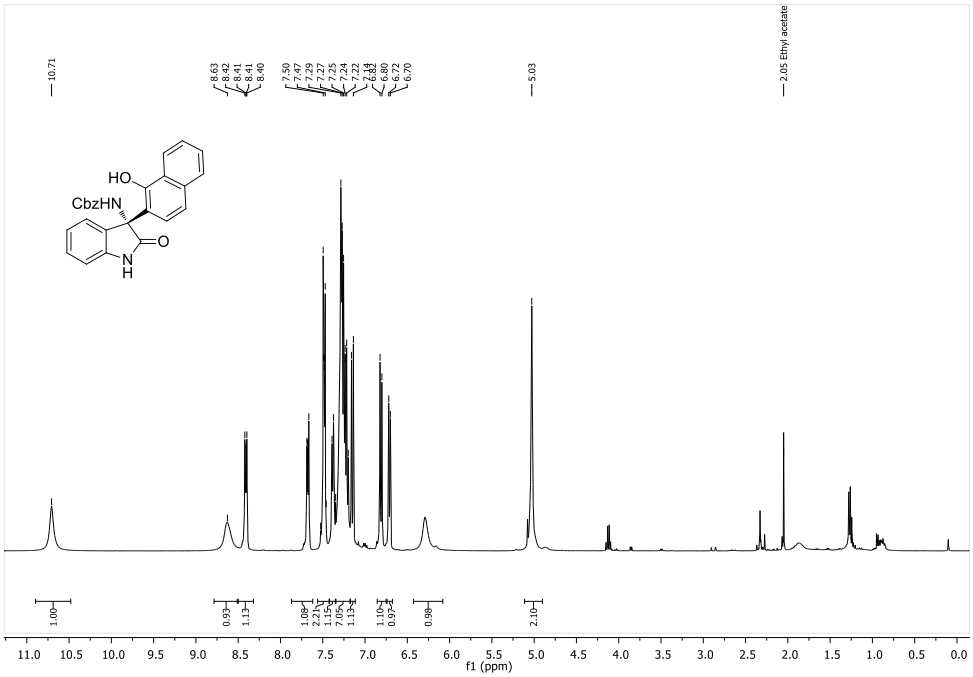

Figure A. 8 ^{1}H NMR spectrum of **95b**.

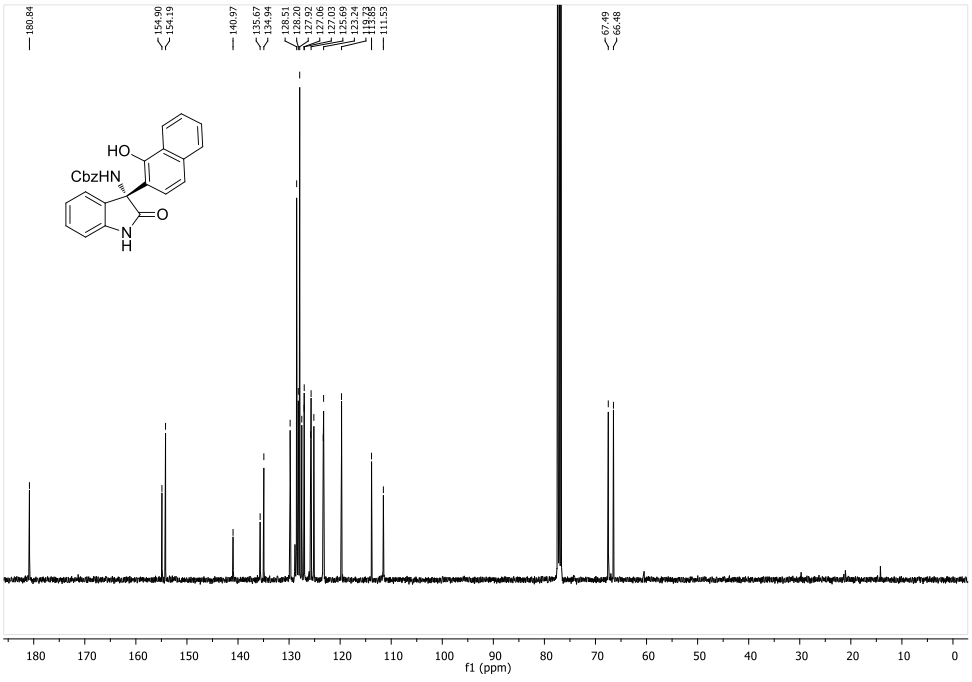

Figure A. 9 ^{13}C NMR spectrum of **95b**.

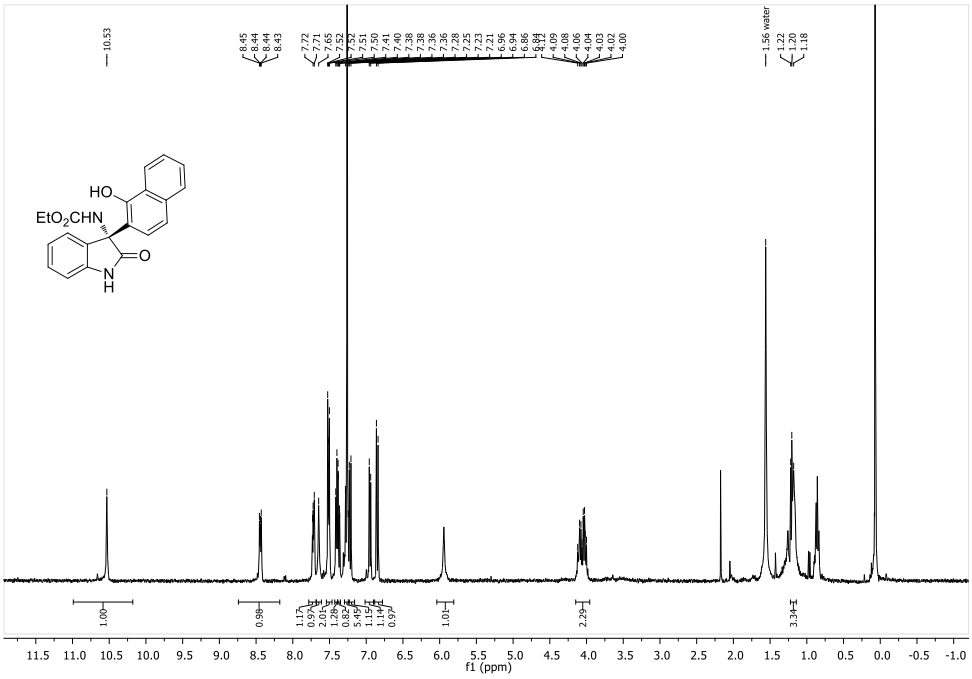

Figure A. 10 ^{1}H NMR spectrum of **95c**.

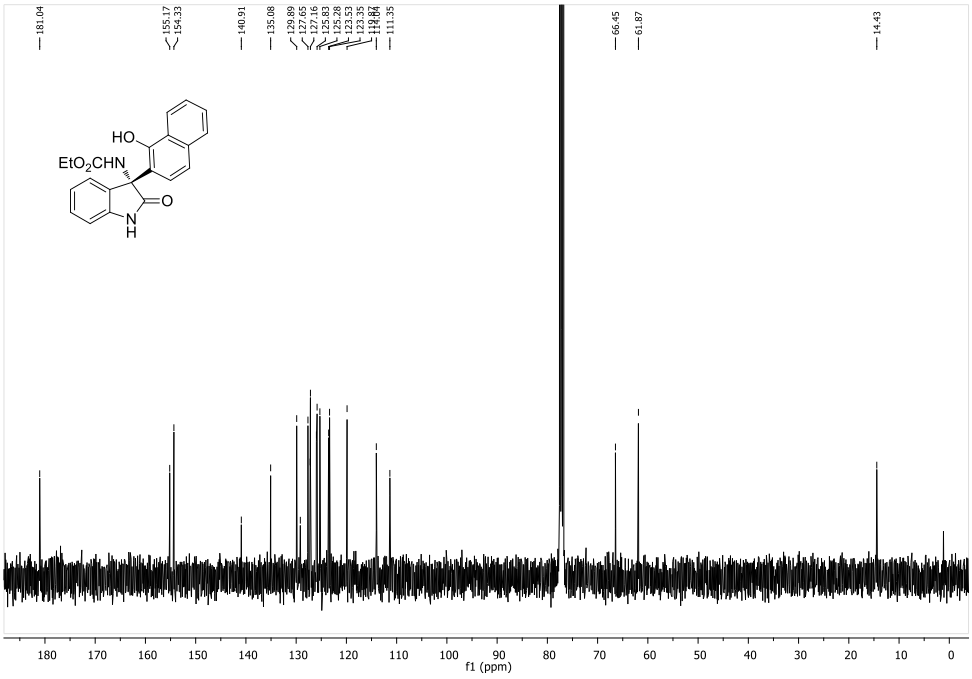

Figure A. 11 ^{13}C NMR spectrum of **95c**.

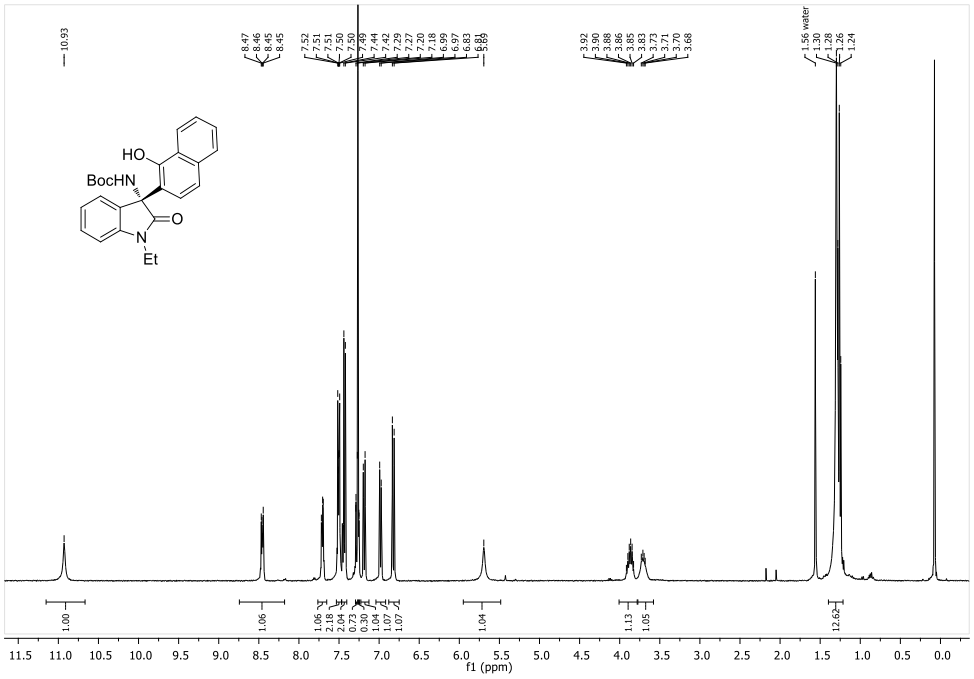

Figure A. 12 ^{1}H NMR spectrum of **95d**.

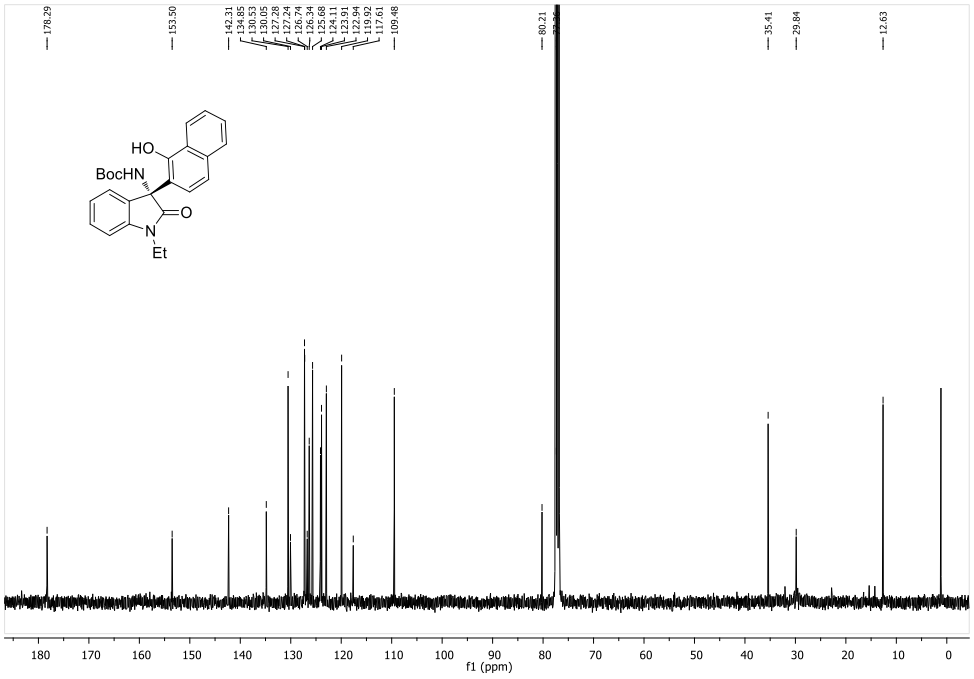

Figure A. 13 ^{13}C NMR spectrum of **95d**.

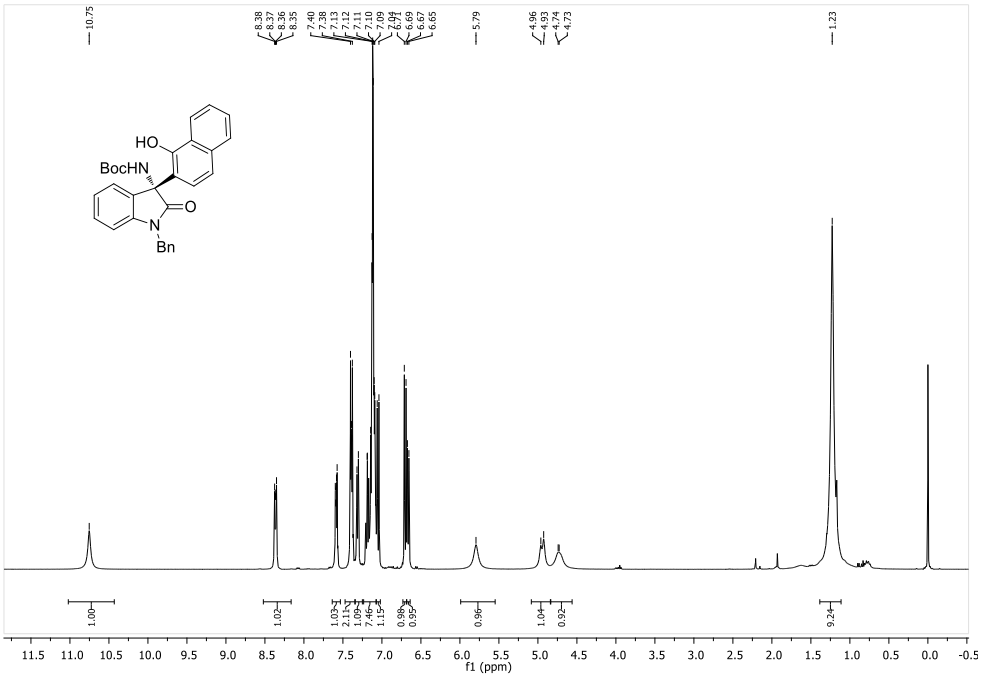

Figure A. 14 ^{1}H NMR spectrum of **95e**.

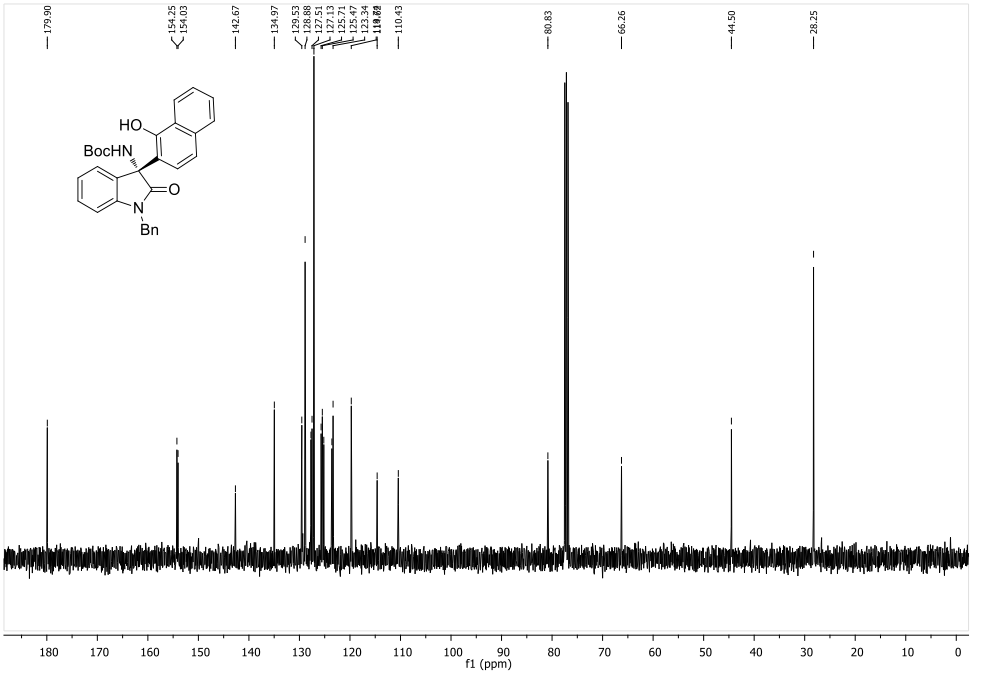

Figure A. 15 ^{13}C NMR spectrum of **95e**.

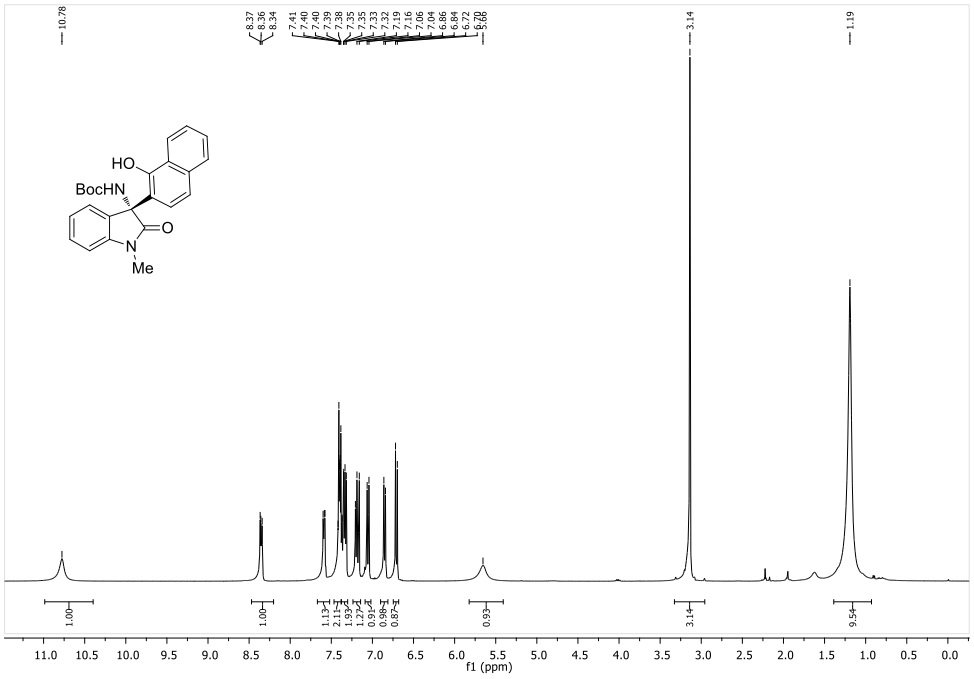

Figure A. 16 ^{1}H NMR spectrum of **95f**.

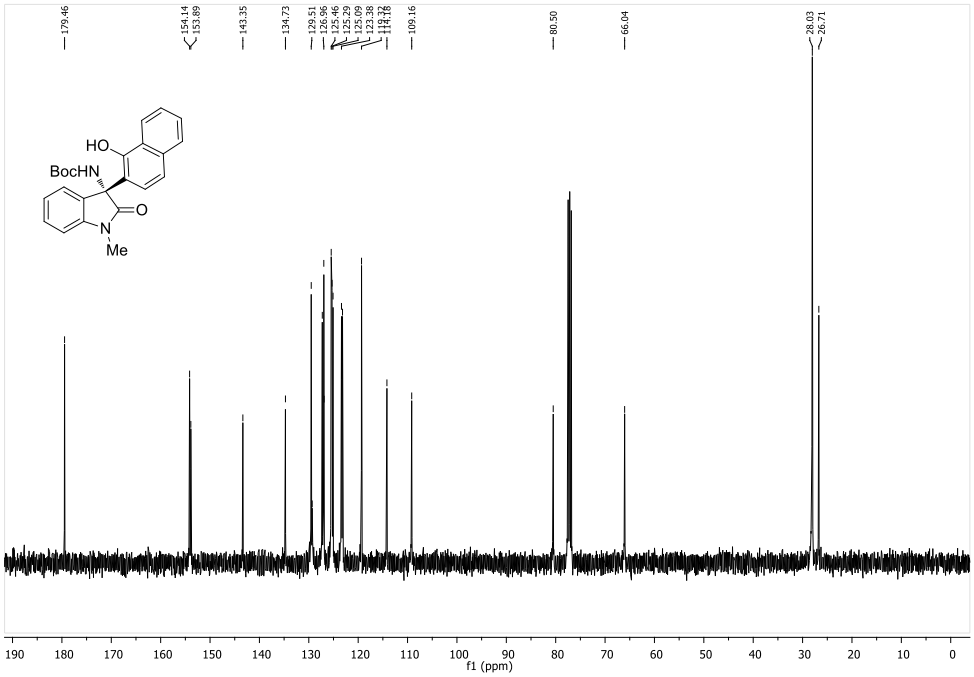

Figure A. 17 ^{13}C NMR spectrum of **95f**.

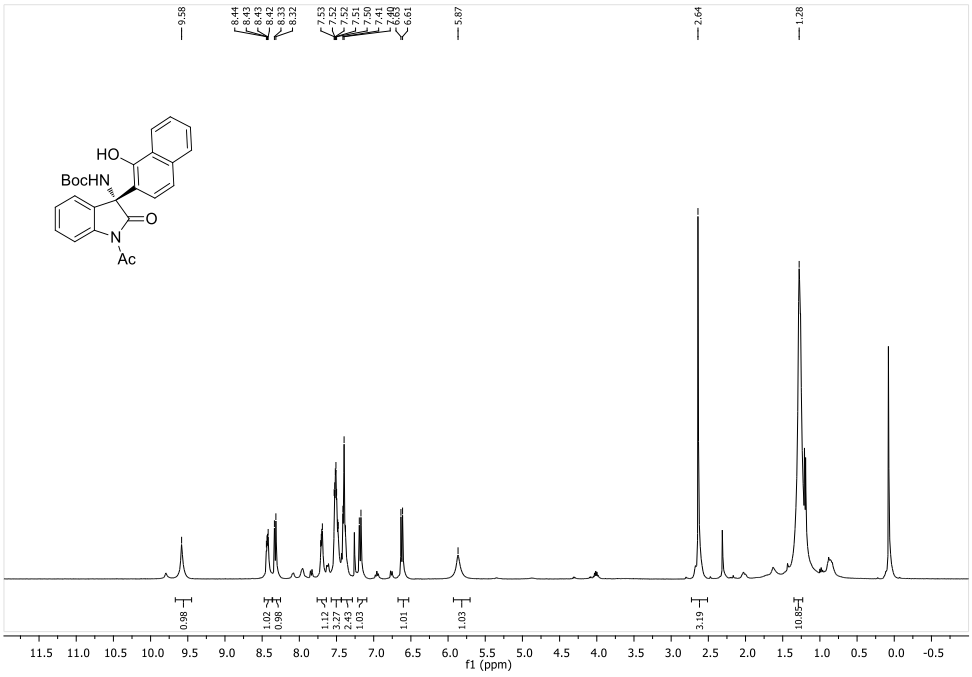

Figure A. 18 ^{1}H NMR spectrum of **95g**.

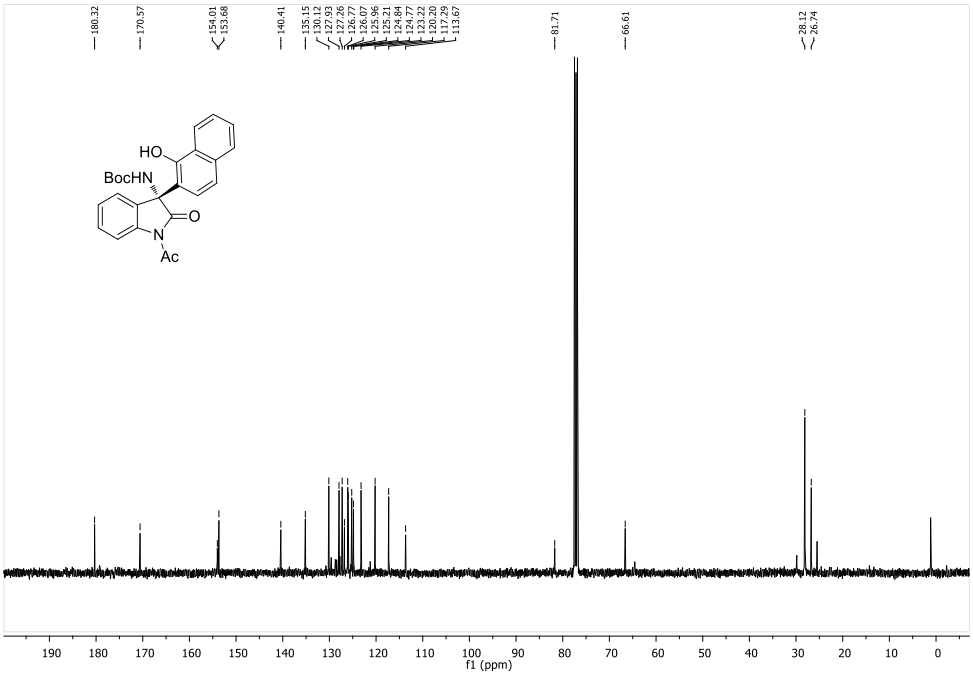

Figure A. 19 ^{13}C NMR spectrum of **95g**.

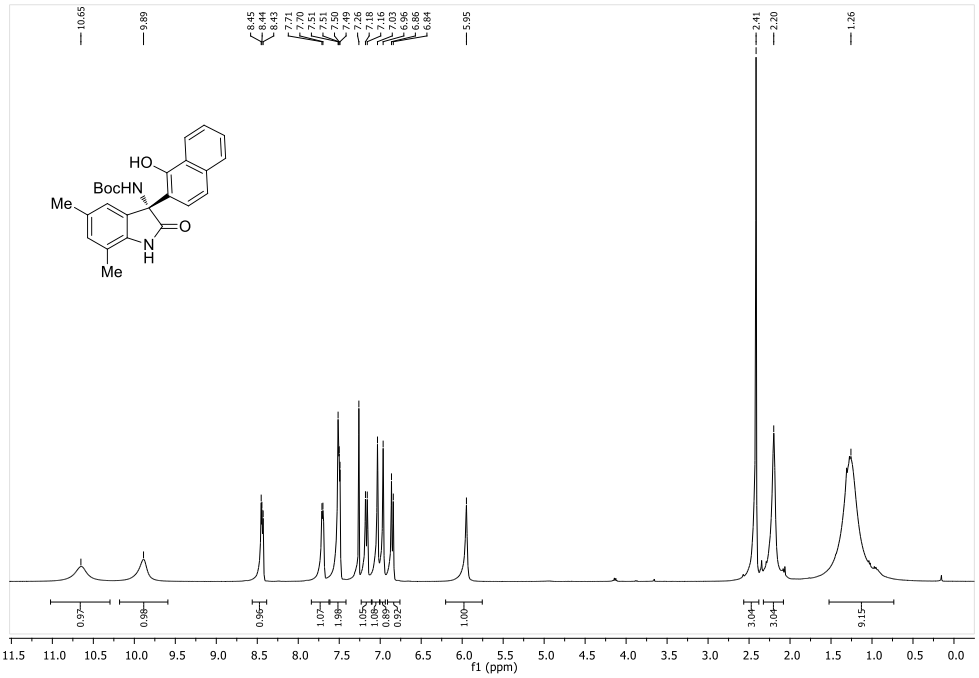

Figure A. 20 ^{1}H NMR spectrum of **95h**.

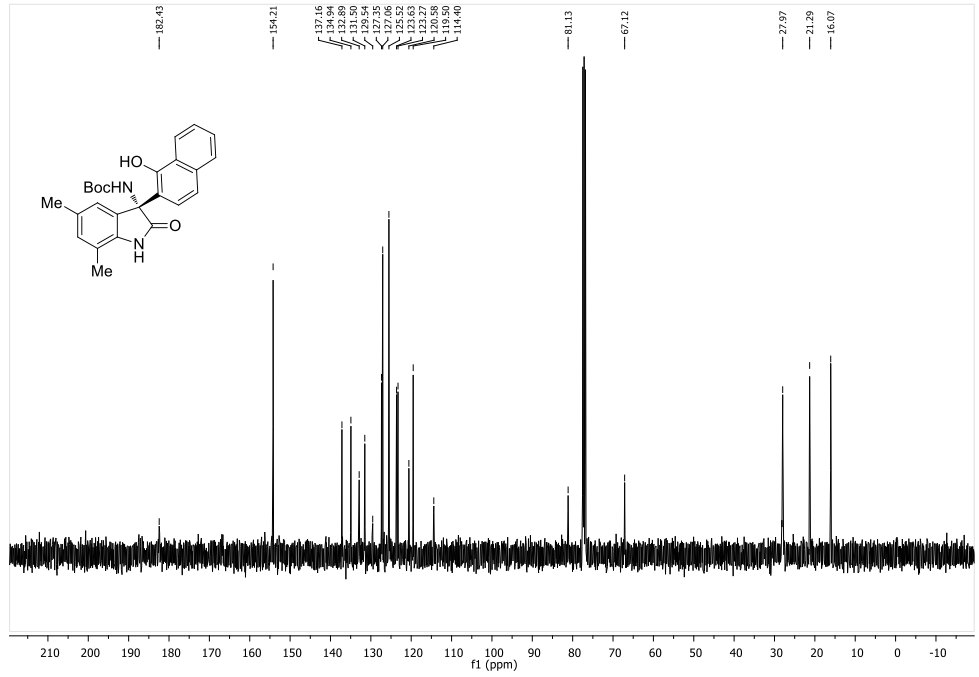

Figure A. 21 ^{13}C NMR spectrum of **95h**.

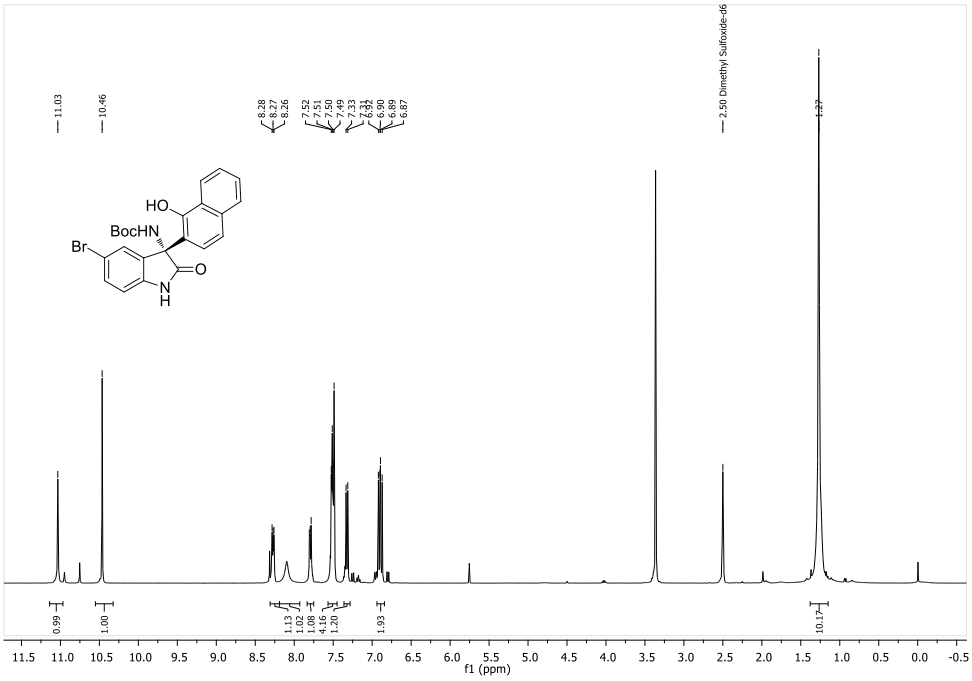

Figure A. 22 ^{1}H NMR spectrum of **95i**.

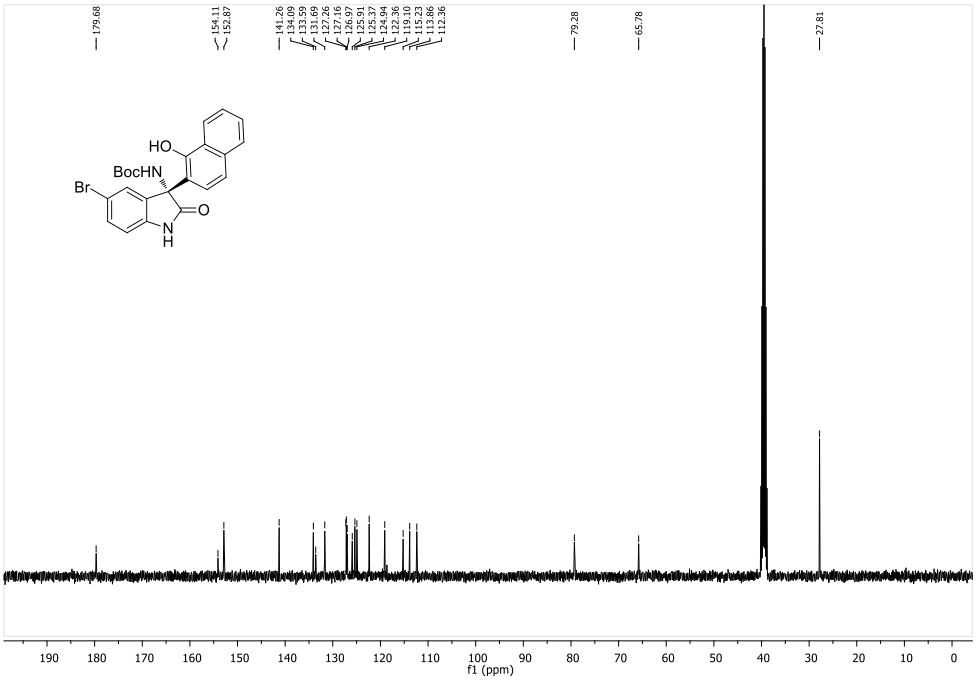

Figure A. 23 ^{13}C NMR spectrum of **95i**.

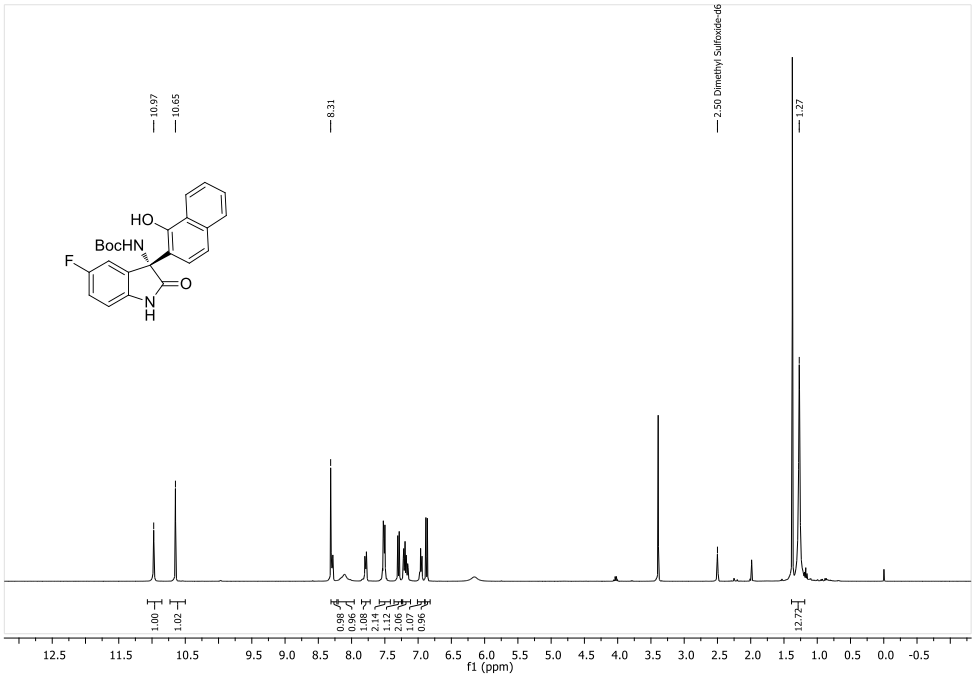

Figure A. 24 ^{1}H NMR spectrum of **95j**.

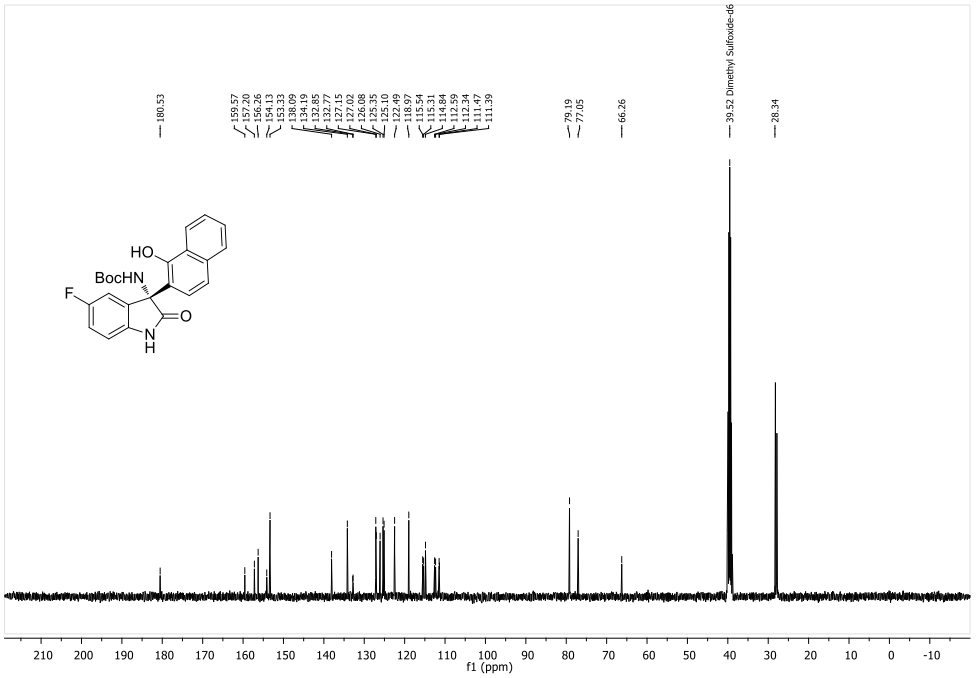

Figure A. 25 ^{13}C NMR spectrum of **95j**.

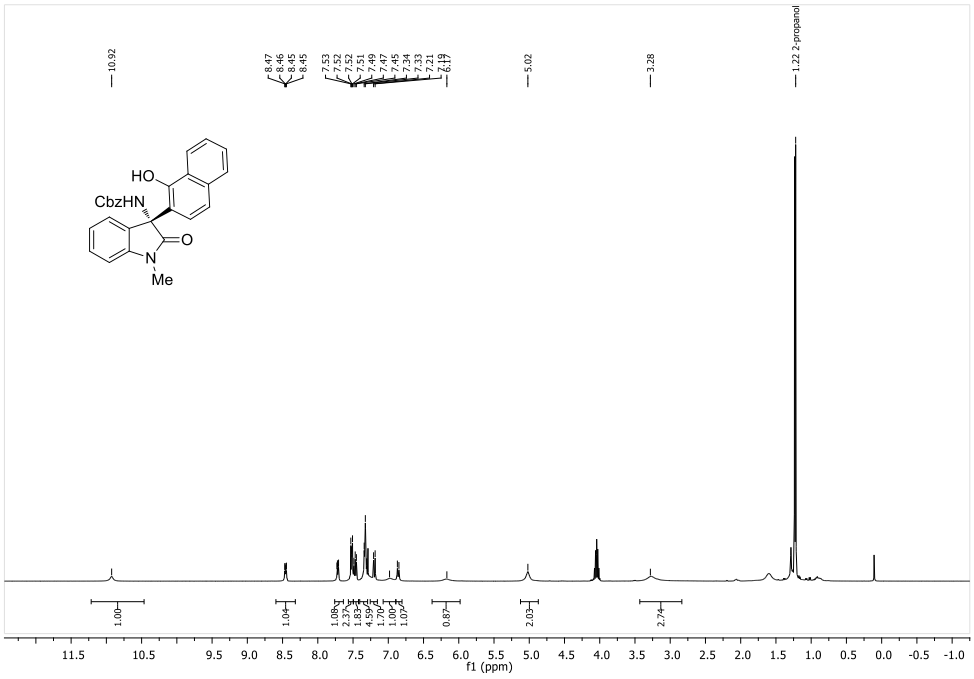

Figure A. 26 ^{1}H NMR spectrum of **95k**.

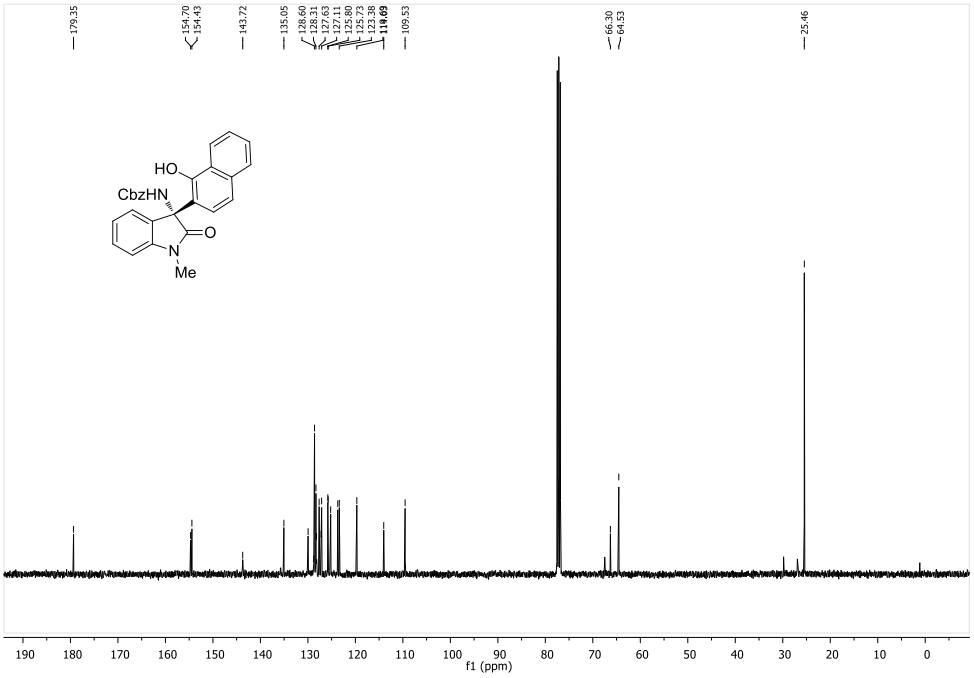

Figure A. 27 ^{13}C NMR spectrum of **95k**.

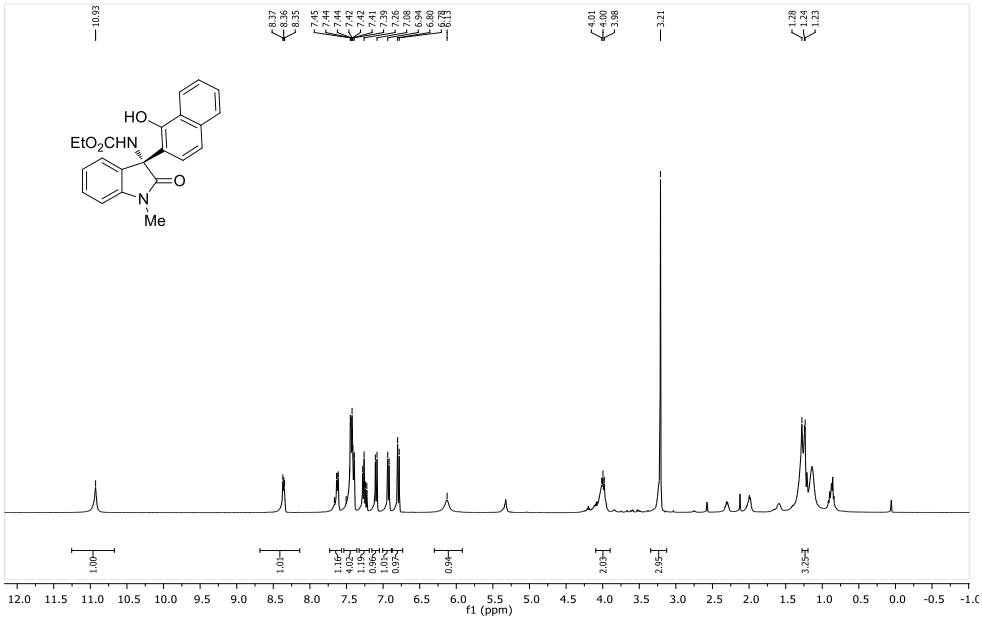

Figure A. 28 ^{1}H NMR spectrum of **95l**.

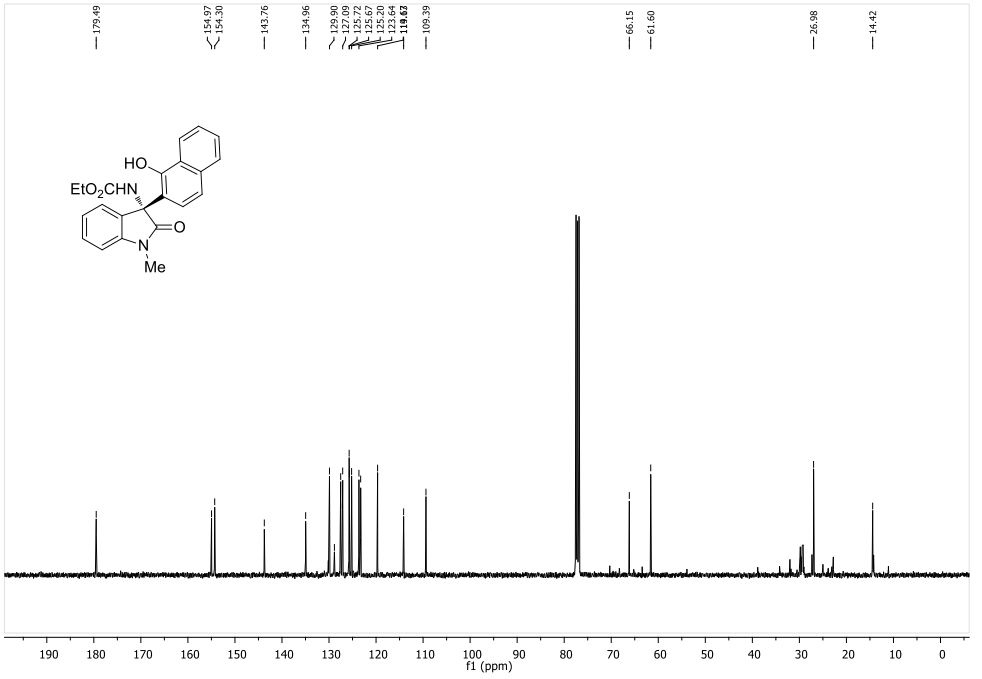

Figure A. 29 ^{13}C NMR spectrum of **95l**.

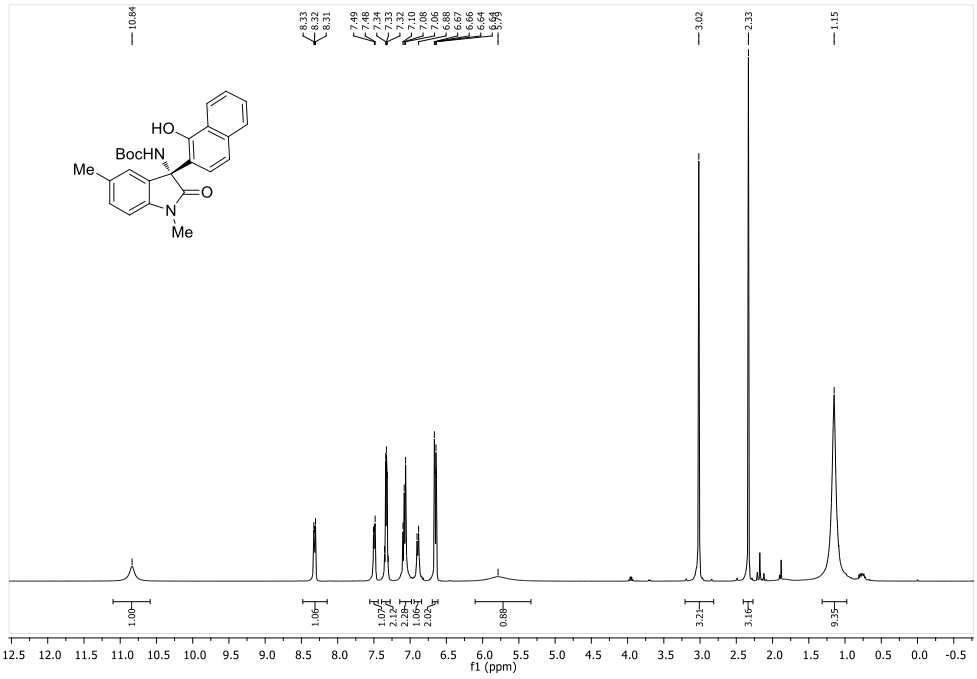

Figure A. 30 ^{1}H NMR spectrum of **95m**.

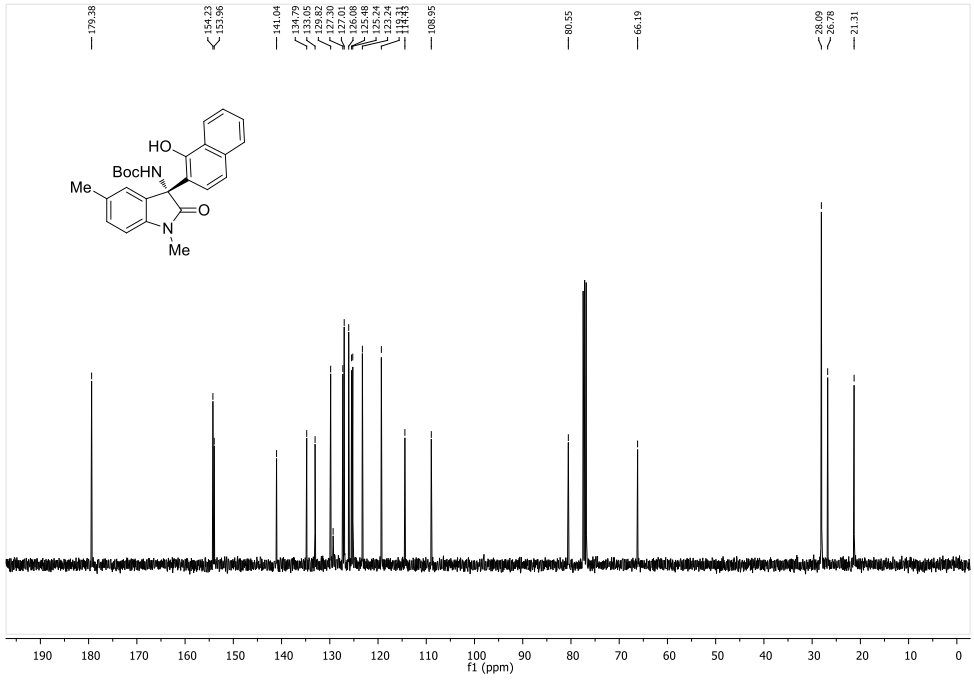

Figure A. 31 ^{13}C NMR spectrum of **95m**.

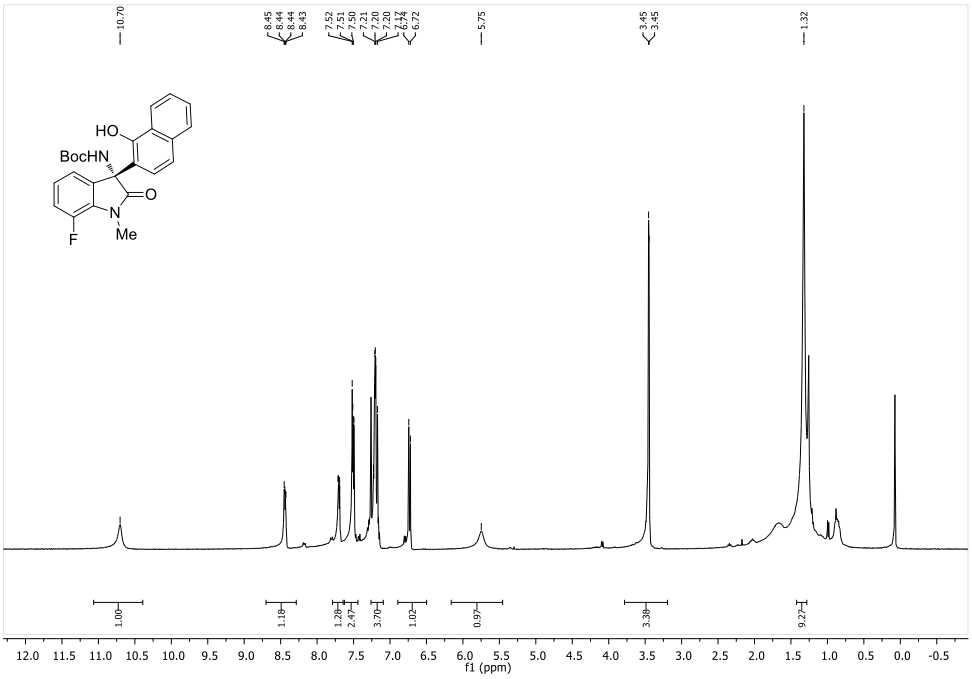

Figure A. 32 ^{1}H NMR spectrum of **95n**.

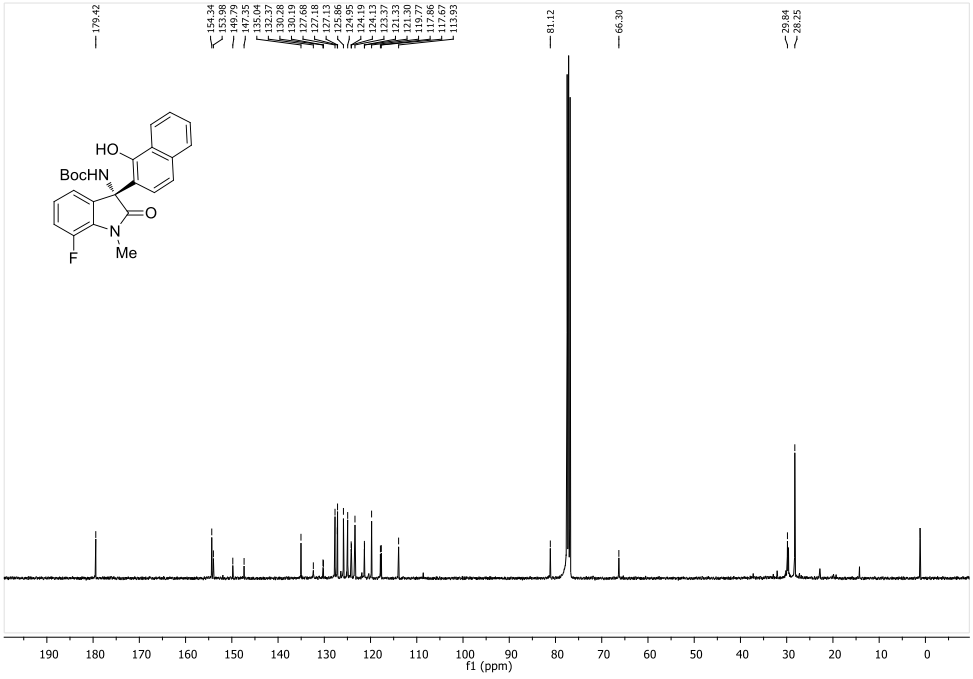

Figure A. 33 ^{13}C NMR spectrum of **95n**.

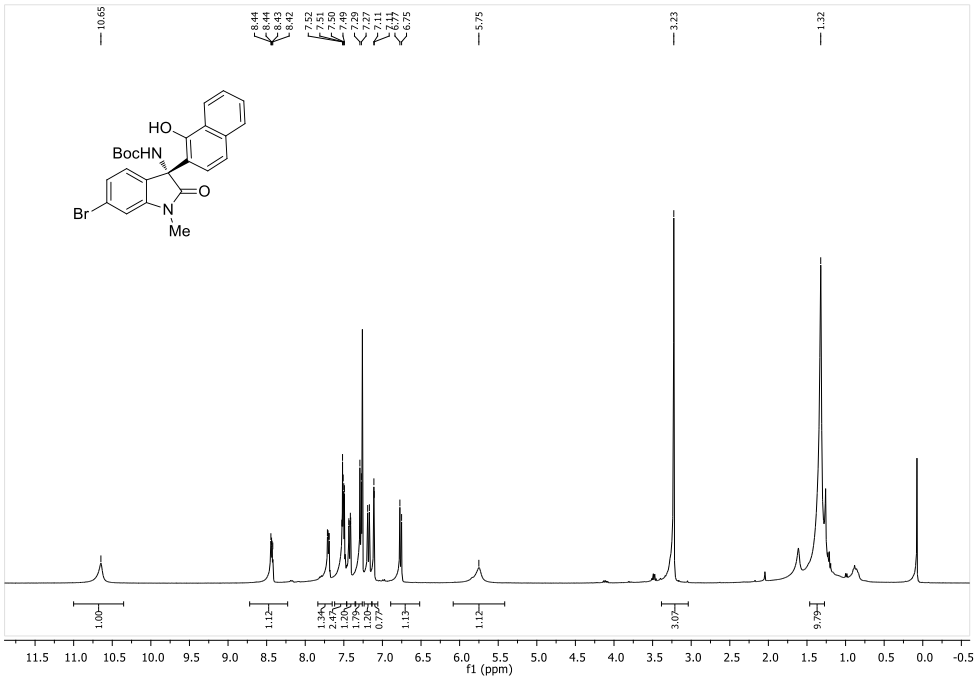

Figure A. 34 ^{1}H NMR spectrum of **95o**.

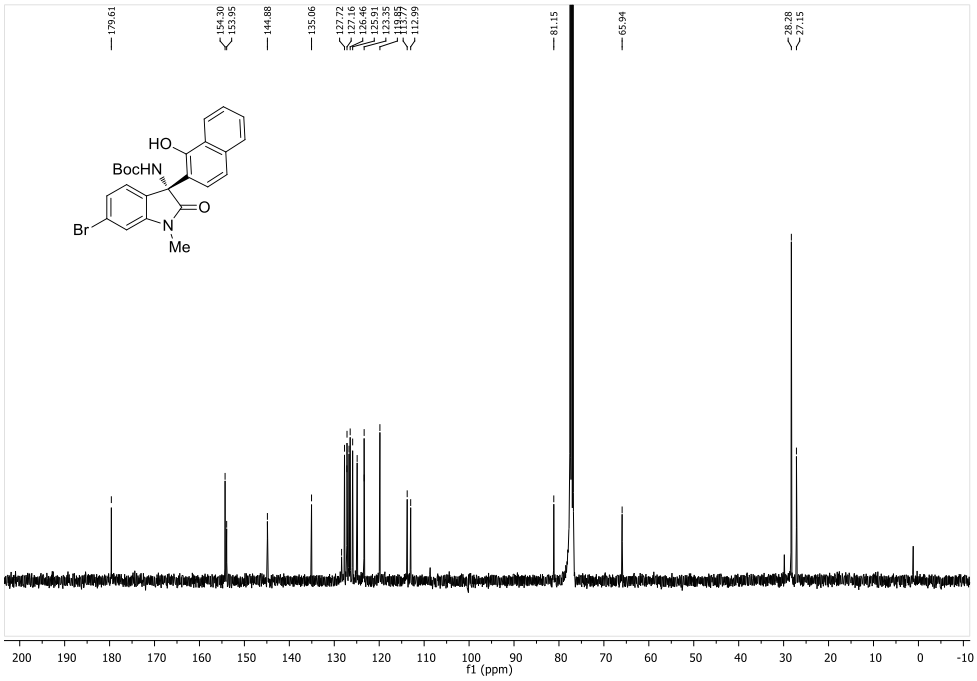

Figure A. 35 ^{13}C NMR spectrum of **95o**.

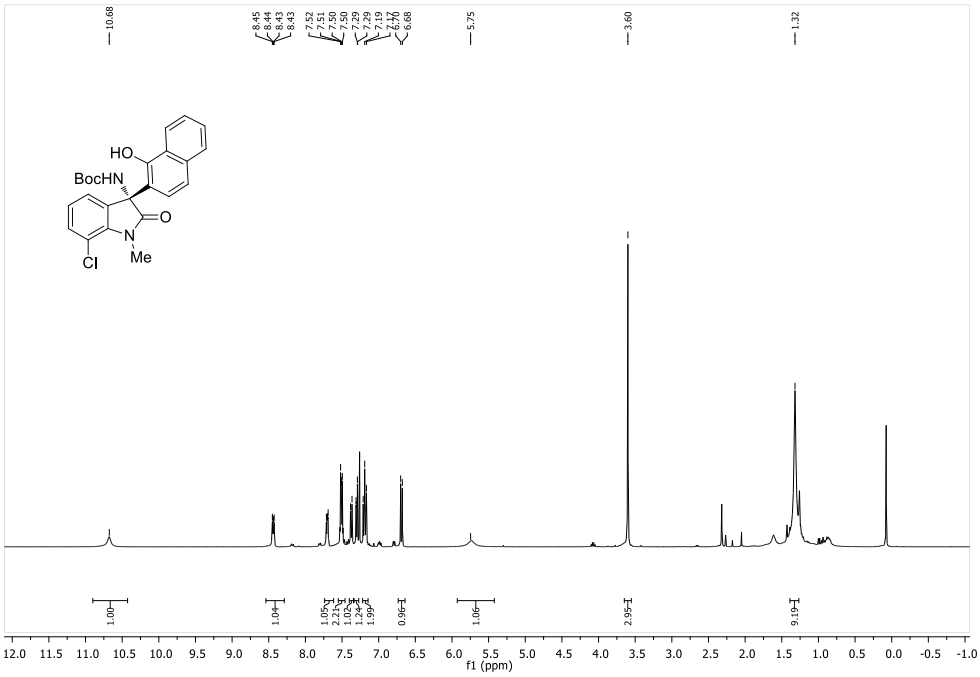

Figure A. 36 ^{1}H NMR spectrum of **95p**.

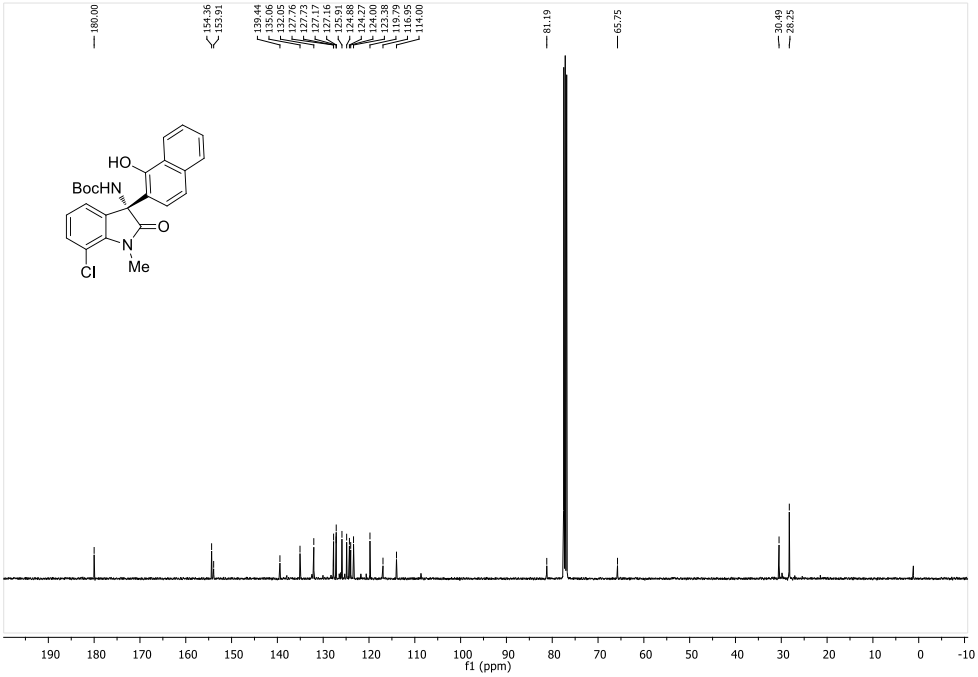

Figure A. 37 ^{13}C NMR spectrum of **95p**.

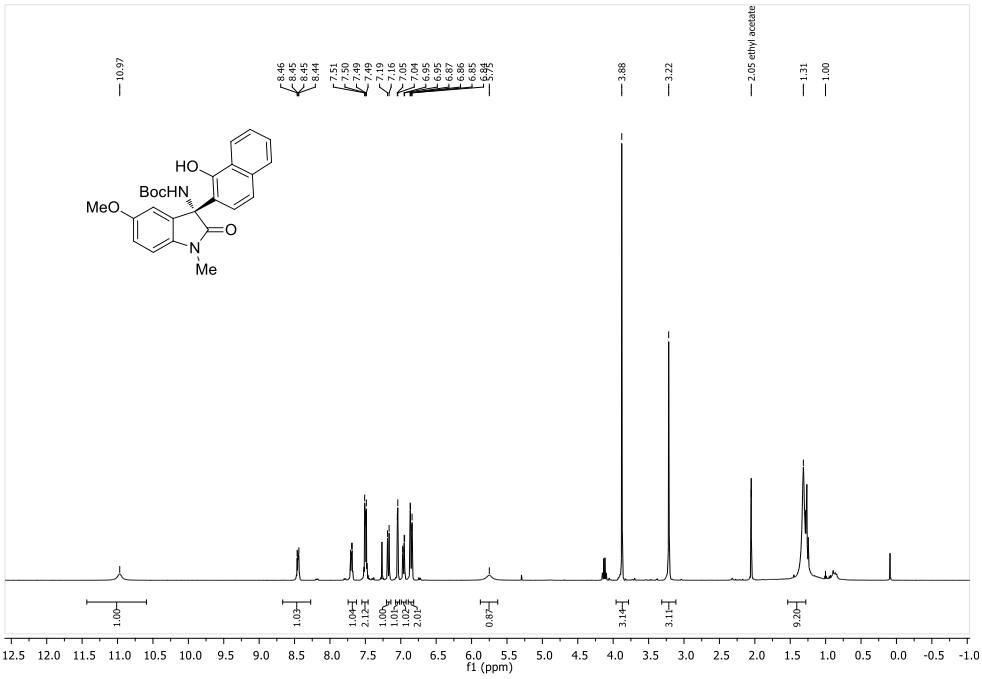

Figure A. 38 ^{1}H NMR spectrum of **95q**.

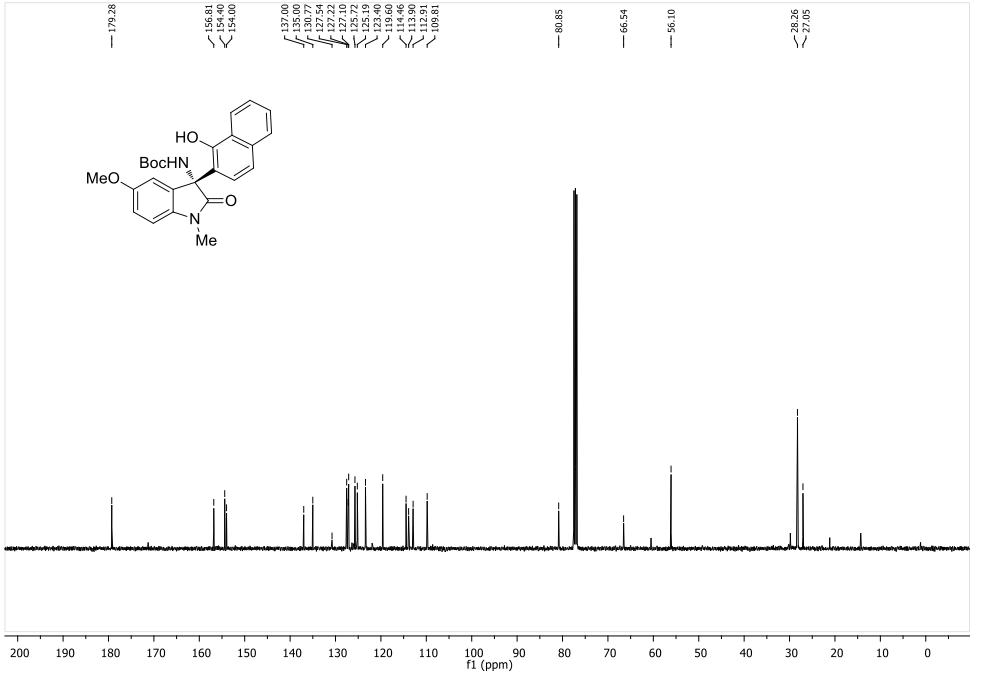

Figure A. 39 ^{13}C NMR spectrum of **95q**.

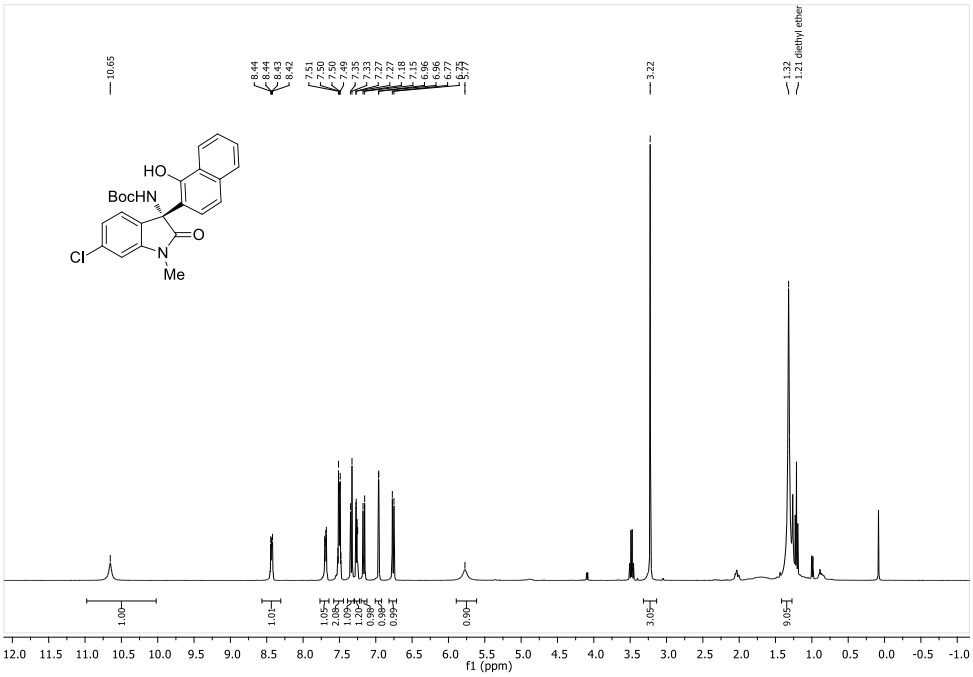

Figure A. 40 ^{1}H NMR spectrum of **95r**.

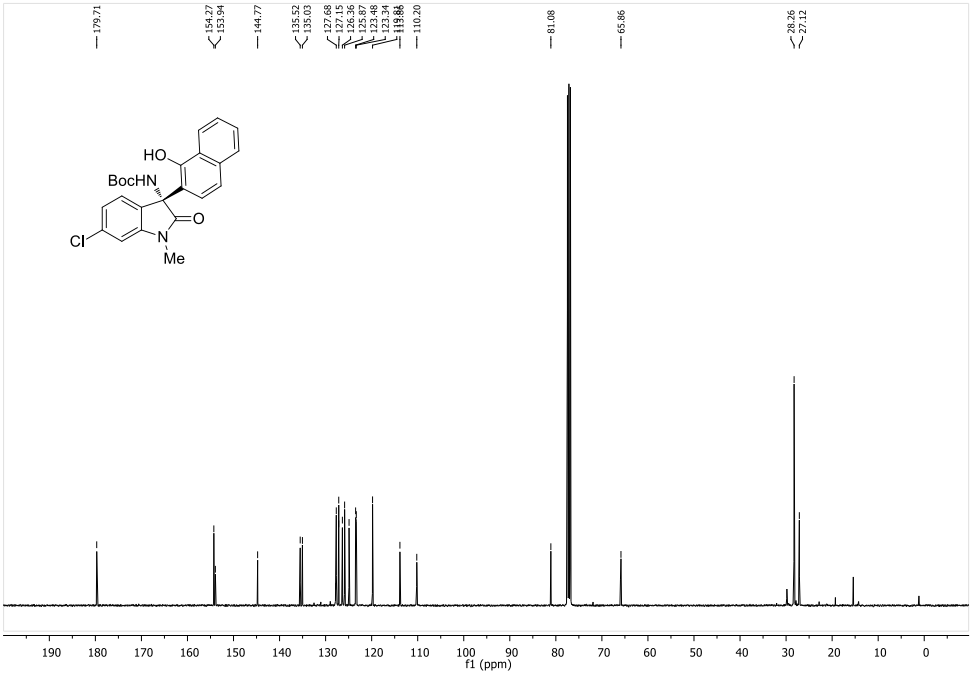

Figure A. 41 ^{13}C NMR spectrum of **95r**.

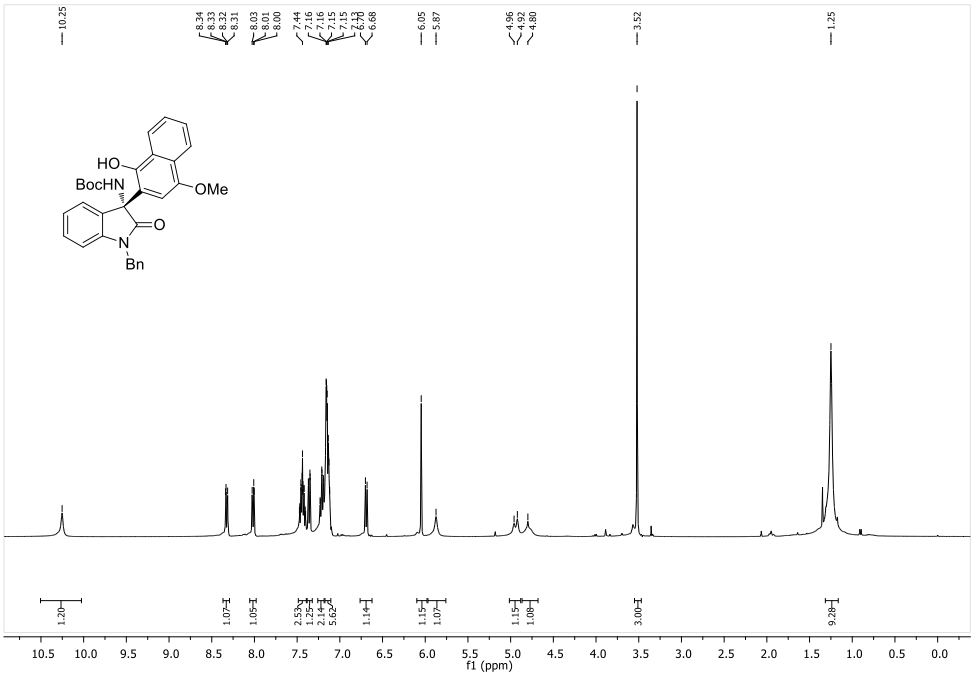

Figure A. 42 ^{1}H NMR spectrum of **95s**.

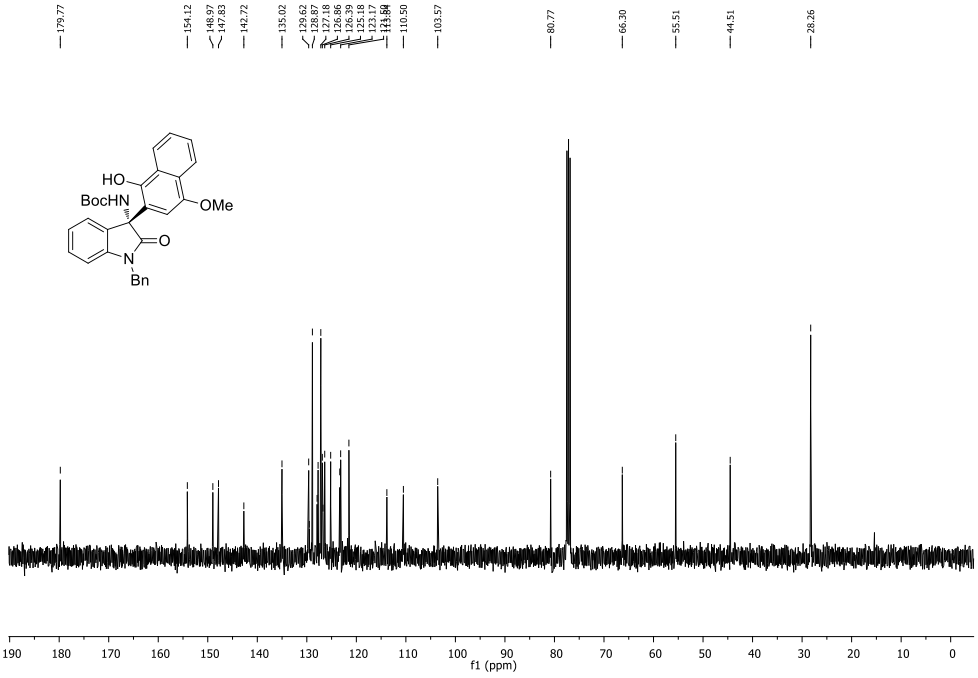

Figure A. 43 ^{13}C NMR spectrum of **95s**.

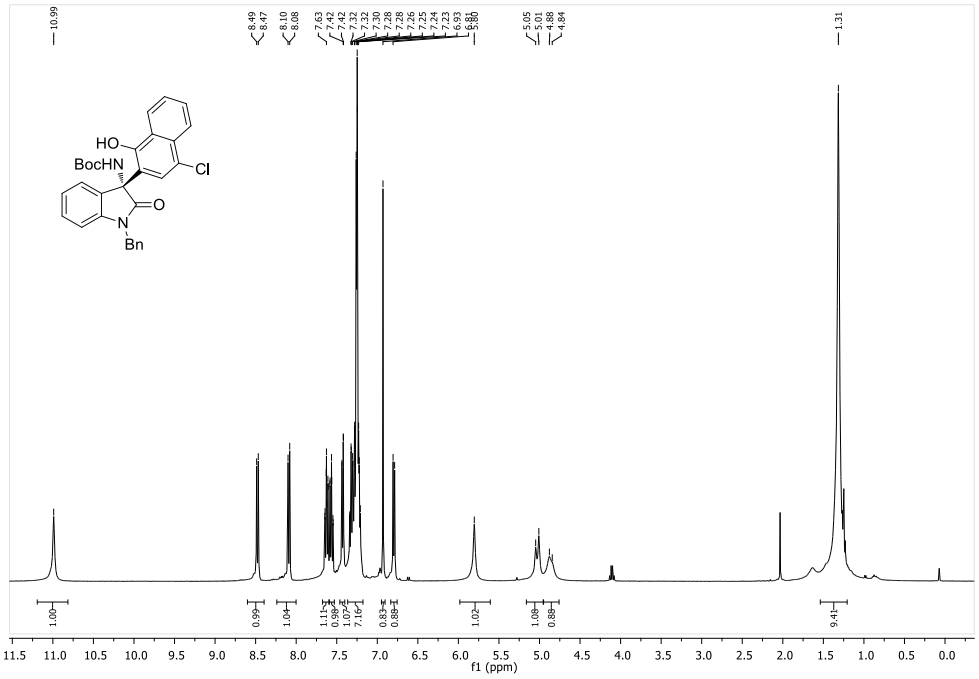

Figure A. 44 ^{1}H NMR spectrum of **95t**.

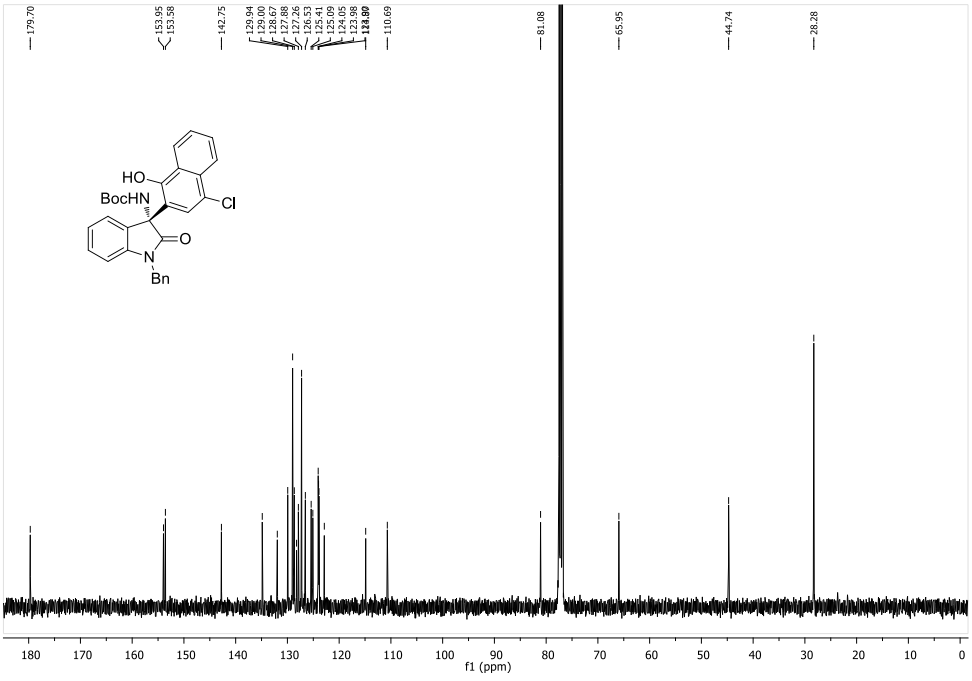

Figure A. 45 ^{13}C NMR spectrum of **95t**.

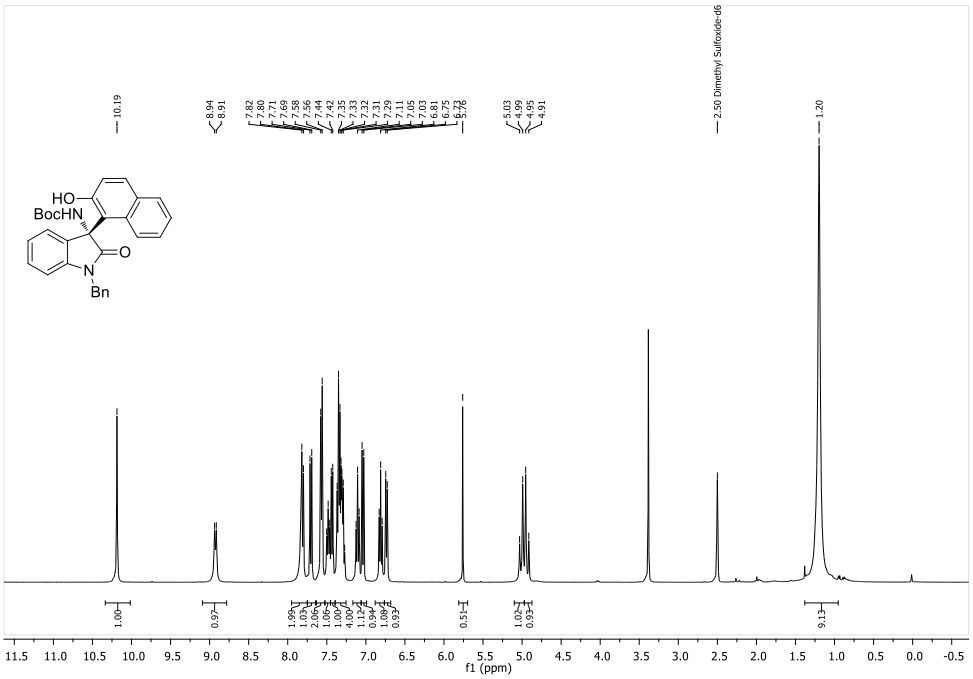

Figure A. 46 ^{1}H NMR spectrum of **96a**.

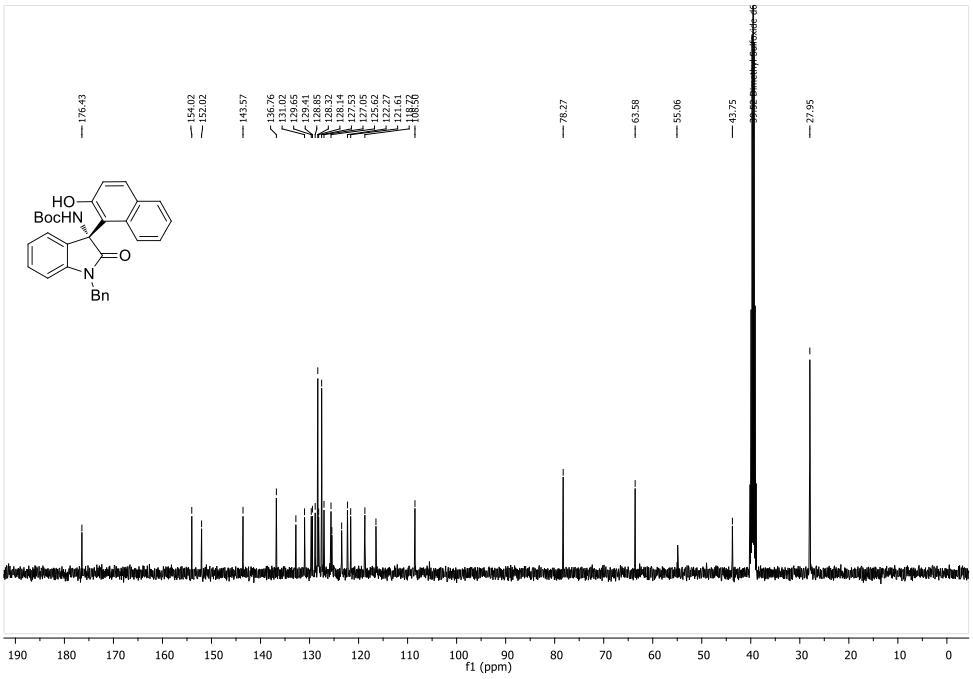

Figure A. 47 ^{13}C NMR spectrum of **96a**.

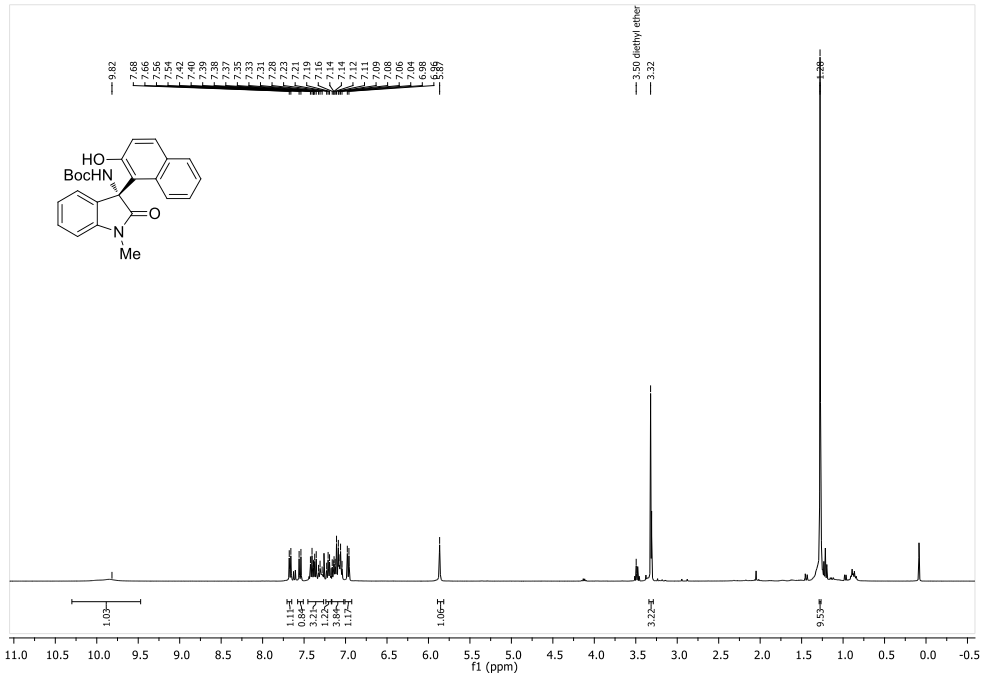

Figure A. 48 ^{1}H NMR spectrum of **96b**.

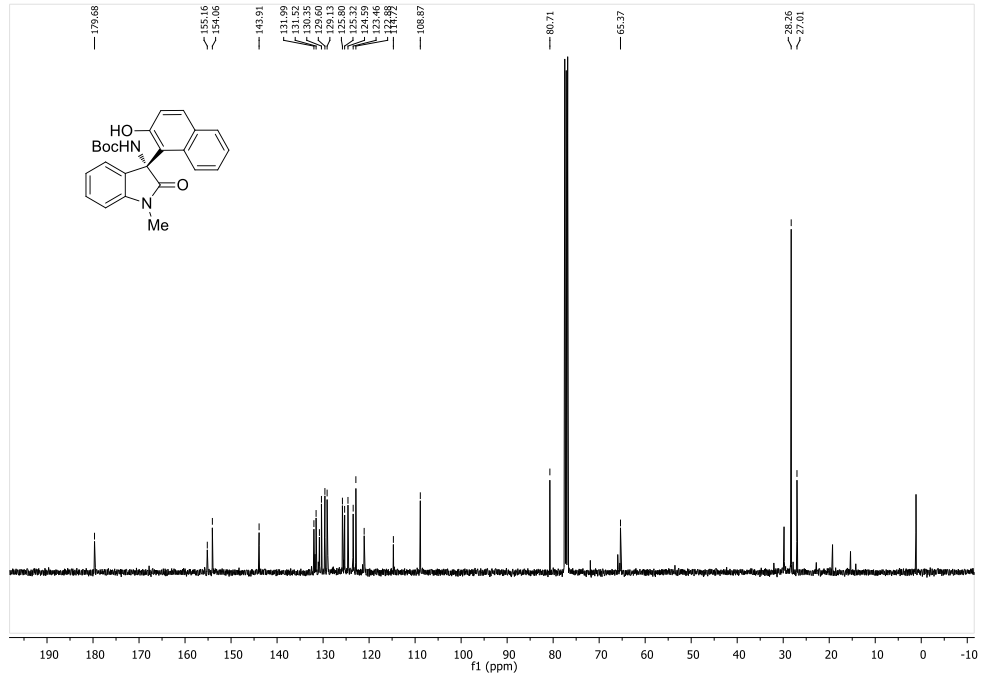

Figure A. 49 ^{13}C NMR spectrum of **96b**.

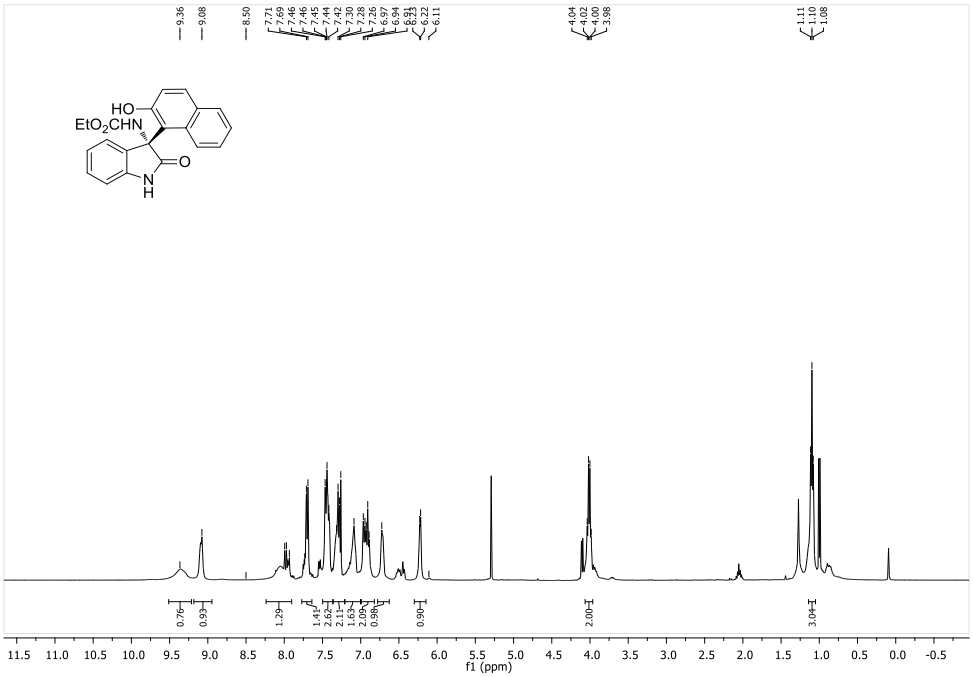

Figure A. 50 ^{1}H NMR spectrum of **96c**.

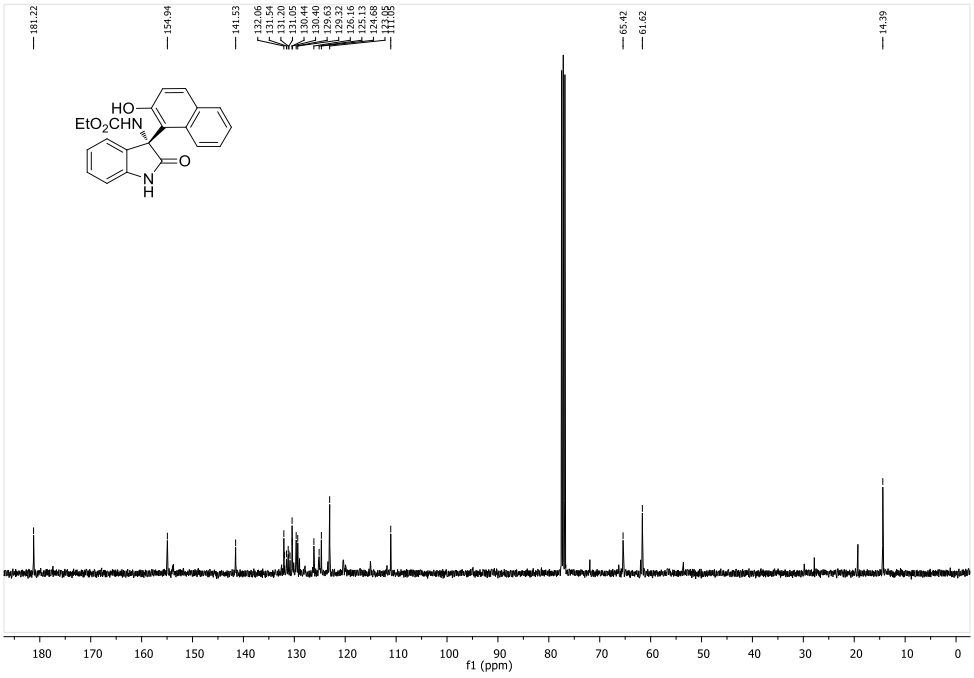

Figure A. 51 ^{13}C NMR spectrum of **96c**.

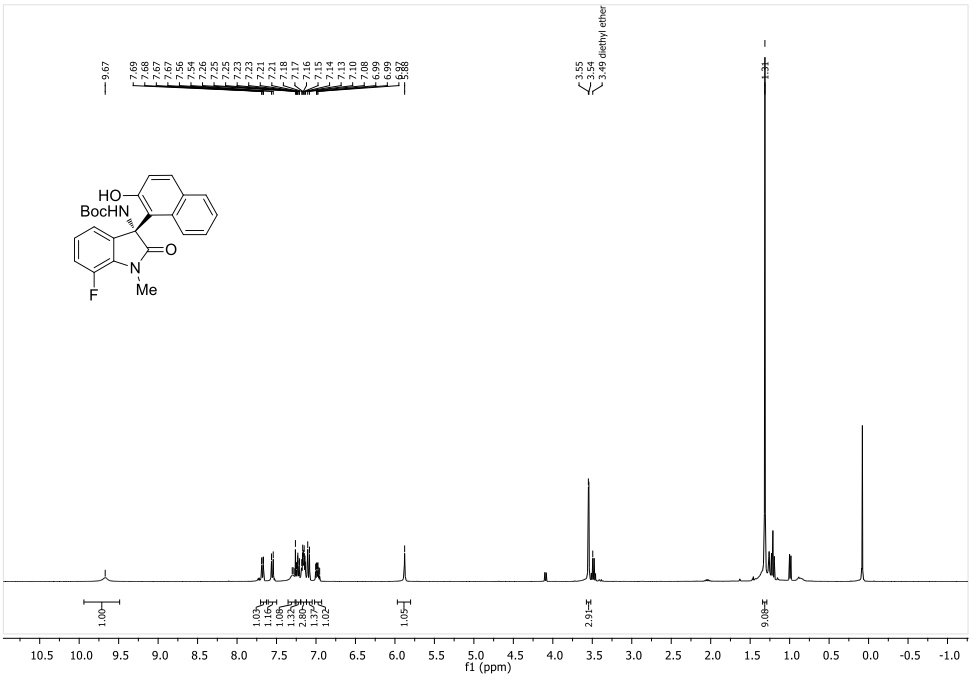

Figure A. 52 ^{1}H NMR spectrum of **96d**.

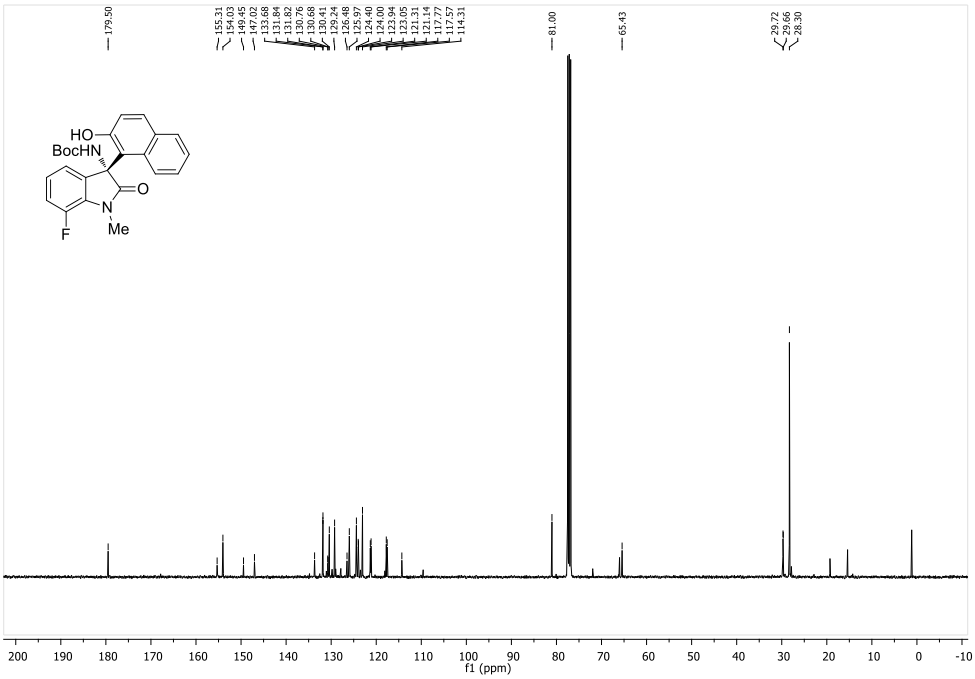

Figure A. 53 ^{13}C NMR spectrum of **96d**.

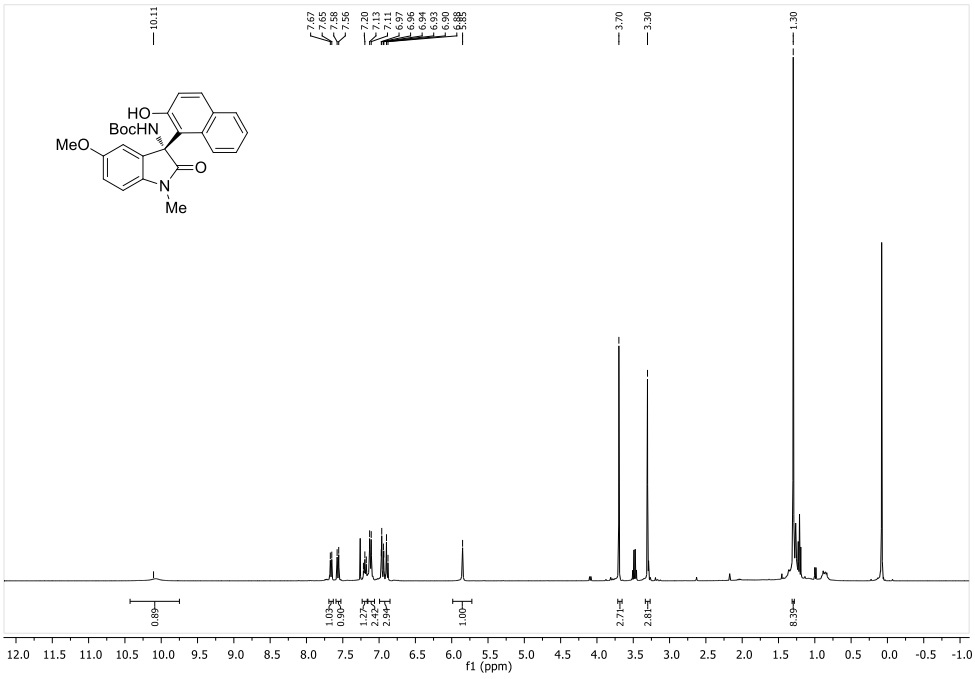

Figure A. 54 ^{1}H NMR spectrum of **96e**.

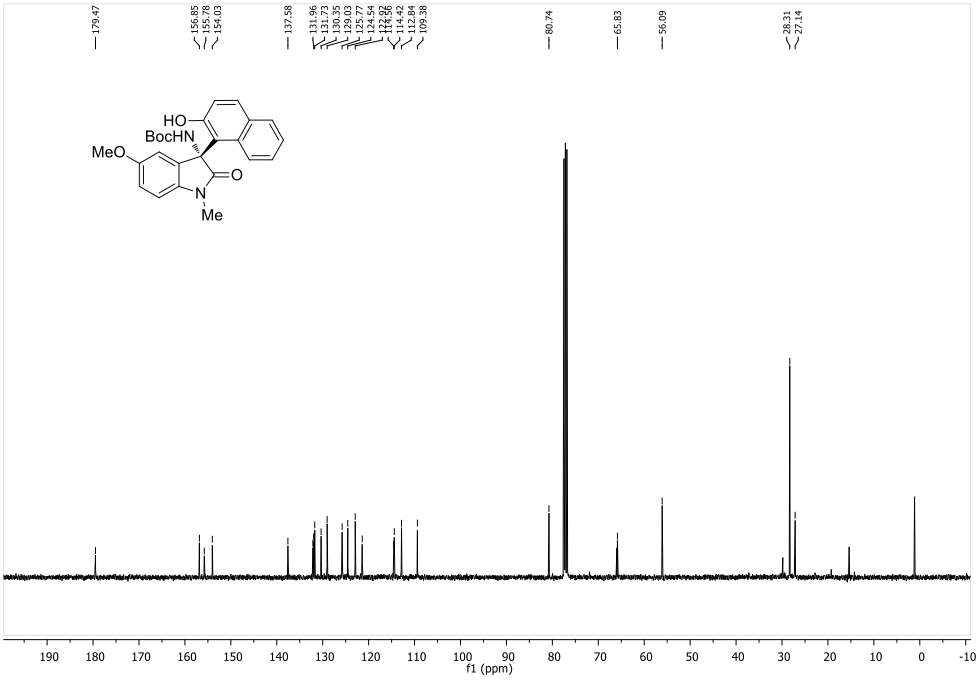

Figure A. 55 ^{13}C NMR spectrum of **96e**.

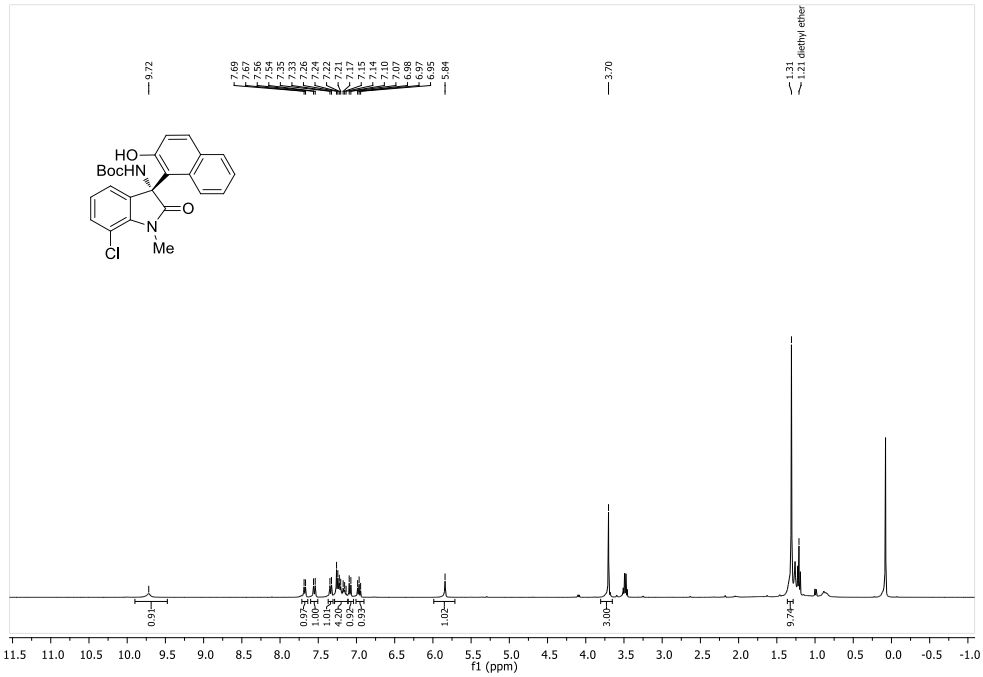

Figure A. 56 ^{1}H NMR spectrum of **96f**.

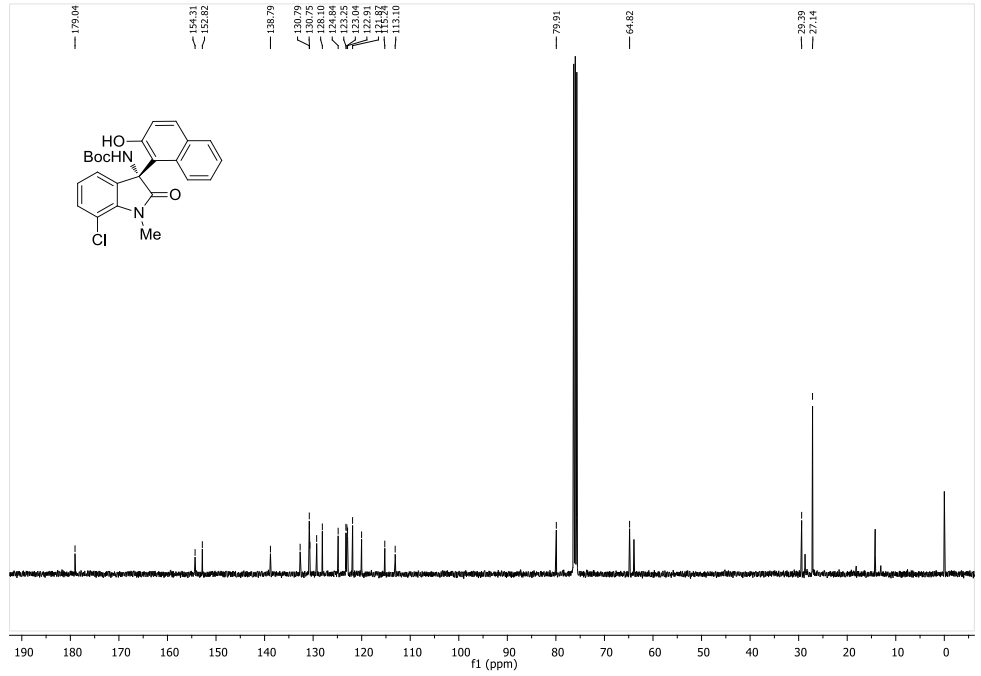

Figure A. 57 ^{13}C NMR spectrum of **96f**.

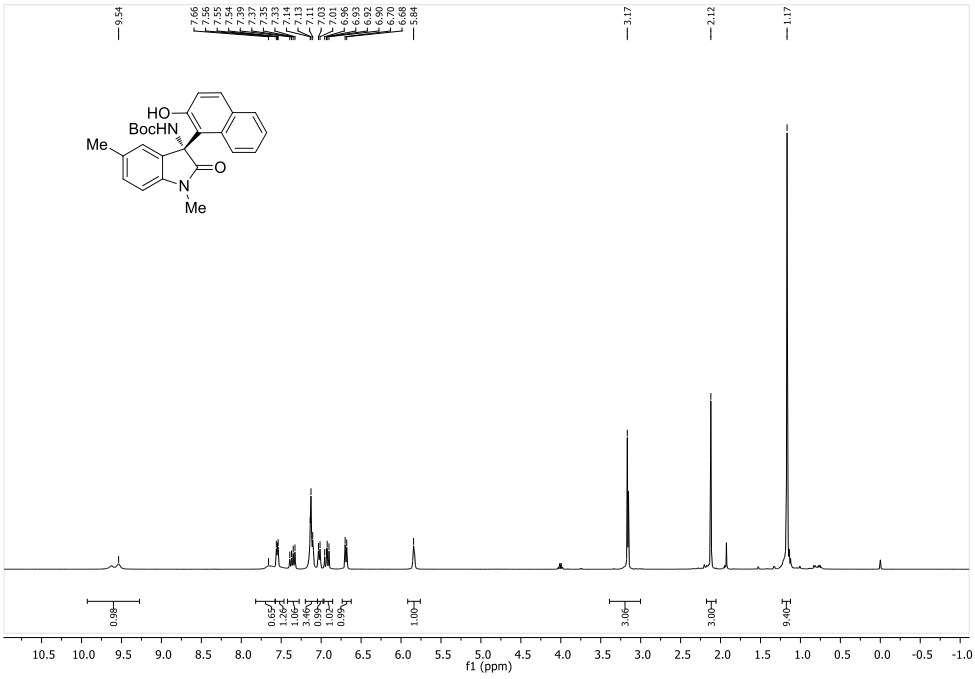

Figure A. 58 ^{1}H NMR spectrum of **96g**.

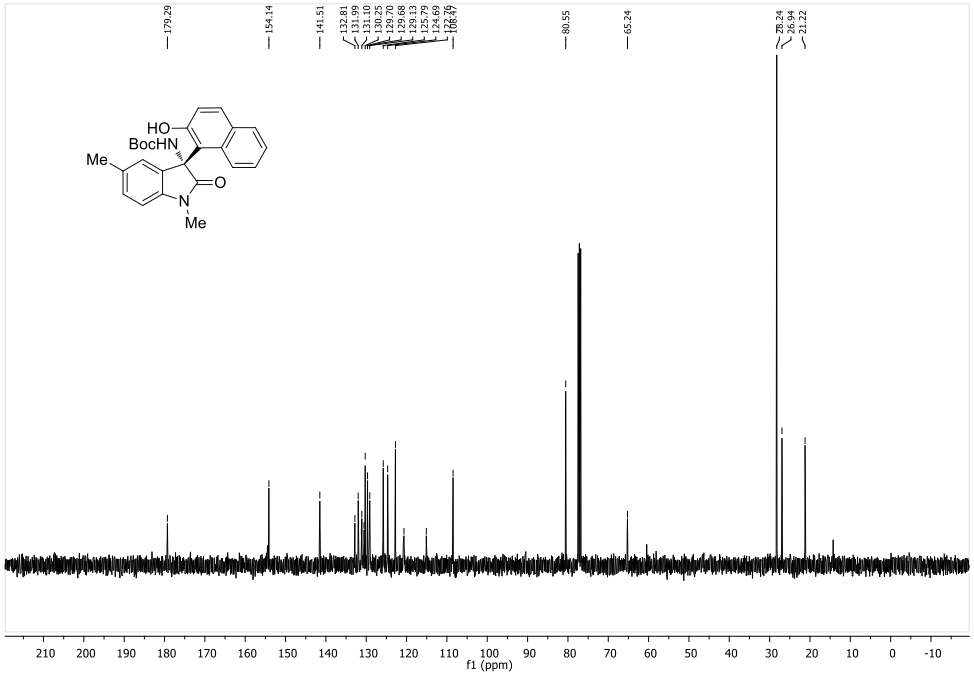

Figure A. 59 ^{13}C NMR spectrum of **96g**.

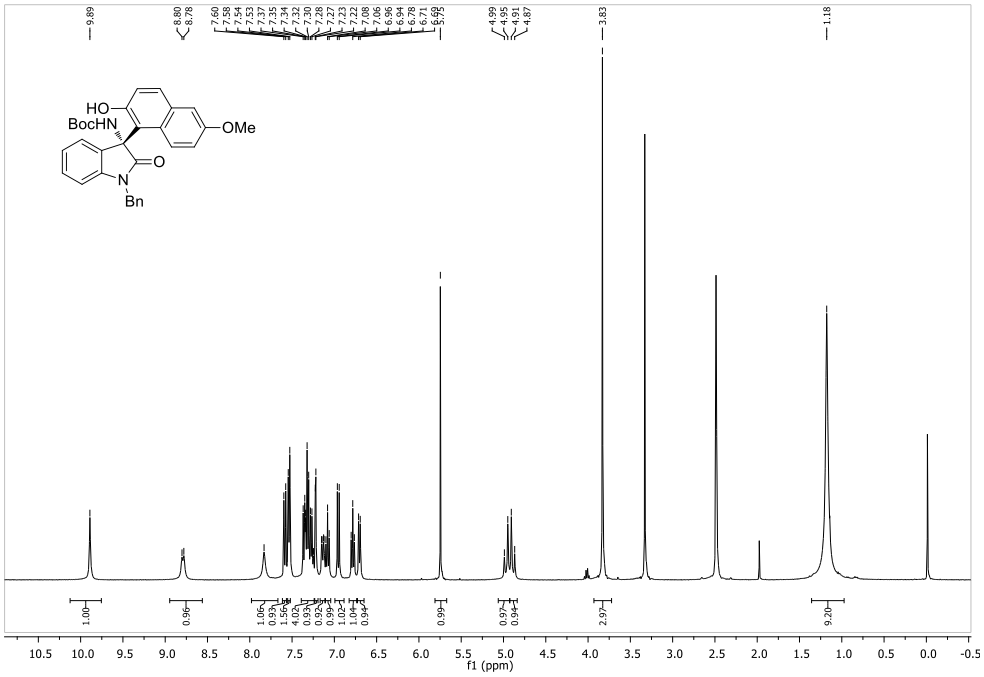

Figure A. 60 ^{1}H NMR spectrum of **96h**.

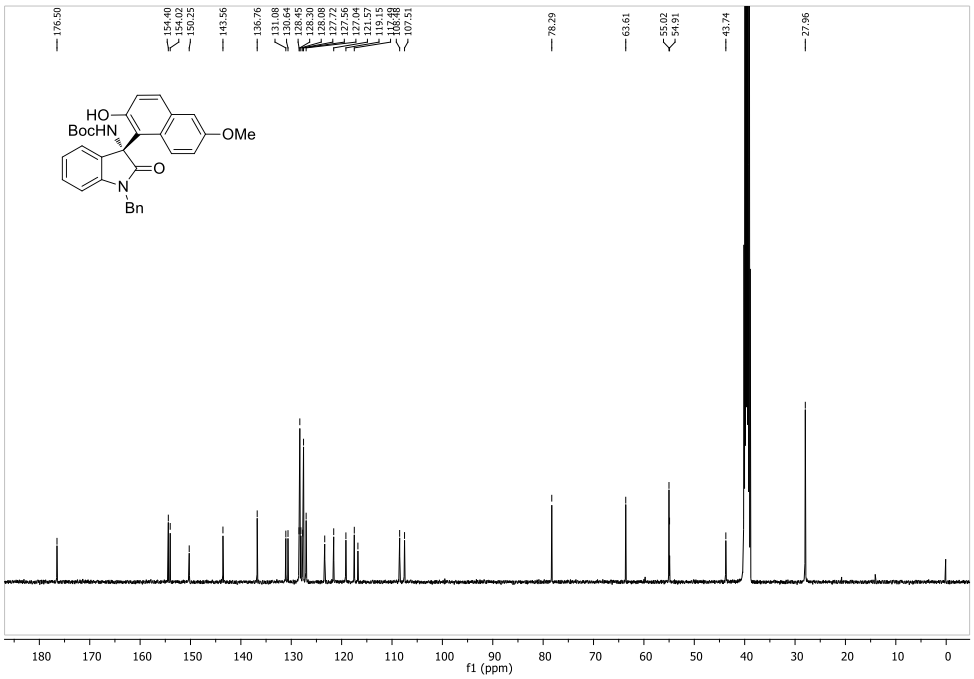

Figure A. 61 ^{13}C NMR spectrum of **96h**.

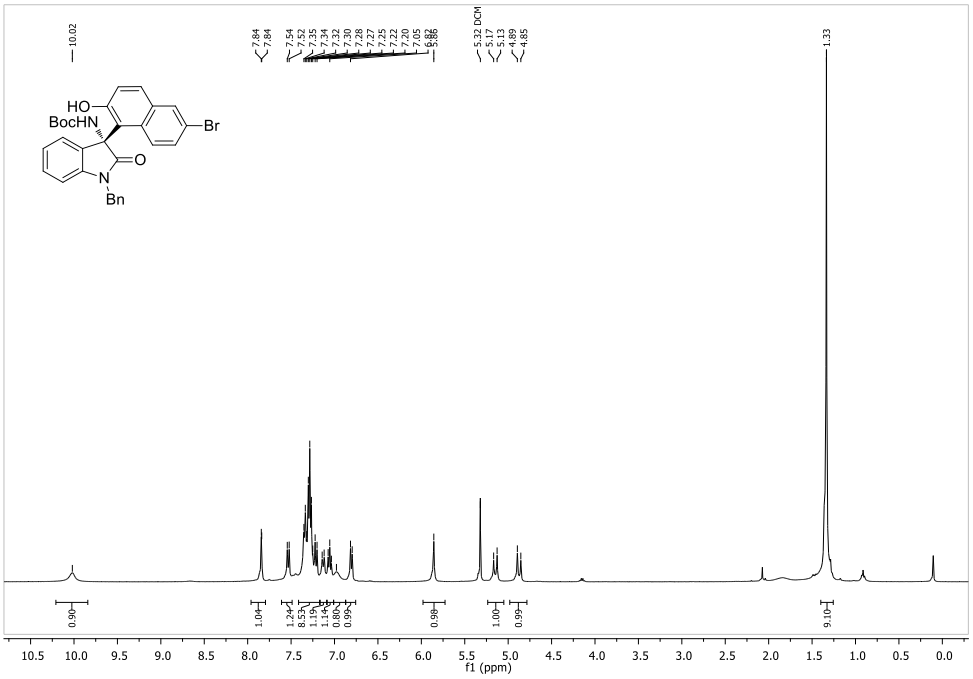

Figure A. 62 ^{1}H NMR spectrum of **96i**.

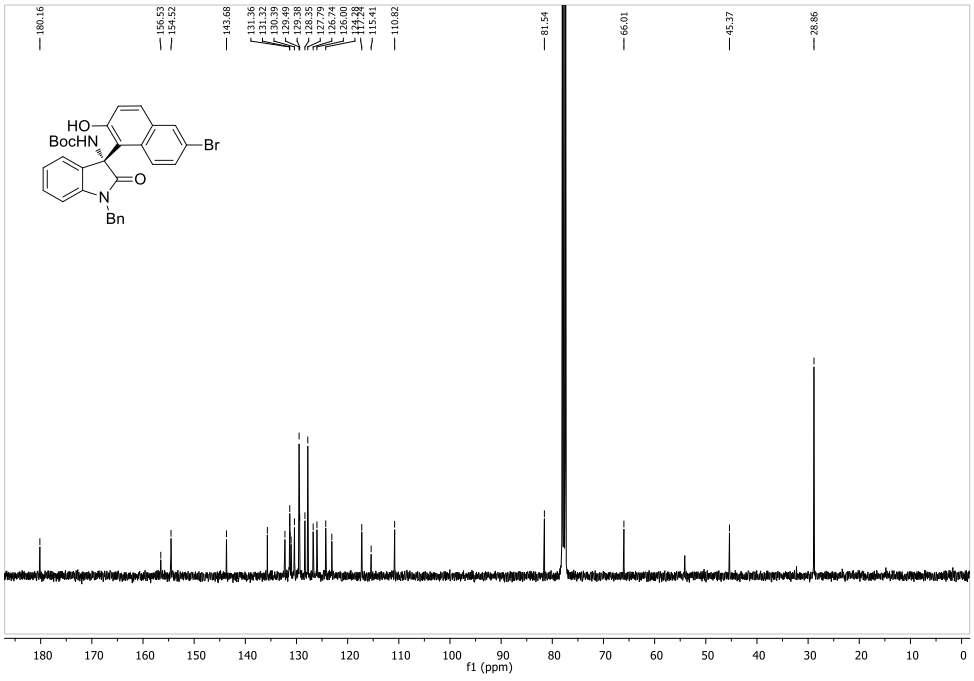

Figure A. 63 ^{13}C NMR spectrum of **96i**.

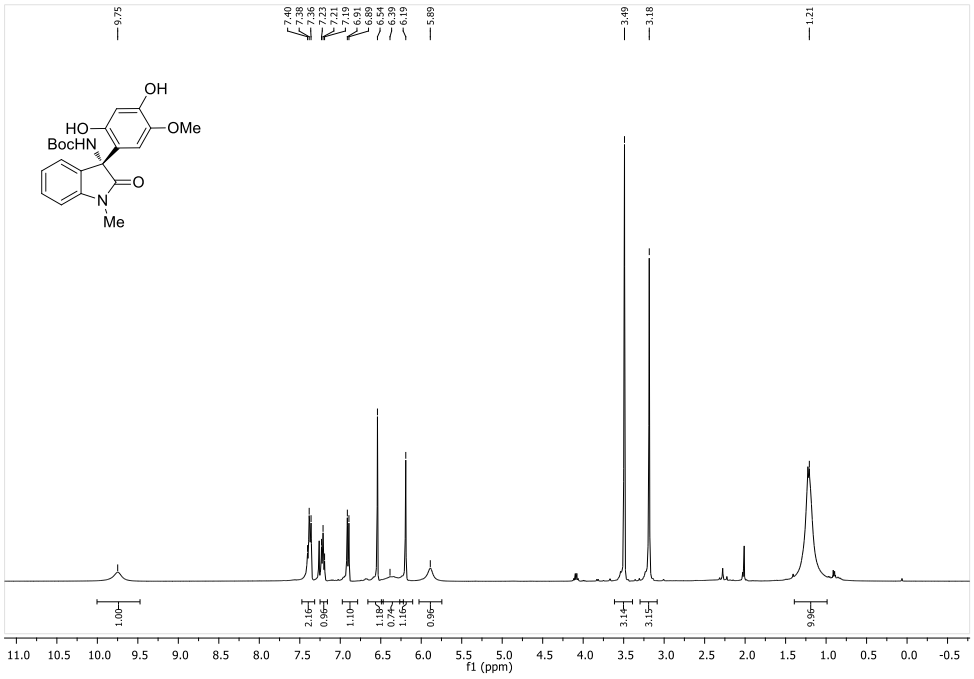

Figure A. 64 ^{1}H NMR spectrum of **98b**.

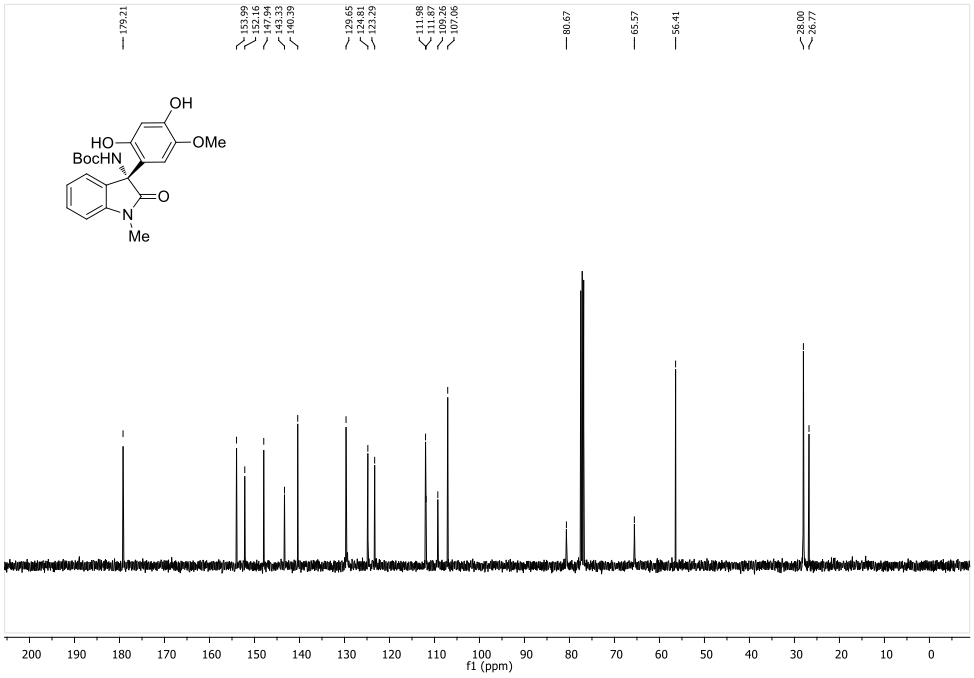

Figure A. 65 ^{13}C NMR spectrum of **98b**.

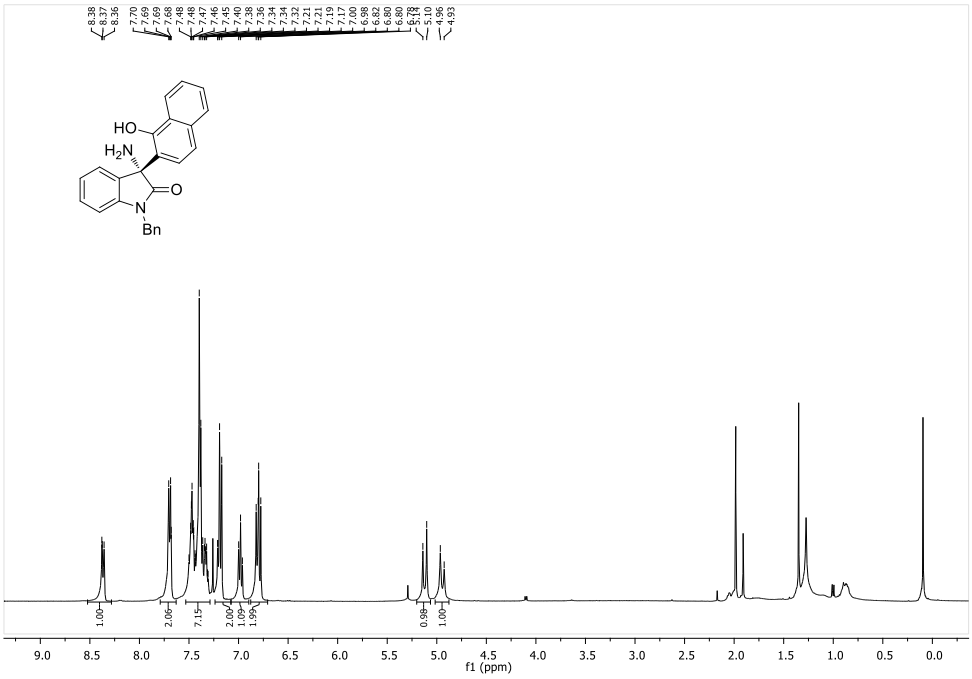

Figure A. 66 ^{1}H NMR spectrum of **99**.

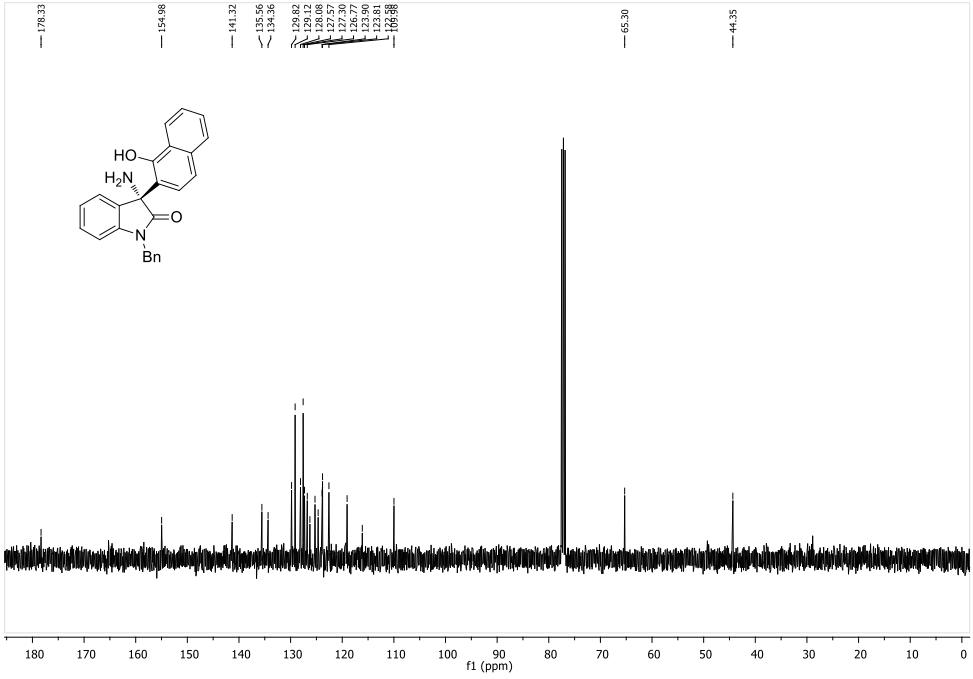

Figure A. 67 ^{13}C NMR spectrum of **99**.

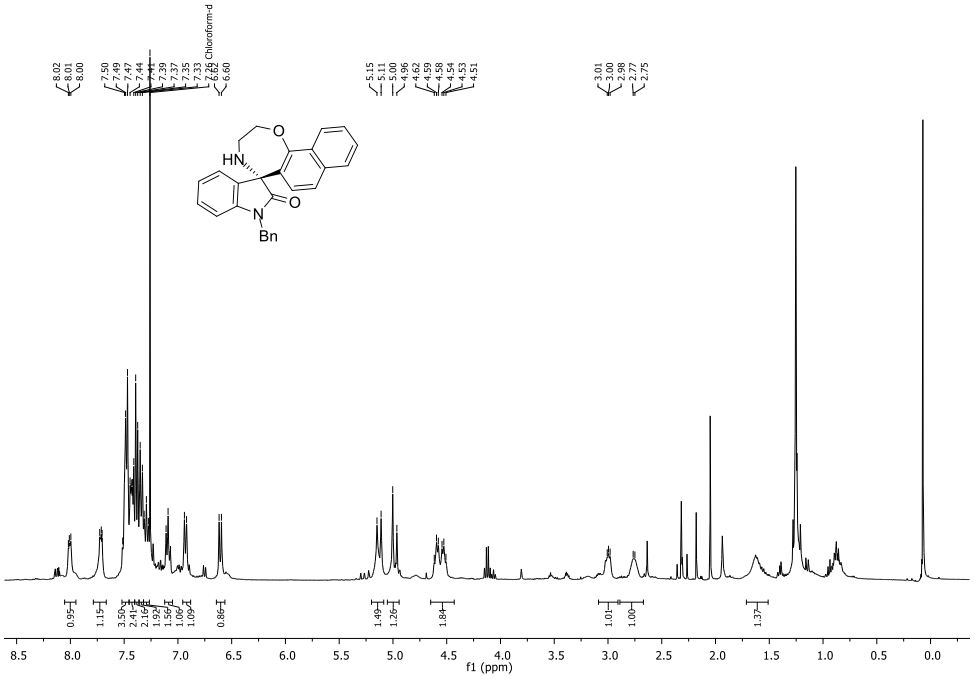

Figure A. 68 ^{1}H NMR spectrum of **100**.

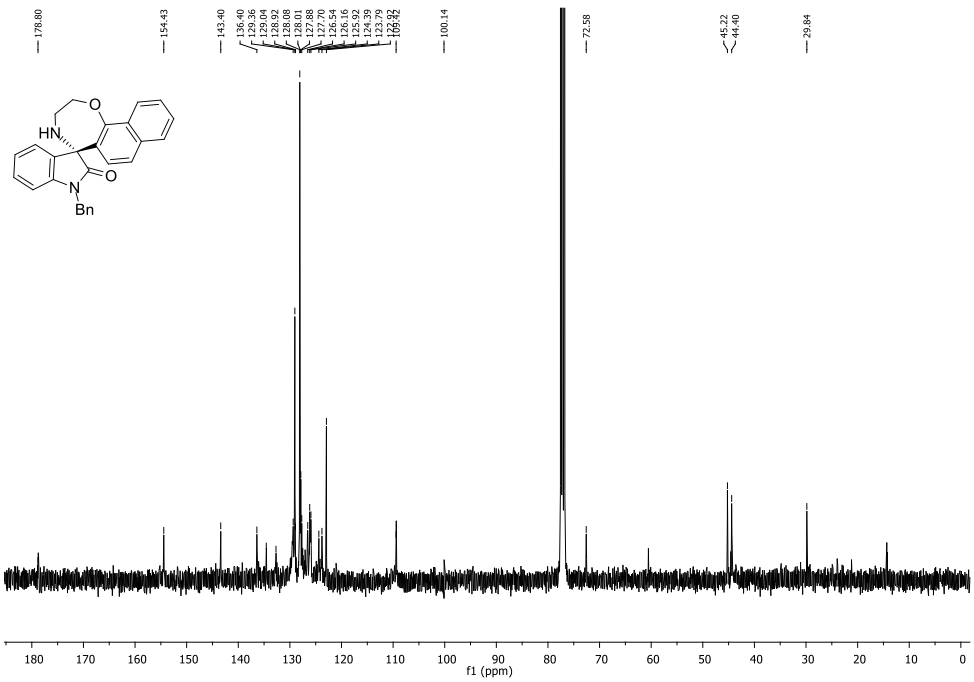

Figure A. 69 ^{13}C NMR spectrum of **100**.

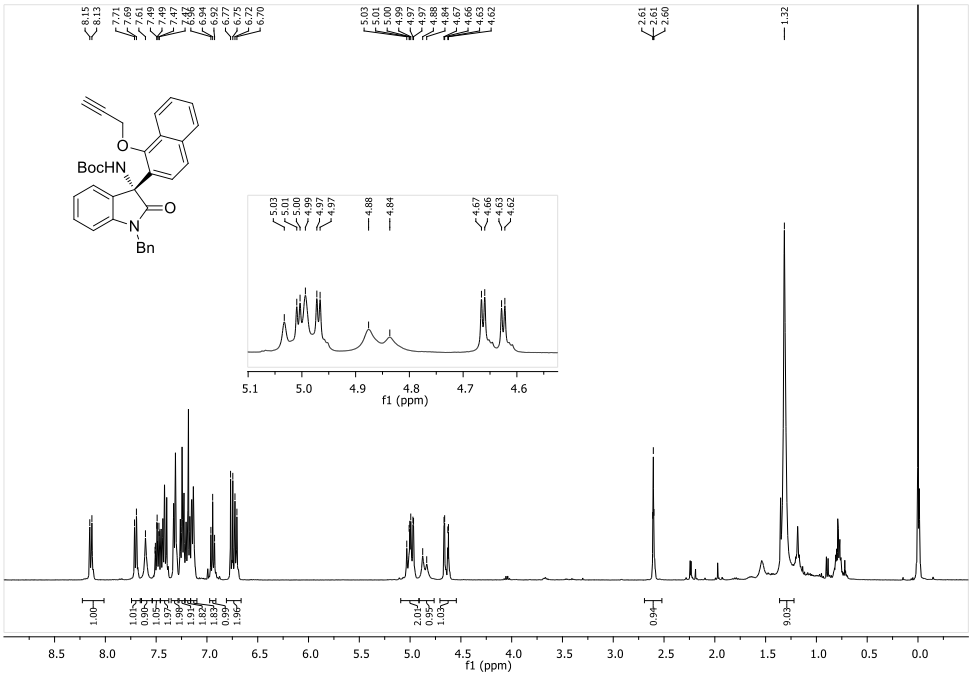

Figure A. 70 ^{1}H NMR spectrum of **102**.

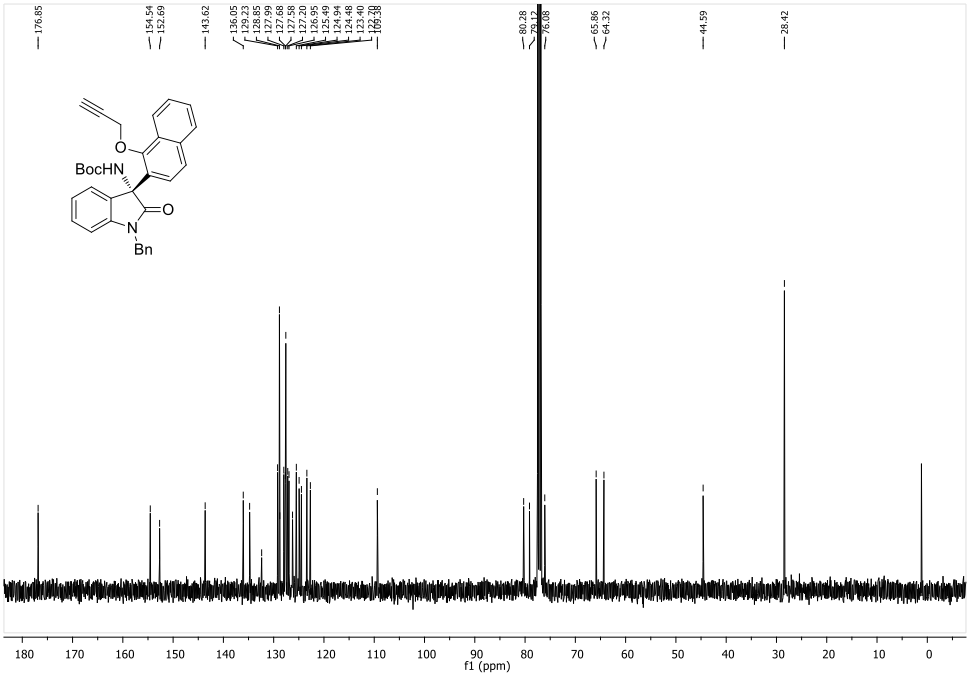

Figure A. 71 ^{13}C NMR spectrum of **102**.

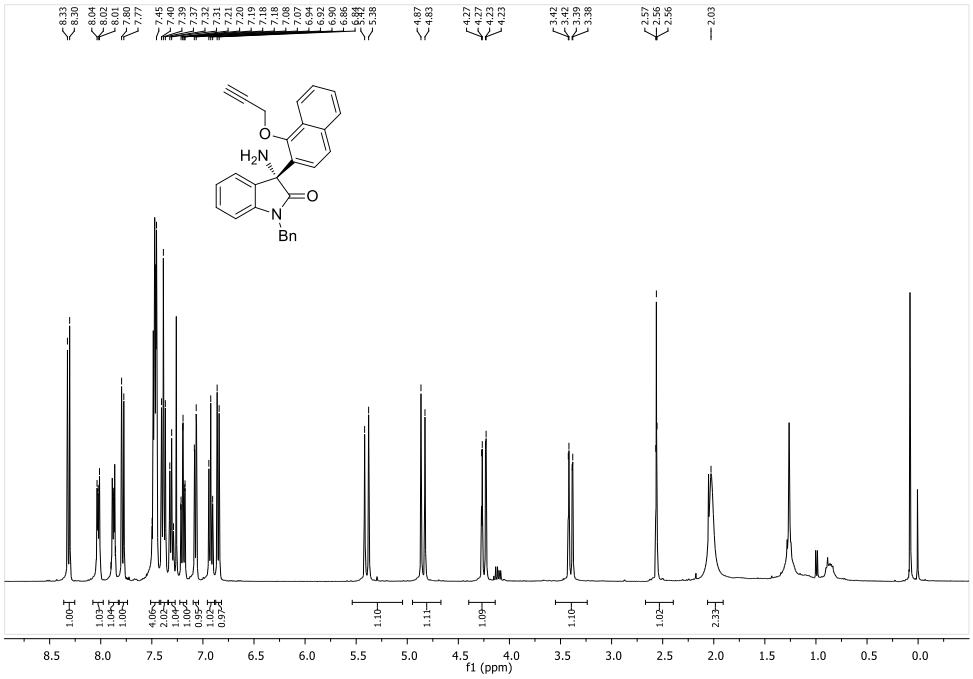

Figure A. 72 ^{1}H NMR spectrum of **103**.

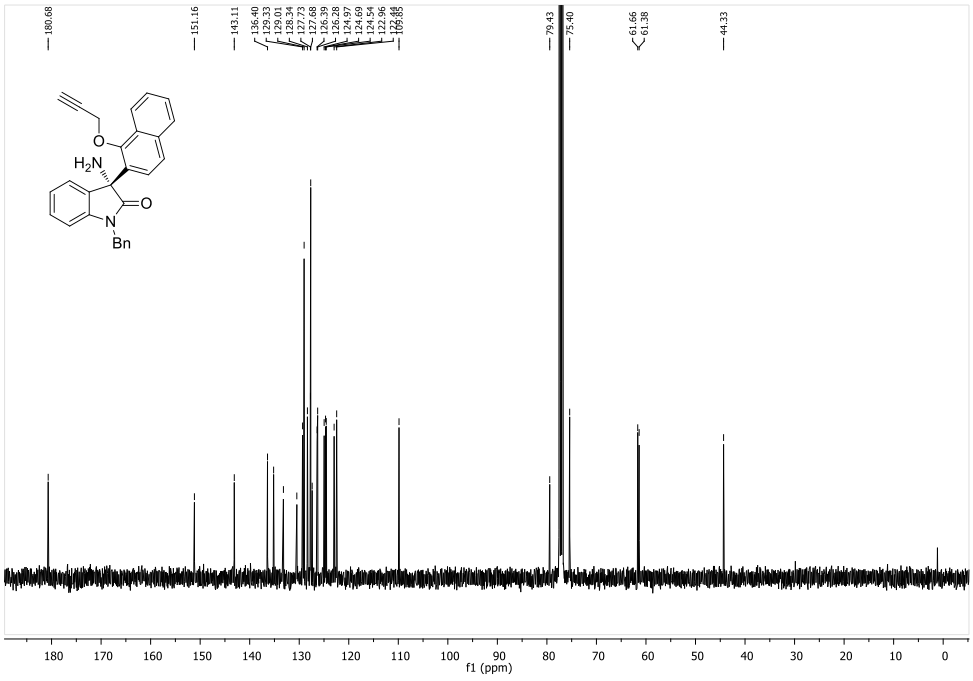

Figure A. 73 ^{13}C NMR spectrum of **103**.

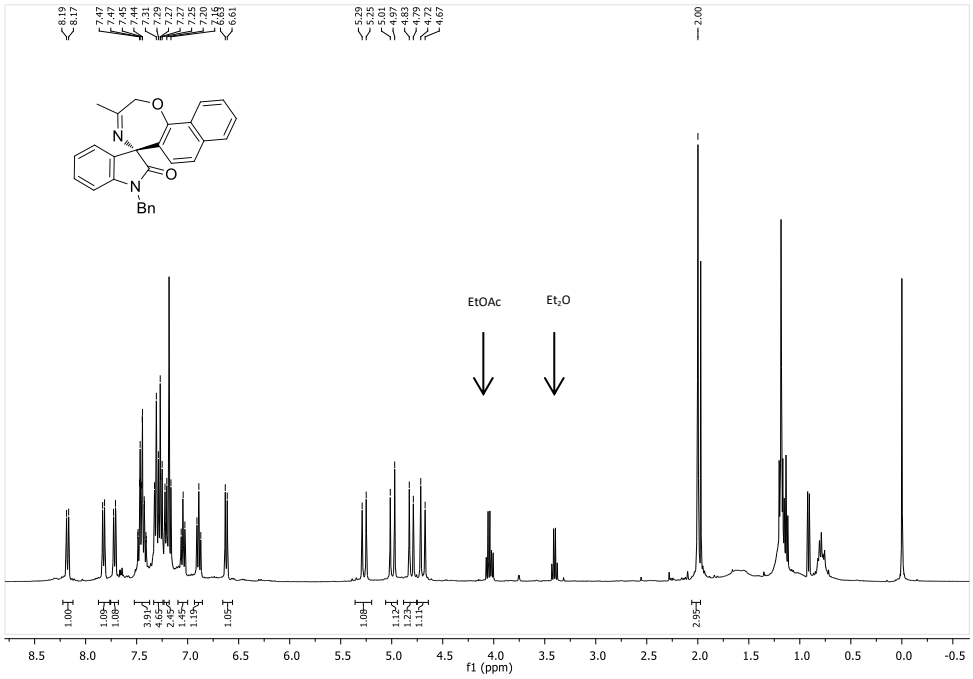

Figure A. 74 ^{1}H NMR spectrum of **105**.

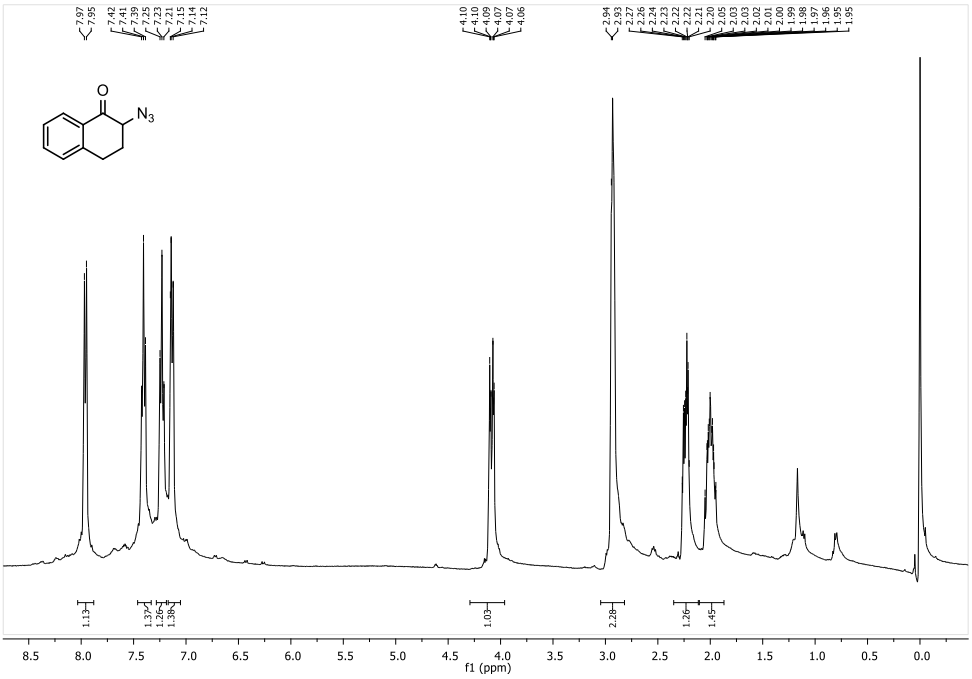

Figure A. 75 ^{1}H NMR spectrum of **93m**.

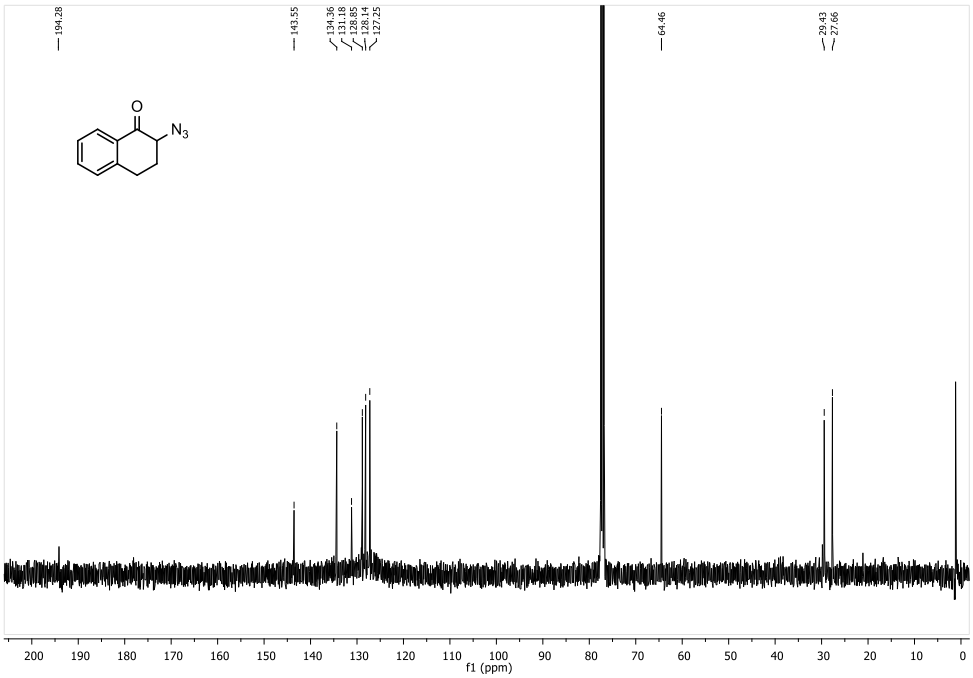

Figure A. 76 ^{13}C NMR spectrum of **93m**.

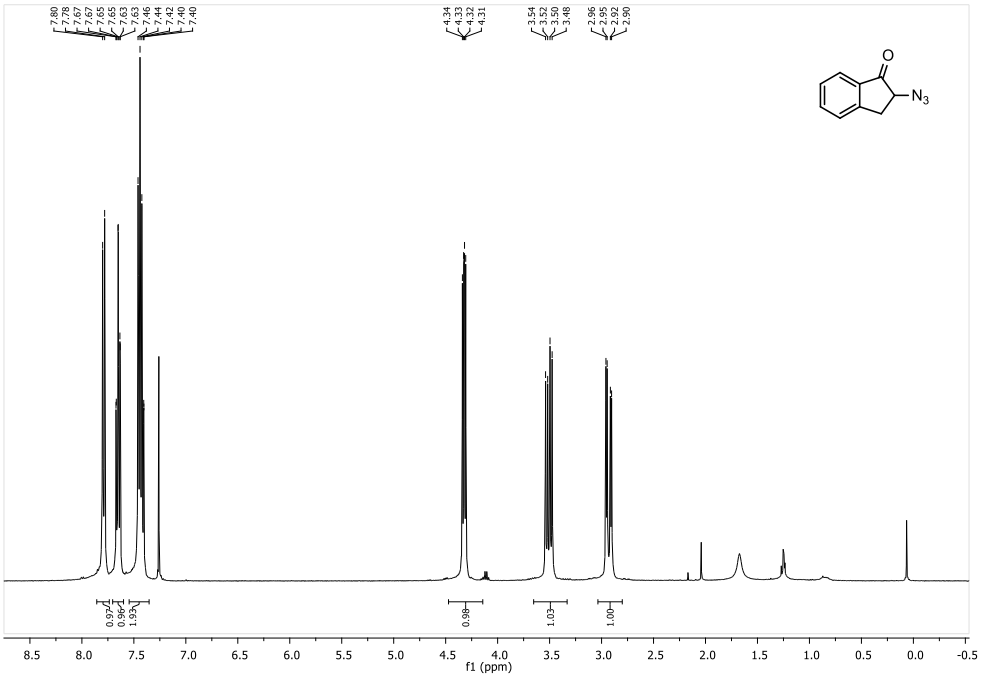

Figure A. 77 ^{1}H NMR spectrum of **93n**.

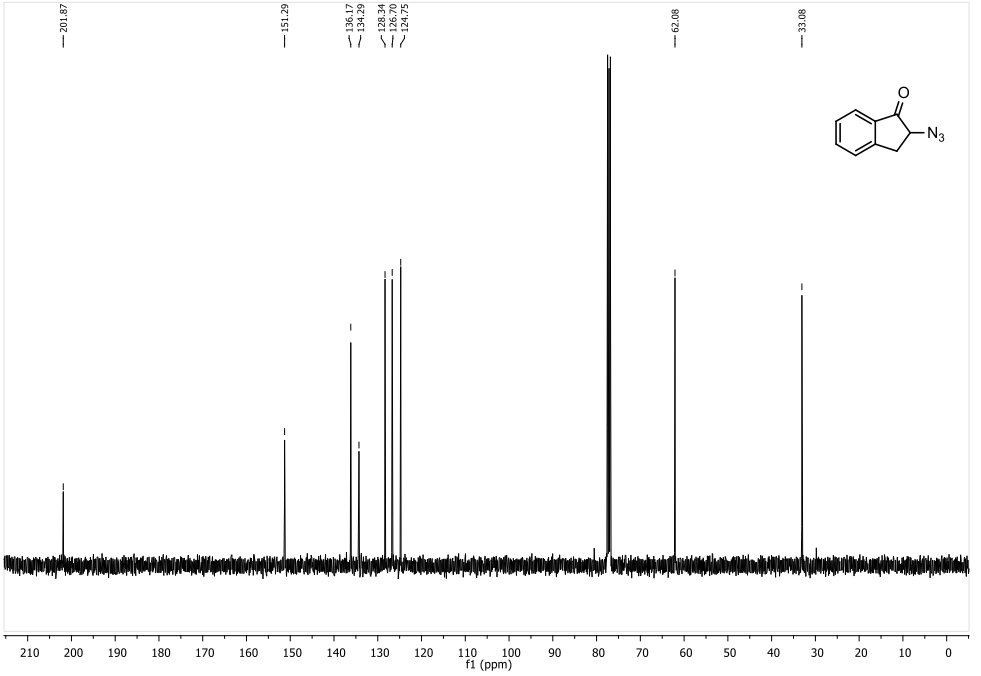

Figure A. 78^{13}C NMR spectrum of **93n**.

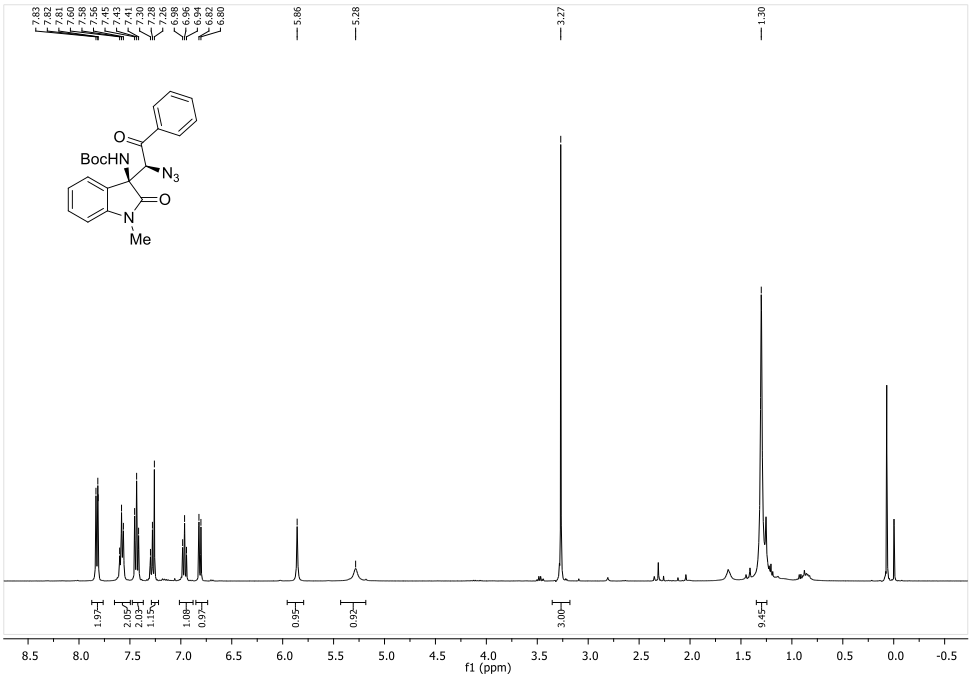

Figure A. 79 ^{1}H NMR spectrum of **107a**.

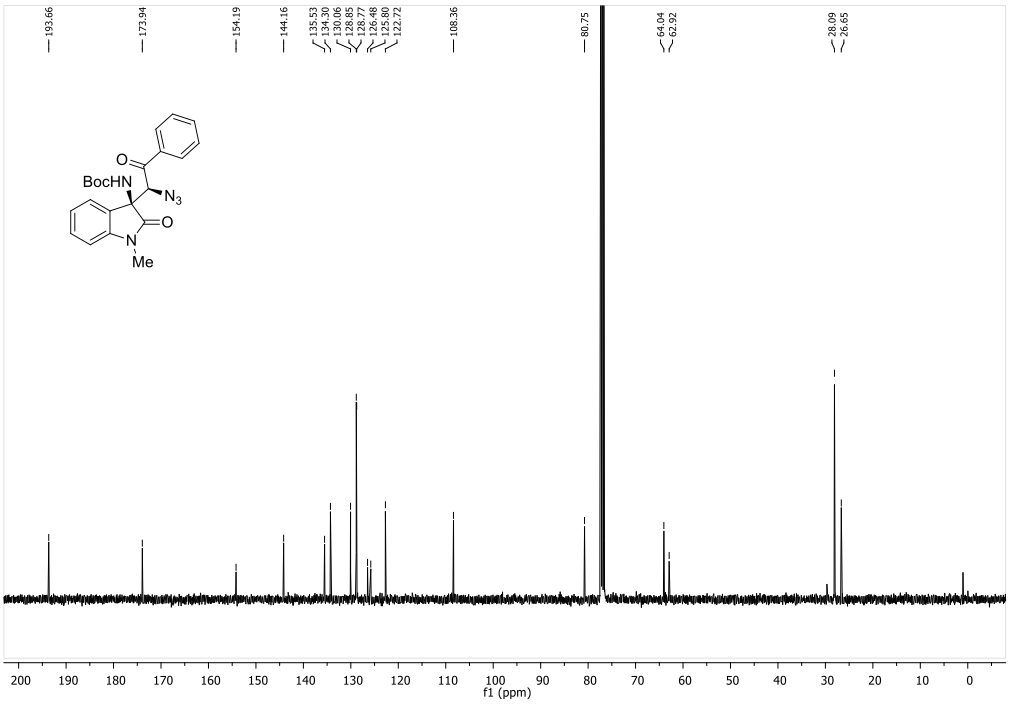

Figure A. 80 ^{13}C NMR spectrum of **107a**.

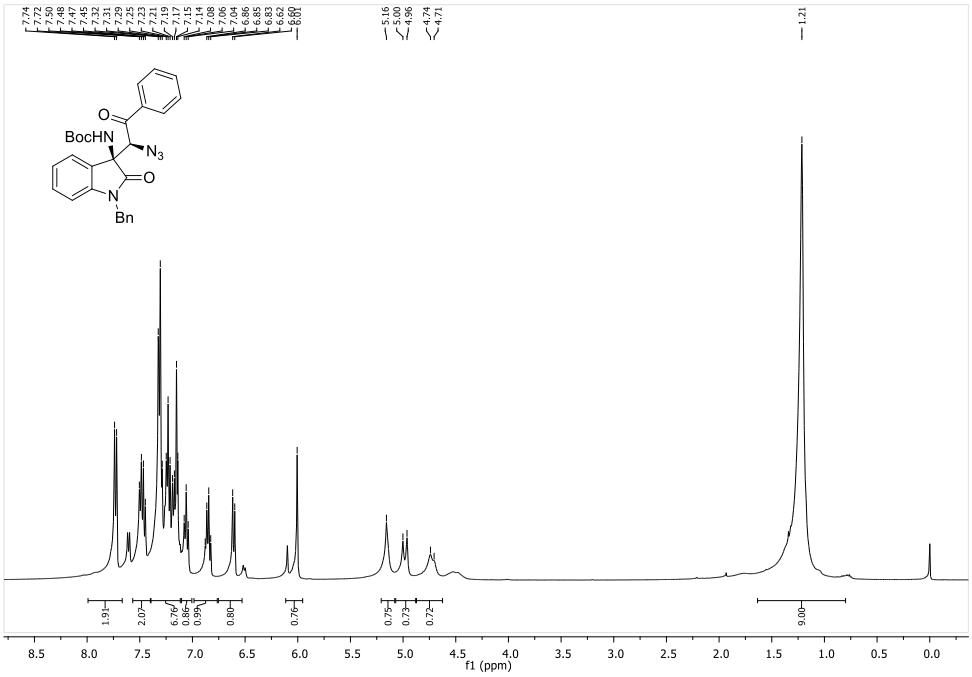

Figure A. 81 ^{1}H NMR spectrum of **107b**.

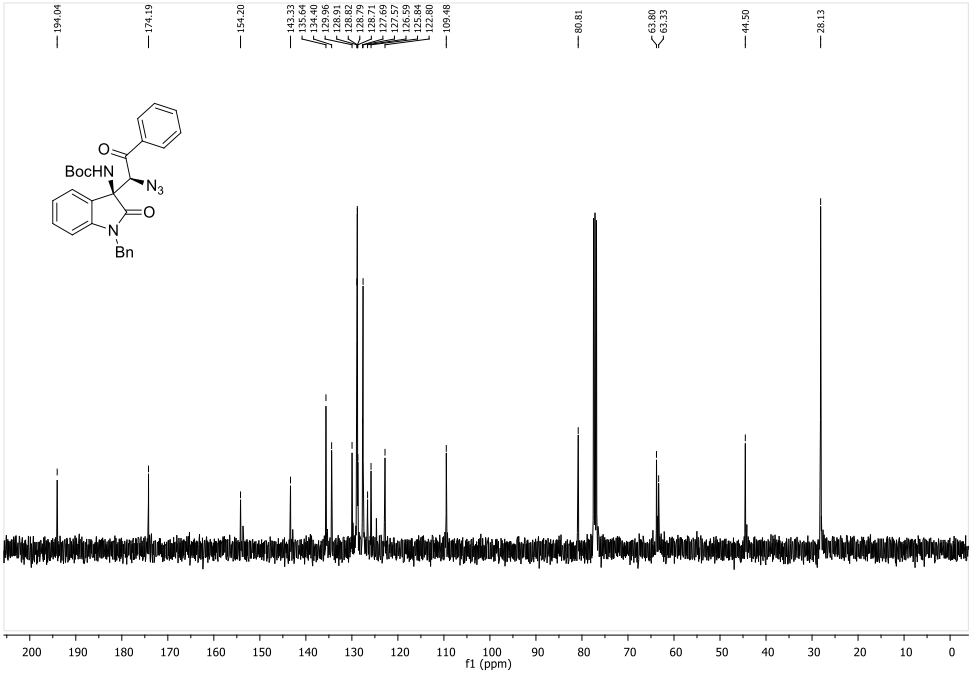

Figure A. 82 ^{13}C NMR spectrum of **107b**.

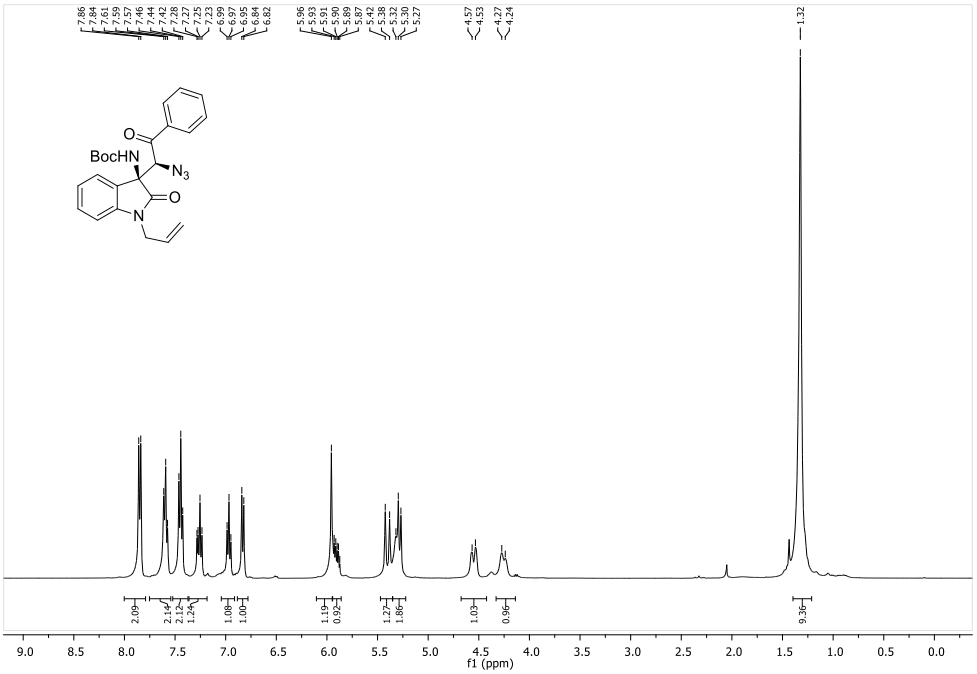

Figure A. 83 ^{1}H NMR spectrum of **107c**.

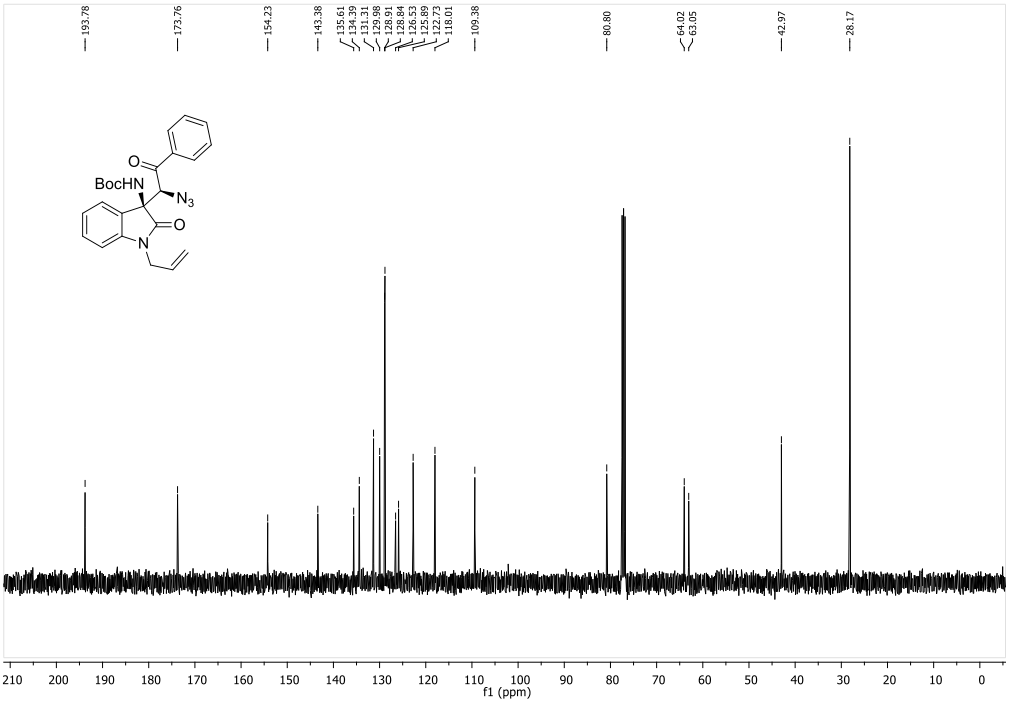

Figure A. 84 ^{13}C NMR spectrum of **107c**.

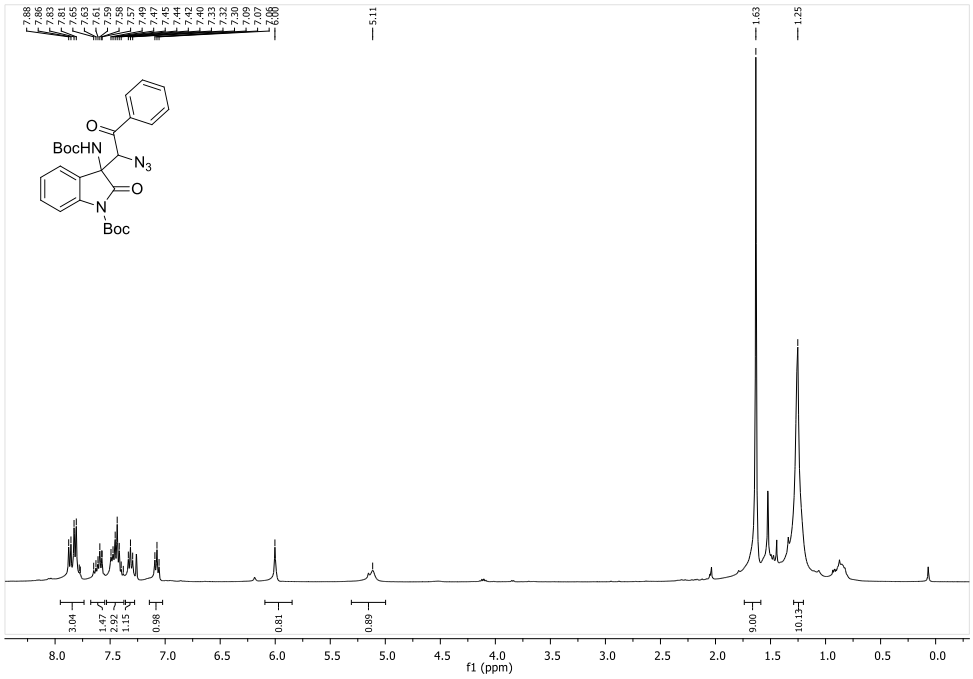

Figure A. 85 ^{1}H NMR spectrum of **107d**.

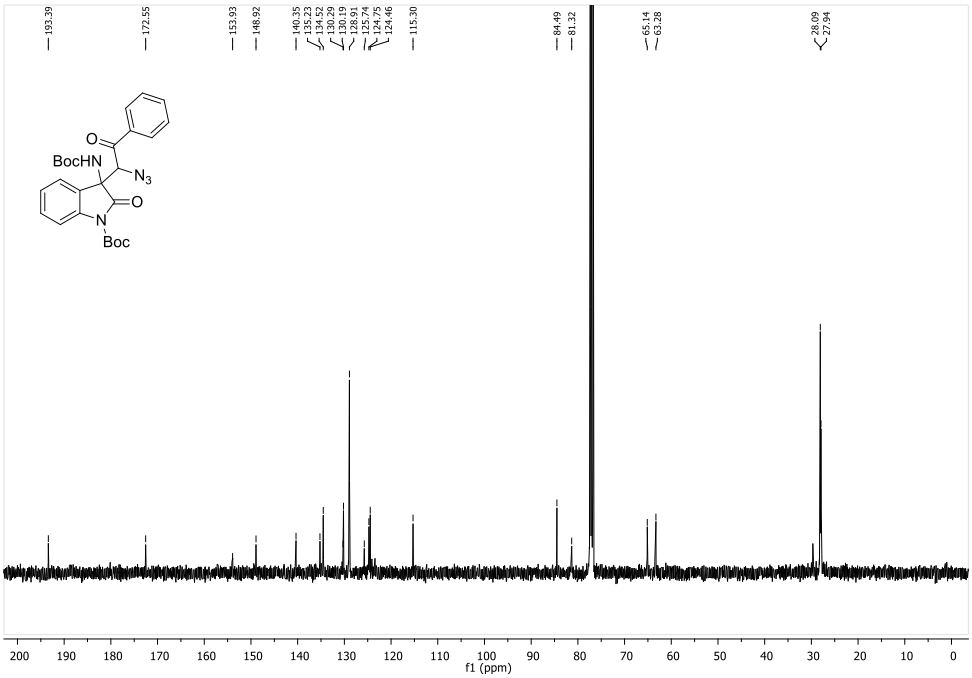

Figure A. 86 ^{13}C NMR spectrum of **107d**.

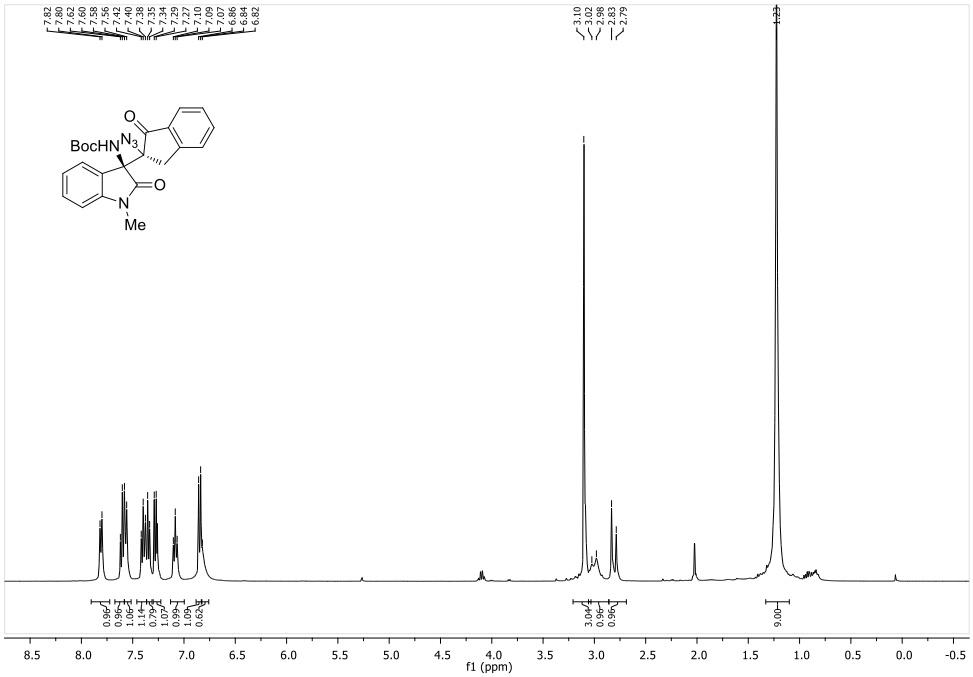

Figure A. 87 ^{1}H NMR spectrum of **107e**.

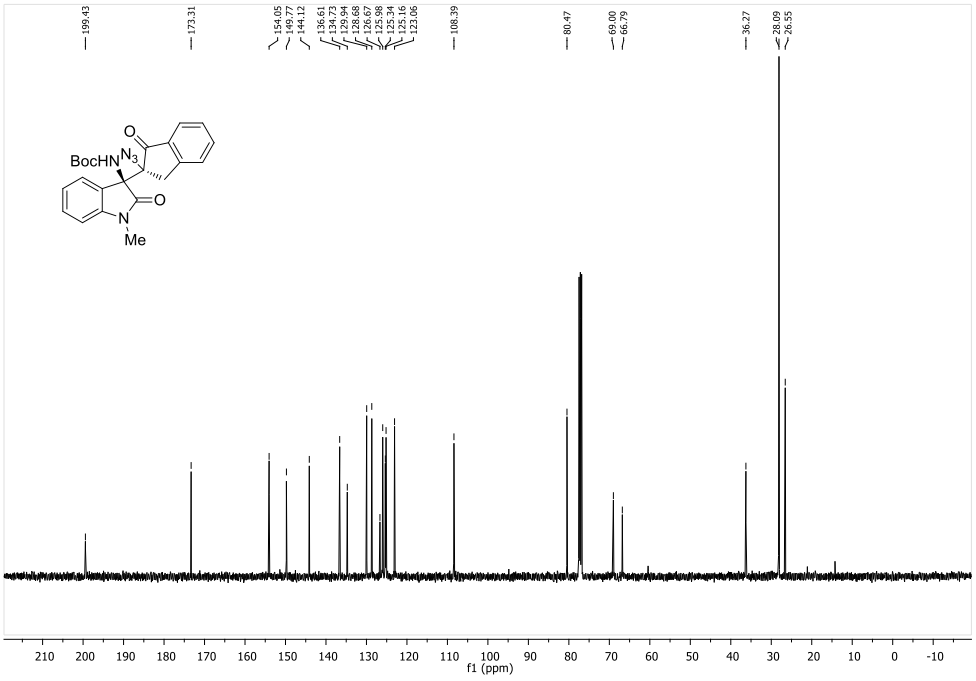

Figure A. 88 ^{13}C NMR spectrum of **107e**.

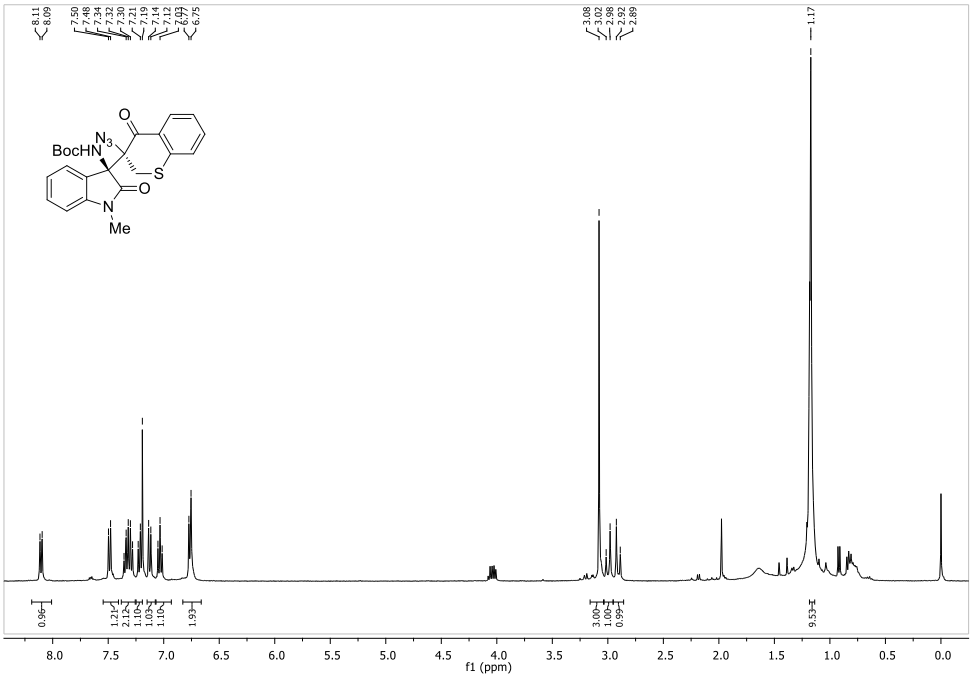

Figure A. 89 ^{1}H NMR spectrum of **107f**.

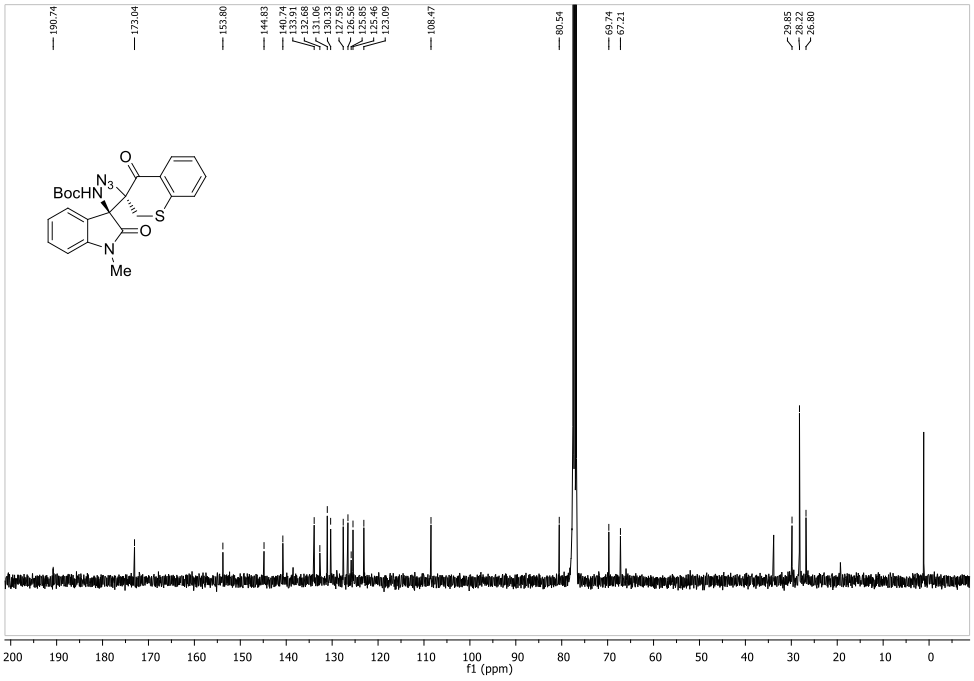

Figure A. 90 ^{13}C NMR spectrum of **107f**.

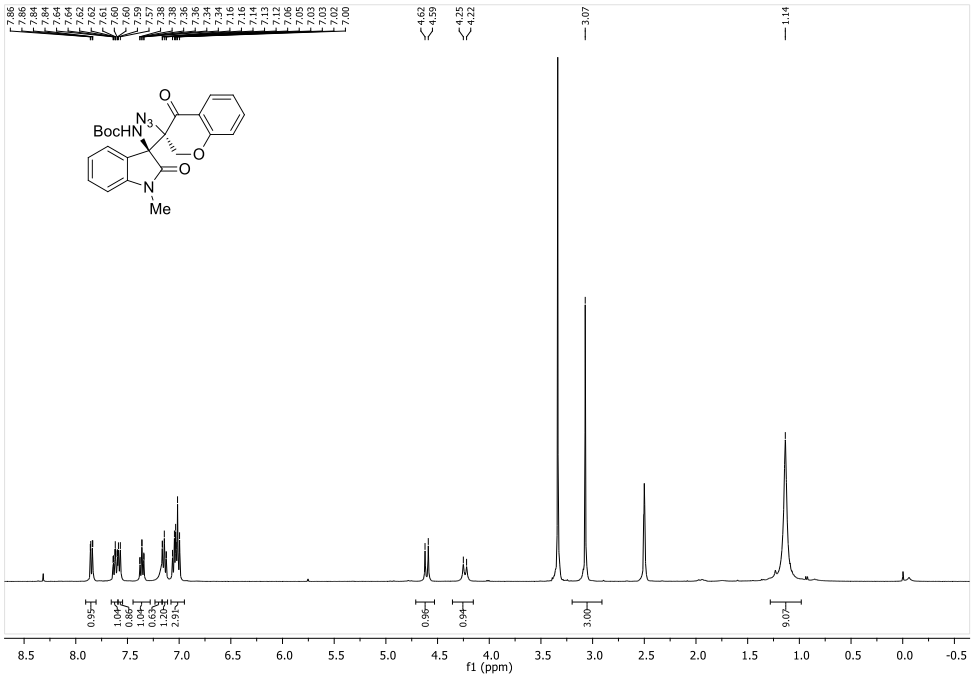

Figure A. 91 ^{1}H NMR spectrum of **107g**.

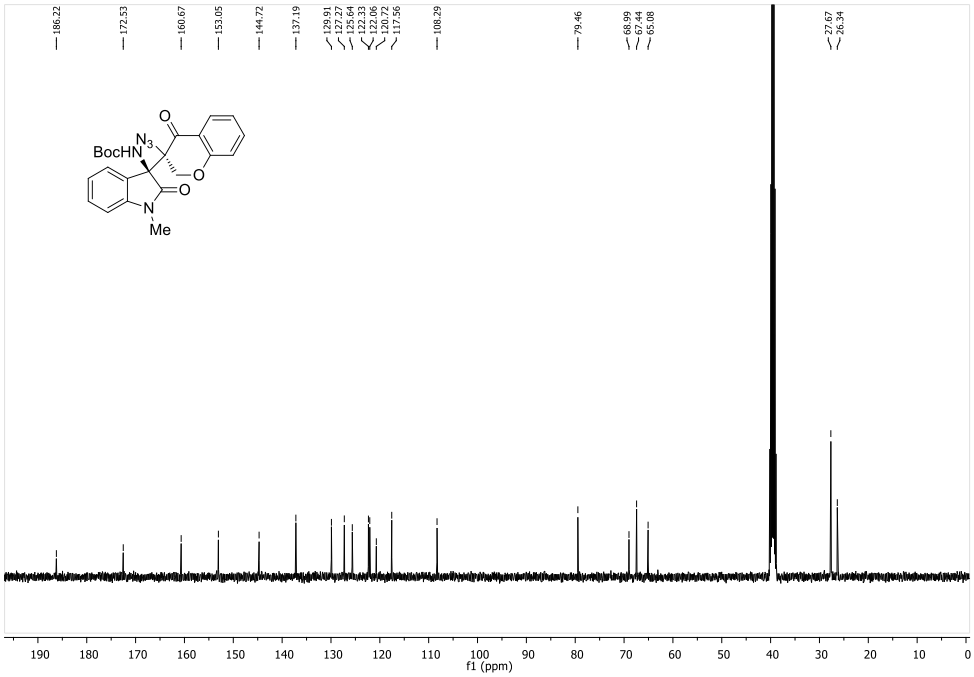

Figure A. 92 ^{13}C NMR spectrum of **107g**.

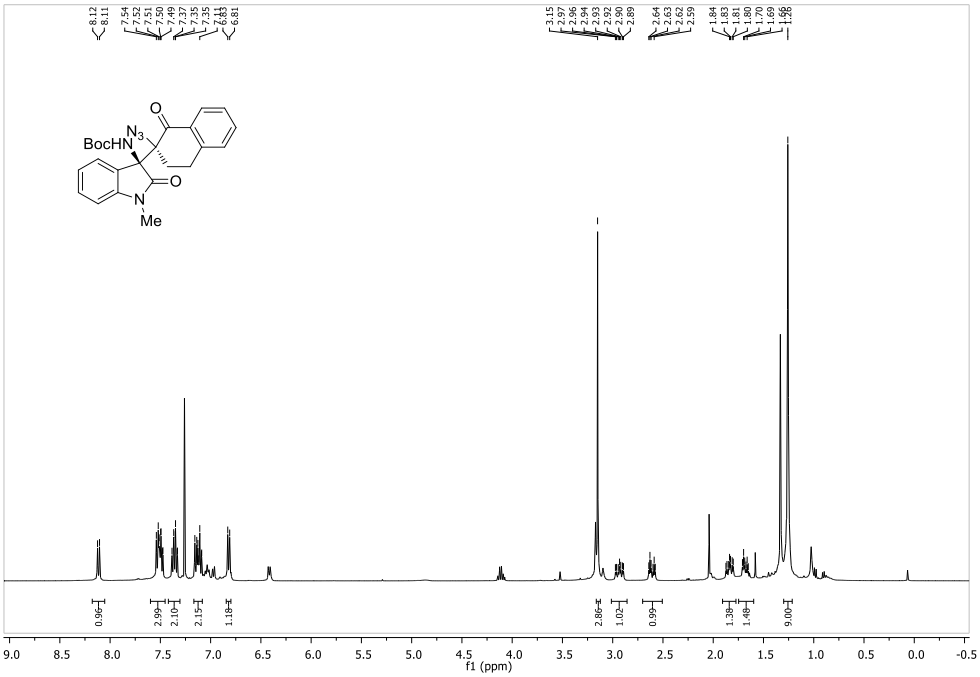

Figure A. 93 ^{1}H NMR spectrum of **107h**.

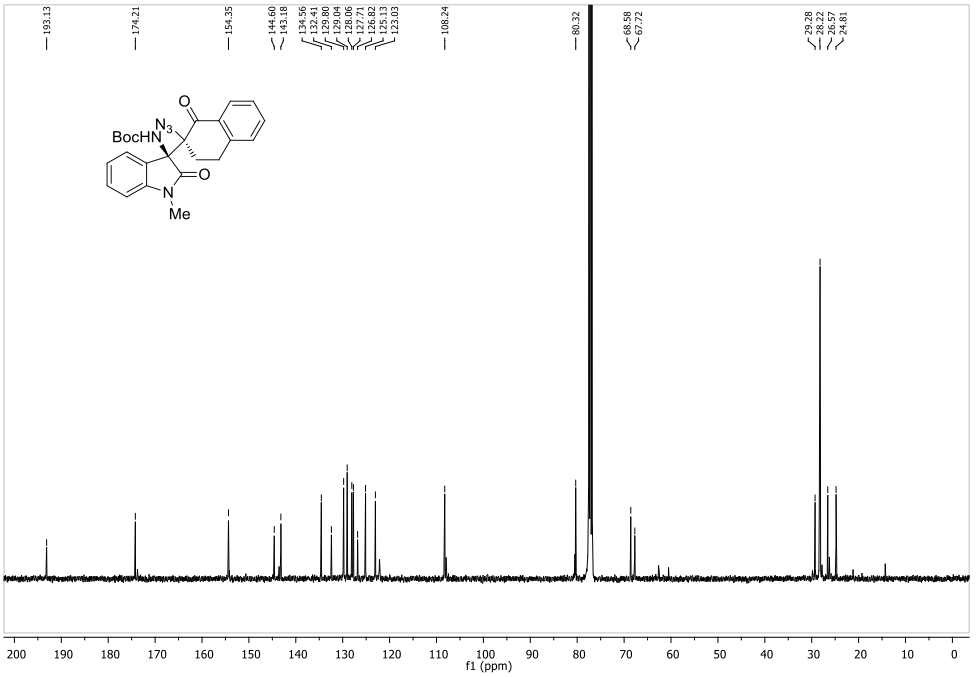

Figure A. 94 ^{13}C NMR spectrum of **107h**.

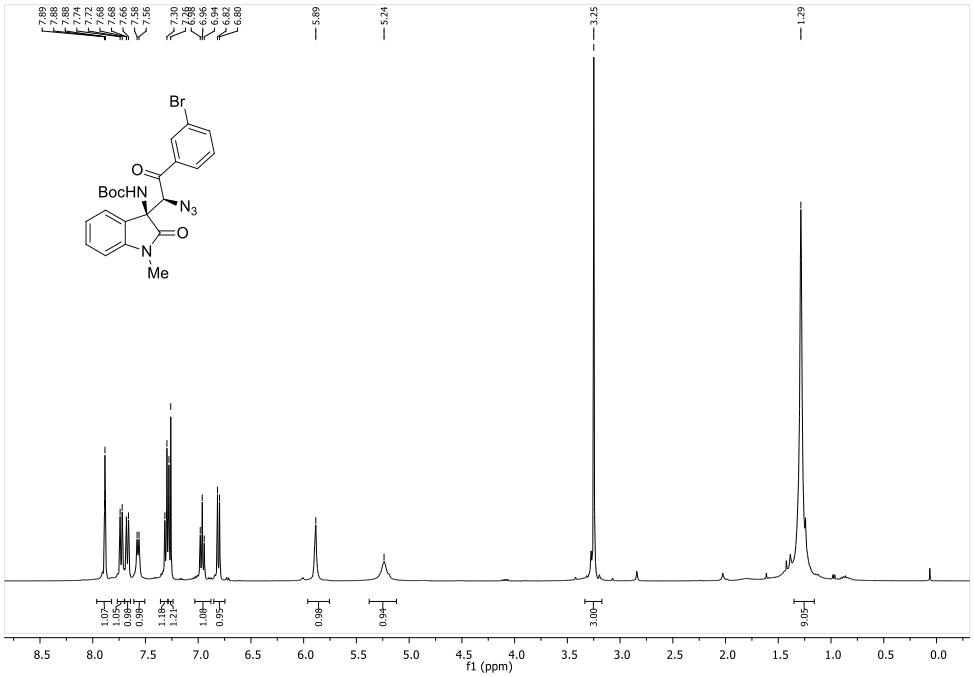

Figure A. 95 ^{1}H NMR spectrum of **107i**.

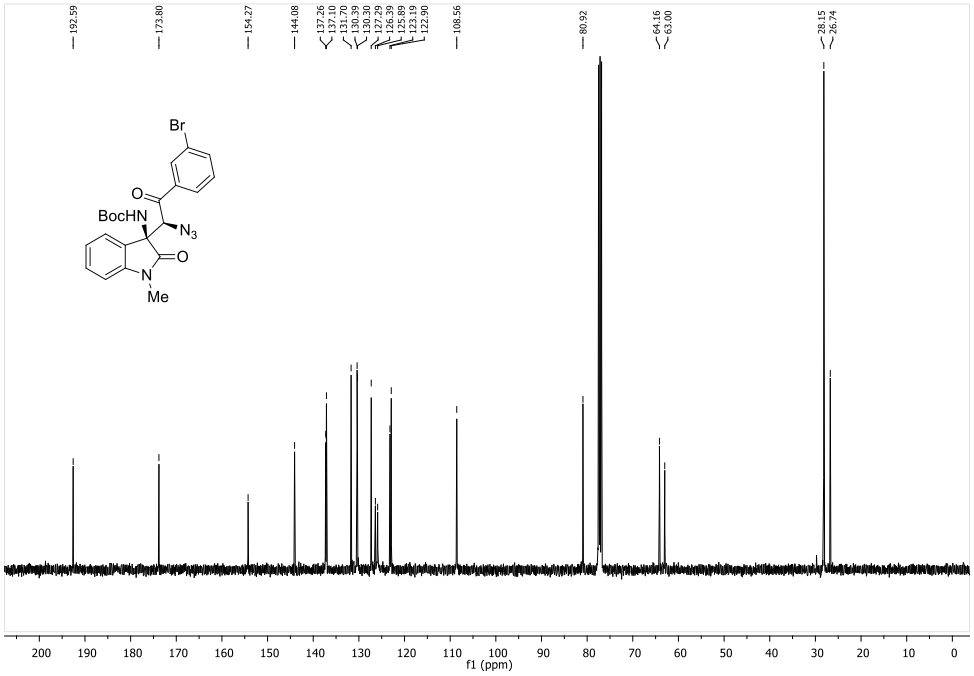

Figure A. 96 ^{13}C NMR spectrum of **107i**.

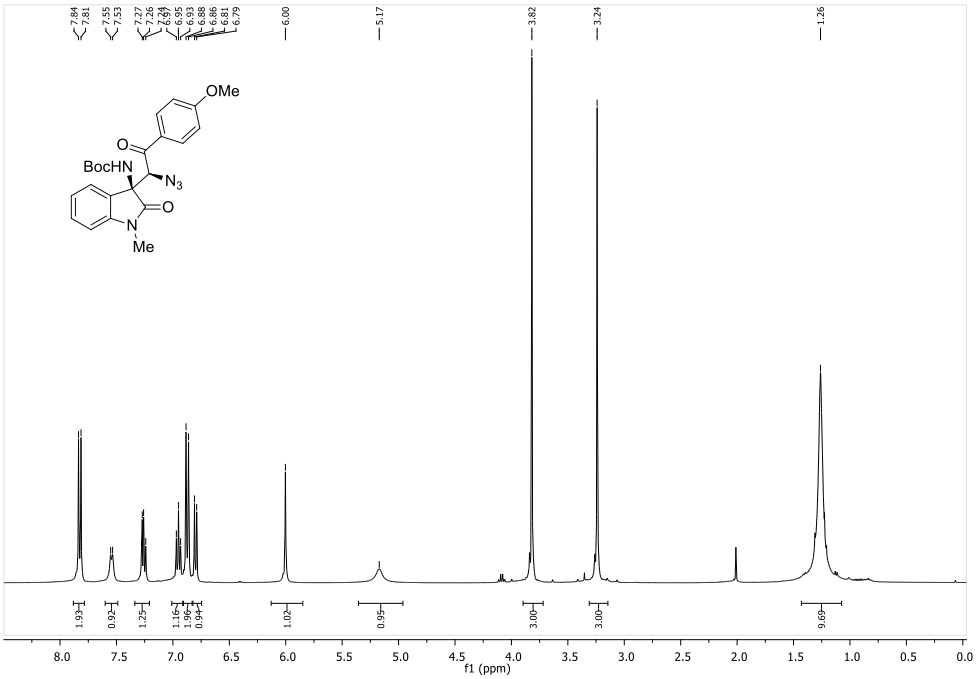

Figure A. 97 ^{1}H NMR spectrum of **107j**.

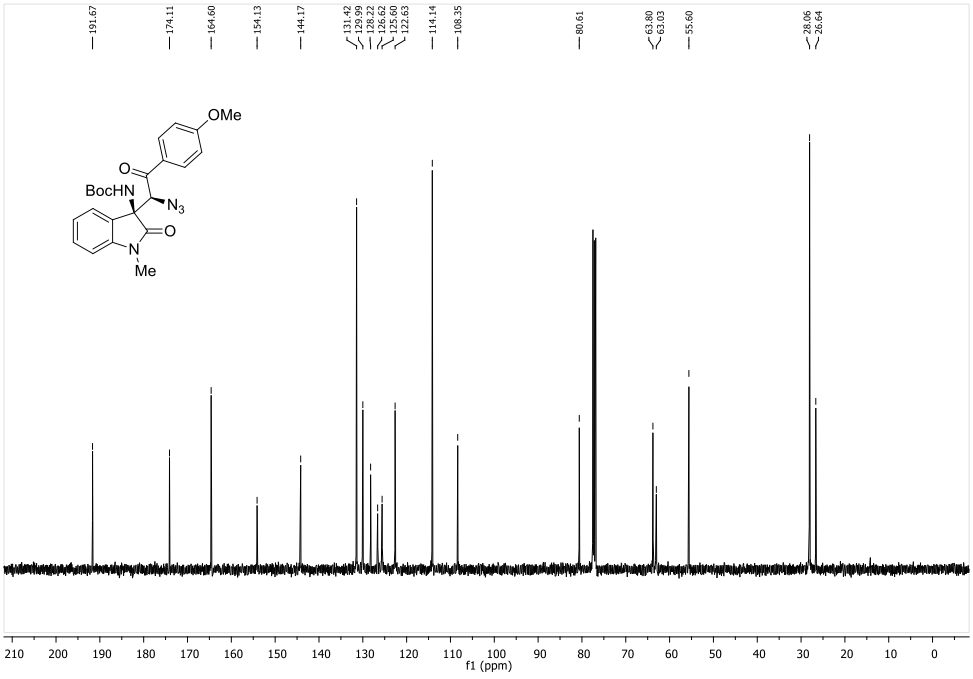

Figure A. 98 ^{13}C NMR spectrum of **107j**.

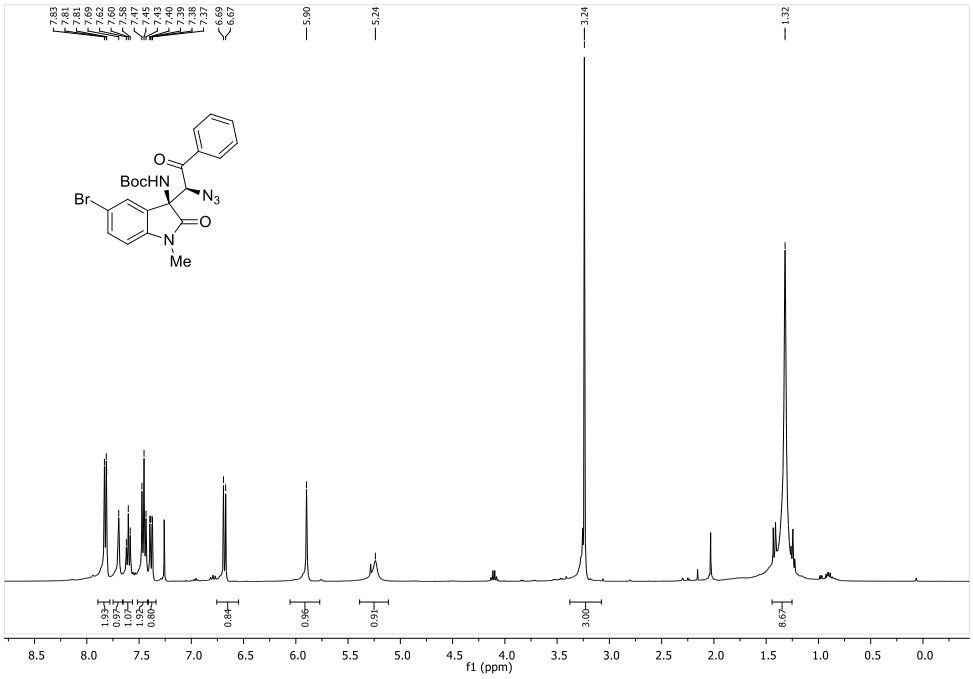

Figure A. 99 ^{1}H NMR spectrum of **107k**.

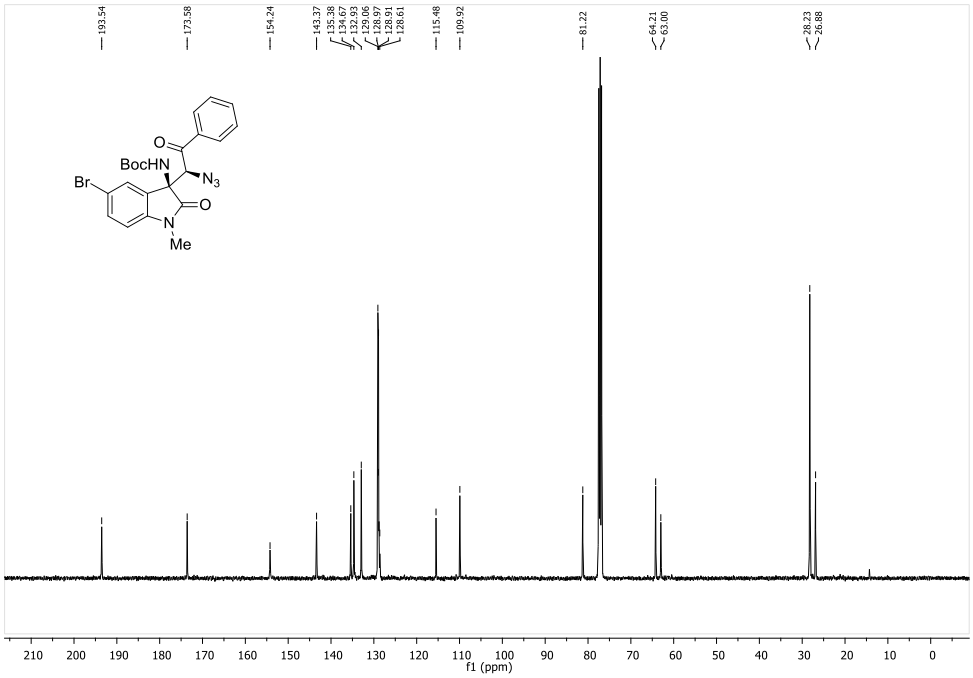

Figure A. 100 ^{13}C NMR spectrum of **107k**.

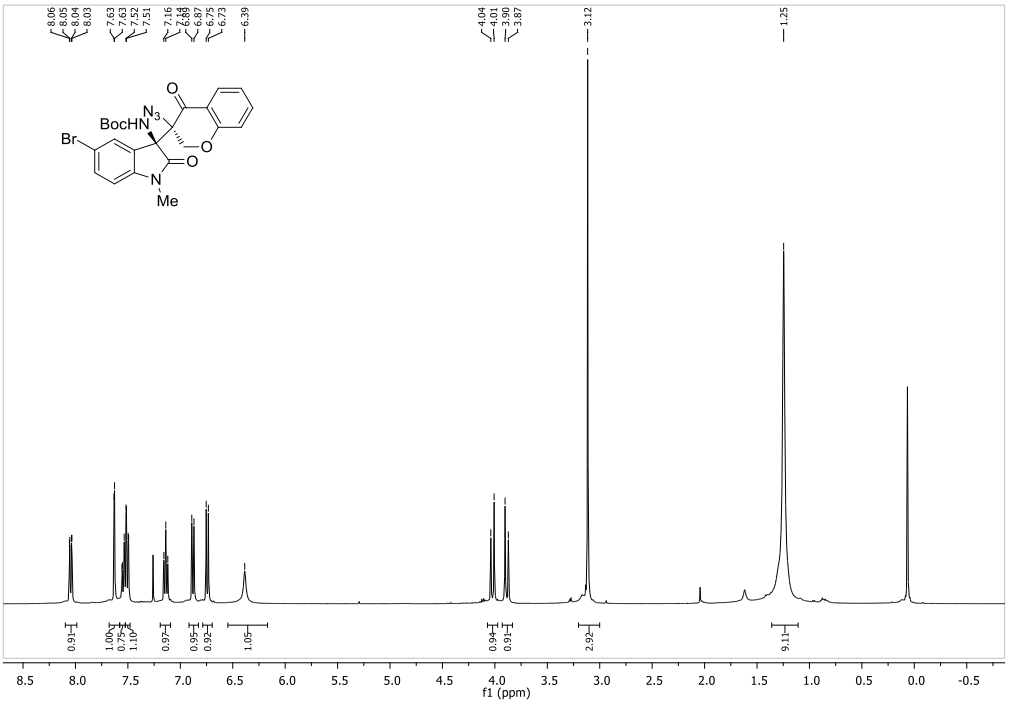

Figure A. 101 ^{1}H NMR spectrum of **107l**.

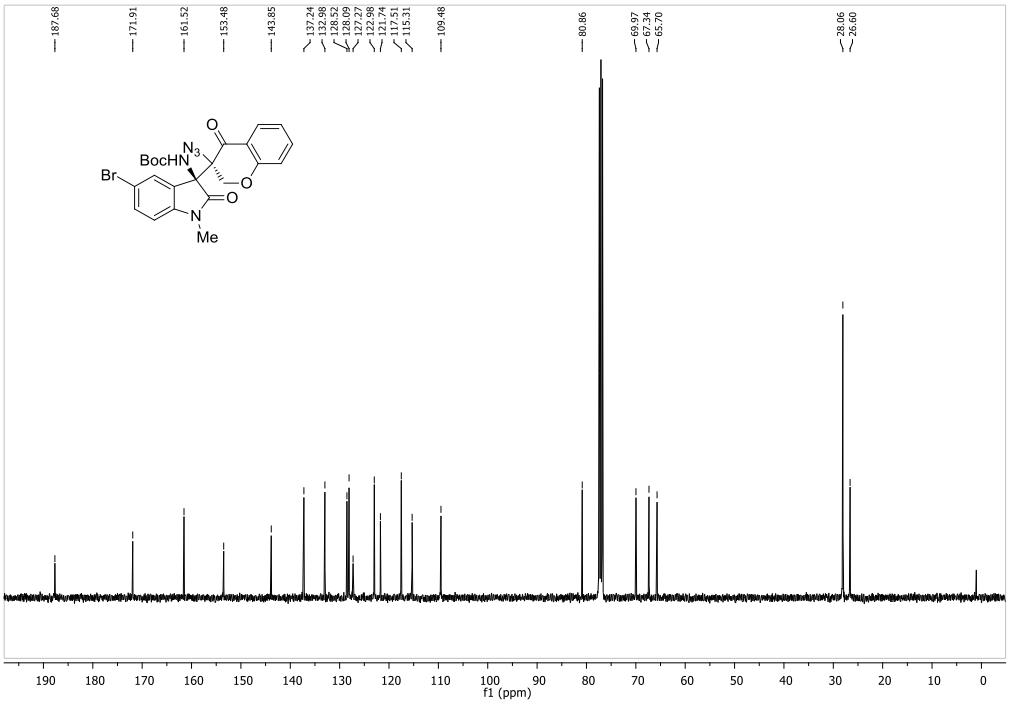

Figure A. 102 ^{13}C NMR spectrum of **107l**.

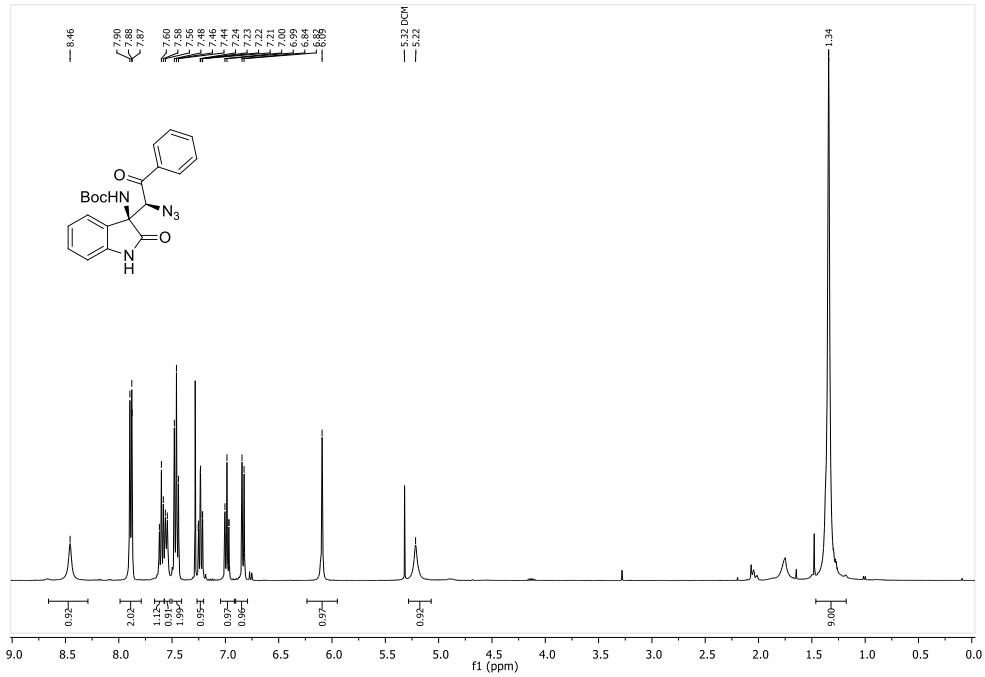

Figure A. 103 ^{1}H NMR spectrum of **107m**.

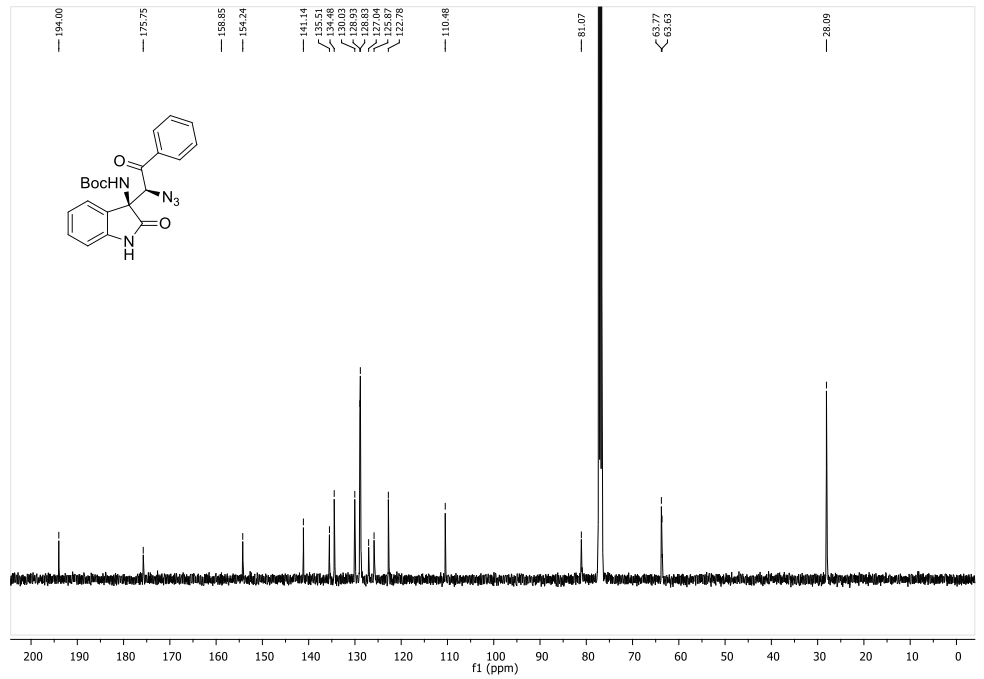

Figure A. 104 ^{13}C NMR spectrum of **107m**.

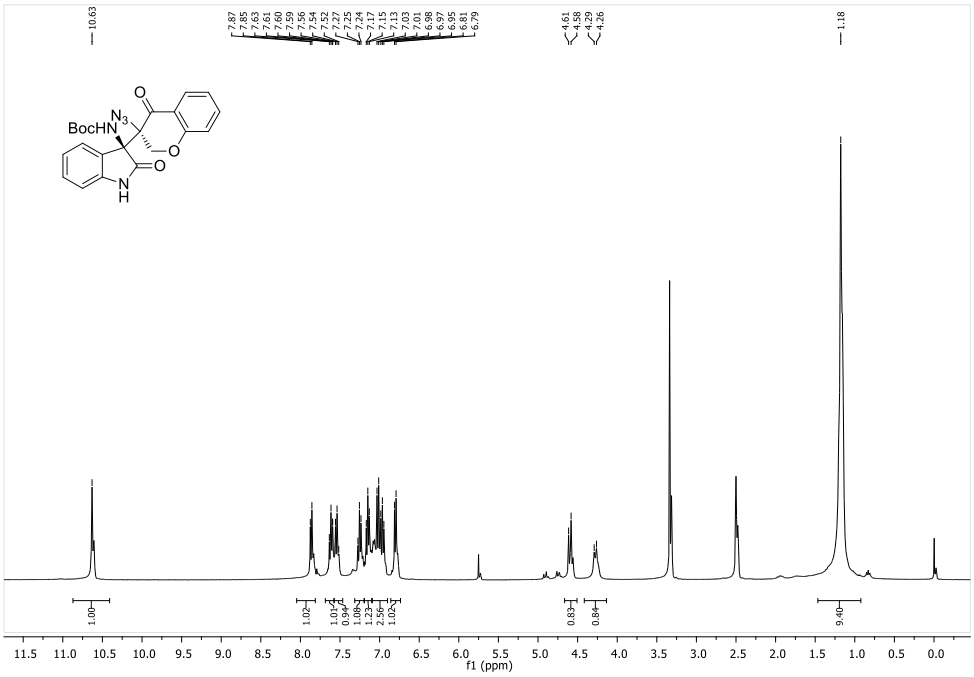

Figure A. 105 ^{1}H NMR spectrum of **107n**.

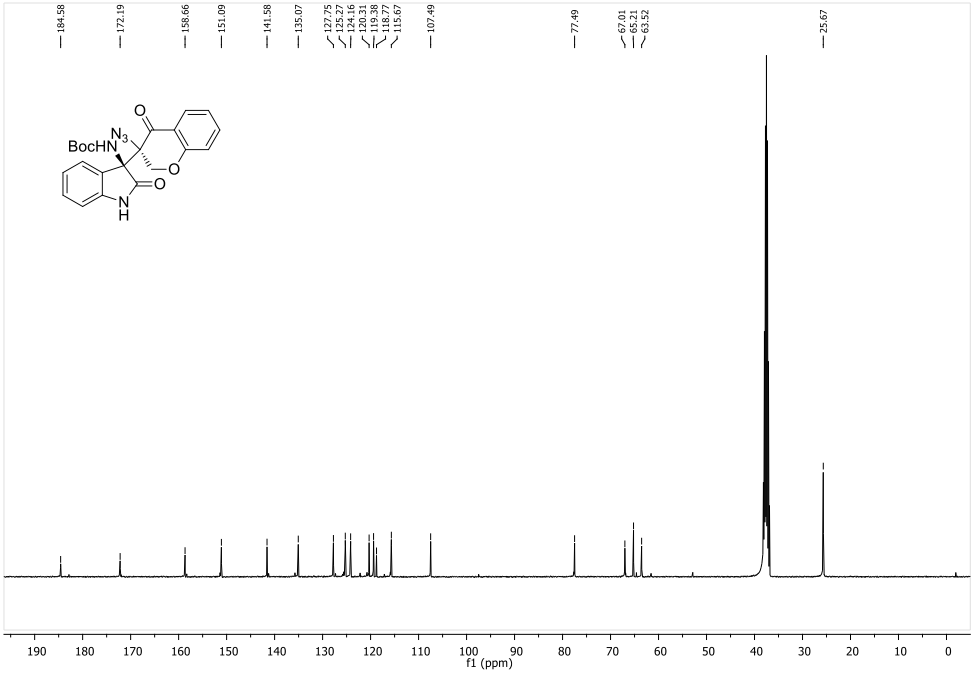

Figure A. 106 ^{13}C NMR spectrum of **107n**.

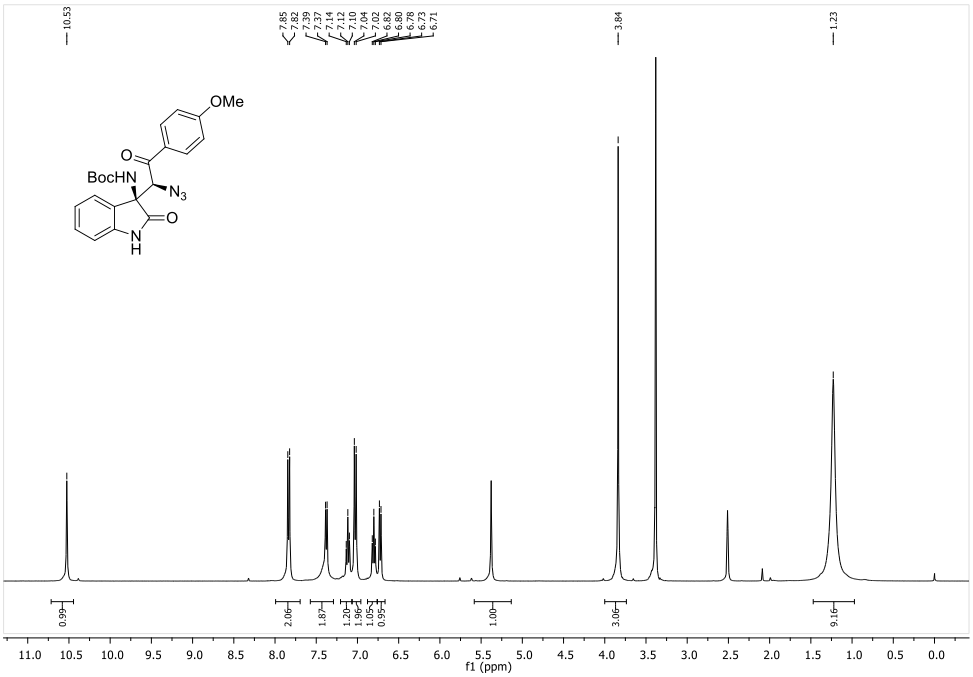

Figure A. 107 ^{1}H NMR spectrum of **107o**.

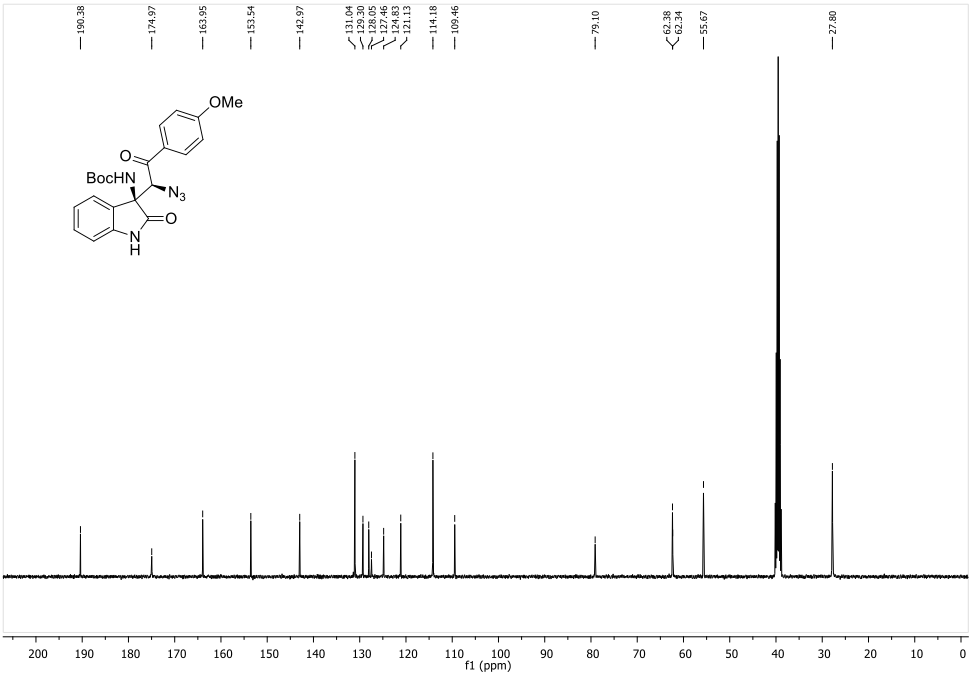

Figure A. 108 ^{13}C NMR spectrum of **107o**.

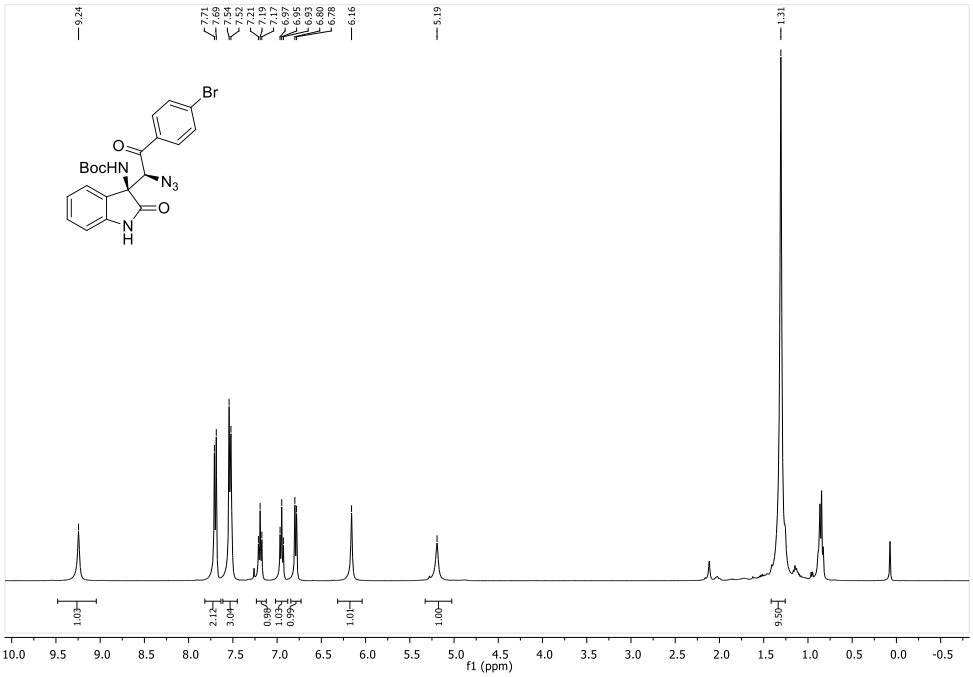

Figure A. 109 ^{1}H NMR spectrum of **107p**.

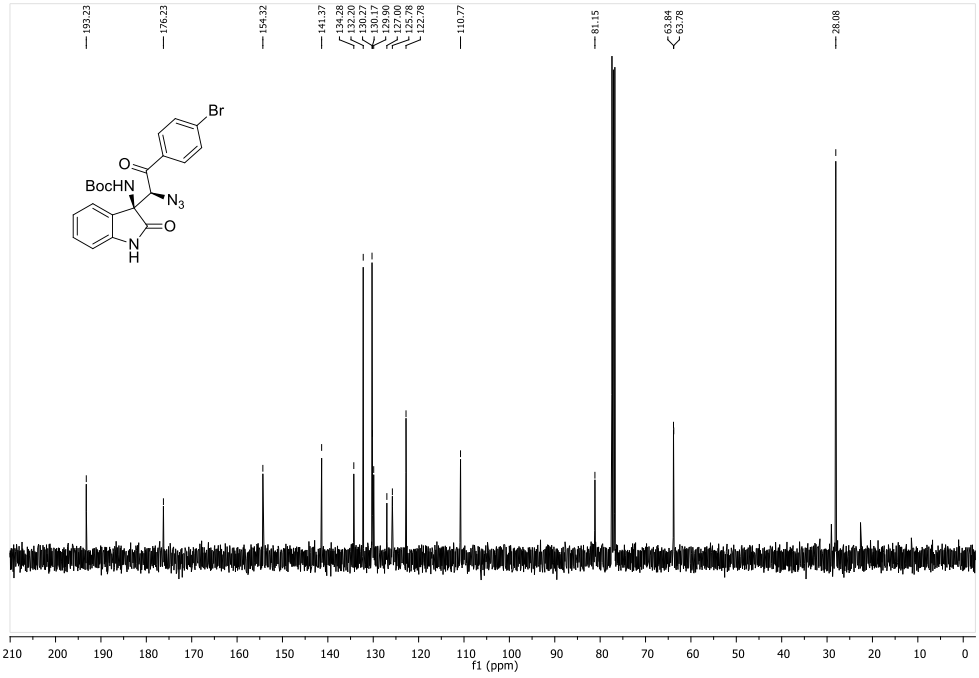

Figure A. 110 ^{13}C NMR spectrum of **107p**.

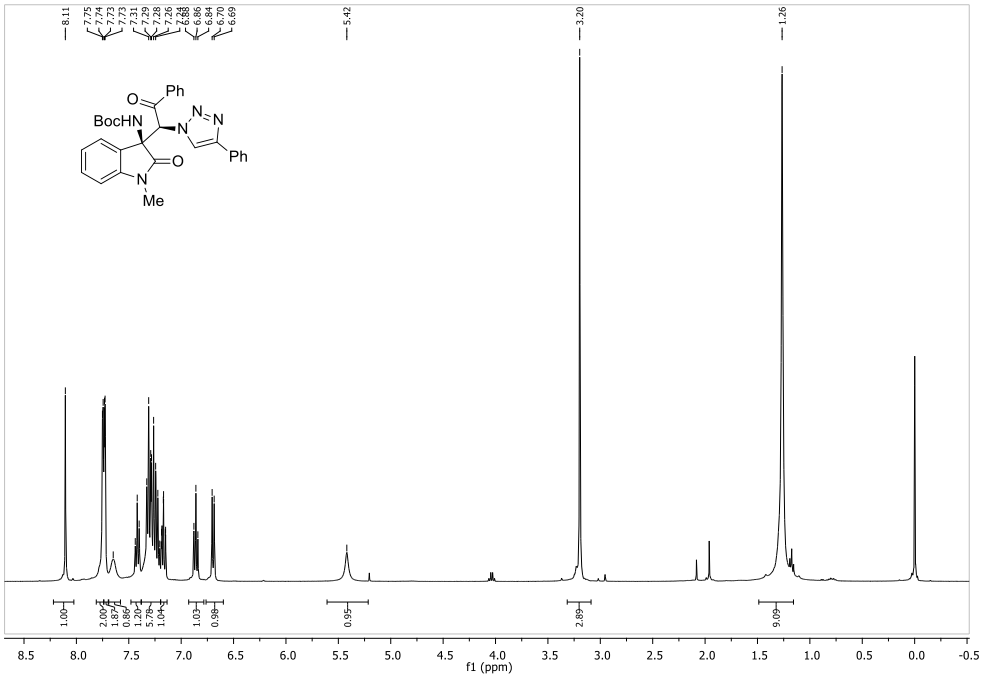

Figure A. 111 ^{1}H NMR spectrum of **109**.

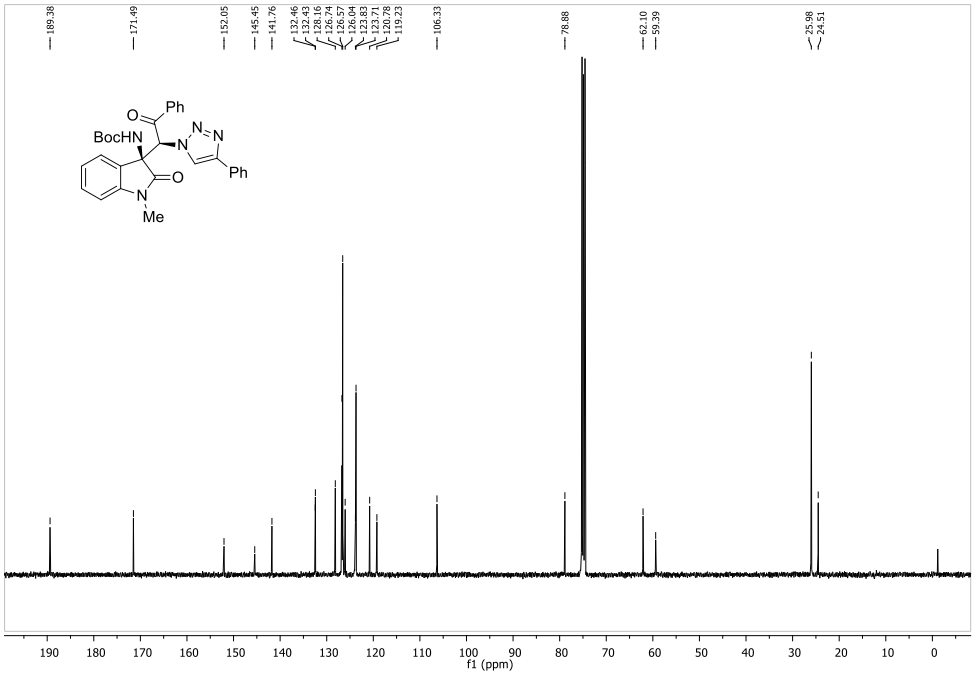

Figure A. 112 ^{13}C NMR spectrum of **109**.

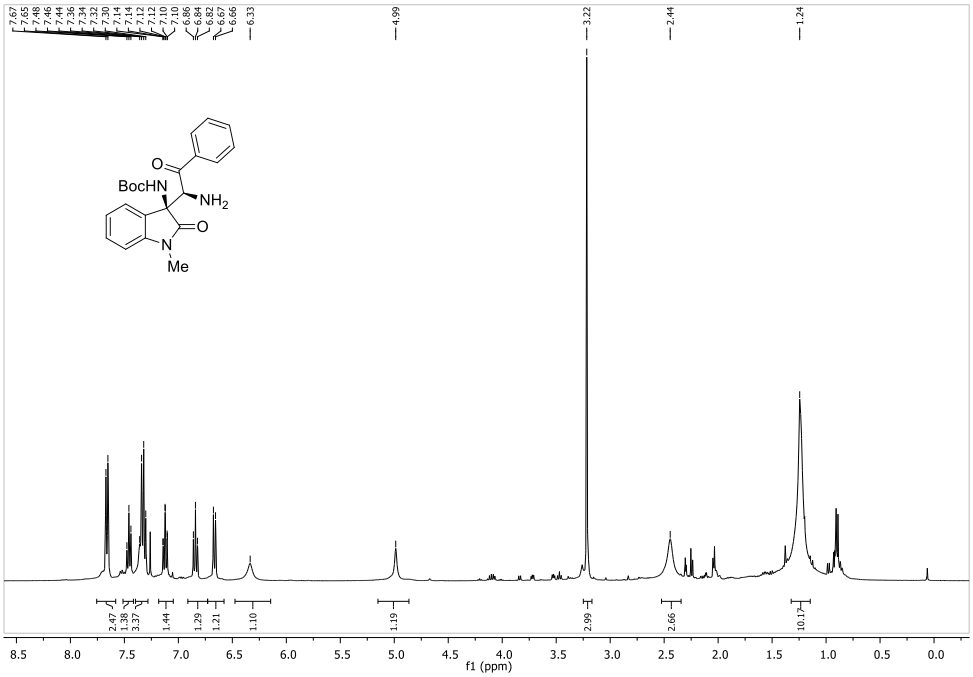

Figure A. 113 ^{1}H NMR spectrum of **111a**.

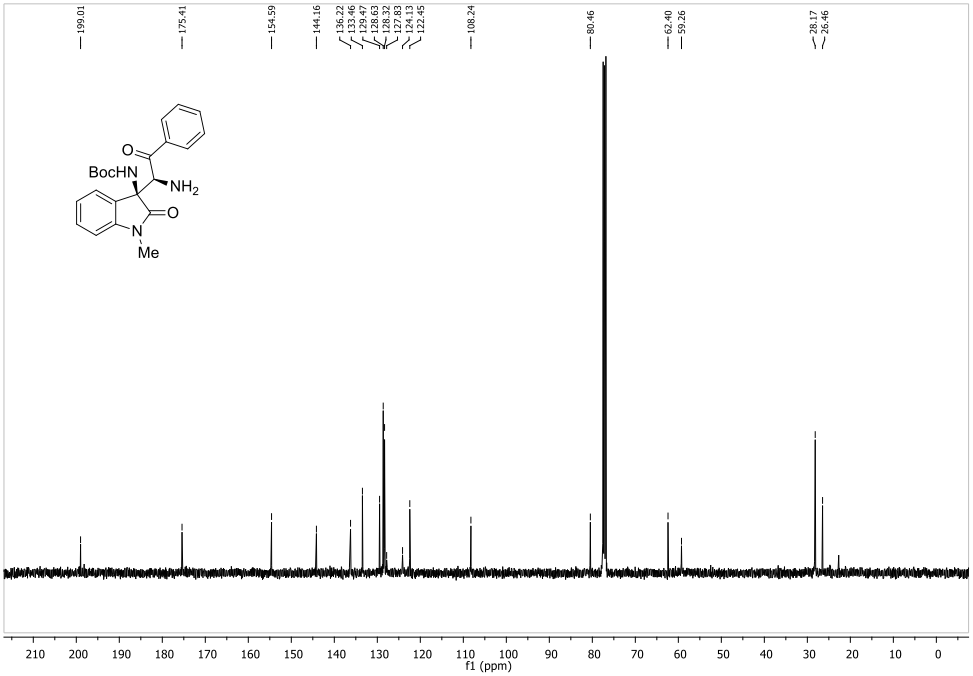

Figure A. 114 ^{13}C NMR spectrum of **111a**.

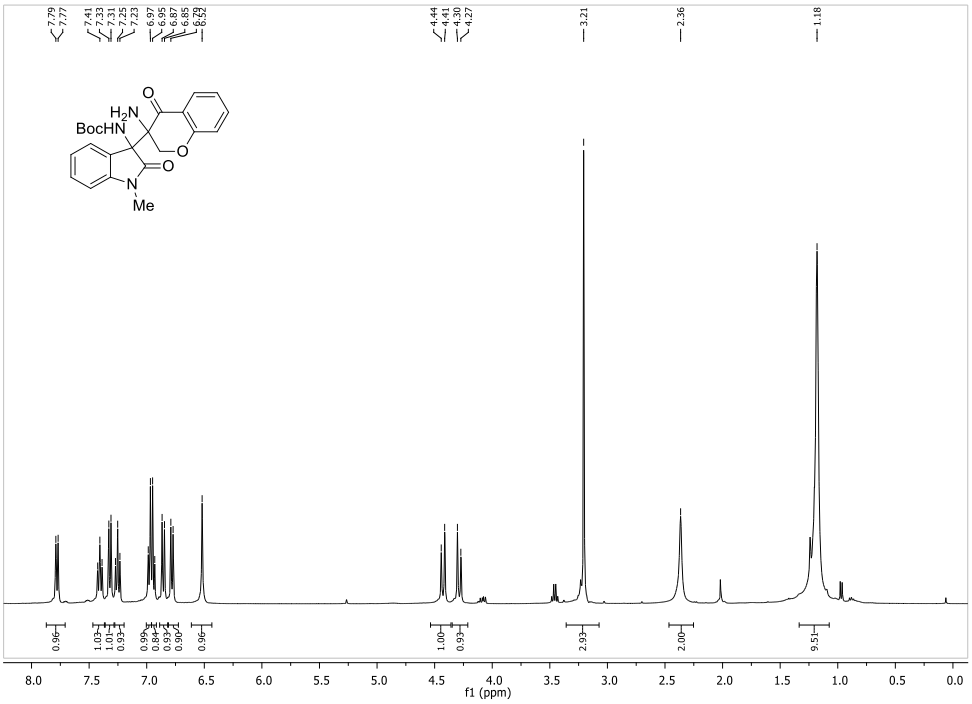

Figure A. 115 ^{1}H NMR spectrum of **111g**.

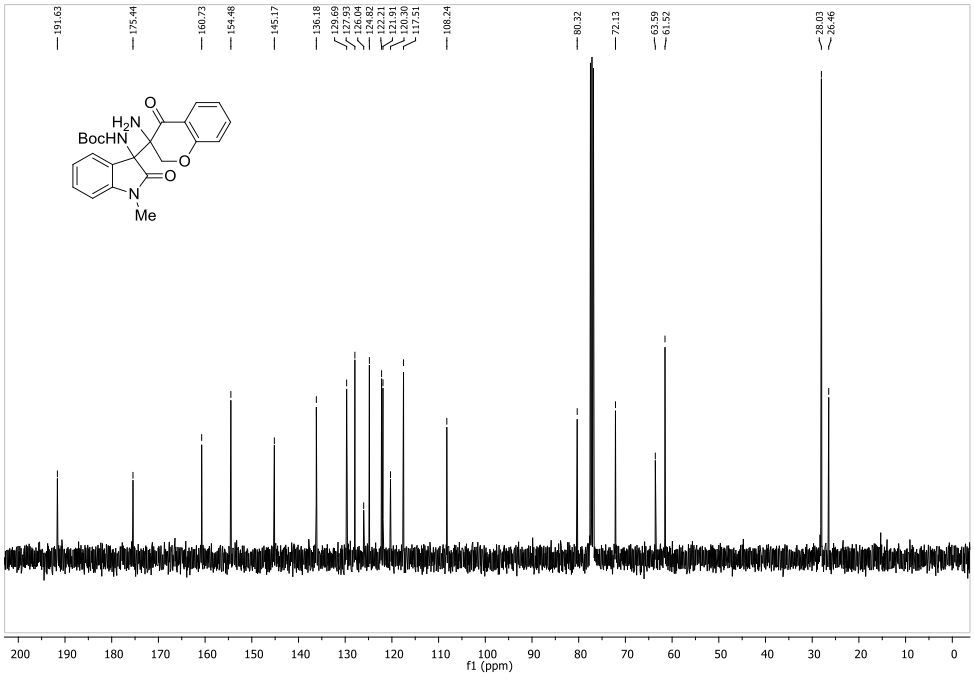

Figure A. 116 ^{13}C NMR spectrum of **111g**.

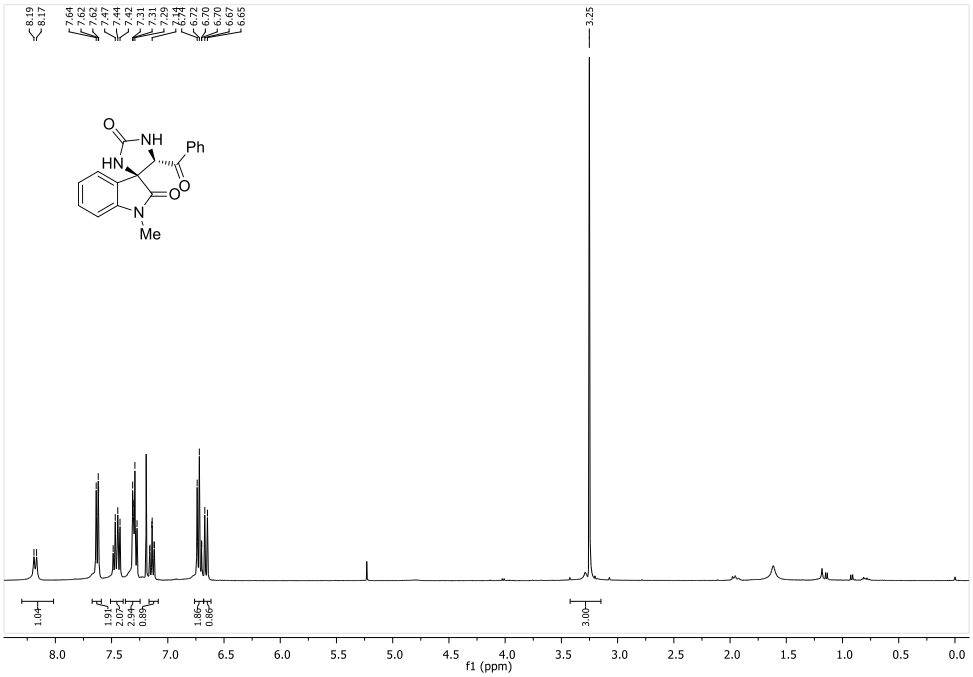

Figure A. 117 ^{1}H NMR spectrum of **112a**.

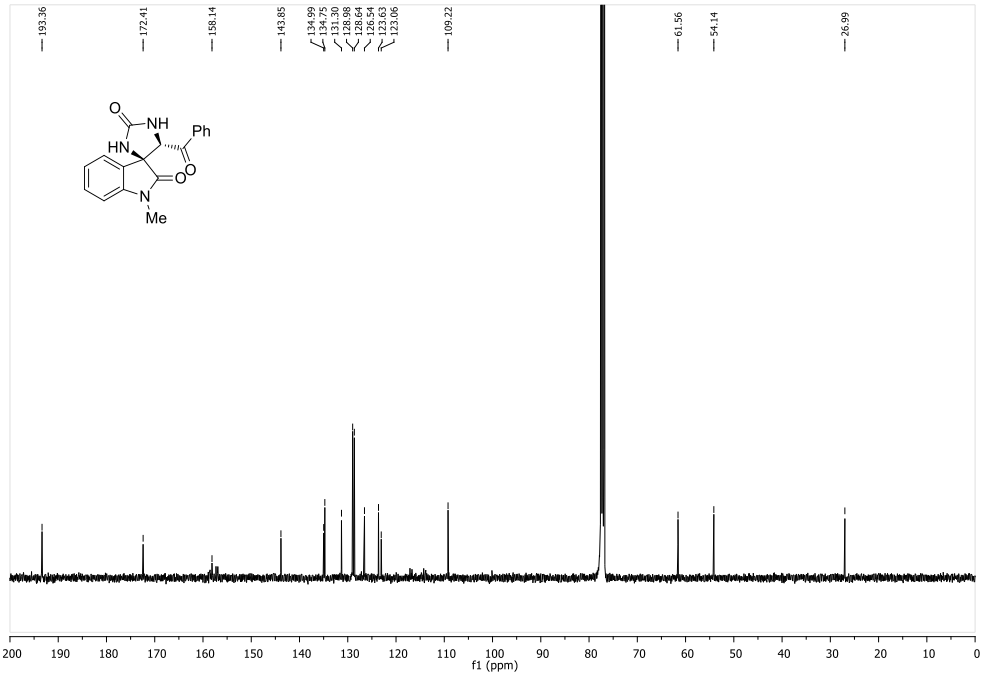

Figure A. 118 ^{13}C NMR spectrum of **112a**.

APPENDIX B

HPLC CHROMATOGRAMS

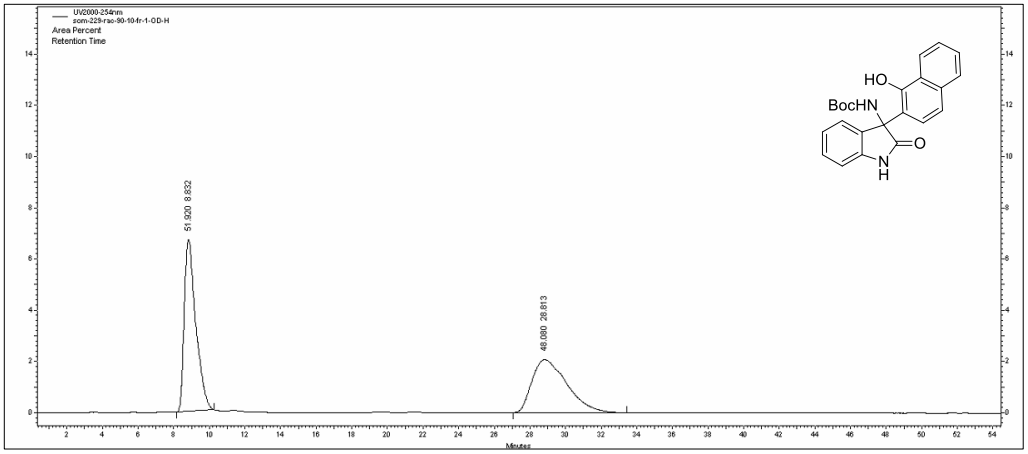

Figure B. 1 HPLC chromatogram of *rac*-**95a**.

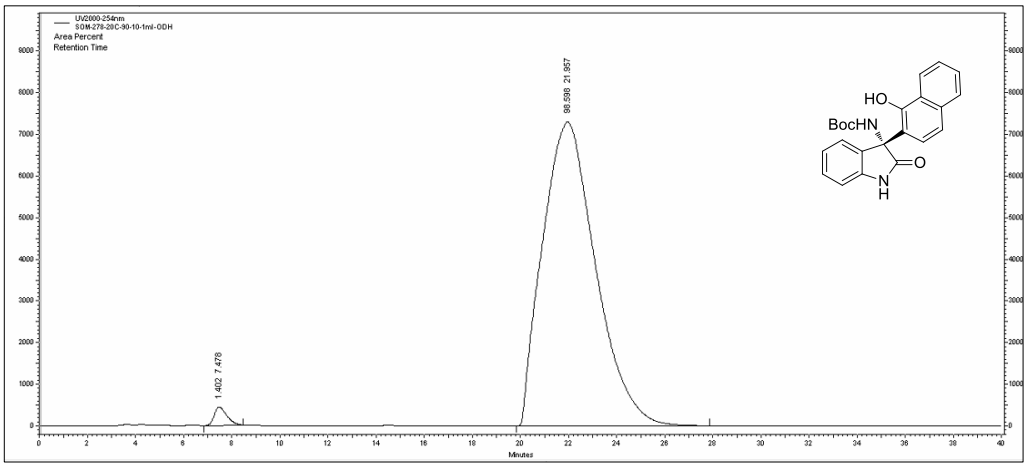

Figure B. 2 HPLC chromatogram of enantiomerically enriched **95a**.

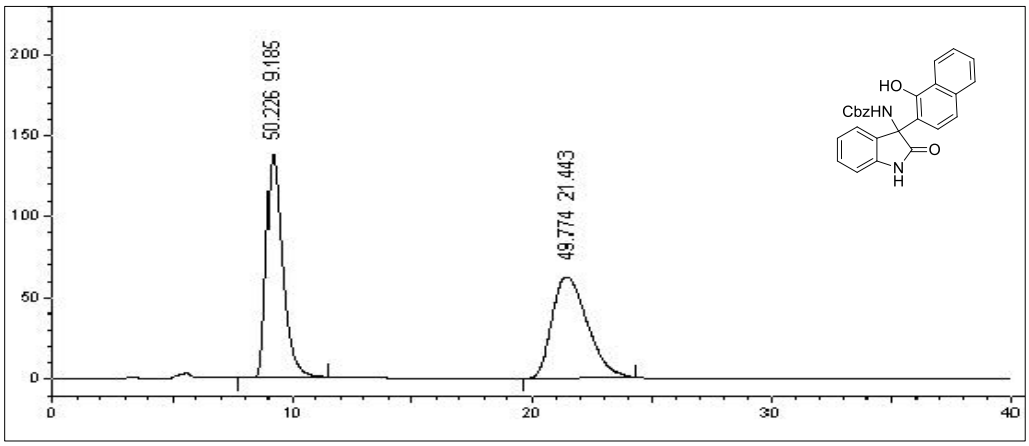

Figure B. 3 HPLC chromatogram of *rac*-**95b**.

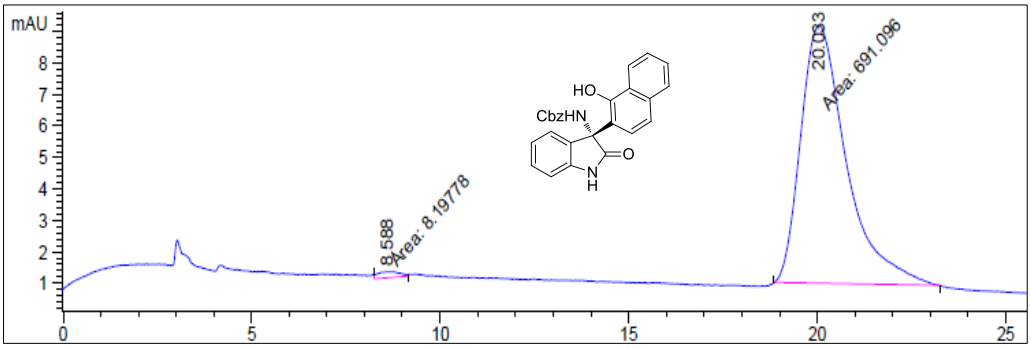

Figure B. 4 HPLC chromatogram of enantiomerically enriched **95b**.

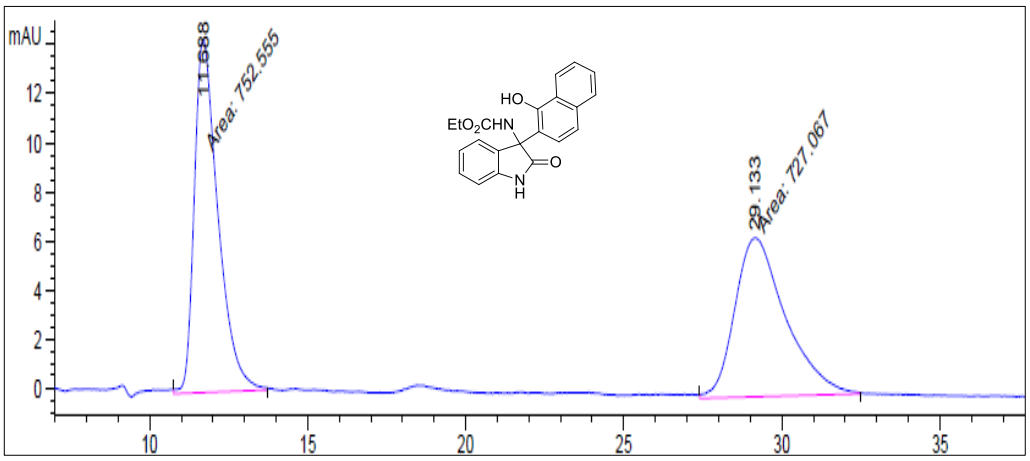

Figure B. 5 HPLC chromatogram of *rac*-**95c**.

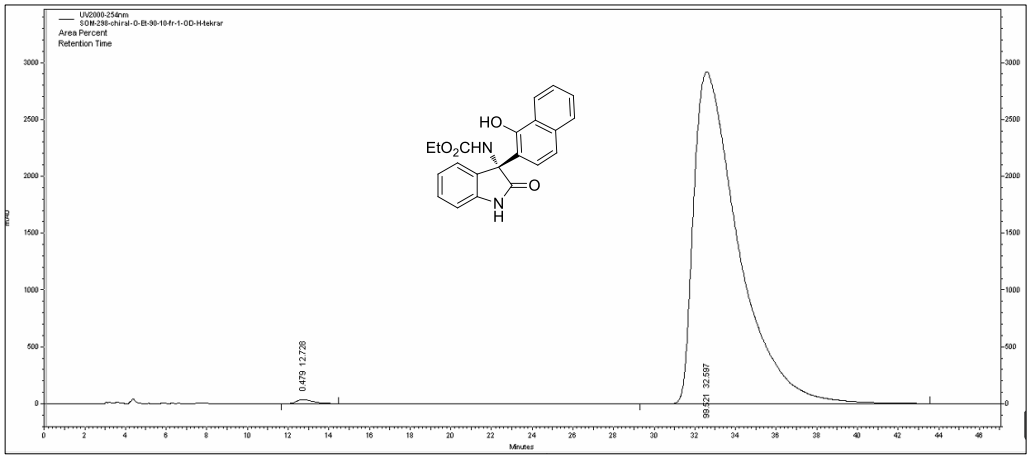

Figure B. 6 HPLC chromatogram of enantiomerically enriched **95c**.

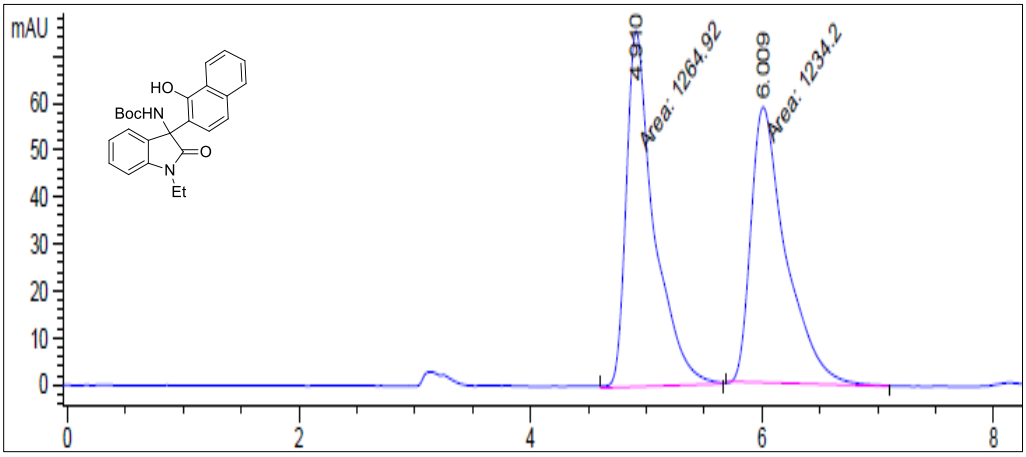

Figure B. 7 HPLC chromatogram of *rac*-**95d**.

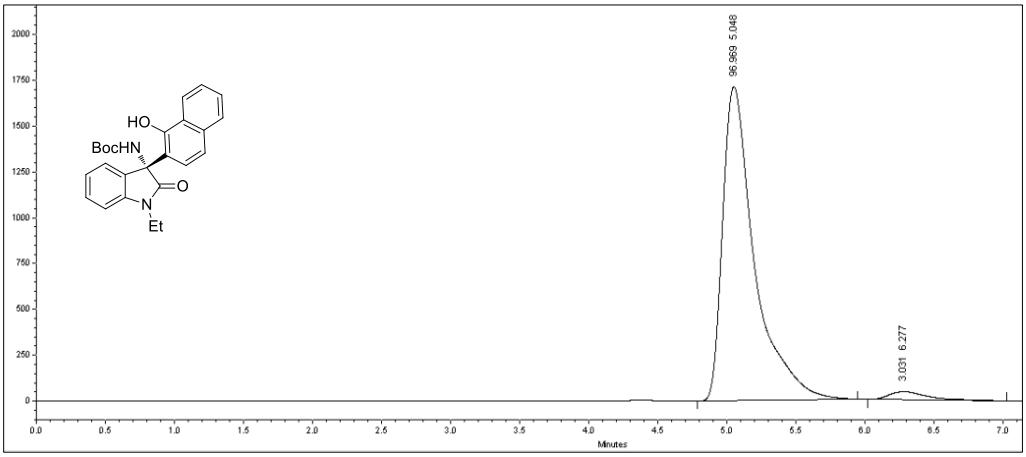

Figure B. 8 HPLC chromatogram of enantiomerically enriched **95d**.

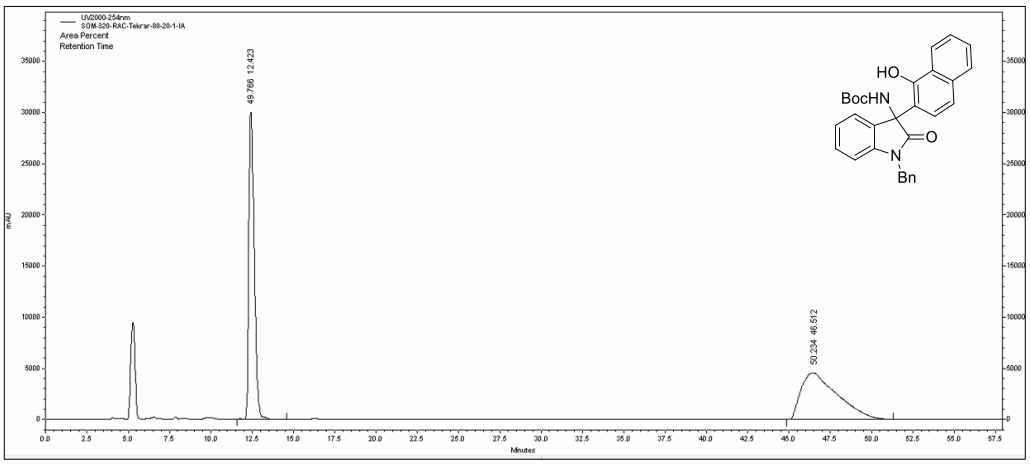

Figure B. 9 HPLC chromatogram of *rac*-**95e**.

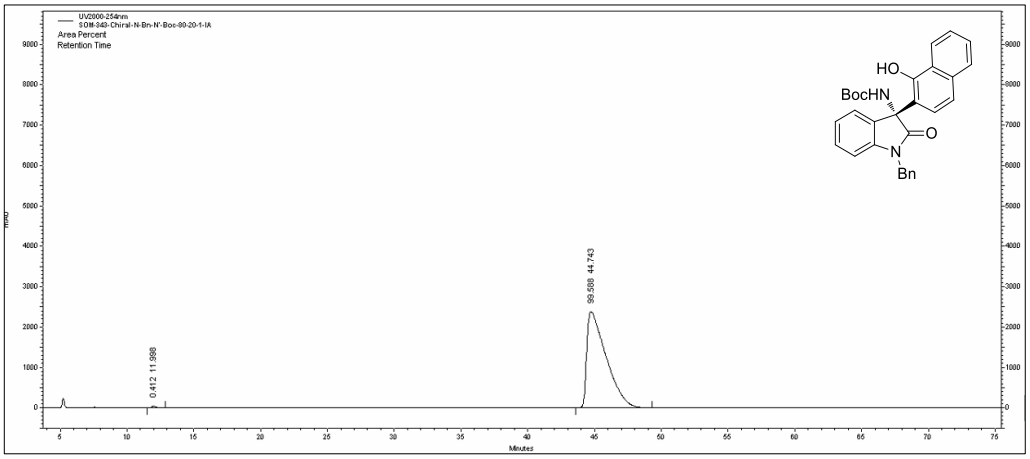

Figure B. 10 HPLC chromatogram of enantiomerically enriched **95e**.

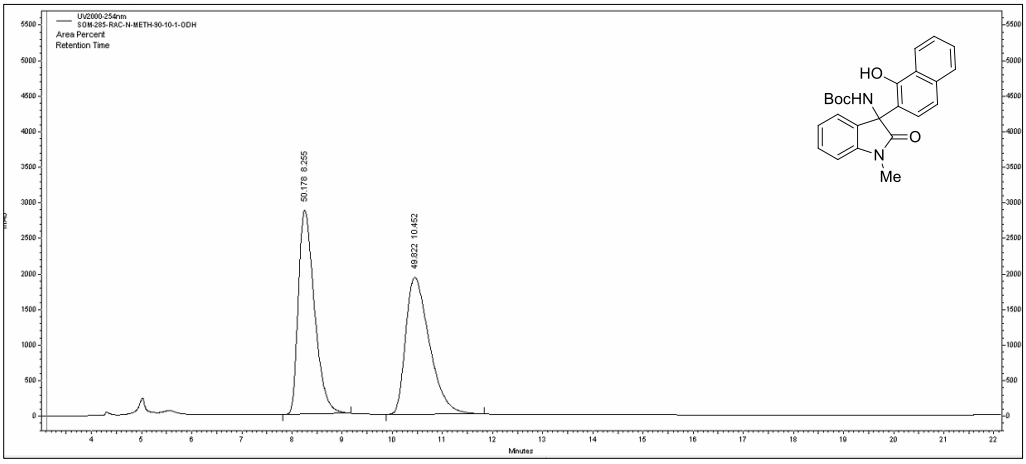

Figure B. 11 HPLC chromatogram of *rac*-**95f**.

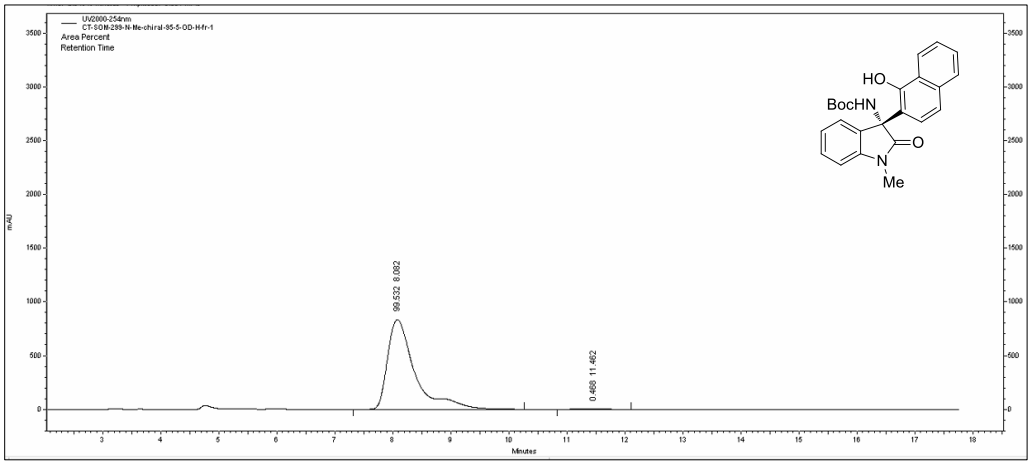

Figure B. 12 HPLC chromatogram of enantiomerically enriched **95f**.

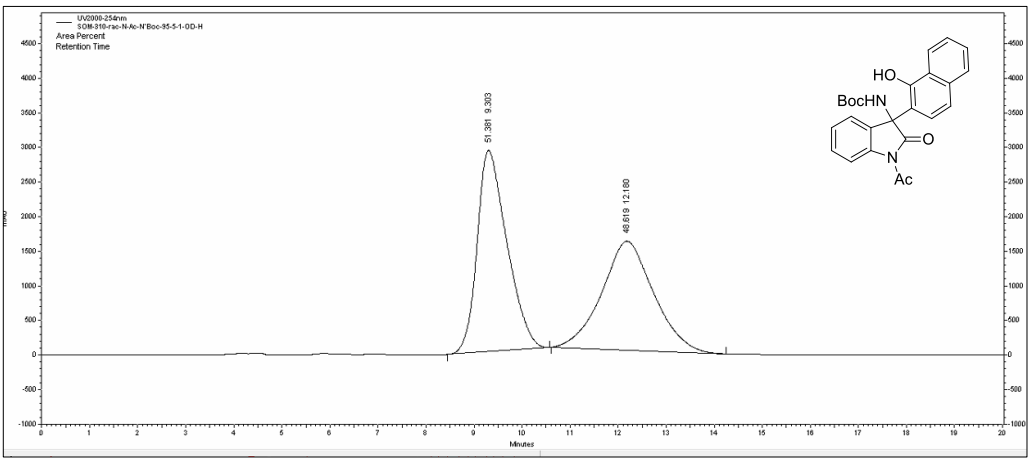

Figure B. 13 HPLC chromatogram of *rac*-**95g**.

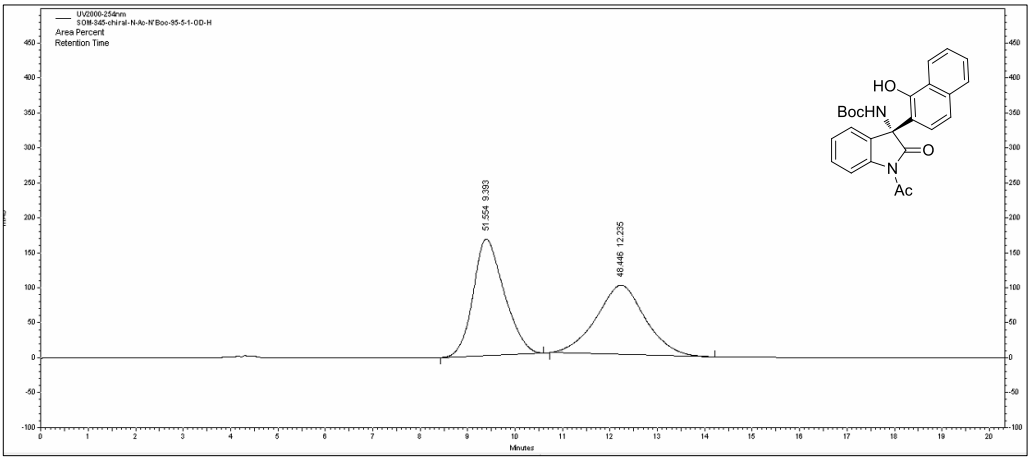

Figure B. 14 HPLC chromatogram of enantiomerically enriched **95g**.

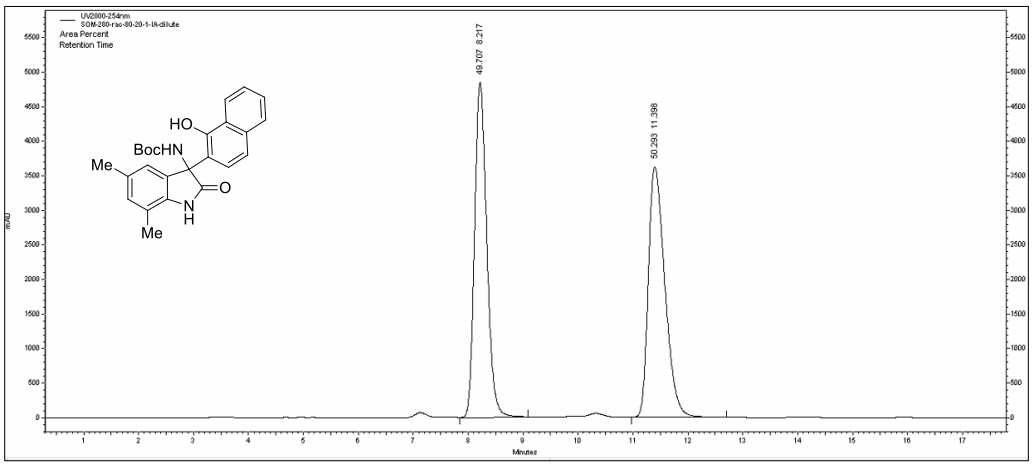

Figure B. 15 HPLC chromatogram of *rac*-**95h**.

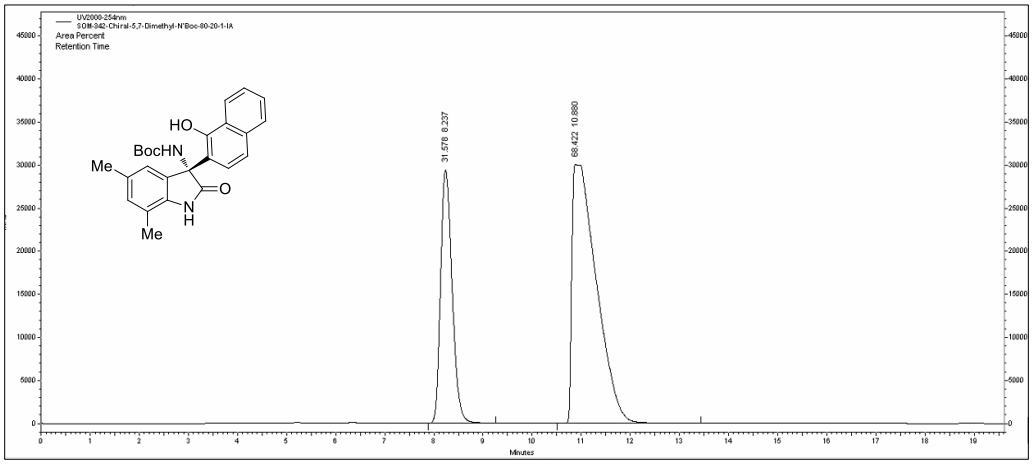

Figure B. 16 HPLC chromatogram of enantiomerically enriched **95h**.

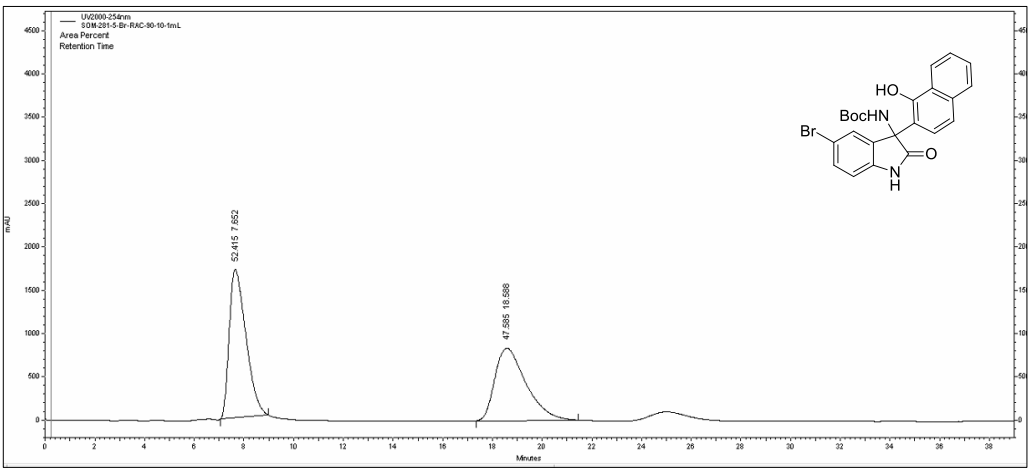

Figure B. 17 HPLC chromatogram of *rac*-**95i**.

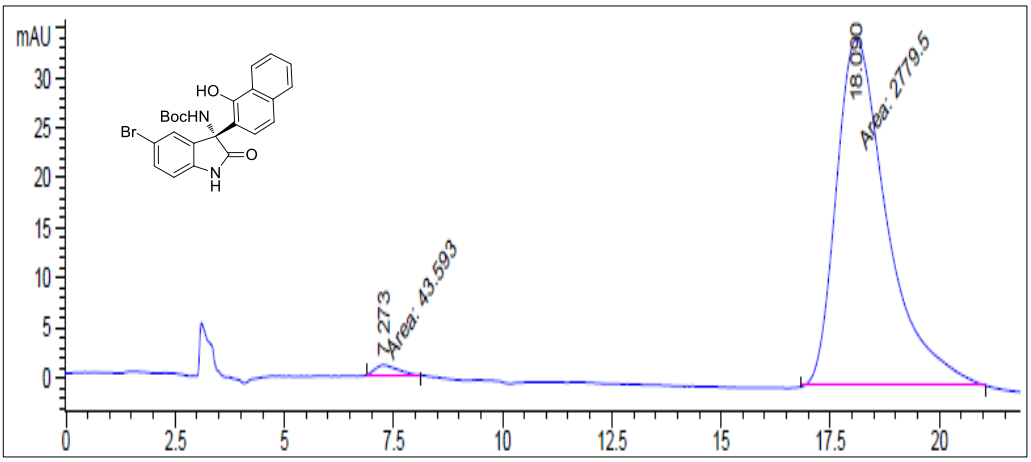

Figure B. 18 HPLC chromatogram of enantiomerically enriched **95i**.

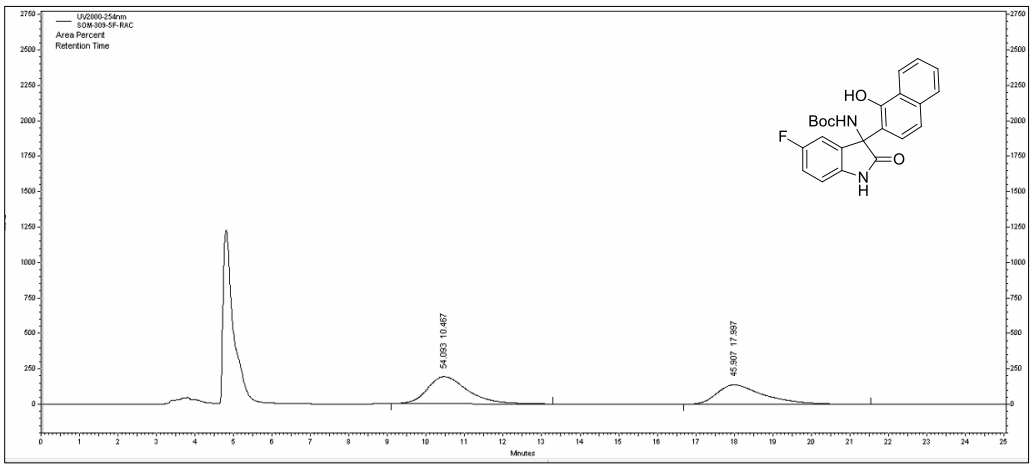

Figure B. 19 HPLC chromatogram of *rac*-**95j**.

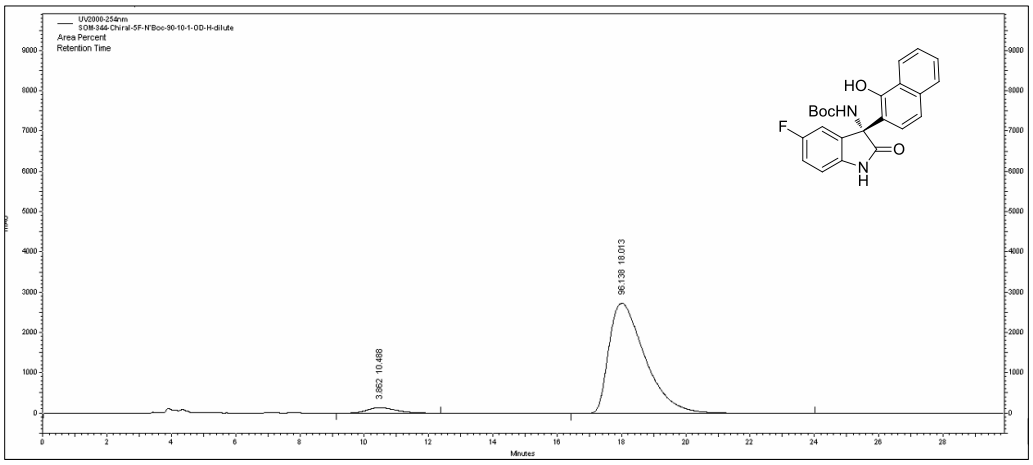

Figure B. 20 HPLC chromatogram of enantiomerically enriched **95j**.

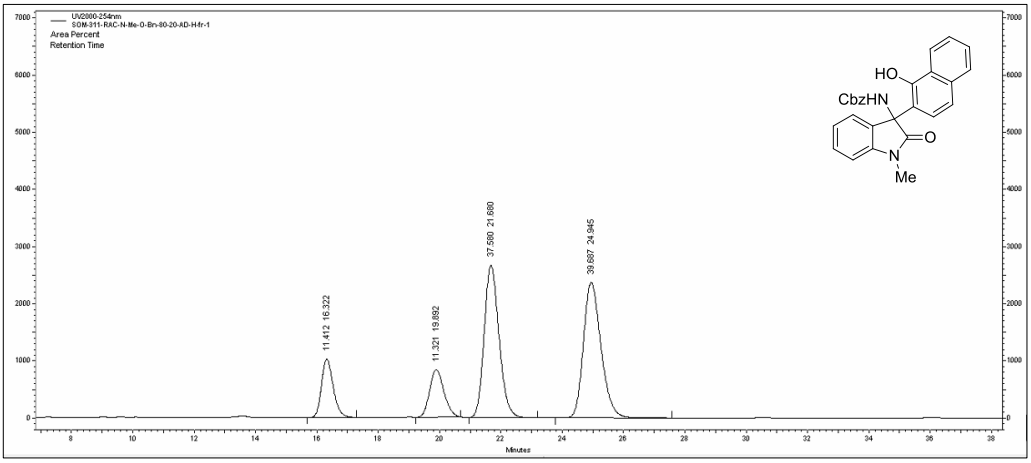

Figure B. 21 HPLC chromatogram of *rac*-**95k**.

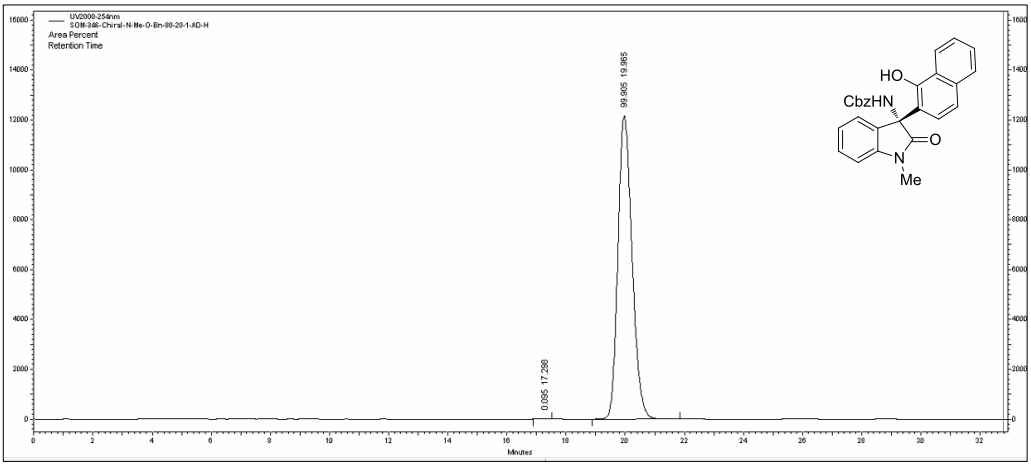

Figure B. 22 HPLC chromatogram of enantiomerically enriched **95k**.

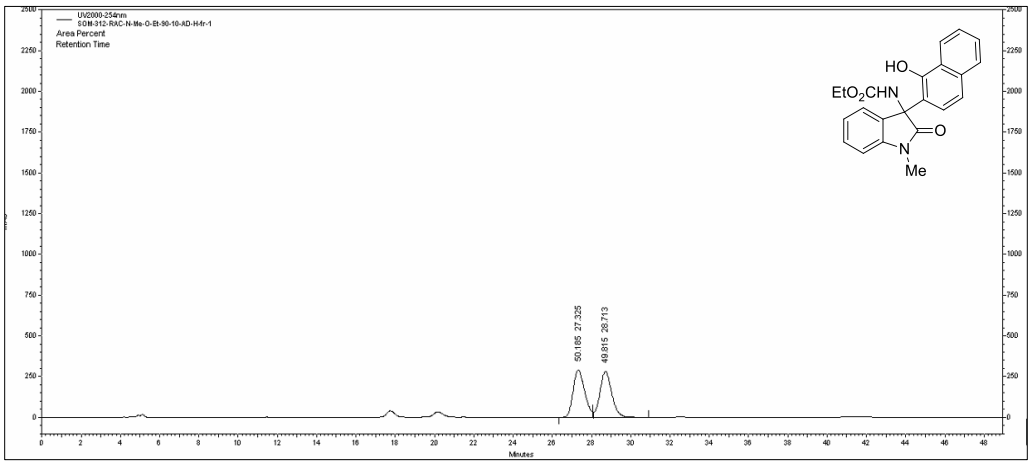

Figure B. 23 HPLC chromatogram of *rac*-**95l**.

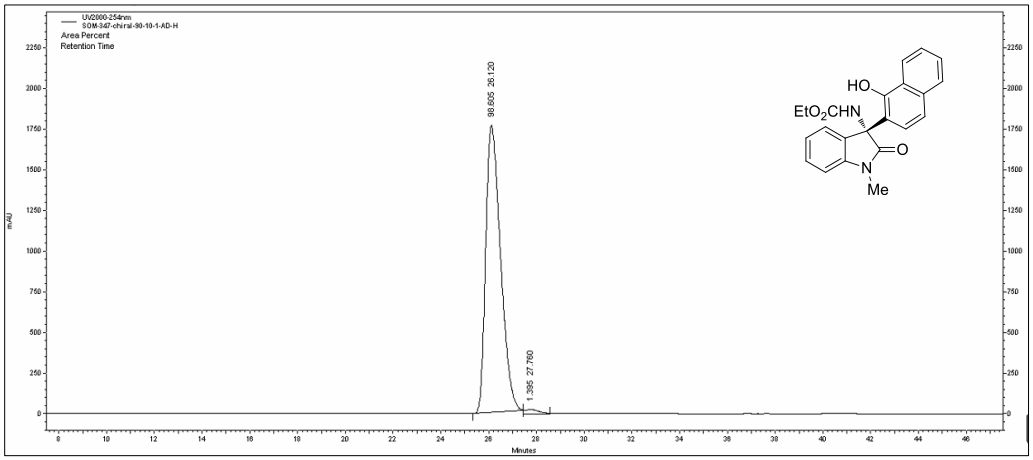

Figure B. 24 HPLC chromatogram of enantiomerically enriched **95l**.

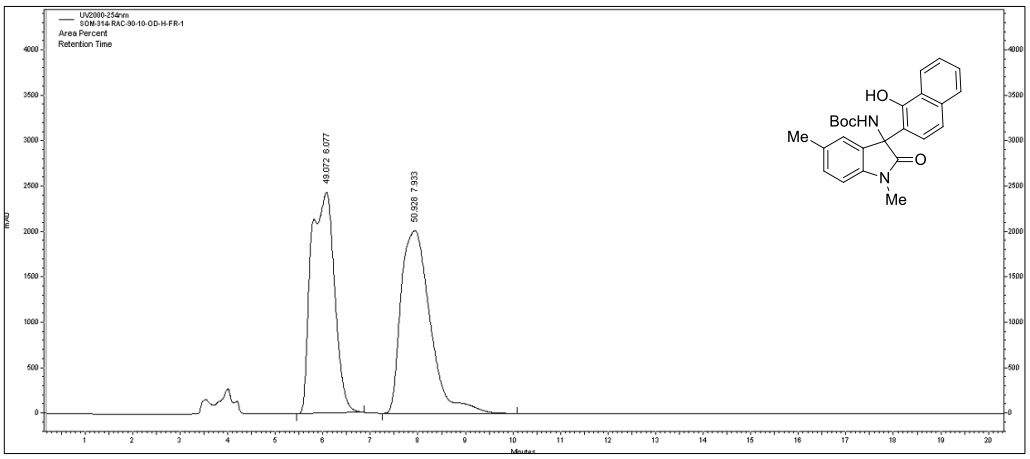

Figure B. 25 HPLC chromatogram of *rac*-**95m**.

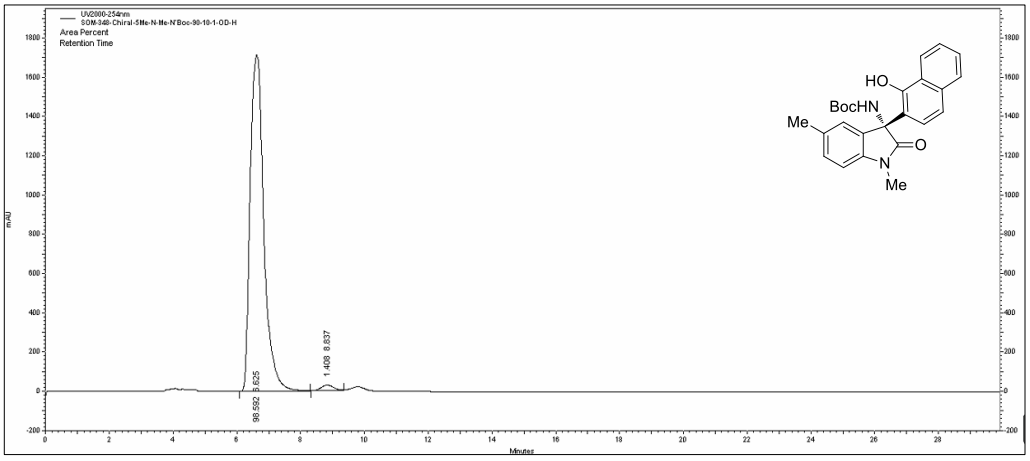

Figure B. 26 HPLC chromatogram of enantiomerically enriched **95m**.

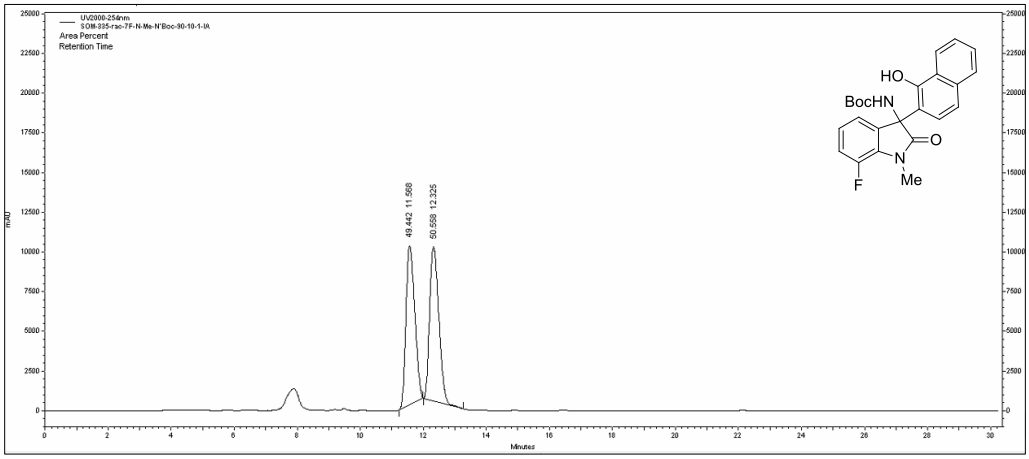

Figure B. 27 HPLC chromatogram of *rac*-**95n**.

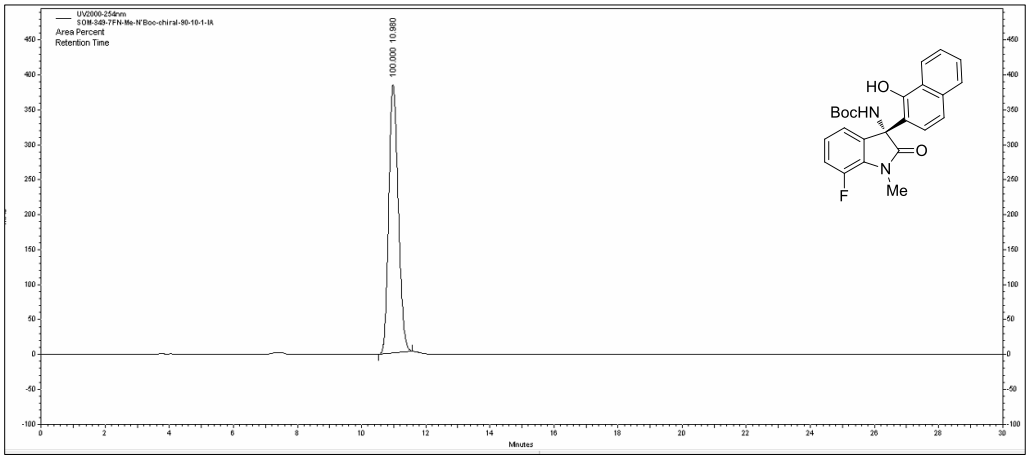

Figure B. 28 HPLC chromatogram of enantiomerically enriched **95n**.

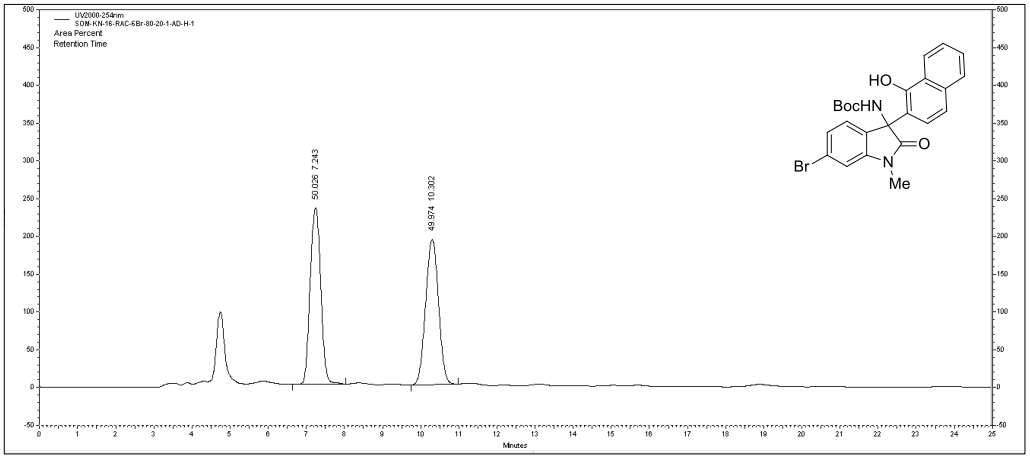

Figure B. 29 HPLC chromatogram of *rac*-**95o**.

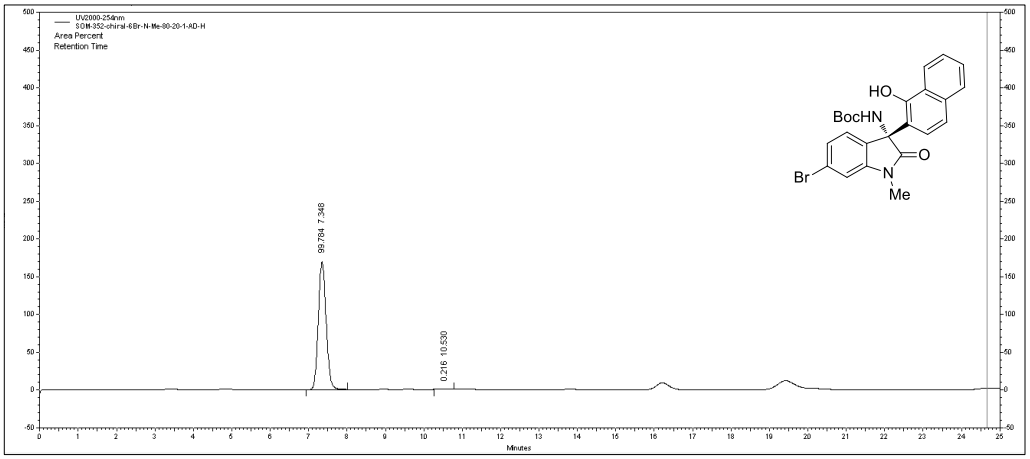

Figure B. 30 HPLC chromatogram of enantiomerically enriched **95o**.

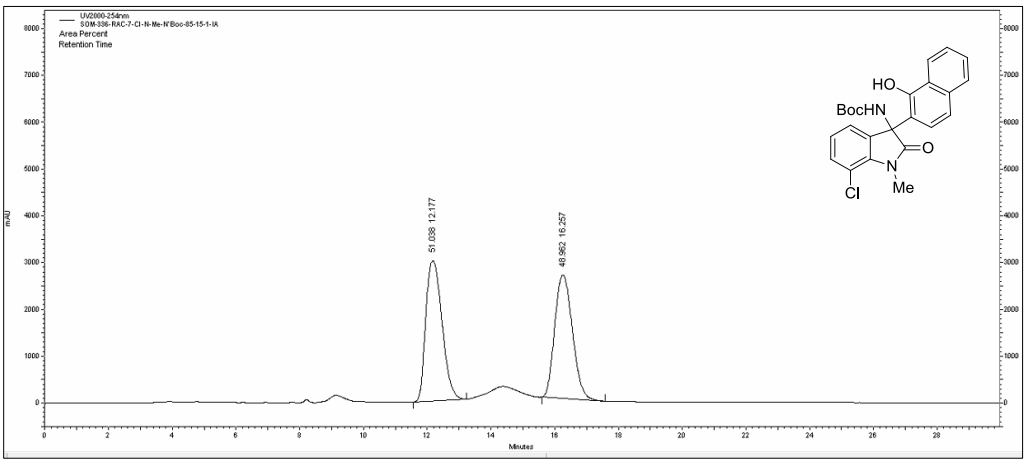

Figure B. 31 HPLC chromatogram of *rac*-**95p**.

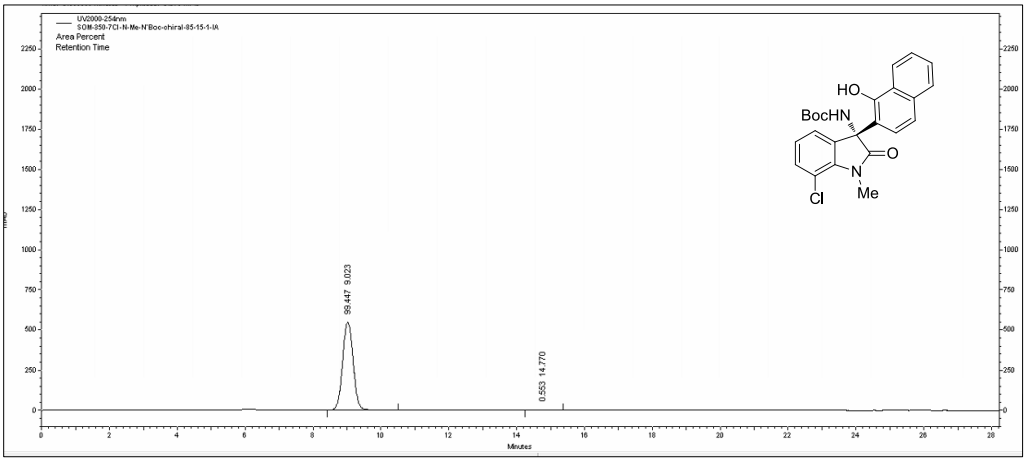

Figure B. 32 HPLC chromatogram of enantiomerically enriched **95p**.

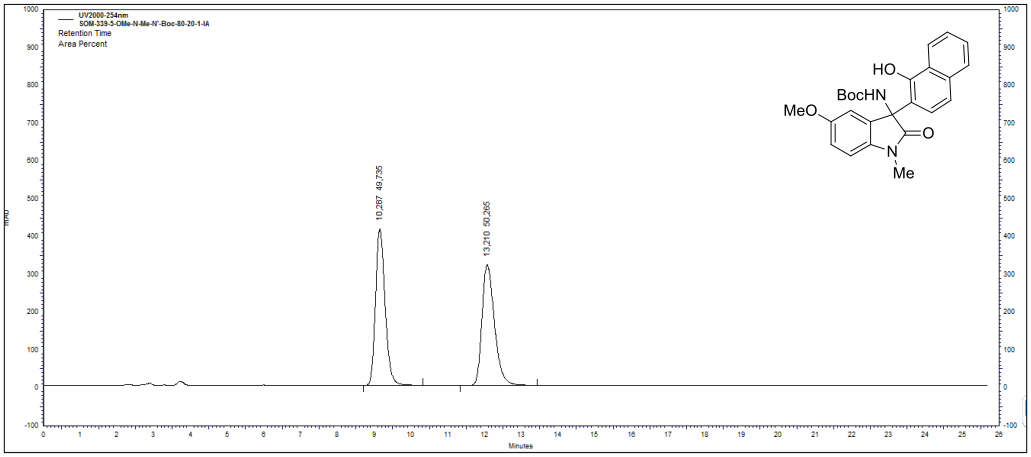

Figure B. 33 HPLC chromatogram of *rac*-**95q**.

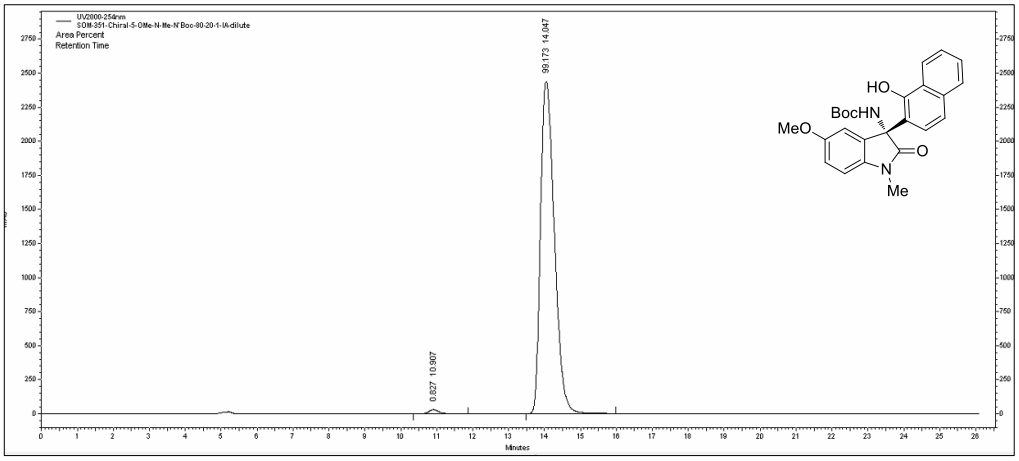

Figure B. 34 HPLC chromatogram of enantiomerically enriched **95q**.

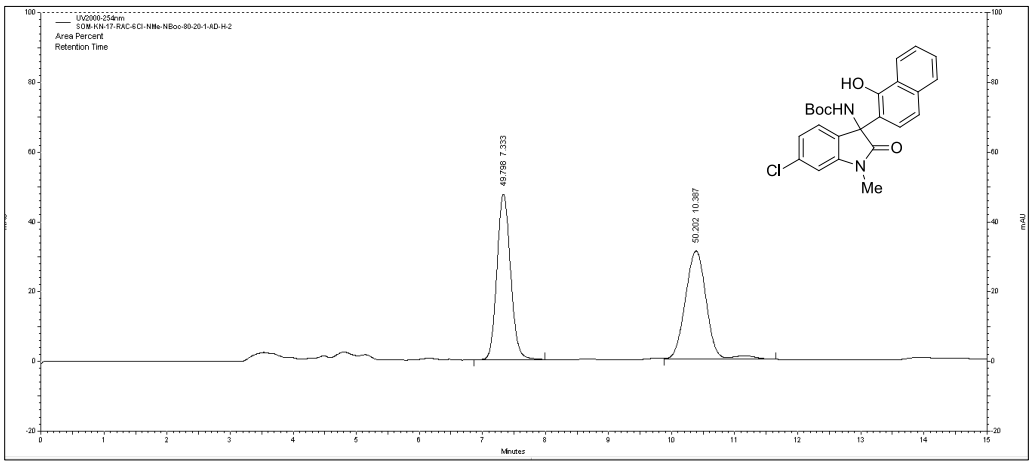

Figure B. 35 HPLC chromatogram of *rac*-**95r**.

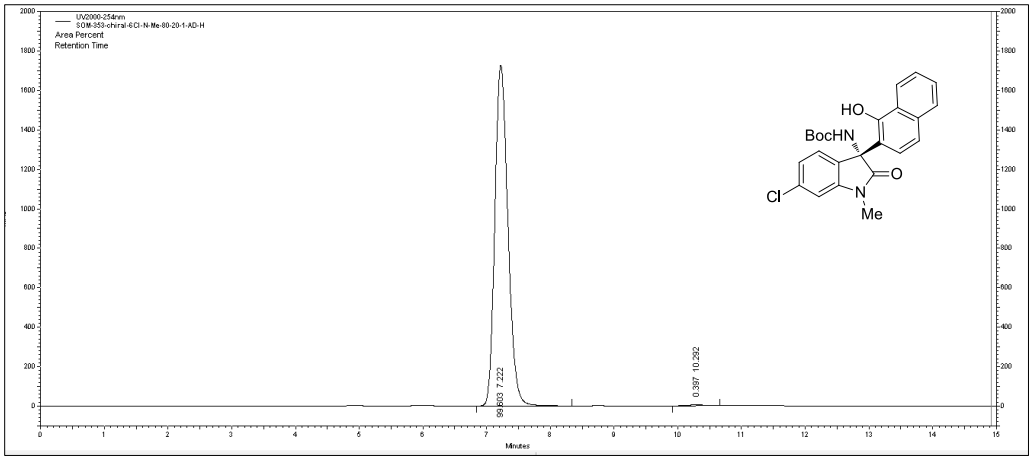

Figure B. 36 HPLC chromatogram of enantiomerically enriched **95r**.

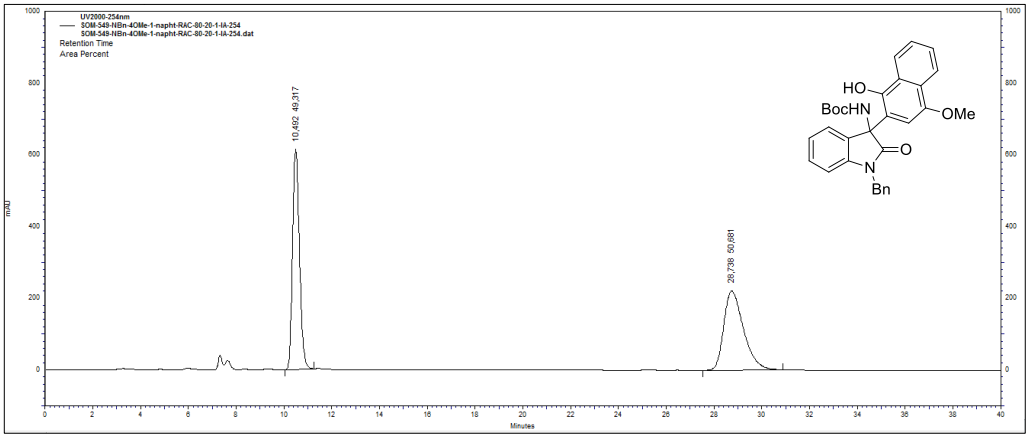

Figure B. 37 HPLC chromatogram of *rac*-**95s**.

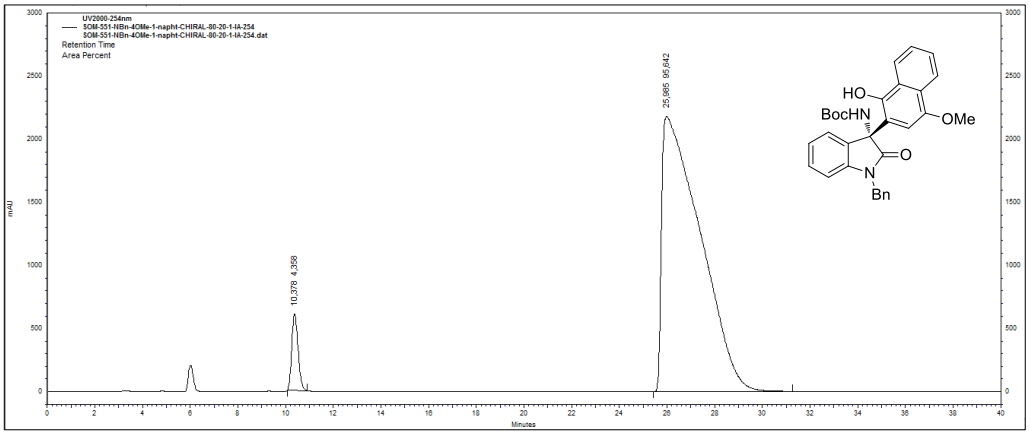

Figure B. 38 HPLC chromatogram of enantiomerically enriched **95s**.

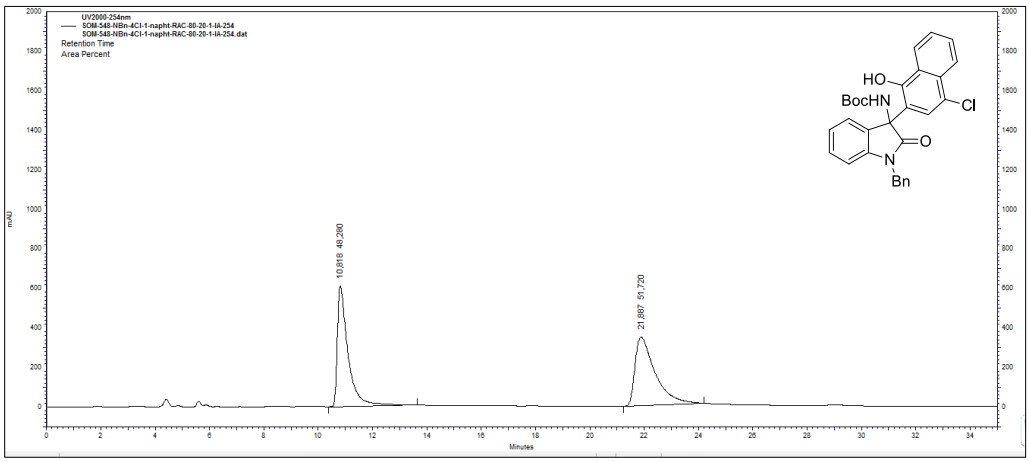

Figure B. 39 HPLC chromatogram of *rac*-**95t**.

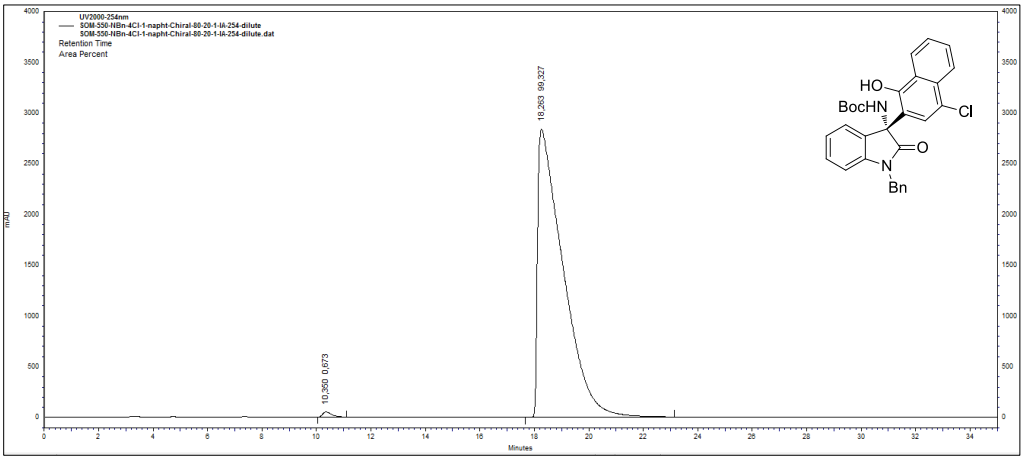

Figure B. 40 HPLC chromatogram of enantiomerically enriched **95t**.

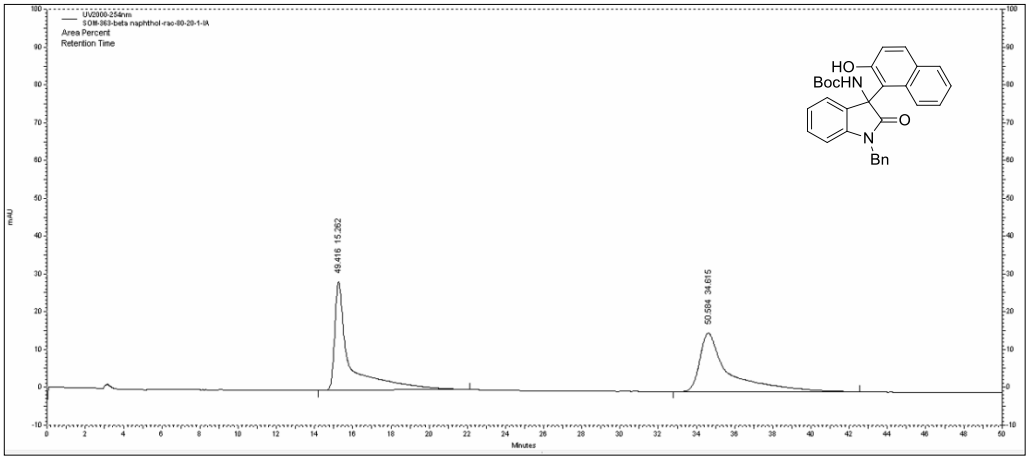

Figure B. 41 HPLC chromatogram of *rac*-**96a**.

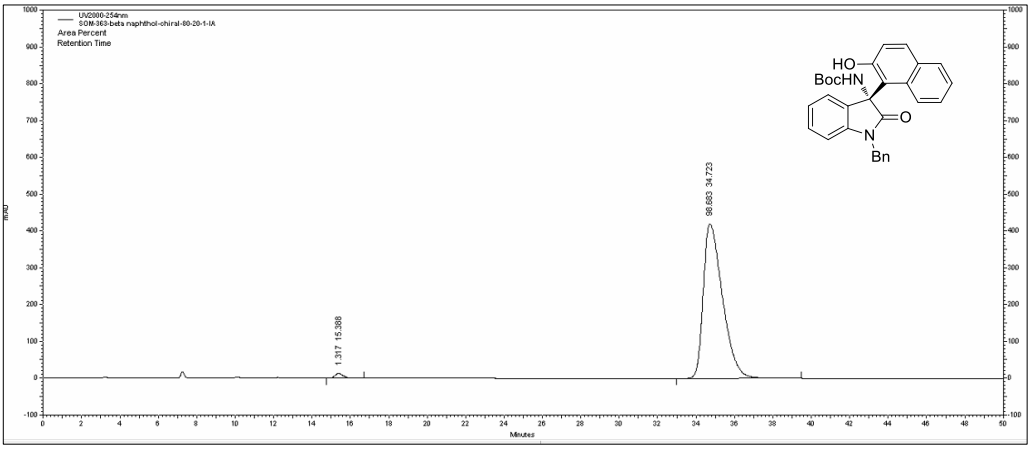

Figure B. 42 HPLC chromatogram of enantiomerically enriched **96a**.

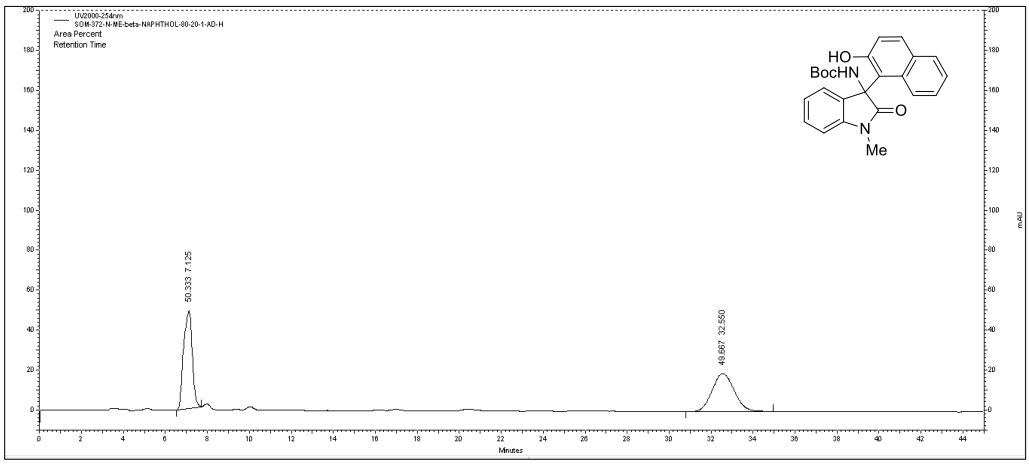

Figure B. 43 HPLC chromatogram of *rac*-**96b**.

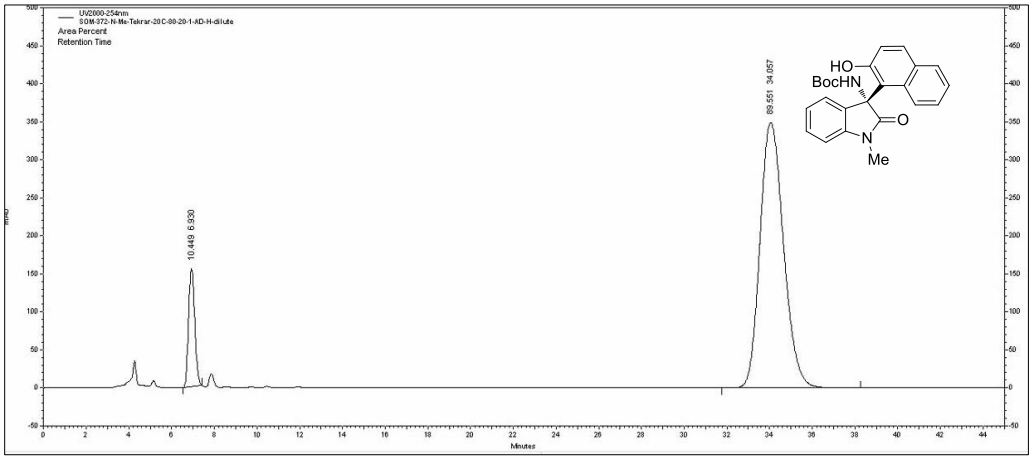

Figure B. 44 HPLC chromatogram of enantiomerically enriched **96b**.

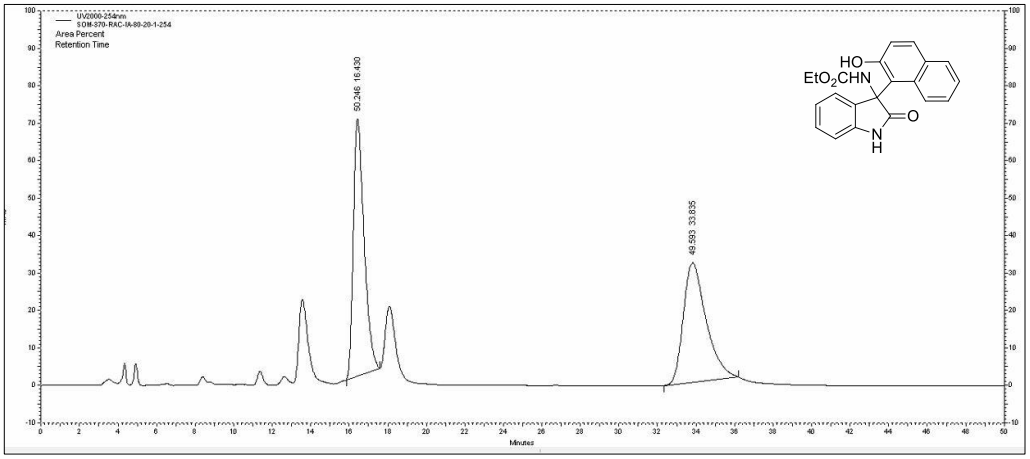

Figure B. 45 HPLC chromatogram of *rac*-**96c**.

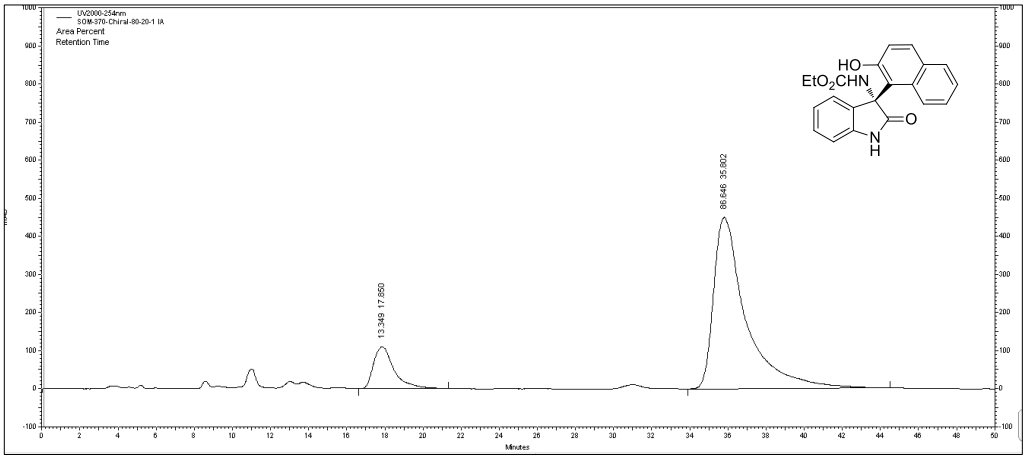

Figure B. 46 HPLC chromatogram of enantiomerically enriched **96c**.

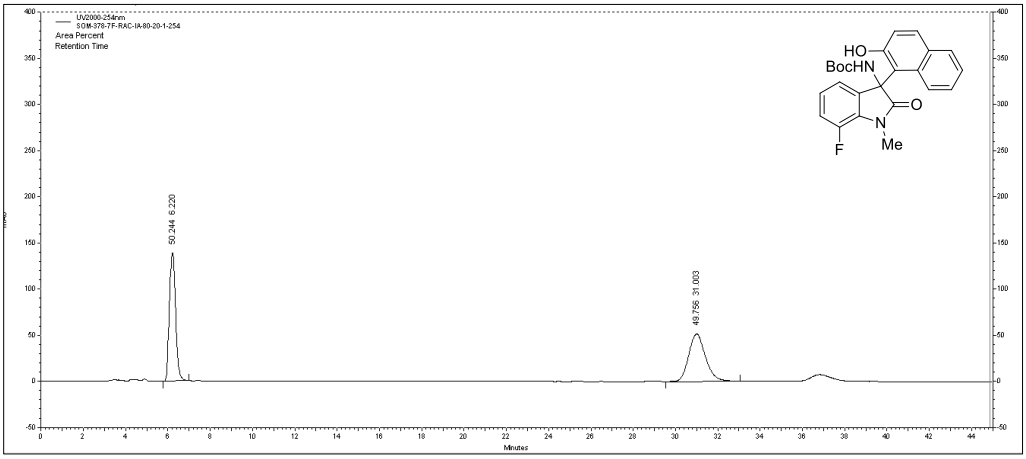

Figure B. 47 HPLC chromatogram of *rac*-**96d**.

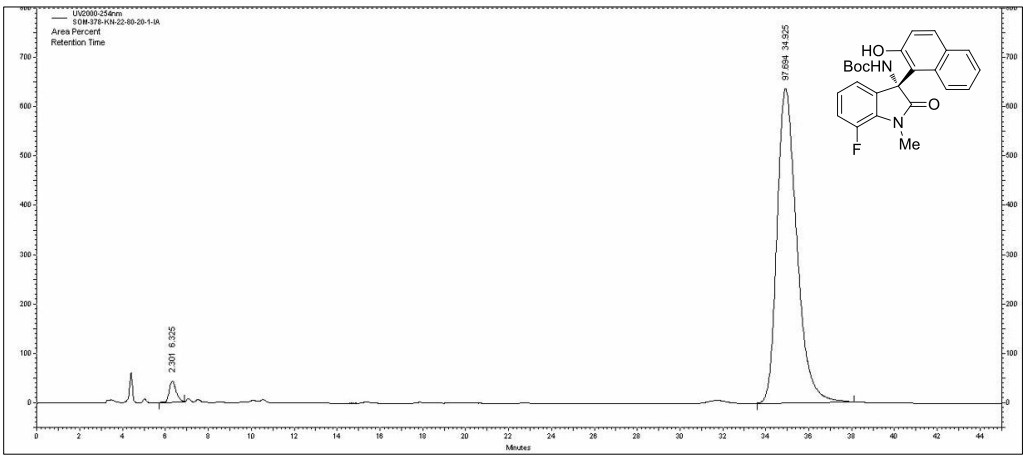

Figure B. 48 HPLC chromatogram of enantiomerically enriched **96d**.

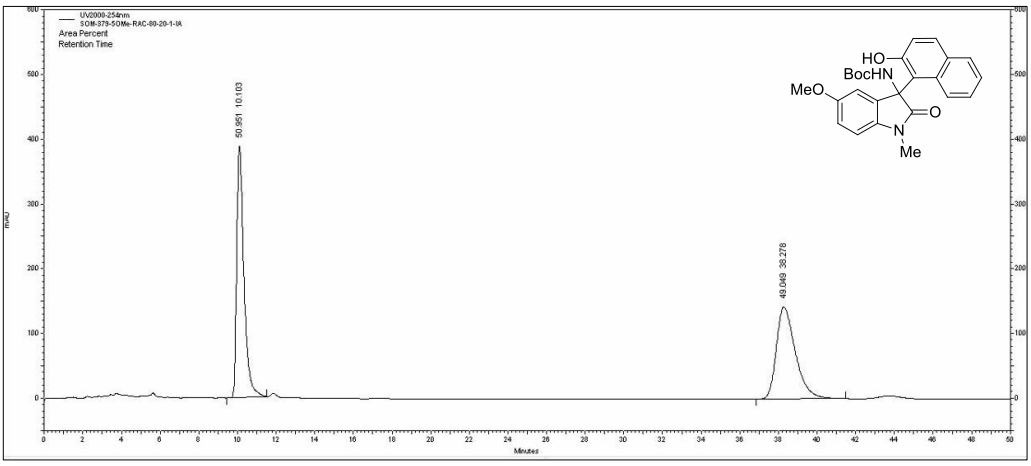

Figure B. 49 HPLC chromatogram of *rac*-**96e**.

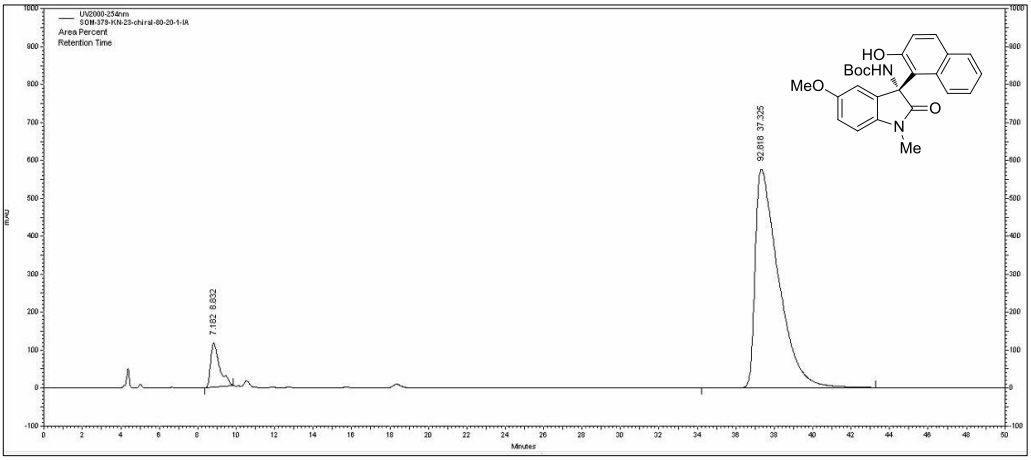

Figure B. 50 HPLC chromatogram of enantiomerically enriched **96e**.

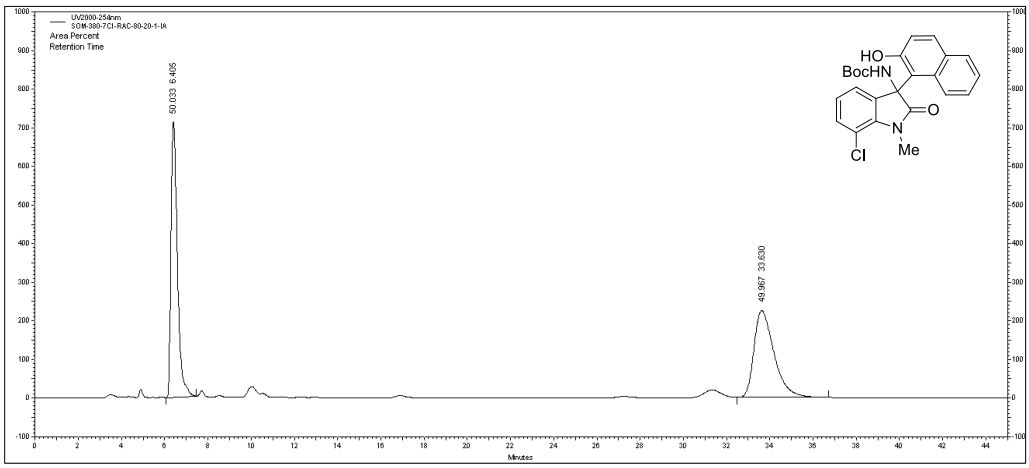

Figure B. 51 HPLC chromatogram of *rac*-**96f**.

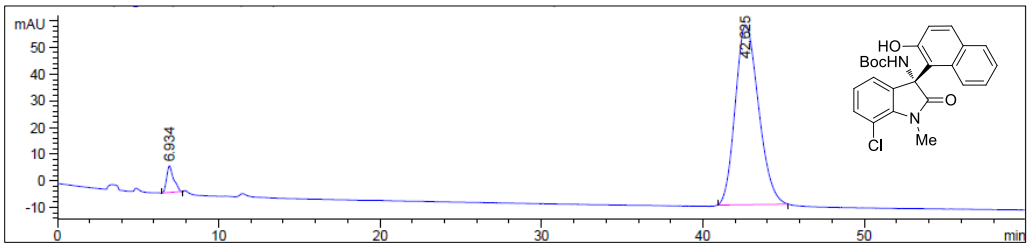

Peak #	RetTime [min]	Type	Width [min]	Area [mAU*s]	Height [mAU]	Area %
1	6.934	BB	0.4371	299.28067	10.00080	4.2268
2	42.625	BB	1.2737	6781.29834	67.52231	95.7732

Figure B. 52 HPLC chromatogram of enantiomerically enriched **96f**.

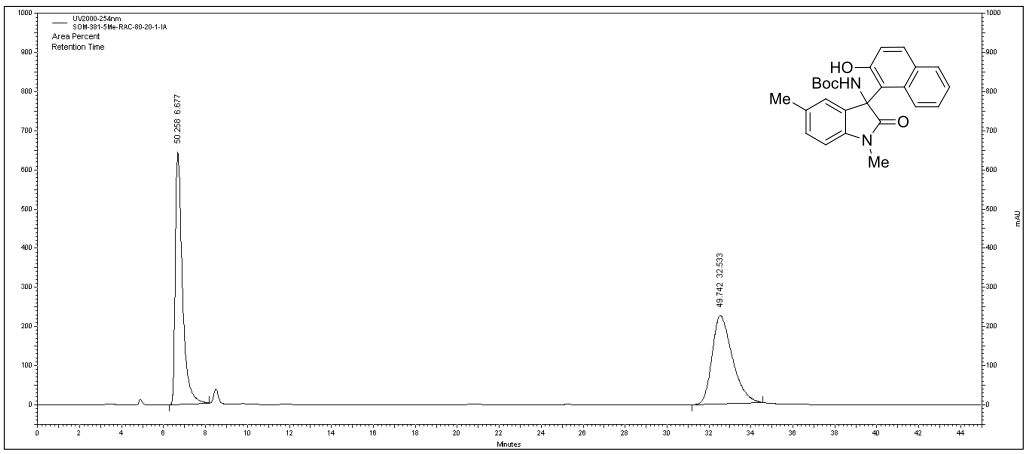

Figure B. 53 HPLC chromatogram of *rac*-**96g**.

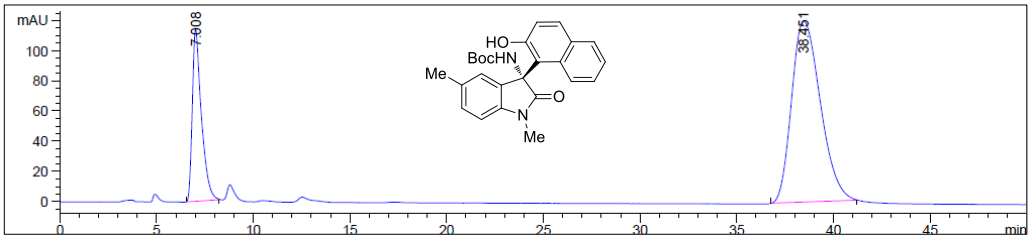

Peak #	RetTime [min]	Type	Width [min]	Area [mAU*s]	Height [mAU]	Area %
1	7.008	BB	0.4689	3728.45581	114.20473	23.0208
2	38.451	BB	1.4713	1.24676e4	120.27791	76.9792

Figure B. 54 HPLC chromatogram of enantiomerically enriched **96g**.

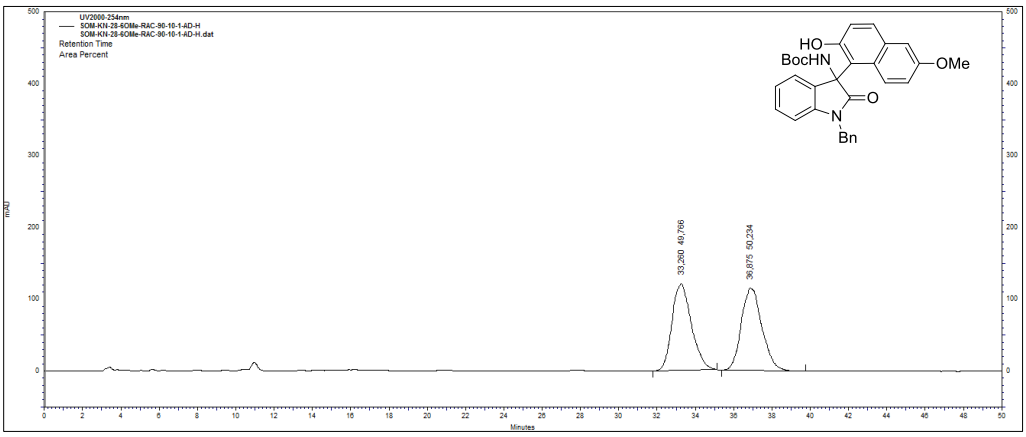

Figure B. 55 HPLC chromatogram of *rac*-**96h**.

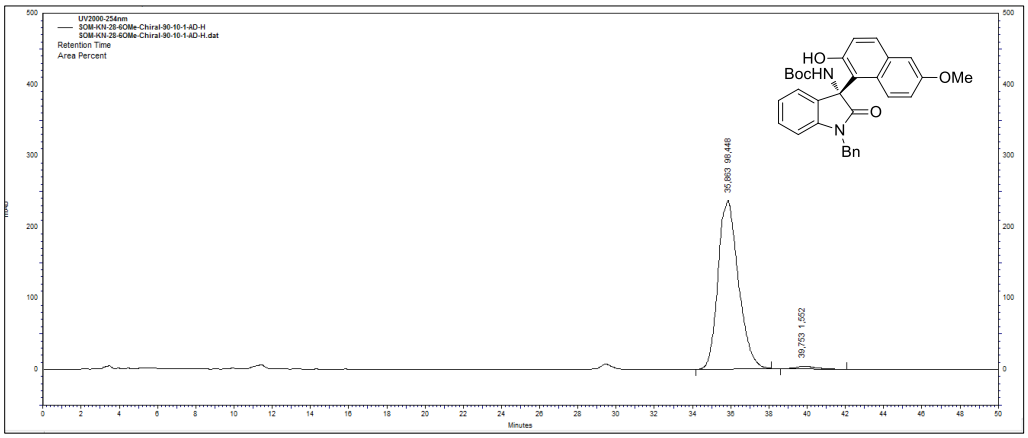

Figure B. 56 HPLC chromatogram of enantiomerically enriched **96h**.

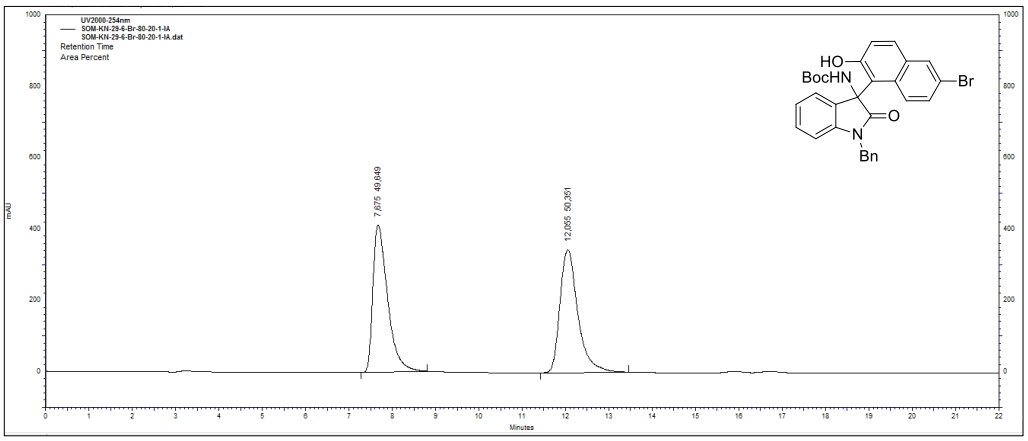

Figure B. 57 HPLC chromatogram of *rac*-**96i**.

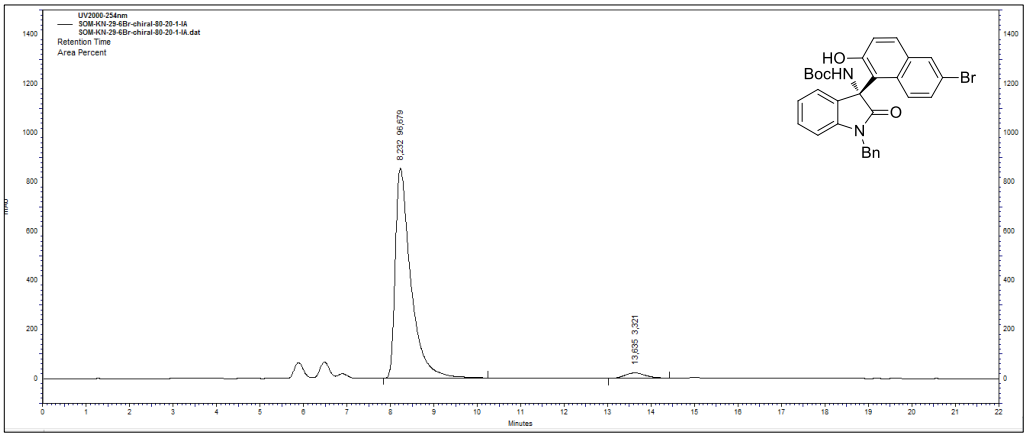

Figure B. 58 HPLC chromatogram of enantiomerically enriched **96i**.

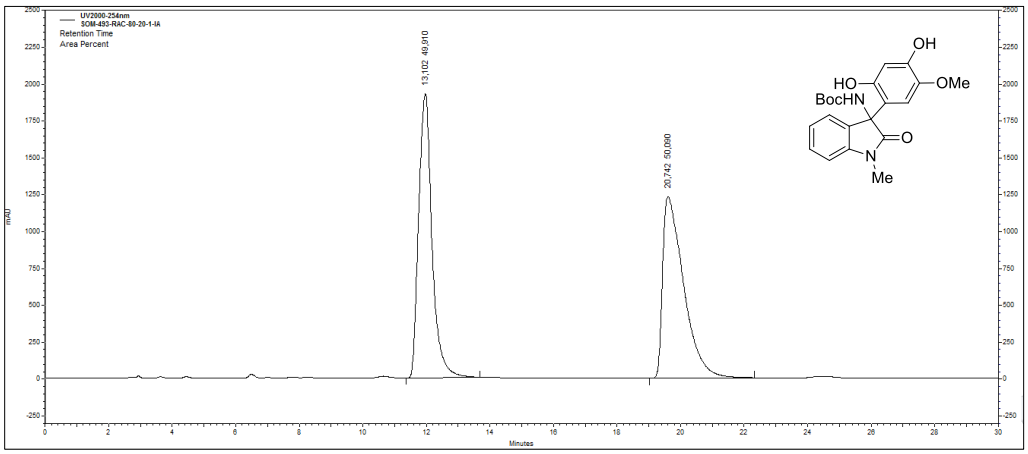

Figure B. 59 HPLC chromatogram of *rac*-**98b**.

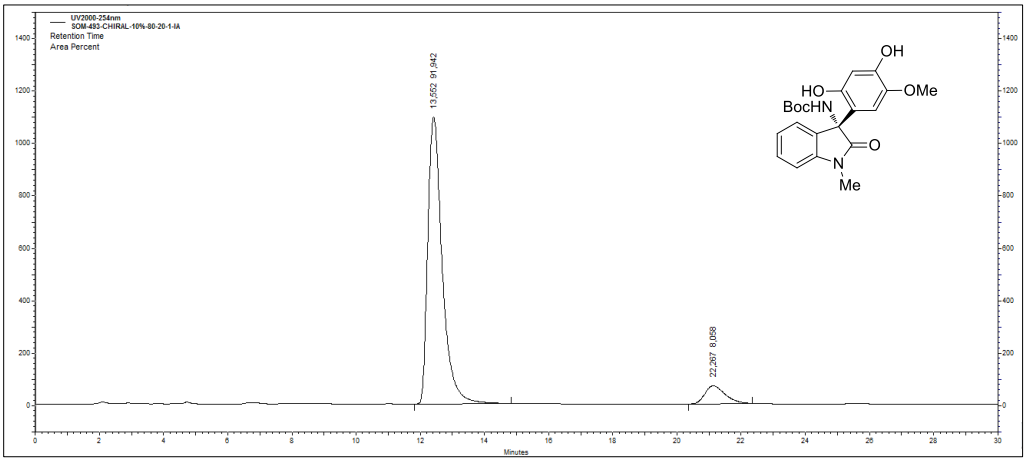

Figure B. 60 HPLC chromatogram of enantiomerically enriched **98b**.

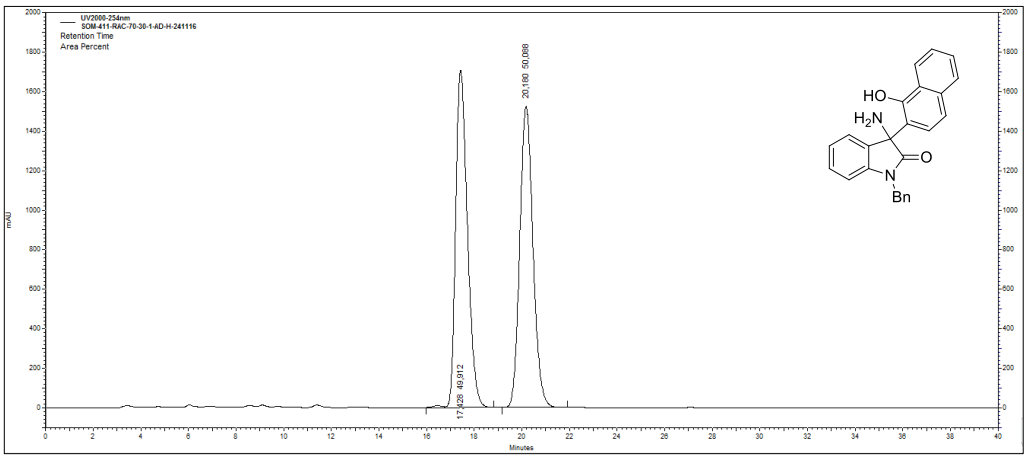

Figure B. 61 HPLC chromatogram of *rac*-**99**.

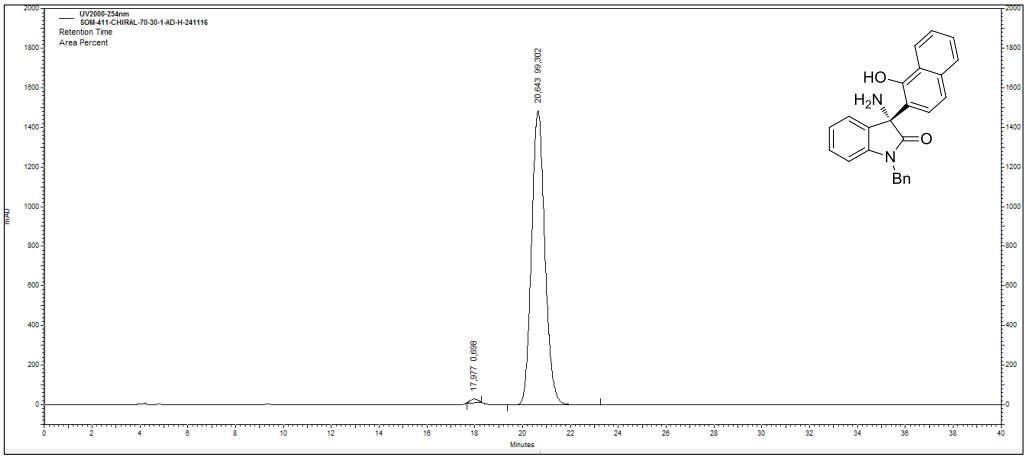

Figure B. 62 HPLC chromatogram of enantiomerically enriched **99**.

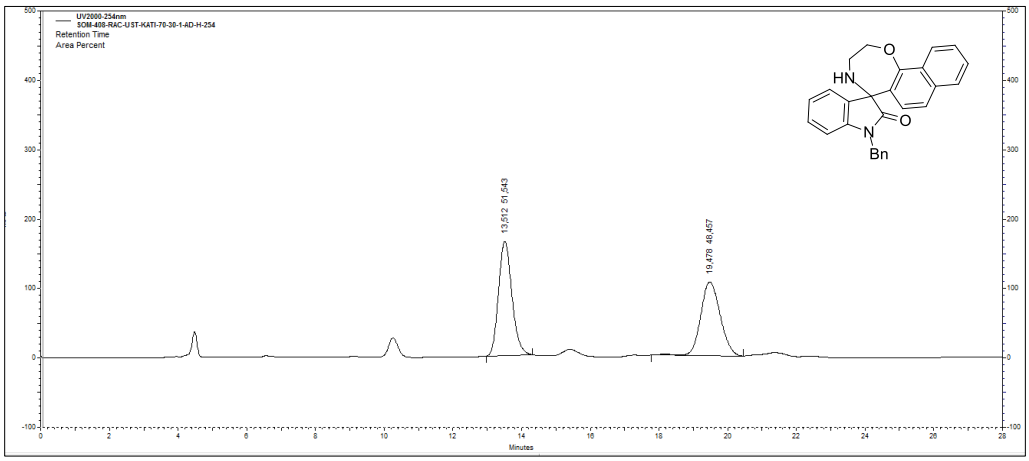

Figure B. 63 HPLC chromatogram of *rac*-**100**.

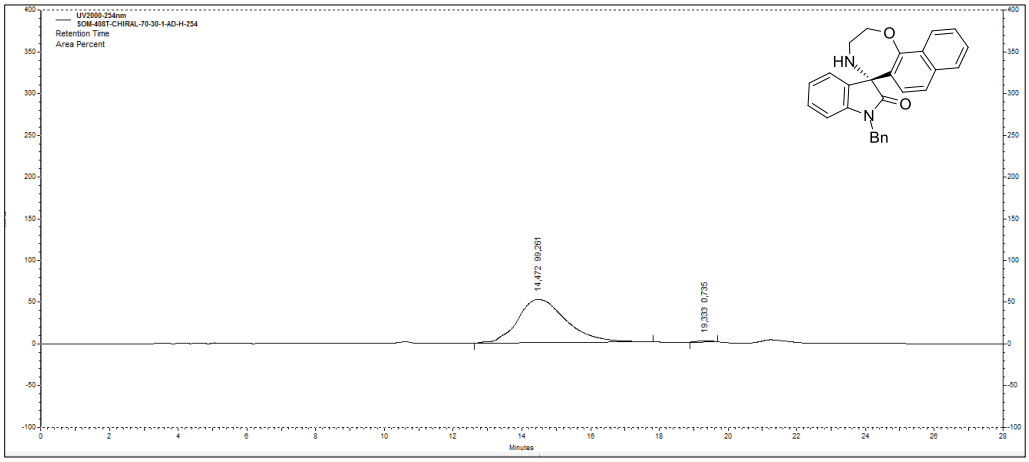

Figure B. 64 HPLC chromatogram of enantiomerically enriched **100**.

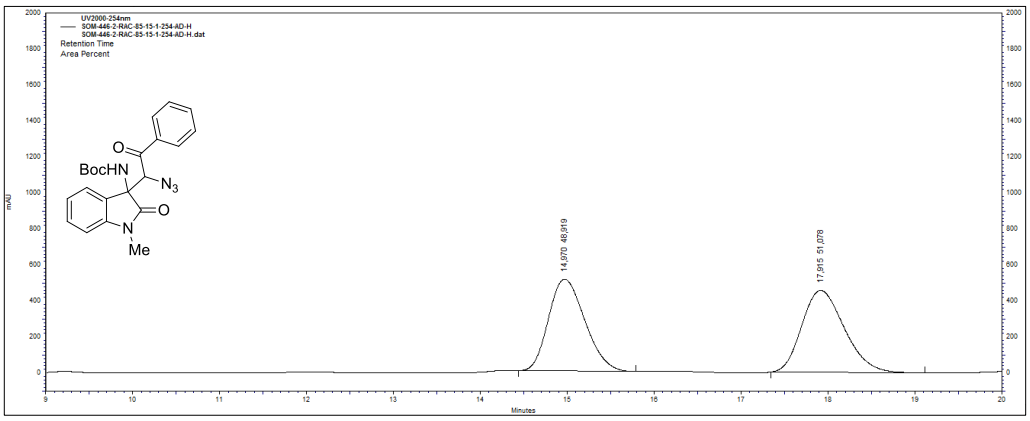

Figure B. 65 HPLC chromatogram of *rac*-**107a**.

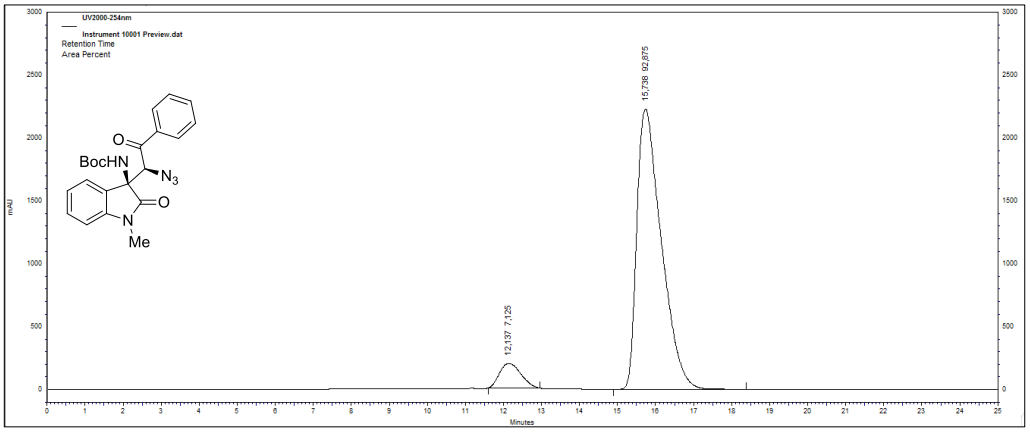

Figure B. 66 HPLC chromatogram of enantiomerically enriched **107a**.

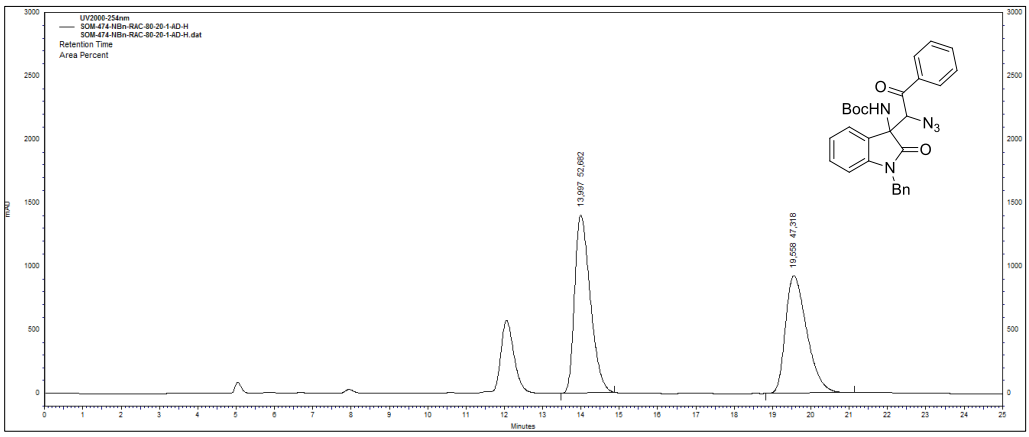

Figure B. 67 HPLC chromatogram of *rac*-**107b**.

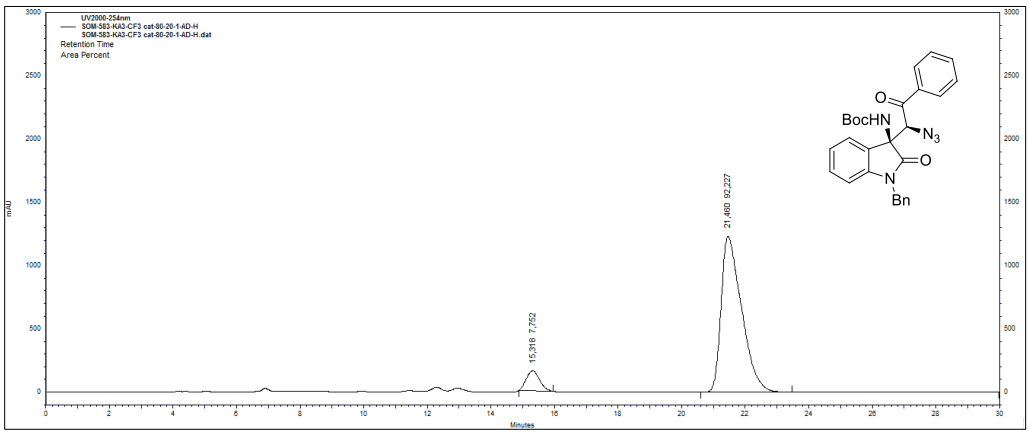

Figure B. 68 HPLC chromatogram of enantiomerically enriched **107b**.

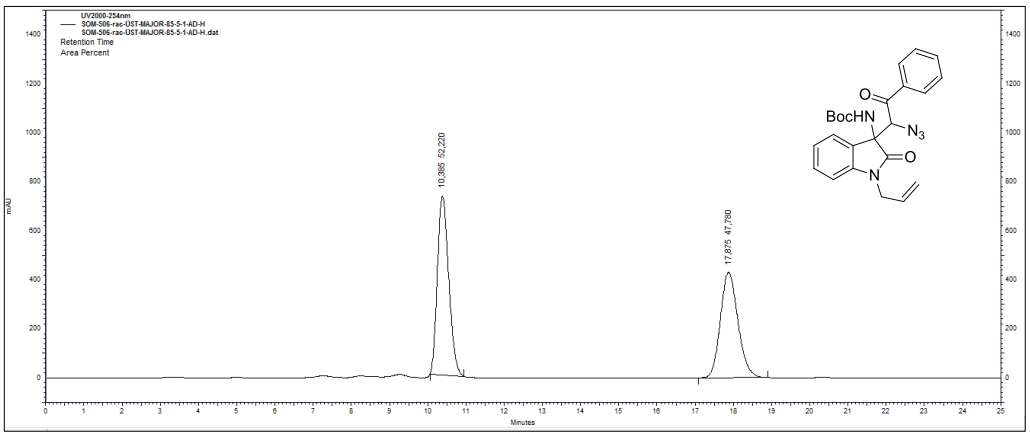

Figure B. 69 HPLC chromatogram of *rac*-**107c**.

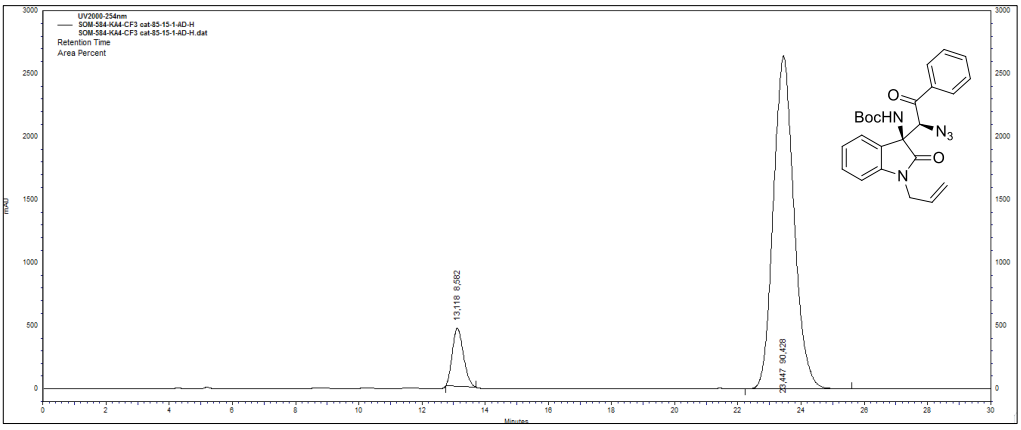

Figure B. 70 HPLC chromatogram of enantiomerically enriched **107c**.

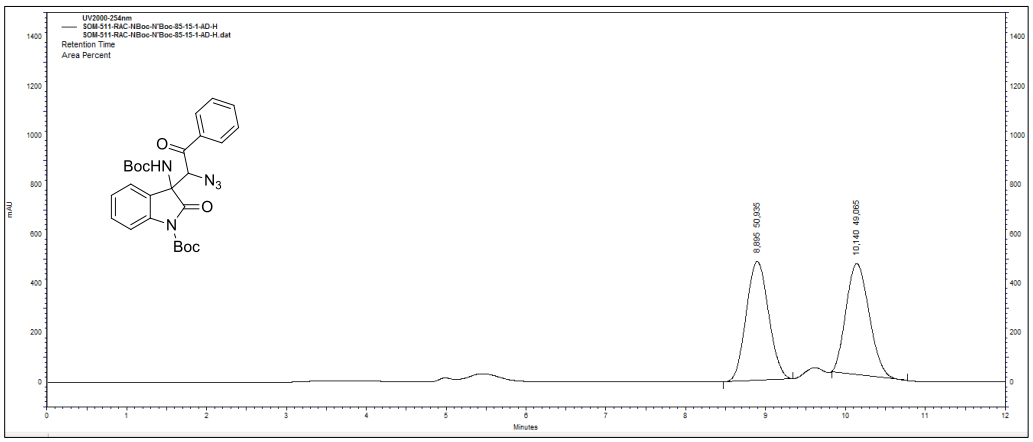

Figure B. 71 HPLC chromatogram of *rac*-**107d**.

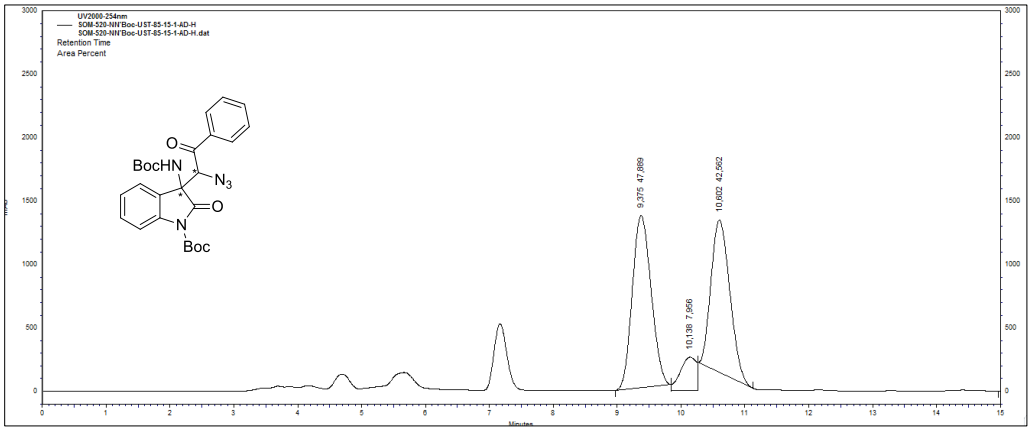

Figure B. 72 HPLC chromatogram of enantiomerically enriched **107d**.

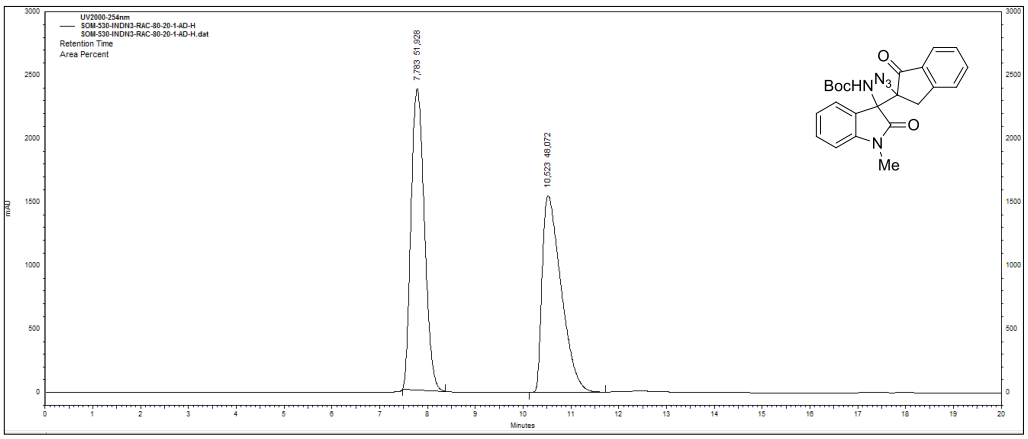

Figure B. 73 HPLC chromatogram of *rac*-**107e**.

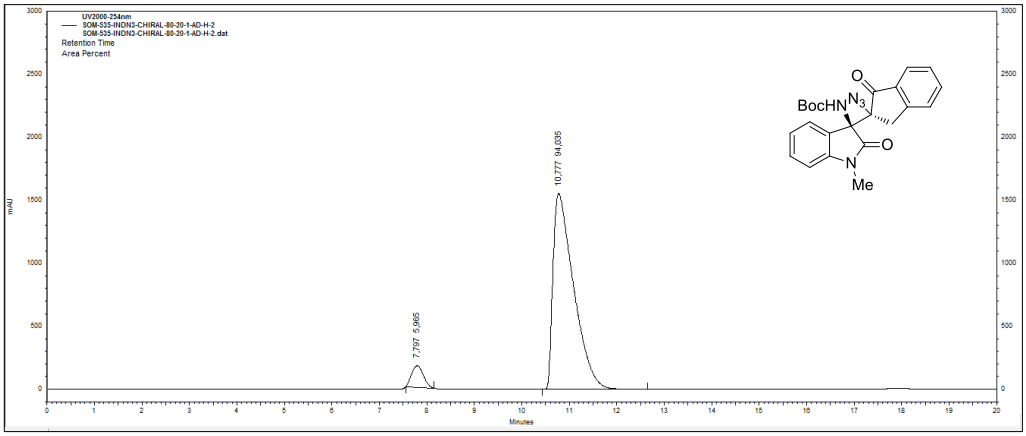

Figure B. 74 HPLC chromatogram of enantiomerically enriched **107e**.

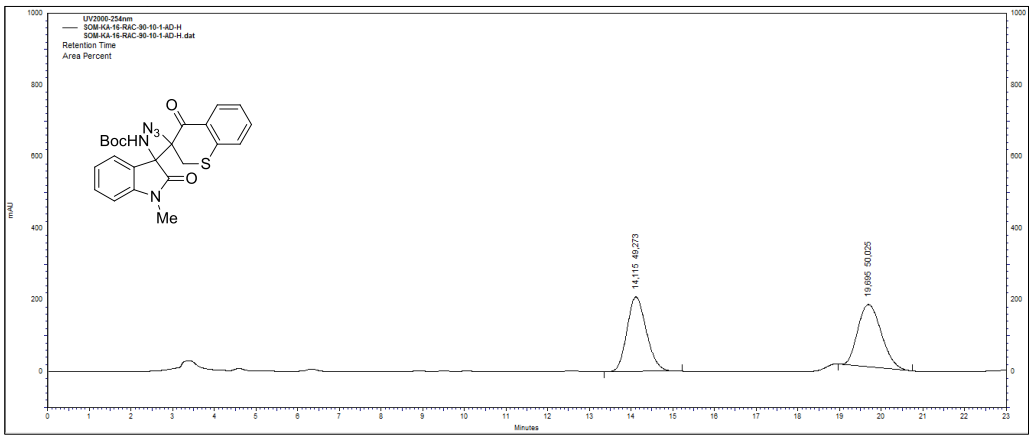

Figure B. 75 HPLC chromatogram of *rac*-**107f**.

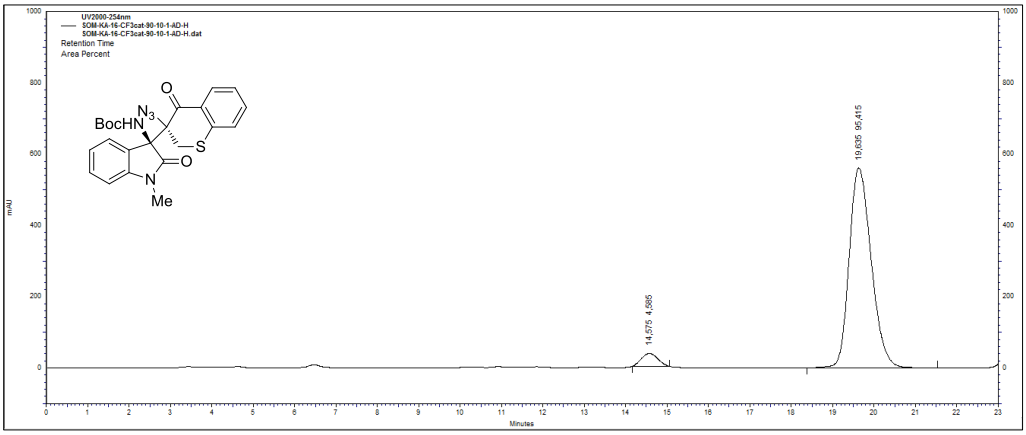

Figure B. 76 HPLC chromatogram of enantiomerically enriched **107f**.

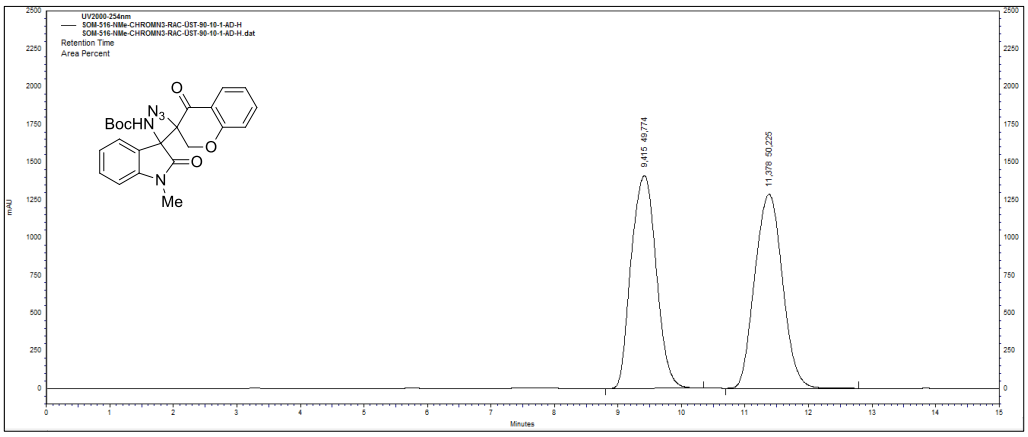

Figure B. 77 HPLC chromatogram of *rac*-**107g**.

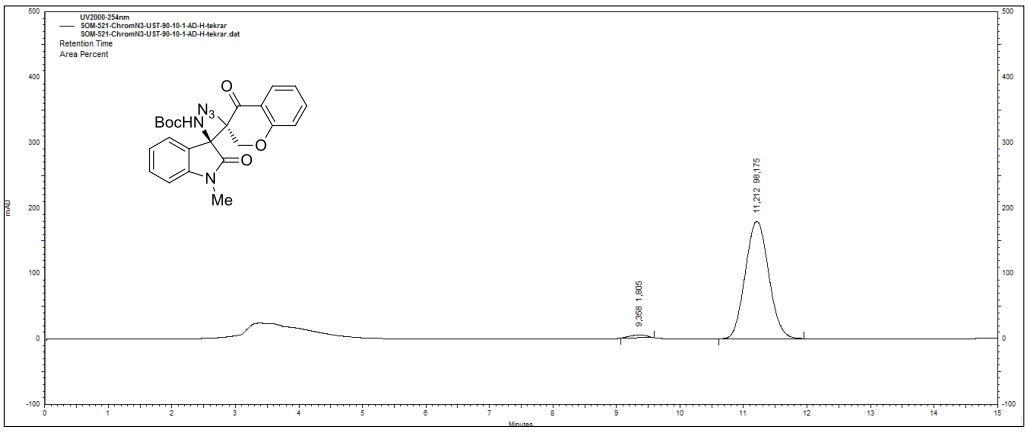

Figure B. 78 HPLC chromatogram of enantiomerically enriched **107g**.

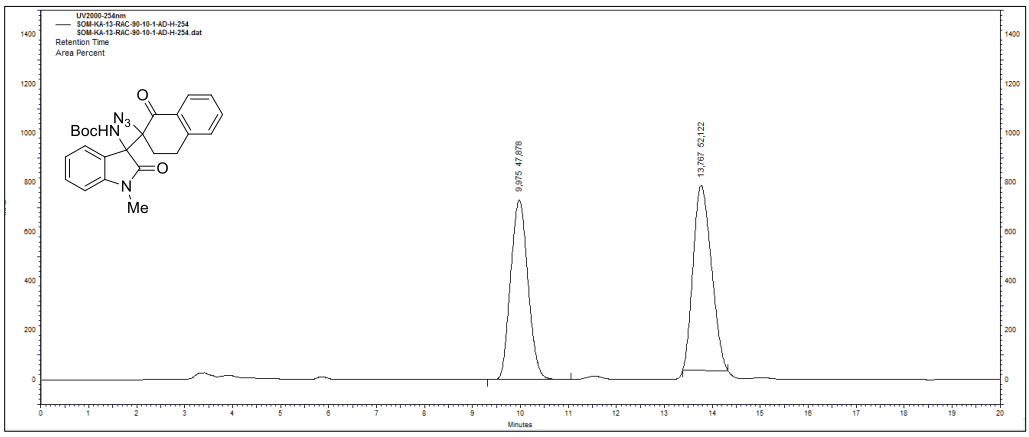

Figure B. 79 HPLC chromatogram of *rac*-**107h**.

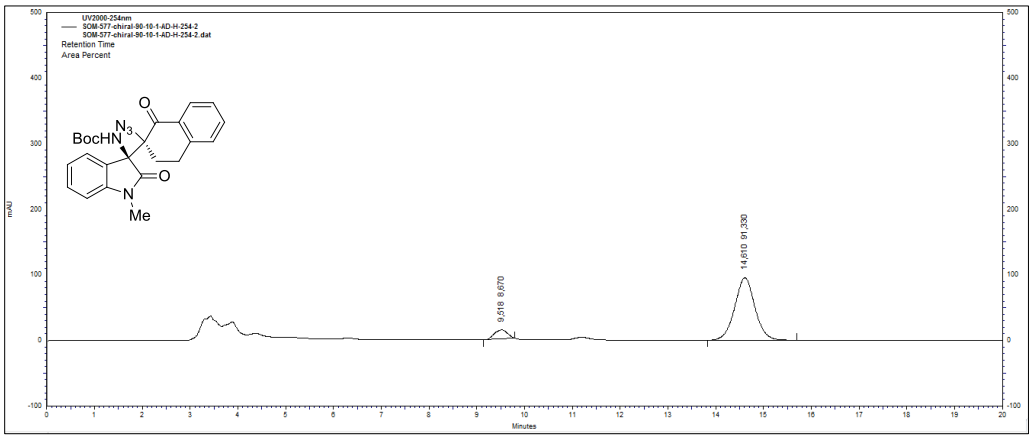

Figure B. 80 HPLC chromatogram of enantiomerically enriched **107h**.

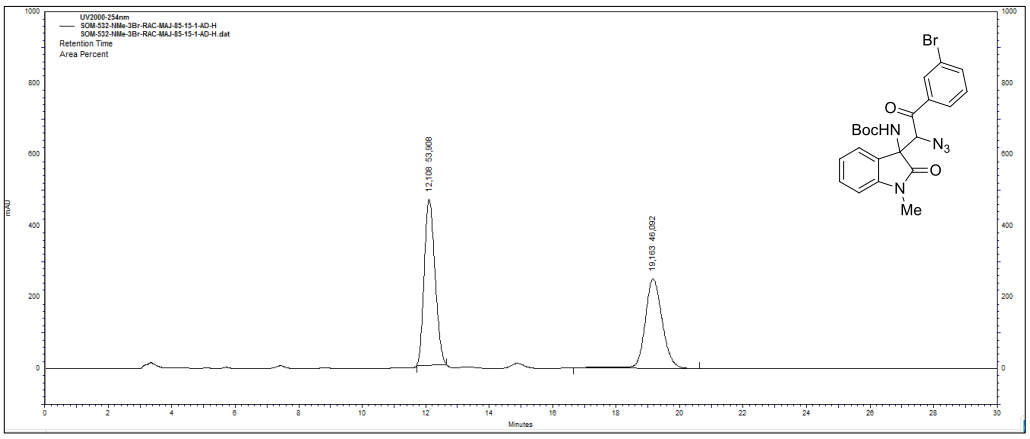

Figure B. 81 HPLC chromatogram of *rac*-**107i**.

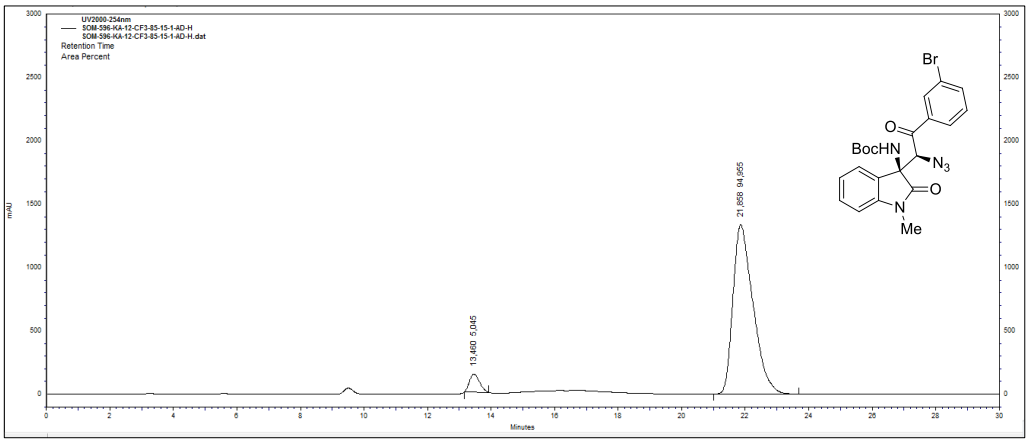

Figure B. 82 HPLC chromatogram of enantiomerically enriched **107i**.

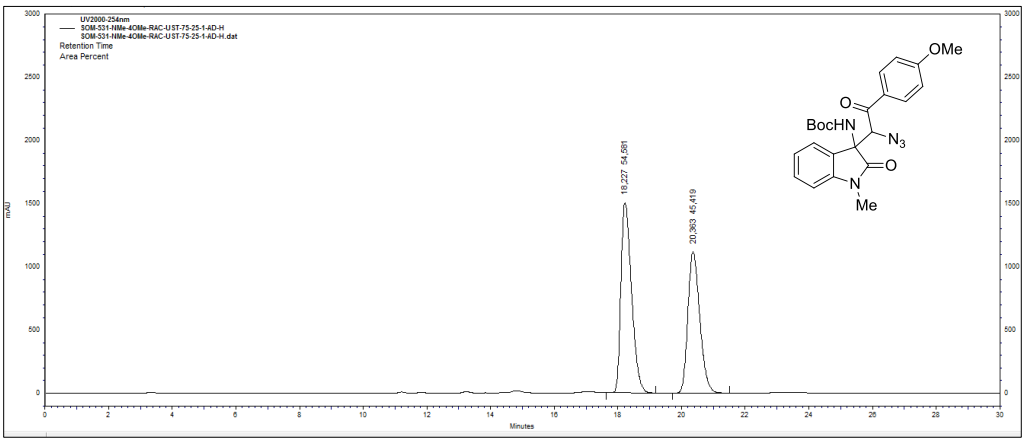

Figure B. 83 HPLC chromatogram of *rac*-**107j**.

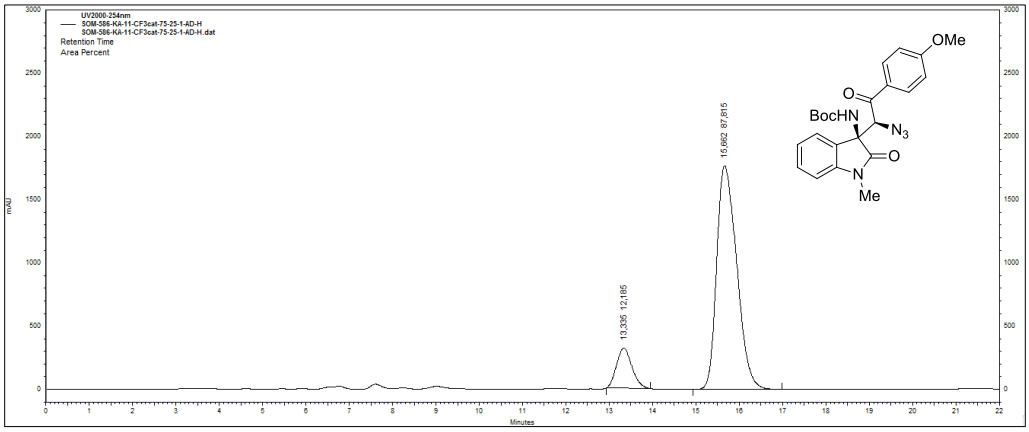

Figure B. 84 HPLC chromatogram of enantiomerically enriched **107j**.

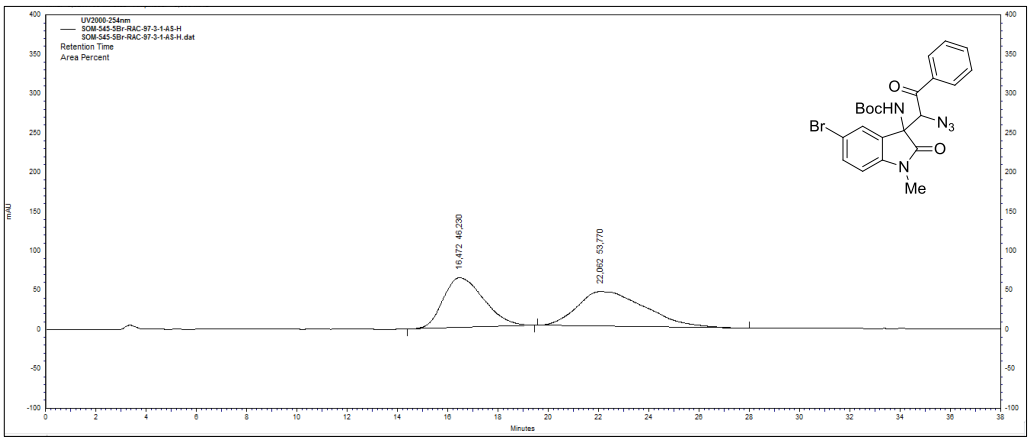

Figure B. 85 HPLC chromatogram of *rac*-**107k**.

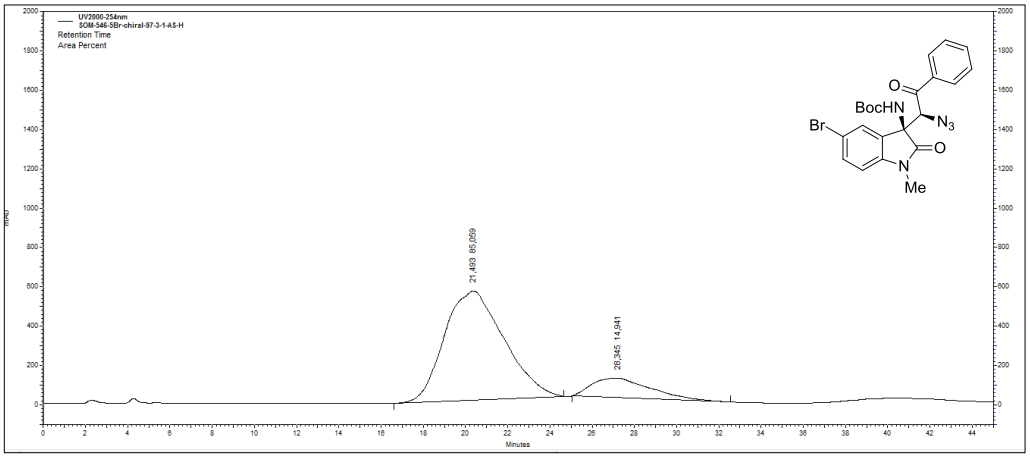

Figure B. 86 HPLC chromatogram of enantiomerically enriched **107k**.

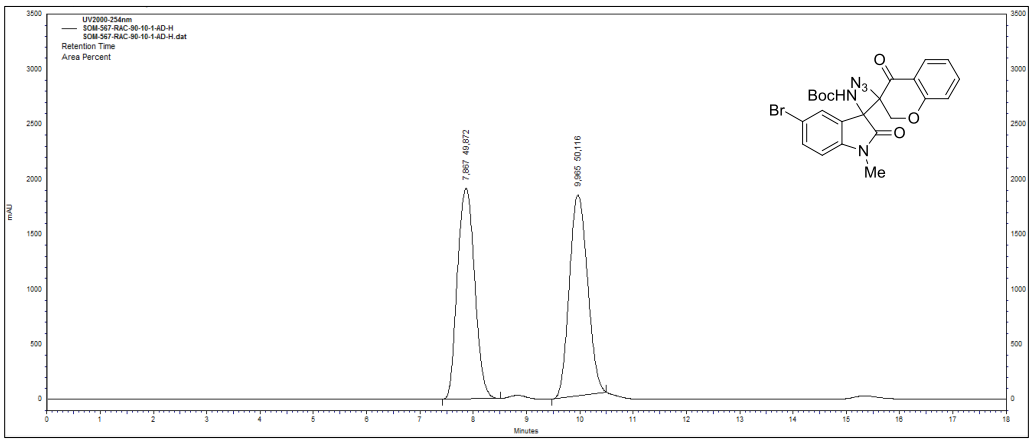

Figure B. 87 HPLC chromatogram of *rac*-**107l**.

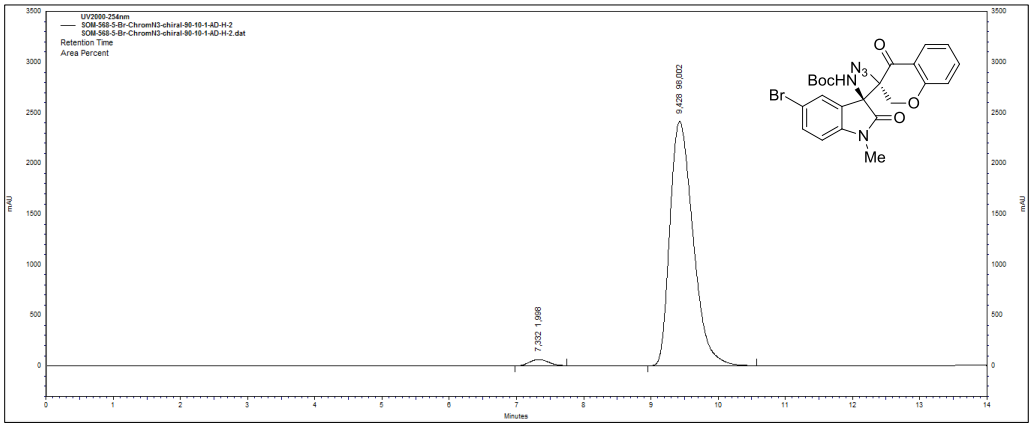

Figure B. 88 HPLC chromatogram of enantiomerically enriched **107l**.

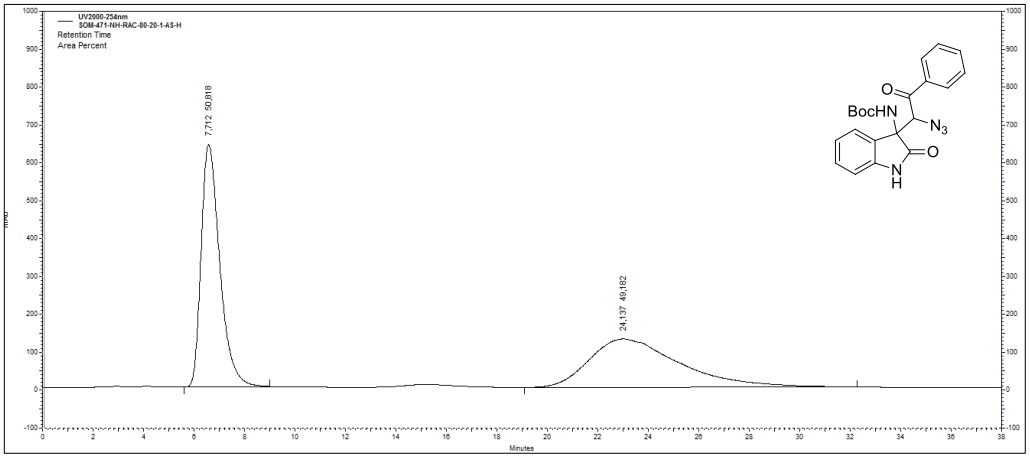

Figure B. 89 HPLC chromatogram of *rac*-**107m**.

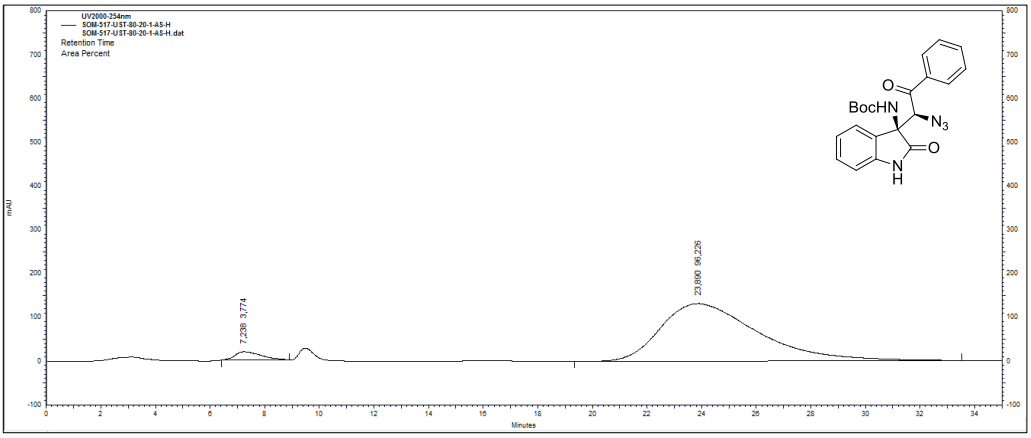

Figure B. 90 HPLC chromatogram of enantiomerically enriched **107m**.

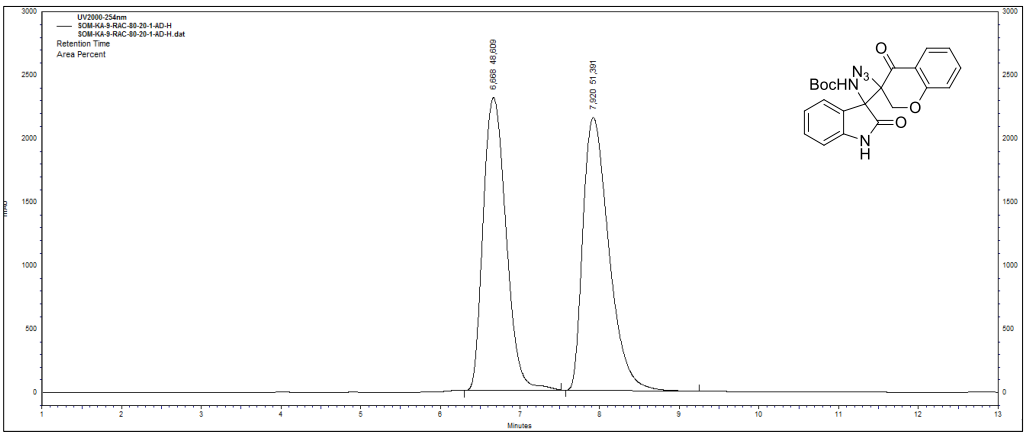

Figure B. 91 HPLC chromatogram of *rac*-**107n**.

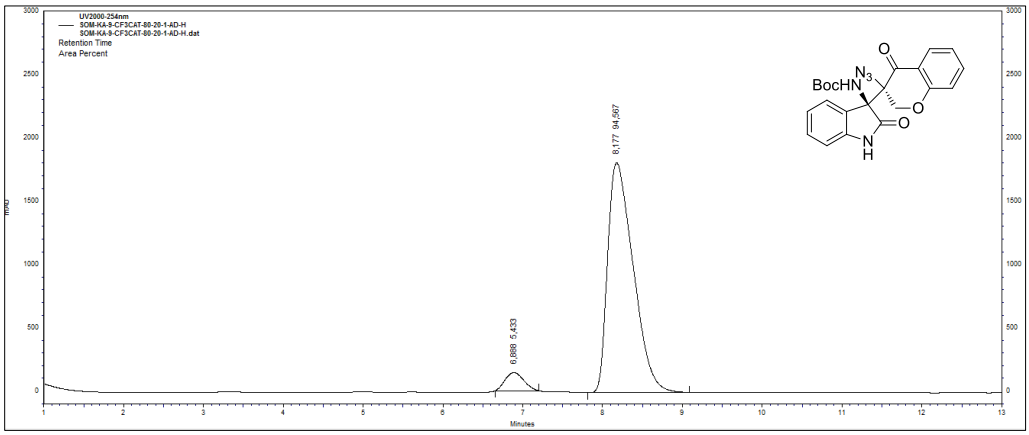

Figure B. 92 HPLC chromatogram of enantiomerically enriched **107n**.

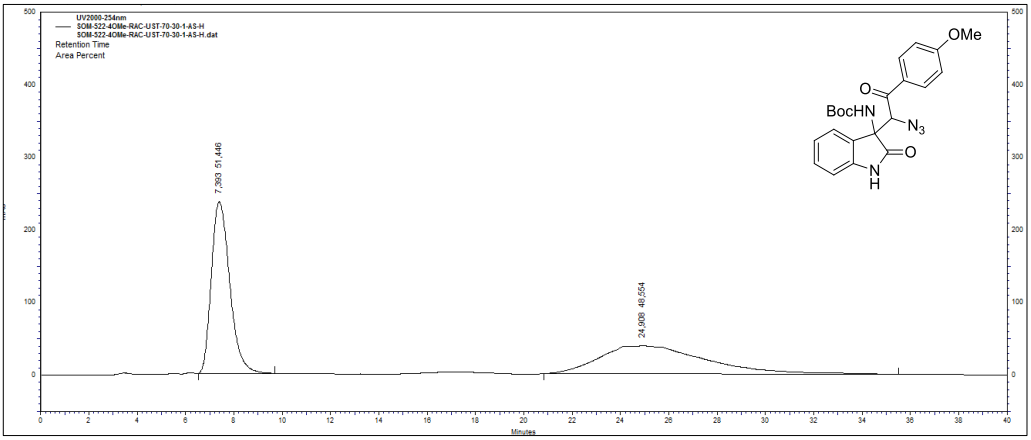

Figure B. 93 HPLC chromatogram of *rac*-**107o**.

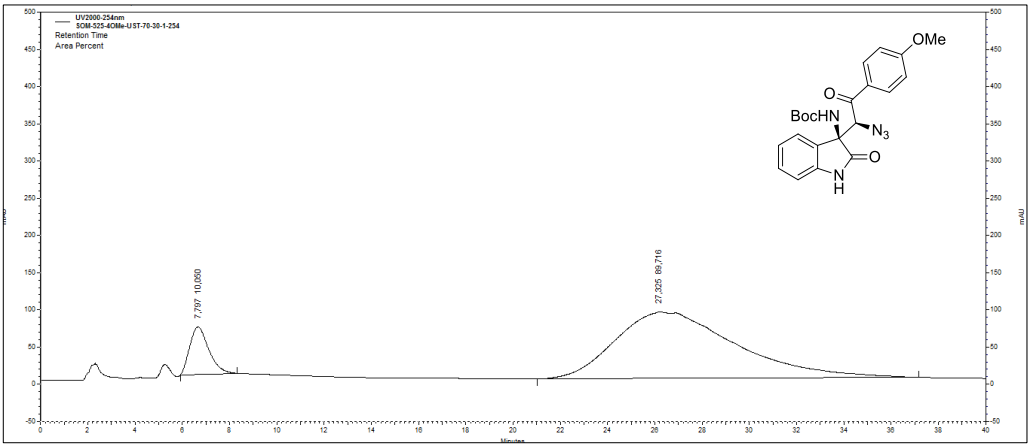

Figure B. 94 HPLC chromatogram of enantiomerically enriched **107o**.

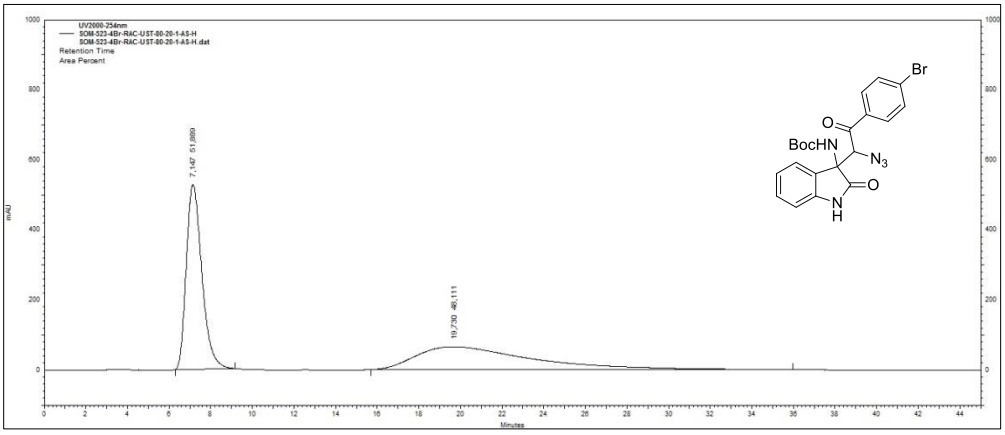

Figure B. 95 HPLC chromatogram of *rac*-**107p**.

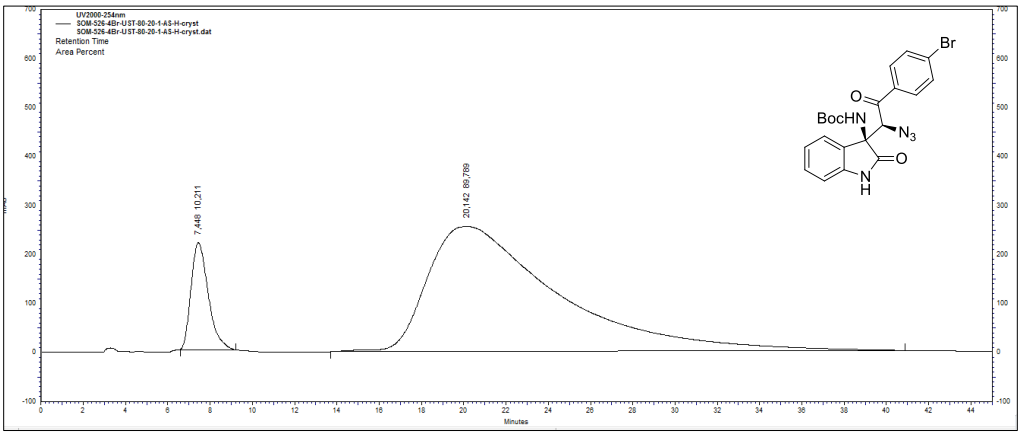

Figure B. 96 HPLC chromatogram of enantiomerically enriched **107p**.

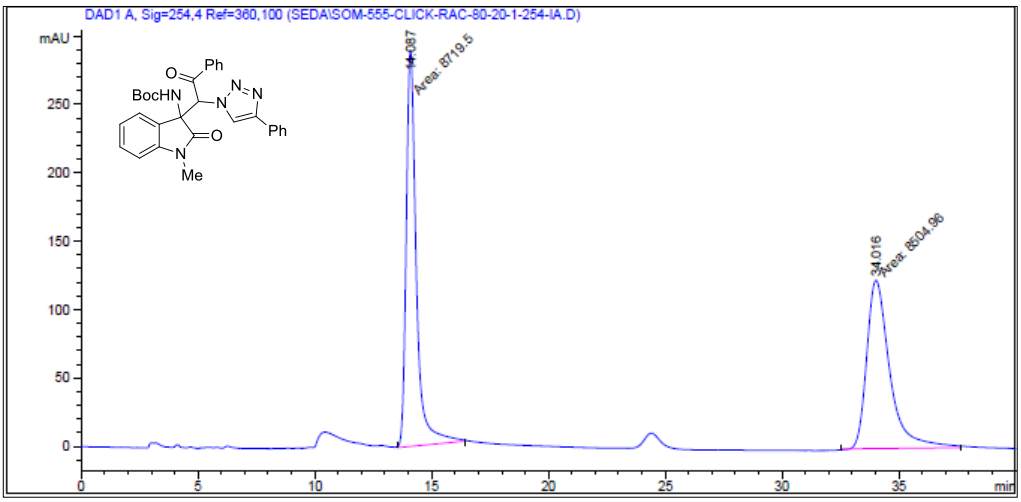

Peak #	RetTime [min]	Type	Width [min]	Area [mAU*s]	Height [mAU]	Area %
1	14.087	MM	0.5015	8719.49609	289.79175	50.6228
2	34.016	MM	1.1507	8504.96191	123.18912	49.3772

Figure B. 97 HPLC chromatogram of *rac*-**109**.

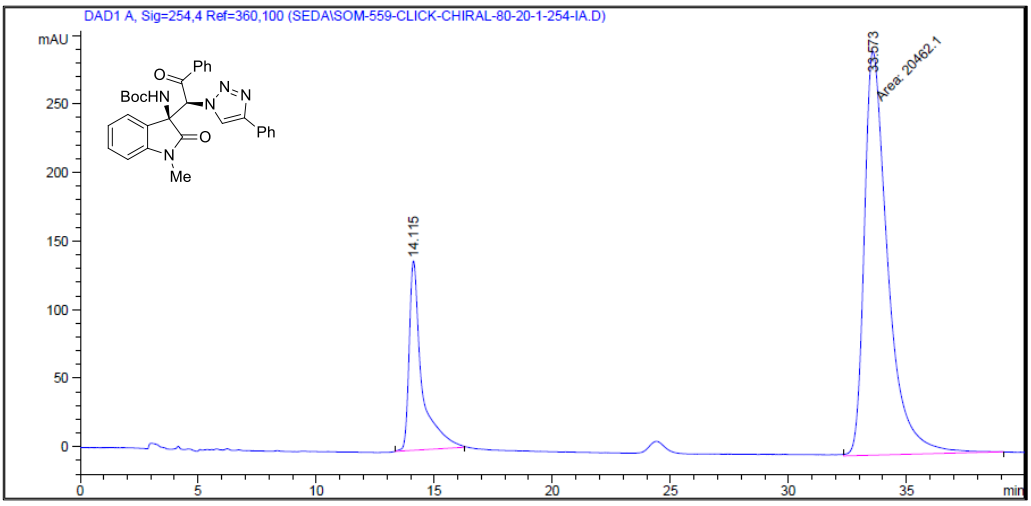

Peak #	RetTime [min]	Type	Width [min]	Area [mAU*s]	Height [mAU]	Area %
1	14.115	BB	0.5348	5175.16943	138.21825	20.1861
2	33.573	MM	1.1578	2.04621e4	294.55768	79.8139

Figure B. 98 HPLC chromatogram of enantiomerically enriched **109**.

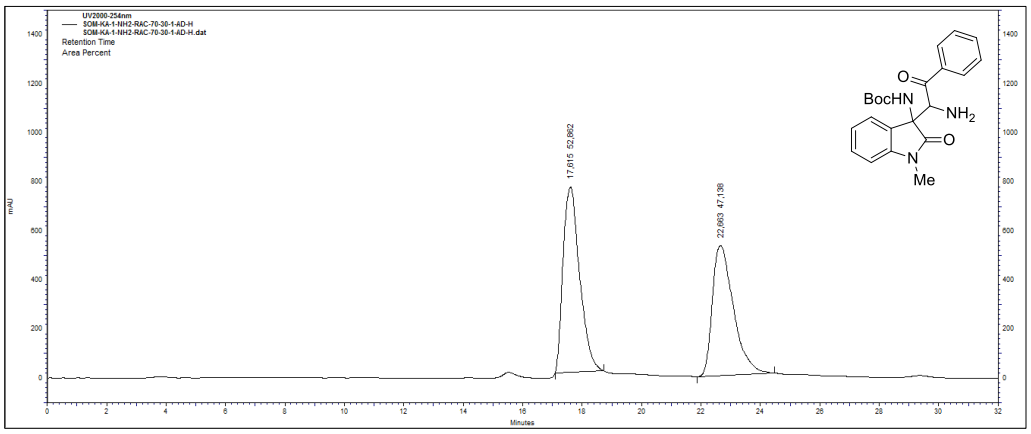

Figure B. 99 HPLC chromatogram of *rac*-**111a**.

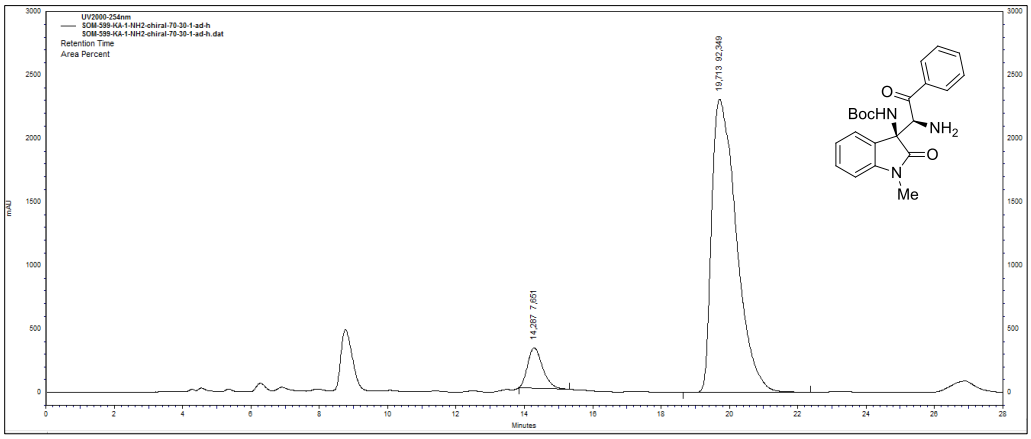

Figure B. 100 HPLC chromatogram of enantiomerically enriched **111a**.

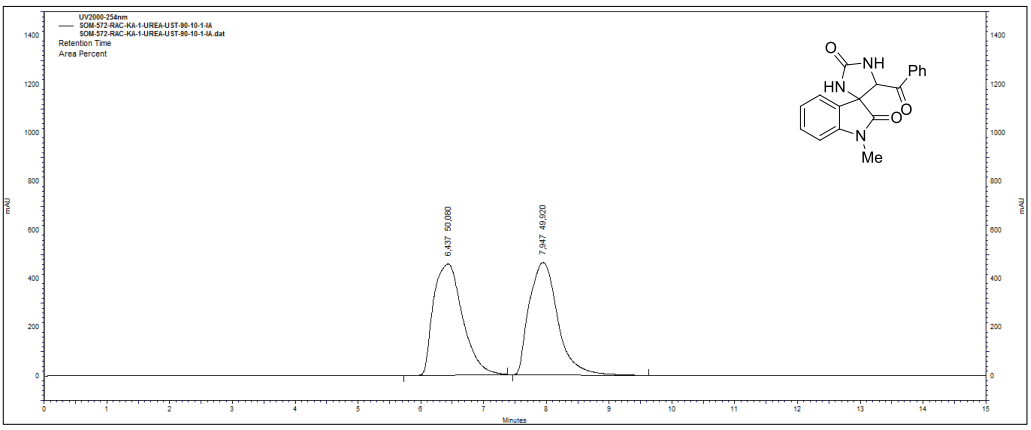

Figure B. 101 HPLC chromatogram of *rac*-**112a**.

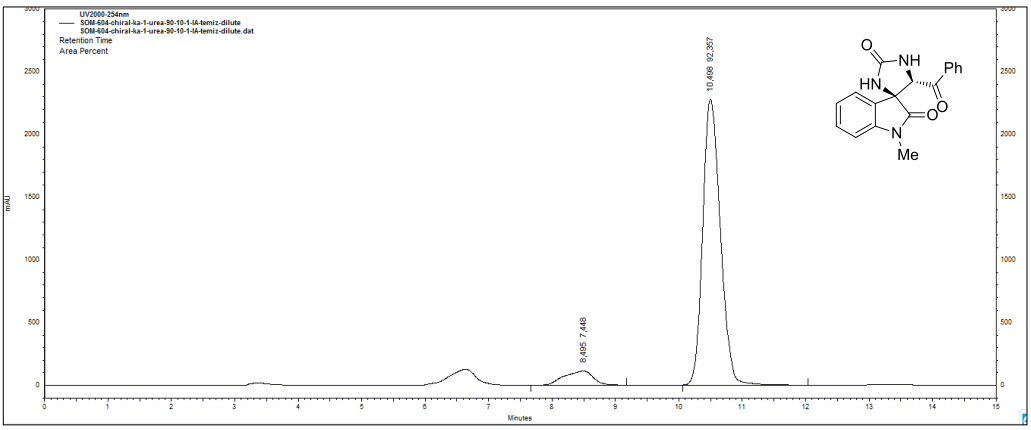

Figure B. 102 HPLC chromatogram of enantiomerically enriched **112a**.

APPENDIX C

X-RAY CRYSTALLOGRAPHIC DATA

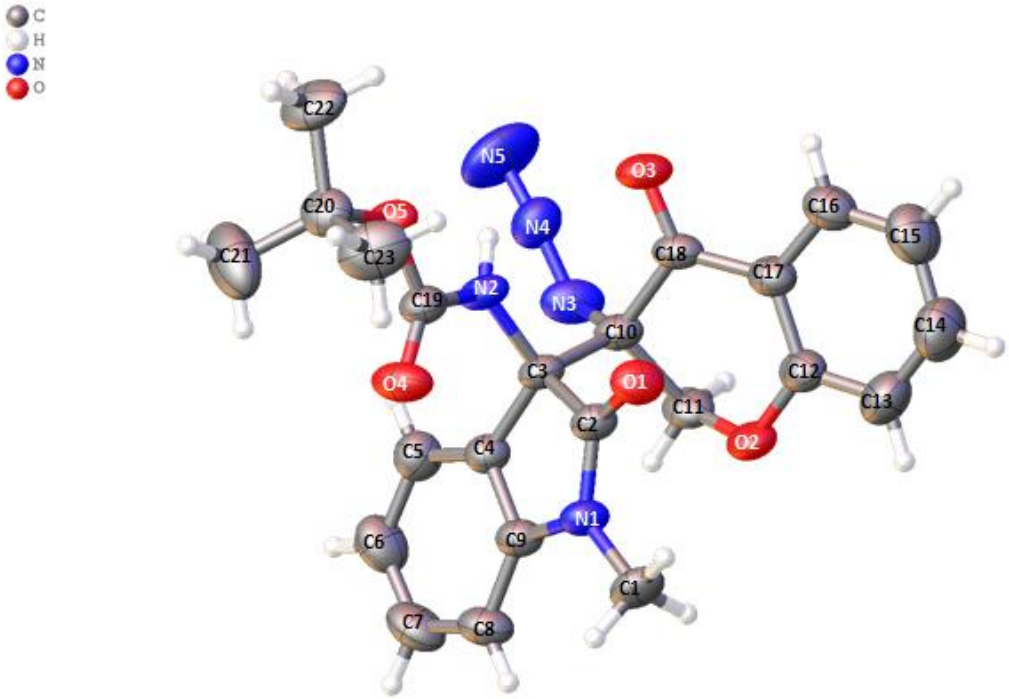

Figure C. 1 ORTEP plot for the X-ray structure of compound **107g**.

```
data_shelxl
_audit_creation_date              2018-04-11
_audit_creation_method
;
Olex2 1.2
(compiled 2017.03.28 svn.r3405 for OlexSys, GUI svn.r5337)
;
_chemical_name_systematic         Crystal
_chemical_formula_moiety          'C23 H23 N5 O5'
_chemical_formula_sum             'C23 H23 N5 O5'
_chemical_formula_weight          449.47
loop_
  _atom_type_symbol
  _atom_type_scat_dispersion_real
  _atom_type_scat_dispersion_imag
  _atom_type_scat_Cromer_Mann_a1
  _atom_type_scat_Cromer_Mann_a2
```

```
  _atom_type_scat_Cromer_Mann_a3
  _atom_type_scat_Cromer_Mann_a4
  _atom_type_scat_Cromer_Mann_b1
  _atom_type_scat_Cromer_Mann_b2
  _atom_type_scat_Cromer_Mann_b3
  _atom_type_scat_Cromer_Mann_b4
  _atom_type_scat_Cromer_Mann_c
  _atom_type_scat_source
  _atom_type_scat_dispersion_source
 H 0.00000 0.00000 0.49300 0.32291 0.14019 0.04081 10.51090
26.12570 3.14236
 57.79970 0.0030380000826
 'International Tables Volume C Table 6.1.1.4 (pp. 500-502)'
 'Henke, Gullikson and Davis, At. Data and Nucl. Data
Tables, 1993, 54, 2'
 C 0.00347 0.00161 2.31000 1.02000 1.58860 0.86500 20.84390
10.20750 0.56870
 51.65120 0.215599998832
 'International Tables Volume C Table 6.1.1.4 (pp. 500-502)'
 'Henke, Gullikson and Davis, At. Data and Nucl. Data
Tables, 1993, 54, 2'
 O 0.01158 0.00611 3.04850 2.28680 1.54630 0.86700 13.27710
5.70110 0.32390
 32.90890 0.250800013542
 'International Tables Volume C Table 6.1.1.4 (pp. 500-502)'
 'Henke, Gullikson and Davis, At. Data and Nucl. Data
Tables, 1993, 54, 2'
 N 0.00653 0.00323 12.21260 3.13220 2.01250 1.16630 0.00570
9.89330 28.99750
 0.58260 -11.5290002823
 'International Tables Volume C Table 6.1.1.4 (pp. 500-502)'
 'Henke, Gullikson and Davis, At. Data and Nucl. Data
Tables, 1993, 54, 2'

_space_group_crystal_system       'triclinic'
_space_group_IT_number            2
_space_group_name_H-M_alt         'P -1'
_space_group_name_Hall            '-P 1'
loop_
  _space_group_symop_id
  _space_group_symop_operation_xyz
 1 x,y,z
 2 -x,-y,-z

_symmetry_Int_Tables_number       2
_cell_length_a                    10.2450(2)
_cell_length_b                    10.9607(2)
_cell_length_c                    11.1338(7)
_cell_angle_alpha                 74.014(5)
_cell_angle_beta                  74.695(5)
```

```
_cell_angle_gamma                  72.702(5)
_cell_volume                       1124.73(9)
_cell_formula_units_Z              2
_cell_measurement_temperature      295
_exptl_absorpt_coefficient_mu      0.096
_exptl_crystal_colour              clear
_exptl_crystal_colour_lustre       clear
_exptl_crystal_density_diffrn      1.3271
_exptl_crystal_description         block
_exptl_crystal_F_000               472.2417
_exptl_crystal_preparation         ?
_exptl_crystal_size_max            25.0
_exptl_crystal_size_mid            5.0
_exptl_crystal_size_min            5.0
_diffrn_reflns_av_R_equivalents    0.0245
_diffrn_reflns_av_unetI/netI       0.0155
_diffrn_reflns_limit_h_max         13
_diffrn_reflns_limit_h_min         -13
_diffrn_reflns_limit_k_max         14
_diffrn_reflns_limit_k_min         -14
_diffrn_reflns_limit_l_max         14
_diffrn_reflns_limit_l_min         -14
_diffrn_reflns_number              29145
_diffrn_reflns_theta_full          28.2574
_diffrn_reflns_theta_max           28.26
_diffrn_reflns_theta_min           3.07
_diffrn_ambient_temperature        295
_diffrn_measured_fraction_theta_full 0.9969
_diffrn_measured_fraction_theta_max 0.9969
_diffrn_radiation_type             'Mo K\a'
_diffrn_radiation_wavelength       0.71075
_diffrn_special_details            ?
_reflns_Friedel_coverage           0.0
_reflns_limit_h_max                13
_reflns_limit_h_min                -12
_reflns_limit_k_max                14
_reflns_limit_k_min                -13
_reflns_limit_l_max                14
_reflns_limit_l_min                0
_reflns_number_gt                  4872
_reflns_number_total               5552
_reflns_threshold_expression       I>=2u(I)
_computing_molecular_graphics      'Olex2 (Dolomanov et al.,
2009)'
_computing_publication_material    'Olex2 (Dolomanov et al.,
2009)'
_computing_structure_refinement    'olex2.refine (Bourhis et
al., 2015)'
_computing_structure_solution      'SIR2004 (Burla et al.,
2007)'
```

```
_refine_diff_density_max          0.3754
_refine_diff_density_min          -0.4439
_refine_diff_density_rms          0.1277
_refine_ls_d_res_high             0.7506
_refine_ls_d_res_low              6.6456
_refine_ls_goodness_of_fit_ref    1.0697
_refine_ls_hydrogen_treatment     constr
_refine_ls_matrix_type            full
_refine_ls_number_constraints     37
_refine_ls_number_parameters      302
_refine_ls_number_reflns          5552
_refine_ls_number_restraints      0
_refine_ls_R_factor_all           0.0633
_refine_ls_R_factor_gt            0.0588
_refine_ls_restrained_S_all       1.0697
_refine_ls_shift/su_max           0.0000
_refine_ls_shift/su_mean          0.0000
_refine_ls_structure_factor_coef  Fsqd
_refine_ls_weighting_details
'w=1/[\s^2^(Fo^2^)+(0.0973P)^2^+0.1929P] where
P=(Fo^2^+2Fc^2^)/3'
_refine_ls_weighting_scheme       calc
_refine_ls_wR_factor_gt           0.1530
_refine_ls_wR_factor_ref          0.1599
_olex2_refinement_description
;
1. Fixed Uiso
 At 1.2 times of:
  All C(H) groups, All C(H,H) groups, All N(H) groups
 At 1.5 times of:
  All C(H,H,H) groups
2.a Secondary CH2 refined with riding coordinates:
 C11(H11a,H11b)
2.b Aromatic/amide H refined with riding coordinates:
 C5(H5), C6(H6), C7(H7), C8(H8), C16(H16), C15(H15),
C14(H14), C13(H13), N2(H2)
2.c Idealised Me refined as rotating group:
 C1(H1a,H1b,H1c), C23(H23a,H23b,H23c), C22(H22a,H22b,H22c),
C21(H21a,H21b,H21c)
;
_atom_sites_solution_primary      direct
loop_
  _atom_site_label
  _atom_site_type_symbol
  _atom_site_fract_x
  _atom_site_fract_y
  _atom_site_fract_z
  _atom_site_U_iso_or_equiv
  _atom_site_adp_type
  _atom_site_occupancy
```

```
  _atom_site_refinement_flags_posn
 O5 O 0.06874(10) 0.01362(9) 0.78766(10) 0.0450(2) Uani
1.000000 .
 O1 O -0.23712(11) 0.35964(10) 0.79541(9) 0.0481(2) Uani
1.000000 .
 O3 O -0.36837(12) 0.05620(9) 0.84692(10) 0.0540(3) Uani
1.000000 .
 O2 O -0.49148(11) 0.43538(9) 0.65918(10) 0.0523(3) Uani
1.000000 .
 O4 O 0.07340(12) 0.21188(10) 0.65296(11) 0.0573(3) Uani
1.000000 .
 N5 N -0.2744(3) -0.10897(17) 0.6408(2) 0.1039(8) Uani
1.000000 .
 N2 N -0.10849(12) 0.11922(9) 0.69168(11) 0.0401(2) Uani
1.000000 .
 H2 H -0.13632(12) 0.04797(9) 0.71953(11) 0.0481(3) Uiso
1.000000 R
 N1 N -0.19563(12) 0.46050(10) 0.58252(10) 0.0405(2) Uani
1.000000 .
 N4 N -0.30418(14) -0.00055(12) 0.61832(14) 0.0539(3) Uani
1.000000 .
 N3 N -0.33961(17) 0.11721(13) 0.57565(12) 0.0557(3) Uani
1.000000 .
 C22 C 0.1953(3) 0.0983(2) 0.8920(2) 0.0782(6) Uani 1.000000
.
 H22a H 0.190(2) 0.1805(4) 0.8319(4) 0.1173(9) Uiso 1.000000
GR
 H22b H 0.1137(11) 0.1045(12) 0.9588(12) 0.1173(9) Uiso
1.000000 GR
 H22c H 0.2769(9) 0.0768(9) 0.9279(15) 0.1173(9) Uiso
1.000000 GR
 C15 C -0.6527(2) 0.3369(2) 1.04472(18) 0.0708(5) Uani
1.000000 .
 H15 H -0.6932(2) 0.3163(2) 1.13061(18) 0.0850(6) Uiso
1.000000 R
 C14 C -0.6763(2) 0.4668(2) 0.9784(2) 0.0764(5) Uani
1.000000 .
 H14 H -0.7287(2) 0.5327(2) 1.0215(2) 0.0917(6) Uiso
1.000000 R
 C21 C 0.3206(2) -0.0143(3) 0.7103(2) 0.0968(8) Uani
1.000000 .
 H21a H 0.3137(14) -0.0745(17) 0.6652(12) 0.1452(13) Uiso
1.000000 GR
 H21b H 0.3143(14) 0.0708(5) 0.6551(11) 0.1452(13) Uiso
1.000000 GR
 H21c H 0.4085(2) -0.044(2) 0.7374(3) 0.1452(13) Uiso
1.000000 GR
 C3 C -0.19598(13) 0.23723(11) 0.62809(11) 0.0353(2) Uani
1.000000 .
```

```
 C2 C -0.21177(13) 0.35819(11) 0.68281(12) 0.0371(3) Uani
1.000000 .
 C18 C -0.40799(14) 0.16928(12) 0.79126(12) 0.0406(3) Uani
1.000000 .
 C4 C -0.14027(13) 0.28504(12) 0.48800(12) 0.0381(3) Uani
1.000000 .
 C10 C -0.34610(13) 0.21269(11) 0.64862(11) 0.0379(3) Uani
1.000000 .
 C9 C -0.14952(13) 0.41901(12) 0.46658(12) 0.0394(3) Uani
1.000000 .
 C19 C 0.01806(14) 0.12291(12) 0.70660(12) 0.0397(3) Uani
1.000000 .
 C17 C -0.51122(14) 0.26934(13) 0.85295(13) 0.0428(3) Uani
1.000000 .
 C12 C -0.54248(14) 0.39964(14) 0.78681(14) 0.0476(3) Uani
1.000000 .
 C11 C -0.45185(15) 0.33270(14) 0.59234(13) 0.0483(3) Uani
1.000000 .
 H11a H -0.53452(15) 0.30624(14) 0.59334(13) 0.0579(4) Uiso
1.000000 R
 H11b H -0.41187(15) 0.36530(14) 0.50416(13) 0.0579(4) Uiso
1.000000 R
 C5 C -0.08766(16) 0.22110(15) 0.38852(14) 0.0492(3) Uani
1.000000 .
 H5 H -0.08016(16) 0.13188(15) 0.40222(14) 0.0590(4) Uiso
1.000000 R
 C20 C 0.20354(15) -0.00724(15) 0.82510(14) 0.0501(3) Uani
1.000000 .
 C8 C -0.11110(16) 0.49239(15) 0.34555(14) 0.0513(3) Uani
1.000000 .
 H8 H -0.11971(16) 0.58185(15) 0.33136(14) 0.0615(4) Uiso
1.000000 R
 C16 C -0.56981(17) 0.23907(17) 0.98357(14) 0.0530(3) Uani
1.000000 .
 H16 H -0.55245(17) 0.15271(17) 1.02867(14) 0.0636(4) Uiso
1.000000 R
 C1 C -0.22632(17) 0.59467(13) 0.59677(16) 0.0509(3) Uani
1.000000 .
 H1a H -0.3128(7) 0.6429(3) 0.5706(12) 0.0763(5) Uiso
1.000000 GR
 H1b H -0.2338(13) 0.59523(14) 0.6844(3) 0.0763(5) Uiso
1.000000 GR
 H1c H -0.1526(7) 0.6345(4) 0.5447(10) 0.0763(5) Uiso
1.000000 GR
 C6 C -0.04582(18) 0.2929(2) 0.26670(15) 0.0609(4) Uani
1.000000 .
 H6 H -0.00874(18) 0.2510(2) 0.19868(15) 0.0731(5) Uiso
1.000000 R
 C7 C -0.05908(19) 0.42564(19) 0.24651(14) 0.0614(4) Uani
1.000000 .
```

```
 H7 H -0.03245(19) 0.47189(19) 0.16425(14) 0.0737(5) Uiso
1.000000 R
 C23 C 0.2139(2) -0.13838(18) 0.9189(2) 0.0726(5) Uani
1.000000 .
 H23a H 0.1362(10) -0.1318(5) 0.9893(8) 0.1088(8) Uiso
1.000000 GR
 H23b H 0.2127(18) -0.2037(4) 0.8770(5) 0.1088(8) Uiso
1.000000 GR
 H23c H 0.2992(9) -0.1625(8) 0.9495(13) 0.1088(8) Uiso
1.000000 GR
 C13 C -0.6228(2) 0.49868(17) 0.8498(2) 0.0659(4) Uani
1.000000 .
 H13 H -0.6402(2) 0.58539(17) 0.8056(2) 0.0791(5) Uiso
1.000000 R

loop_
  _atom_site_aniso_label
  _atom_site_aniso_U_11
  _atom_site_aniso_U_22
  _atom_site_aniso_U_33
  _atom_site_aniso_U_12
  _atom_site_aniso_U_13
  _atom_site_aniso_U_23
 O5 0.0474(5) 0.0369(4) 0.0535(5) -0.0112(4) -0.0266(4)
0.0027(4)
 O1 0.0638(6) 0.0474(5) 0.0375(5) -0.0174(4) -0.0140(4) -
0.0078(4)
 O3 0.0691(7) 0.0366(5) 0.0487(5) -0.0143(4) -0.0167(5)
0.0097(4)
 O2 0.0546(6) 0.0387(5) 0.0500(6) -0.0031(4) -0.0153(4)
0.0082(4)
 O4 0.0613(6) 0.0514(6) 0.0615(6) -0.0287(5) -0.0250(5)
0.0130(5)
 N5 0.155(2) 0.0461(9) 0.1167(17) -0.0003(10) -0.0490(15) -
0.0317(10)
 N2 0.0476(6) 0.0270(5) 0.0469(6) -0.0092(4) -0.0218(5)
0.0024(4)
 N1 0.0532(6) 0.0285(5) 0.0410(5) -0.0137(4) -0.0133(4) -
0.0013(4)
 N4 0.0561(7) 0.0450(7) 0.0635(8) -0.0082(5) -0.0152(6) -
0.0176(6)
 N3 0.0840(9) 0.0477(7) 0.0486(7) -0.0293(6) -0.0251(6) -
0.0054(5)
 C22 0.0993(15) 0.0731(12) 0.0854(14) -0.0293(11) -
0.0524(12) -0.0124(10)
 C15 0.0710(11) 0.0883(13) 0.0509(9) -0.0179(10) -0.0052(8)
-0.0192(9)
 C14 0.0746(12) 0.0772(13) 0.0719(12) -0.0030(9) -0.0083(9)
-0.0296(10)
```

```
 C21 0.0505(10) 0.157(2) 0.0687(12) -0.0113(12) -0.0141(9) -
0.0155(14)
 C3 0.0442(6) 0.0266(5) 0.0364(6) -0.0087(4) -0.0166(5) -
0.0004(4)
 C2 0.0448(6) 0.0308(5) 0.0381(6) -0.0109(4) -0.0148(5) -
0.0027(4)
 C18 0.0486(7) 0.0369(6) 0.0384(6) -0.0172(5) -0.0182(5)
0.0051(5)
 C4 0.0426(6) 0.0356(6) 0.0369(6) -0.0104(5) -0.0133(5) -
0.0031(4)
 C10 0.0469(6) 0.0334(5) 0.0363(6) -0.0134(5) -0.0177(5)
0.0011(4)
 C9 0.0446(6) 0.0360(6) 0.0382(6) -0.0130(5) -0.0145(5)
0.0006(5)
 C19 0.0471(6) 0.0342(6) 0.0389(6) -0.0101(5) -0.0158(5) -
0.0023(5)
 C17 0.0436(6) 0.0438(7) 0.0413(6) -0.0145(5) -0.0152(5)
0.0012(5)
 C12 0.0428(6) 0.0452(7) 0.0496(7) -0.0085(5) -0.0150(5)
0.0013(6)
 C11 0.0489(7) 0.0512(7) 0.0405(6) -0.0117(6) -0.0214(5)
0.0088(5)
 C5 0.0528(7) 0.0507(7) 0.0477(7) -0.0121(6) -0.0116(6) -
0.0154(6)
 C20 0.0467(7) 0.0562(8) 0.0516(7) -0.0123(6) -0.0252(6) -
0.0038(6)
 C8 0.0592(8) 0.0501(8) 0.0437(7) -0.0233(6) -0.0165(6)
0.0081(6)
 C16 0.0571(8) 0.0598(9) 0.0424(7) -0.0212(7) -0.0133(6) -
0.0005(6)
 C1 0.0628(8) 0.0298(6) 0.0630(9) -0.0127(5) -0.0199(7) -
0.0058(5)
 C6 0.0608(9) 0.0843(12) 0.0417(7) -0.0228(8) -0.0055(6) -
0.0187(7)
 C7 0.0668(9) 0.0818(11) 0.0362(7) -0.0328(8) -0.0098(6)
0.0022(7)
 C23 0.0702(11) 0.0602(10) 0.0879(13) -0.0100(8) -0.0504(10)
0.0100(9)
 C13 0.0622(10) 0.0510(9) 0.0758(11) 0.0005(7) -0.0160(8) -
0.0127(8)

loop_
  _geom_bond_atom_site_label_1
  _geom_bond_atom_site_label_2
  _geom_bond_distance
  _geom_bond_site_symmetry_2
  _geom_bond_publ_flag
 O5 C19 1.3420(14) . ?
 O5 C20 1.4821(15) . ?
 O1 C2 1.2149(16) . ?
```

```
O3 C18 1.2229(15) . ?
O2 C12 1.3670(18) . ?
O2 C11 1.4196(19) . ?
O4 C19 1.2076(16) . ?
N5 N4 1.109(2) . ?
N2 H2 0.8600 . ?
N2 C3 1.4556(14) . ?
N2 C19 1.3634(16) . ?
N1 C2 1.3619(15) . ?
N1 C9 1.4035(17) . ?
N1 C1 1.4539(16) . ?
N4 N3 1.2240(18) . ?
N3 C10 1.4691(17) . ?
C22 H22a 0.9600 . ?
C22 H22b 0.9600 . ?
C22 H22c 0.9600 . ?
C22 C20 1.511(2) . ?
C15 H15 0.9300 . ?
C15 C14 1.393(3) . ?
C15 C16 1.375(3) . ?
C14 H14 0.9300 . ?
C14 C13 1.378(3) . ?
C21 H21a 0.9600 . ?
C21 H21b 0.9600 . ?
C21 H21c 0.9600 . ?
C21 C20 1.506(3) . ?
C3 C2 1.5558(16) . ?
C3 C4 1.5135(16) . ?
C3 C10 1.5863(17) . ?
C18 C10 1.5434(17) . ?
C18 C17 1.461(2) . ?
C4 C9 1.3994(17) . ?
C4 C5 1.3771(19) . ?
C10 C11 1.5342(17) . ?
C9 C8 1.3889(18) . ?
C17 C12 1.3992(18) . ?
C17 C16 1.406(2) . ?
C12 C13 1.389(2) . ?
C11 H11a 0.9700 . ?
C11 H11b 0.9700 . ?
C5 H5 0.9300 . ?
C5 C6 1.396(2) . ?
C20 C23 1.519(2) . ?
C8 H8 0.9300 . ?
C8 C7 1.392(2) . ?
C16 H16 0.9300 . ?
C1 H1a 0.9600 . ?
C1 H1b 0.9600 . ?
C1 H1c 0.9600 . ?
C6 H6 0.9300 . ?
```

```
 C6 C7 1.380(3) . ?
 C7 H7 0.9300 . ?
 C23 H23a 0.9600 . ?
 C23 H23b 0.9600 . ?
 C23 H23c 0.9600 . ?
 C13 H13 0.9300 . ?

loop_
  _geom_angle_atom_site_label_1
  _geom_angle_atom_site_label_2
  _geom_angle_atom_site_label_3
  _geom_angle
  _geom_angle_site_symmetry_1
  _geom_angle_site_symmetry_3
  _geom_angle_publ_flag
 C20 O5 C19 121.25(10) . . ?
 C11 O2 C12 114.55(11) . . ?
 C3 N2 H2 120.37(6) . . ?
 C19 N2 H2 120.37(6) . . ?
 C19 N2 C3 119.26(10) . . ?
 C9 N1 C2 111.17(10) . . ?
 C1 N1 C2 123.19(12) . . ?
 C1 N1 C9 125.63(11) . . ?
 N3 N4 N5 169.95(19) . . ?
 C10 N3 N4 121.25(12) . . ?
 H22b C22 H22a 109.5 . . ?
 H22c C22 H22a 109.5 . . ?
 H22c C22 H22b 109.5 . . ?
 C20 C22 H22a 109.5 . . ?
 C20 C22 H22b 109.5 . . ?
 C20 C22 H22c 109.5 . . ?
 C14 C15 H15 119.89(11) . . ?
 C16 C15 H15 119.89(11) . . ?
 C16 C15 C14 120.22(17) . . ?
 H14 C14 C15 119.64(11) . . ?
 C13 C14 C15 120.72(18) . . ?
 C13 C14 H14 119.64(12) . . ?
 H21b C21 H21a 109.5 . . ?
 H21c C21 H21a 109.5 . . ?
 H21c C21 H21b 109.5 . . ?
 C20 C21 H21a 109.5 . . ?
 C20 C21 H21b 109.5 . . ?
 C20 C21 H21c 109.5 . . ?
 C2 C3 N2 112.25(9) . . ?
 C4 C3 N2 115.69(10) . . ?
 C4 C3 C2 101.54(9) . . ?
 C10 C3 N2 108.07(9) . . ?
 C10 C3 C2 108.44(10) . . ?
 C10 C3 C4 110.59(9) . . ?
 N1 C2 O1 127.06(11) . . ?
```

```
C3 C2 O1 125.17(11) . . ?
C3 C2 N1 107.74(10) . . ?
C10 C18 O3 119.73(12) . . ?
C17 C18 O3 123.55(12) . . ?
C17 C18 C10 116.71(10) . . ?
C9 C4 C3 108.15(10) . . ?
C5 C4 C3 131.66(11) . . ?
C5 C4 C9 120.19(12) . . ?
C3 C10 N3 109.94(11) . . ?
C18 C10 N3 111.58(10) . . ?
C18 C10 C3 111.67(9) . . ?
C11 C10 N3 102.00(11) . . ?
C11 C10 C3 113.56(10) . . ?
C11 C10 C18 107.72(11) . . ?
C4 C9 N1 110.11(10) . . ?
C8 C9 N1 128.00(12) . . ?
C8 C9 C4 121.84(13) . . ?
O4 C19 O5 126.83(12) . . ?
N2 C19 O5 109.34(10) . . ?
N2 C19 O4 123.82(11) . . ?
C12 C17 C18 120.61(12) . . ?
C16 C17 C18 120.41(12) . . ?
C16 C17 C12 118.64(14) . . ?
C17 C12 O2 121.64(13) . . ?
C13 C12 O2 117.33(13) . . ?
C13 C12 C17 120.99(15) . . ?
C10 C11 O2 113.32(11) . . ?
H11a C11 O2 108.91(7) . . ?
H11a C11 C10 108.91(7) . . ?
H11b C11 O2 108.91(7) . . ?
H11b C11 C10 108.91(7) . . ?
H11b C11 H11a 107.7 . . ?
H5 C5 C4 120.67(8) . . ?
C6 C5 C4 118.66(14) . . ?
C6 C5 H5 120.67(10) . . ?
C22 C20 O5 109.80(13) . . ?
C21 C20 O5 110.06(13) . . ?
C21 C20 C22 112.94(19) . . ?
C23 C20 O5 102.15(12) . . ?
C23 C20 C22 110.01(15) . . ?
C23 C20 C21 111.34(18) . . ?
H8 C8 C9 121.59(9) . . ?
C7 C8 C9 116.82(14) . . ?
C7 C8 H8 121.59(9) . . ?
C17 C16 C15 120.12(16) . . ?
H16 C16 C15 119.94(11) . . ?
H16 C16 C17 119.94(9) . . ?
H1a C1 N1 109.5 . . ?
H1b C1 N1 109.5 . . ?
H1b C1 H1a 109.5 . . ?
```

```
H1c C1 N1 109.5 . . ?
H1c C1 H1a 109.5 . . ?
H1c C1 H1b 109.5 . . ?
H6 C6 C5 119.77(10) . . ?
C7 C6 C5 120.45(15) . . ?
C7 C6 H6 119.77(9) . . ?
C6 C7 C8 121.99(14) . . ?
H7 C7 C8 119.01(9) . . ?
H7 C7 C6 119.01(9) . . ?
H23a C23 C20 109.5 . . ?
H23b C23 C20 109.5 . . ?
H23b C23 H23a 109.5 . . ?
H23c C23 C20 109.5 . . ?
H23c C23 H23a 109.5 . . ?
H23c C23 H23b 109.5 . . ?
C12 C13 C14 119.17(17) . . ?
H13 C13 C14 120.41(11) . . ?
H13 C13 C12 120.41(10) . . ?
```

CURRICULUM VITAE

PERSONAL INFORMATION

Surname, Name: Karahan, Seda
Nationality: Turkish (T.C.)
Date and Place of Birth: 20.12.1987, Artvin
Marital Status: Married
Maiden Name: Okumuş
Phone: +90 554 764 19 93
E-mail: okumus@metu.edu.tr; sedok87@gmail.com

EDUCATION

Doctor of Philosophy (Ph.D.): (2013-2019)
Organic Chemistry, Middle East Technical University, Ankara, Turkey
CGPA: 3.86/4.00 – **High Honor**

Master of Science (M.Sc.): (2011-2013)
Organic Chemistry, Middle East Technical University, Ankara, Turkey
CGPA: 3.64/4.00 – **High Honor**

Integrated Bachelor's and Non-Thesis Master of Science (B.Sc.): (2006-2011)
Chemistry Education, Middle East Technical University, Ankara, Turkey
CGPA: 3.68/4.00 – **Highest ranking student**

Prep School: (2005-2006)

High School: (2001-2005)
Hasan Ali Yücel Anatolian Teacher Training High School, Ankara, Turkey
Mathematics and Science Branch
CGPA: 4.87/5.00

WORK EXPERIENCE

Research Assistant: (10.2011-10.2018)
Department of Chemistry, Middle East Technical University, Ankara, Turkey

LANGUAGES

English: Advanced

PUBLICATIONS

1. **Karahan, S.**; Tanyeli, C. "Squaramide catalyzed α-chiral amine synthesis" *Tetrahedron Lett.* **2018**, *59*, 3725-3737.

2. İşibol, D.; **Karahan, S.**; Tanyeli, C. "Asymmetric organocatalytic direct Mannich reaction of acetylacetone and isatin derived ketimines: Low catalyst loading in chiral cinchona-squaramides" *Tetrahedron Lett.* **2018**, *59*, 541-545.

3. **Karahan, S.**; Tanyeli, C. "Organocatalytic enantioselective construction of isatin-derived N-alkoxycarbonyl 1,3-aminonaphthols via sterically encumbered hydrocarbon substituted quinine-based squaramide" *New J. Chem*. **2017**, *41*, 9192-9102.

4. **Okumuş, S.**; Tanyeli, C.; Demir, A. S. "Asymmetric aldol addition of α-azido ketones to ethyl pyruvate mediated by a cinchona-based bifunctional urea catalyst" *Tetrahedron Lett.* **2014**, *55*, 4302-4305.

SCHOLARSHIPS & AWARDS

1. TÜBİTAK 2211/A National Scholarship Program for PhD Students
2. Poster Award - 3rd place on Anatolian Conference on Synthetic Organic Chemistry, (ACSOC II)

INTERNATIONAL CONFERENCE PROCEEDINGS

1. **Poster Presentation,** 255th American Chemical Society National Meeting & Exposition, New Orleans, LA, USA (18-22 March 2018) "*Asymmetric Organocatalytic Addition of α-Azido Ketones to Isatin-Derived Ketimines*"

2. **Poster Presentation,** 253rd American Chemical Society National Meeting & Exposition, San Francisco, CA, USA (2-6 April 2017) "*New Quinine-Based Squaramide Catalyst and Its Evaluation in the Asymmetric aza-Friedel-Crafts Reactions of Isatin-Derived Ketimines*"

3. **Poster Presentation,** Anatolian Conference on Synthetic Organic Chemistry (ACSOC II), Aydın, Turkey (21-24 March 2016) "*New Quinine-Based Squaramide Catalyst and Its Evaluation in the Asymmetric Reactions of Isatin-Derived Ketimines"*

4. **Poster Presentation,** IUPAC 2013 44th World Chemistry Congress, İstanbul, Turkey (11-16 August 2013) "*Asymmetric Aldol Addition of α-Azido Ketones via Cinchona Based Bifunctional Urea Catalyst"*

NATIONAL CONFERENCE PROCEEDINGS

1. **Oral Presentation,** Chemistry Discussions, 2018, METU, Ankara, Turkey (30th April 2018) "*Stereoselective Synthesis of 2-Oxindole Derived Heterocycle Precursors: Asymmetric aza-Friedel Crafts Reaction of Isatin Ketimines*"

2. **Poster Presentation,** 29. Ulusal Kimya Kongresi, Ankara, Turkey (10-14 September 2017) "*İsatin Türevi Ketiminlere α-Azido Ketonların Asimetrik Organokatalitik Katılması*"

3. **Poster Presentation,** 23. Ulusal Kimya Kongresi, Sivas, Turkey (16-20 June 2009) "Yeni *Heterosiklik Polifonksiyonel Kiral Katalizörlerin Sentezi*"